Commercially relevant Cd-based quantum dots: environmental transformations' influence on toxicity and the search for sustainable alternatives

Aude Bechu

Department of Chemistry

McGill University, Montreal, Canada

December 2021

A thesis submitted to McGill University in partial fulfillment of the requirements of the degree of Doctor of Philosophy

“In nature, nothing exists alone”

Rachel Carson, Silent Spring

Table of Contents

List of Figures

List of Tables

1 Abstract

Several nanomaterials have transitioned from laboratories into products that the general population use every day. Unfortunately, often nanomaterials are not fully vetted for potential impacts on the environment and human health before introduction onto the market. One such nanomaterial is cadmium-based quantum dots, whose structure contains a carcinogenic heavy metal. Quantum dots are excellent light converters but also have long term stability due to a combination of inorganic shell and organic coatings. Originally, these particles demonstrated promise for use in biomedical applications, so most measures of their toxicity and environmental fate focused on particles designed and functionalized to enhance interactions with a biological system.

However, Cd-containing quantum dots were introduced into displays at scale, not for use with biological systems. In the first chapter of this thesis, we developed a model quantum dot representing the structure of these commercial quantum dots (core, shell, and coating) to determine key transformations of the inorganic particles in aquatic media. After exposure to different environmental factors, we found that the Cd-containing core of quantum dots aggregated and was resistant to dissolution at circumneutral pH, unlike the Zn-containing inorganic shell. We also demonstrated aggregation of inorganic quantum dots, even in the presence of an abundant amount (95wt%) of polymer coating. Toxicity studies indicated that the aged particle alone (no ions released from the quantum dots present) was less toxic than the pristine particle. This shifting toxicity of quantum dots, dependent on previous exposure to the environment, highlighted the importance of studying transformations carefully. In the second chapter of this thesis, we then probed the transformation of quantum dots in simulated human digestive fluids, where we found that quantum dots become more dispersed and loose their Zn-containing shell. These transformations will be correlated to change in QD toxicity by collaborators.

The last chapter in this thesis details the examination of quantum dot alternatives, as the original Cd-containing quantum dot was phased out of production in Europe. We grouped alternative substances into classes, but found no clear frontrunner in terms of safety, sustainability, cost-effectiveness, and performance combined. This assessment, as well as the work done detailing

the transformation of Cd-containing quantum dots, can serve as an interdisciplinary example for probing the possible impacts of commercially-relevant nanomaterials.

2 Resumé

Certains nanomatériaux sont présents dans des produits quotidiens. Malheureusement, leurs effets potentiels sur l'environnement et sur la santé sont rarement examinés avant leur commercialisation. les points quantiques (PQ), à base de cadmium, un métal lourd cancérigène, en font partie. Les points quantiques ont d'excellente propriétés lumineuses, et bénéficient d'une grande stabilité grâce à leurs nombreuse couches tant inorganiques qu'organiques. À l'origine, ces matériaux ayant l'air prometteurs pour des applications biomédicales, les mesures de leur toxicité et de leur sort environnemental ont été limitées aux particules prévues pour améliorer l'interaction avec un biote.

Cependant, des PQ à base de Cd, non prévus pour des biotes, ont été introduits dans des écrans. Dans la première partie de cette thèse, nous avons mis au point un modèle représentatif de la structure de ces PQ du commerce (cœur, coque et enrobage) pour rechercher les transformations majeures des particules inorganiques dans l'eau. Après des contacts avec divers facteurs environnementaux, nous avons constaté que, aux pH approchant la neutralité, le cœur contenant le Cd s'agrège et résiste à la dissolution, à la différence de la coque inorganique contenant du zinc. Nous avons également démontré l'agrégation des PQ, même en présence d'une quantité importante de polymère d'enrobage (95 % par poids). Les études de toxicité ont montré une toxicité inférieure (absence d'ions émis par les QD présents),par rapport aux particules originales, des particules soumises au pH . Ce changement de toxicité, en fonction du contact avec le milieu, a souligné l'importance d'une étude approfondie des transformations. Il a servi de motivation pour la deuxième partie de cette thèse, dans laquelle nous examinons les modifications des PQ dans un système digestif humain simulé. Nous avons observé que les PQ y perdent leur coque de zinc, tout en se désagrégeant. Ces transformations sont alors corrélées à une augmentation de toxicité.

La dernière partie de cette thèse explore les alternatives aux PQ, ceux à base de cadmium n'étant désormais plus fabriqués en Europe. Après avoir groupés les alternatives en catégories, nous n'en avons trouvé aucune se détachant en termes de sécurité, de coût, de durabilité ni de performance. Cette analyse, associée aux études de transformation des PQ, pourra servir d'exemple de recherche interdisciplinaire sur les effets des nanomatériaux du commerce.

Acknowledgements

I would like to thank my two supervisors, Audrey Moores and Subhasis Ghoshal. Your care and attention to both the research and my personal goals has been much appreciated. Audrey, conversations with you about the big picture have kept me on track and motivated to do my best. Subhasis, your patience as we've examined every detail of the research has been invaluable, and your sense of humor has kept our conversations cheerful.

Three other professors – Maureen McKeague, Saji George and Nil Basu have also advised the work in this thesis. Maureen, your systematic approach improved the work and I've appreciated how approachable you have been, even when experiments didn't go according to plan. Saji, your patience and enthusiasm in these bi-weekly meetings has kept up our energy over many months. Nil, thank you for posing questions in a way that somehow guided me without giving me all the answers. Thank you also for our discussions on of the many systems involved in chemical safety outside of academia.

These five professors were all part of the McGill Sustainability Systems Initiative (MSSI), headed by Heather McShane and assisted by Larissa Jarvis. Thank you both for your commitment to organizing all these researchers to expand our connections beyond our respective departments. Krittika, Guillaume, Rana, Iris, and Austin, thank you for believing in MSSI and fostering a network of students outside of the lab.

I'd like to thank the many specialists as well that helped me learn how to effectively use many different instruments – Robin Stein, Petr Fiurasek, Arthath Abdul Rahim, Kelly Sears, and Hatem Titi (who also taught me a lot about plant care). Thank you to Jean Lachaud for tailoring the resumé of this thesis.

Thank you to my coauthors, Jeffrey Liao, Chang Huang, Chany Ahn, Connor Farrell, for your time, help and willingness to explain your valuable contributions. Iris, your determination, and kindness are so admirable. I'm so glad we teamed up as research partners.

To my Moores and Ghoshal lab-mates, past and present, thank you. Your enthusiasm has meant a lot to me. Alain, Sarayu, and Arshath, you paved the way. Alex, Vini, Tony, Blaine, and Julio, your growth as researchers has been awesome to witness throughout this process. Ruby and

Jasmine, the next generation of co-supervised students, thank you for your patience as we try to explain everything, you can do this.

Outside of McGill, my friends and family were incredibly supportive – and listened politely as I talked about little particles in TVs. Harry, I could not thank you enough (and TorTor, of course). You brought me joy every day with your sharp sense of humor and improvised dance parties. Your constant belief in the goal of this PhD has been especially invaluable when I've wavered. To my parents, thank you for always believing I could do this, and thoughtfully asking week after week how the paper writing is going. To my siblings, Noemie, Elsa, and Paul, thank you for being so funny and outgoing on holidays that I forget the worries of research. To Opa and Oma, your kind hearts and open home have been such a refuge. To the rest of the Griffin Gang, thank you for welcoming me with open arms and teaching me so much about having fun in adulthood. To Rikke, Katherine, Alex, and Julio, your friendship and joyfulness have made these last years so fun.

Finally, I would like to acknowledge that this work was conducted on the traditional lands of the Haudenosaunee and Anishinabeg nations.

Preface and Contribution to Knowledge

Preface

This thesis is written in the manuscript format, according to McGill's *"Guidelines for Thesis Preparation."* Chapters 1 details the motivation, objectives, and outline of this thesis. Chapter 2 surveys related literature. Chapters 3-5 cover the methods, results and discussions related to original experimental work. Chapter 6 briefly summarizes this work and identifies future research needs. The results presented in Chapters 3 and 5 have been published in peer-reviewed journals where the author of this thesis is the first author. Chapter 4 presents this author's contribution to a body of work that, combined with a collaborator's results, will be submitted as two different manuscripts.

Contributions to knowledge

1. **Design of commercially-relevant QD for use in toxicity and transformation tests.** Previous reports investigating QD transformation used either QDs covered with small molecules or large polymers. However, for commercially-relevant QDs, the polymers are unknown because they are not disclosed by QD manufacturers (besides hints from patents). We formulated a protocol for the synthesis of a QD, very similar to one described in a patent that describes the preparation of QDs for display applications. We also synthesized this QD such that the inorganic content was relatively low – reflecting the low concentrations of QDs in actual products. This complex structure provided a versatile platform to investigate QD transformation and toxicity, as we could also synthesize its components (i.e., without shell, or without core). Such QDs of complex structure have not been used in previous environmental fate and human toxicity studies
2. **Evaluating the long-term stability of commercially-relevant QDs in environmentally-relevant conditions.** The fate of nanoparticles in the environment is commonly studied with experiments that occur on the order of days. Although those studies often capture many chemical, physical and biological transformations, they do not capture information on the longevity of particles. By studying both dissolution and aggregation state for six months, we saw limited dissolution of Cd from Cd-QDs at

circumneutral pH, but also observed the homo-aggregation of QDs into ~100 nm aggregates.

3. **Tracking the transformation of QDs in biomolecule-containing simulated digestive system.** The fate of nanomaterials in the gastro-intestinal tract is a growing research field due to the increased ingestion of nanoparticles incorporated or accidently present in food. The use of model nanoparticles, such as QDs, can inform the key transformations of small reactive nanoparticles. In this research, the systematic examination of QDs was undertaken in three different environments, simulated salivary, gastric, and intestinal phases. Previous studies have not provided robust information on how the aggregation state of QDs are altered in digestive fluids. For the first time, we used spICP-MS to decipher the general aggregation state of QDs and link it to specific digestion stages. The transformation was explored at every digestion stage rather than at the very end of the digestion, where compounded transformations complicate conclusions.
4. **Adaptation of alternatives assessment method for substance researchers** Alternatives assessment is a powerful tool used by regulators and corporations, but has struggled to gain a foothold in the assessment of emerging technologies. On the other hand, design metrics based on the 12 principles of green chemistry consider efficiency but not hazard. There is therefore a gap in the hazard tools available to substance researchers. The alternatives assessment we developed aims to help these materials researchers by outlining accessible assessments (price, hazard, and performance).
5. **Assessment of perovskites, QDs and organic emitters by the same metrics** Due to the sheer volume of publications introducing new substances, it is difficult to establish which of these holds the most promise in terms of safety and sustainability. There are excellent reviews that summarize the challenges and opportunities of each of these substance types, but there is no comparison using a systematic framework between these candidates. This is surprising because these candidates are all vying for use in the same application, displays. The alternatives assessment served to bring together these various fields to highlight their respective strengths and shared challenges.

Contribution of authors

Prof. Audrey Moores (AM) and Prof. Subhasis Ghoshal (SG) supervised the completion of this thesis.

Chapters 1 and 2 was written by Aude Bechu (AB) and edited by AM and SG.

Chapter 3 was initiated by AB, AM, SG, and Maureen McKeague (MM). AB designed the quantum dot synthesis, and Chany Ahn helped to synthesize those quantum dots during a summer internship. Jeffery Liao and Chang Huang ran toxicity tests under the supervision of MM. AB, MM, SG, and AM co-authored an article, which is adapted for this thesis:

- A. Bechu, J. Liao, C. Huang, C. Ahn, M. McKeague,* S. Ghoshal,* A. Moores*, "Cadmium-Containing Quantum Dots Used in Electronic Displays: Implications for Toxicity and Environmental Transformations" ACS Appl. Nano Mater. 2021, 4, 8, 8417-8428. *indicates corresponding authors

Chapter 4 was initiated by AB, AM, SG, Saji George (SG2) and Ke Xu (KX). KX performed all cell-related experiments with quantum dots prepared by AB. AB tracked the transformation of quantum dots in the digestive system. KX also contributed confocal images. KX also ran all cell toxicity experiments of transformed quantum dots, which she will include in her thesis. Then, KX, AB, SG, AM, SG2, and Nil Basu (NB) co-authored a manuscript on pristine QD toxicity, whose full contents will be in KX's thesis. A concise report AB's contribution is provided in this thesis. The authors, AB, KX, SG, AM, NB, and SG2 plan to combine transformation and toxicity into a manuscript. Only the AB's transformation results are presented in this thesis, while toxicity results will be presented by KX.

- K. Xu, A. Bechu, N. Basu, S. Ghoshal*, A. Moores*, S. George* "Hazard profiling of components constituting a commercially-relevant functional quantum dot revealed synergistic interactions between heavy metals and polymer" Chem. Res. Tox. 2021 (submitted Nov. 10 2021, ID: tx-2021-00382n)

- Bechu & K. Xu. N. Basu, S. Ghoshal*, A. Moores*, S. George* “Linking transformation and toxicity of Cd-containing quantum dots in the simulated human digestive system” manuscript in preparation.

Chapter 5 was initiated by AB, AM, and NB, with SG helping with experimental design. AB structured and performed the analysis. AB, AM, NB, and SG co-authored the manuscript, which was then adapted for this manuscript.

- A. Bechu, S. Ghoshal, A. Moores,* N. Basu* “Are substitutes to Cd-based quantum dots in displays more sustainable, effective, and cost competitive? An alternatives assessment approach” ACS Sustainable Chem. Eng. 2021 (Submitted Jul. 20 2021, sc-2021-04909g, major revisions) ChemRxiv: 10.33774/chemrxiv-2021-sjv53 Appeared on Jul. 20 2021.

Chapter 6 was written by Aude Bechu (AB) and edited by AM and SG.

1 Introduction

1.1 Thesis motivation

The development of various new substances have overall improved and lengthened our lives. However, the history of materials development is also littered with many examples of regrettable substitution and unintended consequences. From the burning of fossil fuels to the generation of tons of plastic waste (some of which include toxic additives), there are many lessons to be learned in safe and sustainable materials development. The relatively recent development of nanomaterials for commercial use provides an opportunity for researchers to design complex products with life cycle consequences and safety in mind.

This effort is traditionally complicated by the current segmentation of research fields. Chemists are just now starting to learn the complexities involved in toxicity testing, while toxicologists are learning the complexities of nanomaterials. All the while, environmental engineers are striving to develop analytical techniques to fully assess environmental transformations of these nanomaterials – keeping both design and toxicity in mind. Health and environmental impact assessors are learning how to effectively group nanomaterials to determine their possible health and environmental impacts. These complex problems cannot be addressed in one discipline alone and demand effective collaboration.

These large trends are reflected in the story of a nanoparticle described in this thesis, quantum dots (QDs). Original implementation of Cd-based QDs in consumer products generated push-back because of the presence of a toxic heavy metal. The initial transformation and toxicity assessment of QDs was complicated by their multi-component structure. Despite massive advancements in the field seeking to address these questions, designing higher performing, sustainable and safe QDs continues to be an obscure goal for all stakeholders involved.

The work presented in this thesis serves as a small example of chemists, environmental engineers, toxicologists, and assessors coming together to advance the development of QDs. The results presented are aimed at a similar multidisciplinary audience and are expressed with accessible terms.

1.2 Research objectives

The overall objective of this thesis was to bring attention to the key transformations and resulting toxicity of a commercially relevant QD, and provide a framework for the development of less hazardous alternatives that was accessible to substance researchers. These objectives serve to build on the connections between the fields of nanoparticle design, environmental transformation, and resulting toxicity for the implementation of safe and sustainable materials.

The specific objectives of this thesis were:

1. Design a commercially-relevant quantum dot and identify how its environmental transformations differed from previously tested QDs of simpler structure. Determine whether the toxicity of this commercially relevant QD after aging arose from the nanoparticle itself, its dissolved ions, organic components, or a combination.
2. Determine how the toxicity of QDs can change after exposure to a biologically-relevant environment, the simulated human gastric digestion system and identify key transformations of QDs when sequentially exposed to the principal digestive fluids.
3. Design an assessment that could be used by materials researchers to easily integrate hazard and price (in addition to standardizing performance). This would inform the next generation of emitting substances.

1.3 Organization of the thesis

- **Chapter 1** introduces the motivation of this thesis, as well as its research objectives, contribution to knowledge and summarizes its organization.
- **Chapter 2** provides a survey of the literature relevant to the research objectives of thesis. The development and wide variety of applications of QDs is summarized. Next, the toxicity drivers and mechanisms of QDs are discussed. The different environmental transformations of nanoparticles are presented as well, using popular nanoparticles as examples of chemical, physical, and biological transformations, as well as resulting toxicity implications. Then the environmental transformation and toxicity of QDs is briefly introduced. Finally, different assessment and design strategies are summarized and connected to the ongoing research in nanomaterial transformation and toxicity.

- **Chapter 3** presents the design and synthesis of a commercially-relevant Cd-based QD. Chemical and physical transformations of these particles are investigated in response to O_2 levels and acetic acid (pH 2-8). ZnS shells dissolved, while Cd remained in QDs that formed homo-aggregates. Toxicity resulting from the ageing of QDs at low pH is also investigated, and the toxicity of released ions, rather than aged QDs themselves, is identified as the main driver of toxicity.
- **Chapter 4** uses the same QDs and its components to investigate levers of pristine QD toxicity in a quantitative manner. Then, the transformations of QDs in a simulated human digestive system is presented. The degree of dispersion and dissolution are identified as key transformations linked to the gastric and intestinal stage of digestion.
- **Chapter 5** aims to guide the development of next generation of substances that will eventually replace Cd-QDs in products using an alternatives assessment. The survey of substances included In-QDs, perovskites and emitters in OLEDs. To examine these substances we grouped them into packages with a red, green, and blue material. The packages were then examined with hazard, price and performance assessments. Results indicated no clear winner in terms of decreasing hazard and price while maintaining performance. However, the assessment was designed such that researchers could input their own substances in the future.
- **Chapter 6** summarizes the findings in their thesis while also identifying future work needed to design and assess both safe and sustainable nanomaterials.

2 Literature Review

2.1 Connecting text:

The objectives met in this thesis were only possible because we could stand on the shoulders of giants. Meticulous and in-depth research was involved in the development of QDs, commercialization of QDs, as well as testing of NP toxicity and transformation. A rich body of sustainability-inspired research has set the stage for the alternatives assessment discussed in the previous chapter and developed guiding principles that integrate the lessons of safety and sustainability assessments. We will survey the achievements of these researchers in the next section, and point out further areas of study.

2.2 Quantum Dots: Brief history of a complex particle

2.2.1 The promising particle

The term "nanotechnology" appeared in 1974, following the development of advanced instruments (e.g. transmission electron microscope) in the early-mid 1900s.[1] Such instruments allowed for the analysis of atoms and structures on the nanoscale (~10^{-9} m).[1] Therefore, nanomaterials that had been well known for centuries could be examined in a new light. In addition, new materials were examined and developed in the late 1900s.

One of the new nanomaterials is the focus of this thesis, quantum dots (QDs). QDs were rapidly developed after 1980s because they allowed scientists to probe the electron band structure of very small uniform crystals (Figure 2-1).[2] These crystals had enough atoms such that calculations regarding their energy states was complex, but not impossible. These calculations of energy states built on fundamental research probing the orbitals of individual atoms, as well as the combination of orbitals in small molecules.[3] QDs provided a link between this theoretical and the practical observations because these crystals had properties that could be observed such as a defined band-gap, measured via absorbance and fluorescence. QD synthesis (more details in the following section) allowed scientists to tune crystal size to observe phenomena such as the formation of discrete energy levels due to decreasing crystallite size. Scientists could also

understand the role of charge carriers (electrons and holes) when QDs were synthesized in ordered fashion on substrates.[4] The fact that QDs could absorb and reliably recombine visible light photons was also an advantage compared to the previous state-of-the-art material, silicon.[5] Silicon had weak absorption of high-energy light, which was not practical for most applications.[5] These many properties of quantum dots may seem confined to academic journals, but their implications meant that quantum dots had the potential to disrupt certain industries (see Section 2.2.4).

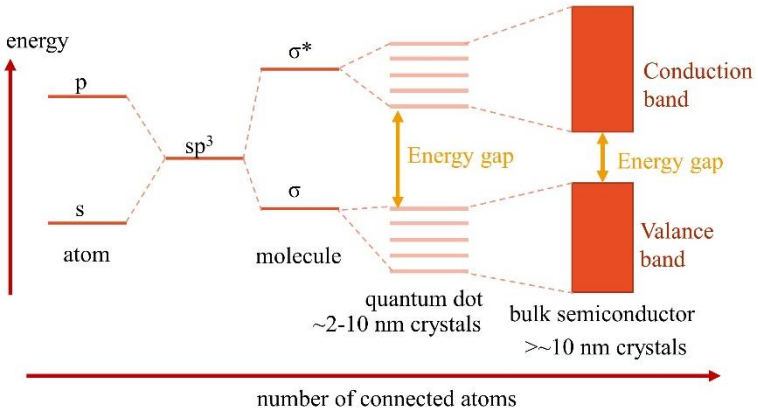

Figure 2-1: Quantum dot energy band structures were novel compared to molecules and bulk semiconductors. Adapted from Gunter et al.[2]

2.2.2 Initial synthesis: Focus on core and shell

Before understanding QDs applications outside of the lab, we must first understand their structure. QDs contain three key components: a core, shell, and an organic coating.

The core of quantum dots is made up of an emissive material. The core is emissive at a certain wavelength because its electrons experience quantum confinement in three directions. Quantum confinement is defined as the emergence of discrete energy levels in a structure. This phenomenon occurs when a wavelength of light interacts with a material whose dimensions are on the order of the light's wavelength.[6] This light excites an electron into a higher energy state (similar to a conduction band in metals) while leaving a hole in the lower energy state (valance band). The electron band structure of QDs allows for the non-radiative relaxation of light into the lowest energy of the conduction band. Non-radiative relaxation is defined as the loss of energy

by an electron without the emission of light. Then, to return to the valance band, the electron must overcome an energy gap. The relaxation of an electron from the conduction to the valance band emits energy in the form of light. Through this mechanism, the core of a QD can absorb many wavelengths of visible light, but their relaxation pathway produces just one wavelength of emitted light.

This core material is generally a semiconductor but can also be carbon-based.[7] For example, the most mature QD synthesis is based on CdSe, a semiconductor whose electrons exhibit quantum confinement at crystallite diameters smaller than ~10 nm.[8] The smaller the core, the more constricted the bandgap, and therefore the more energetic the emission. Once the core reaches a size of >10 nm for CdSe (size cut-off is dependent on semiconductor), the core's emission resembles the "bulk" emission and is therefore no longer considered a quantum dot.[8]

The emission of the core is influenced by both its size and material, but there is also a risk of non-radiative recombination. This mechanism is especially relevant when the surface of the quantum dot is changed (commonly by oxidation) because of reactive uncoordinated surface atoms.[9] The introduction of an inorganic coating whose bandgap is larger than the emissive core is key to decreasing this non-radiative recombination mechanism. Electrons absorbed by the shell are transferred to the excited state of the core and fluoresce. In addition to shuttling electrons to the core, the shell also decreases oxidation of the core. As early as the mid 1990s, Hines and Guyot-Sionnest proved that a ZnS shell on a CdSe core could increase quantum yield to 50%.[10] The shell's structure continued to be improved, with Peng et al. first reporting a CdS shell with more controlled growth (within a tenth of a monolayer!).[11] This type of shell evolved to contain both CdS and ZnS, which further decreased lattice mismatch and improved stability.[12,13] Synthesis was further tuned by many groups until quantum yield became near unity for Cd-containing QDs.[14]

2.2.3 Ligand exchange expands horizons

The next key component of quantum dot structure is the ligand or organic coating. Originally, ligands were present during the synthesis of quantum dots to regulate the growth of these nanoparticles at high temperatures. Once the synthesis and work up was complete, ligands would

remain on the surface of quantum dots. However, originally monodentate phosphine ligands were labile and their dynamic equilibrium with surrounding media decreased colloidal stability of quantum dots.[15] The exchange to other ligands represented a huge opportunity in diversifying applications of quantum dots.

Although originally concentrated in the field of fundamental atomic structures,[6] quantum dots experienced a shift in the early 2000s. This shift coincided with the emergence of (successful) ligand exchange. The emergence of polymer coatings allowed for enhanced stability in polar media.[15] Polydentate ligands also enhanced quantum dot stability and provided versatile platforms for copolymerization into composites.[16] Thiols initially showed promise in dispersing quantum dots in water,[17] but were hindered by the photo-induced formation of disulfides,[18] and a decreased quantum yield.[19] These factors were addressed by mechanistic studies that discovered the behavior of thiolates which could act as detrimental hole traps at high concentrations. Tuning the concentration and pH of ligand exchanges then allowed for the preservation of QD emission while affording the desired suspendability.[20]

In conclusion, advances in ligand exchange meant that quantum dots can be dispersed in a wide variety of media without loosing their photoluminescent properties. This, coupled with diligent studies that fine-tuned quantum dot synthesis for exciton recombination,[21] meant that quantum dots became a versatile substance ready for many applications.

2.2.4 Research-stage applications of quantum dots

Quantum dots can now be tuned to countless applications.[22] Authors often cite the tunability of QD surface as well as the reliable emission properties as the reasons the QDs are competitive candidates in many fields. The following section is a non-exhaustive survey that highlights potential applications of quantum dots that have been extensively studied and reviewed in the literature. It must be noted that these research-stage applications are not exclusive to cadmium-containing QDs. Other semiconductors, as well as carbon QDs, are increasingly being used because of toxicity concerns of Cd.

To categorize these many applications, we divided them into two groups. First, we surveyed applications that rely on the constant fluorescence of quantum dots. Second, applications that

depend on changing the fluorescence of quantum dots were explored. Some of these applications favor the non-emissive relaxation pathways. This categorization method may seem a somewhat unconventional, but it will serve well to explain how quantum dots later transitioned out of the lab into commercial applications.

First, quantum dots were used because of their stable fluorescence emission. Adding a biomolecule to the coating of quantum dots advanced the field of fluorescent labelling of cells. Such biomolecules included proteins, peptides, antibodies, aptamers, nucleic acids, liposomes, and small molecules.[23,24] These bioconjugates of quantum dots found applications in both specific and non-specific cellular labelling. For example, quantum dot cationic lipids and polymers were used to bind non-specifically to cell membranes.[25] When coated with specific antibodies, quantum dots could bind to and detect different extracellular vesicles outside of cells.[26] QD stability also allowed for their use in intracellular applications, as these nanoparticles are small enough to be transported into cells. This transport can be mediated by the coating of quantum dots by both complex biomolecules[27] as well as relatively simple molecules.[28] The key is the presence of receptors on cells that recognize these molecules.[23] These biosensing applications of quantum dots are focused on the coating of quantum dots that preserves the stable fluorescence emission.

The second group of quantum dot applications involve coupling a QD with another substance to mediate either QD absorption or emission. This group can be further divided into two different subcategories, electron transfer and dipole-dipole energy transfer (FRET).[29] The former involves the transfer of electrons between the QD and an electron donor or acceptor.[30] In the latter subcategory (FRET), electronic energy is transferred, usually from the photoexcited quantum dot to its coating molecules.[30] These two subcategories have been applied to diverse sensing applications. For example, QD-based sensors for toxic heavy metal concentrations or pH changes rely on a chromophore coupled to a QD.[29] The latter has been fine-tuned for detection of pH changes inside of cells.[31] Recent interest in quantum dot solar cells also uses the transfer of electrons from QDs to acceptor molecules like TiO_2 or ZnO using various small-molecule linkers.[32] This same concept has also been applied to fashion quantum dots into photocatalysts.[33]

QDs are also attractive platforms for light emitting diodes, where holes and electrons can be delivered with electrical charges and recombined in QDs.[34]

The thorough examination of these quantum dot applications is outside of the scope of this introduction, but there are a few key takeaways from these two categories. The first category, which involved preserving quantum dot emission, is relatively mature. There has been extensive fundamental science relating to the preservation of fluorescence in quantum dots. The second category however, which intentionally changes the recombination path of an exciton in a quantum dot, is relatively young in comparison. There remains a lack of systematic design principles and studies that researchers can use to fashion new complex substances involving QDs.

2.2.5 Current commercial uses of quantum dots

Unsurprisingly, the main commercial use of quantum dots is evolving in a similar way as the research stage applications. By recent estimates, 90% of quantum dots are used in display applications.[35] Quantum dots in this commercial application have been very successful, with the market estimated to grow to USD 8.6 billion by 2026 (up from 4.0 billion in 2021). [36]

Originally introduced in the early 2000s, quantum dots have emerged as a more efficient, stable, and effective solution compared to organic emitters and liquid crystals. The key to quantum dot stability in this application has been its coating. Quantum dots are embedded into a plastic film and used as a down-converter of blue light.[37] The two desired colors in a display, red and green, were achieved with two different core sizes of Cd-based quantum dots.[38] Further plans for quantum dots include a re-design to eliminate the blue blacklight and generate colors by electrically exciting quantum dots.[39]

In short, the evolution of QDs in display applications mirrors that of research applications (Figure 2-2). First, quantum dots were commercialized because they could efficiently absorb a wide spectrum of blue light and emit at a narrow wavelength. The emission of QDs at specific wavelengths remains the key to their successful applications in displays. Second (at the demonstration phase) is patterning QDs directly on hole and electron transmitting layers, changing the absorption pathway of energy. There are also certain companies pursuing the

commercialization of QD solar cells[40] and QD light emitting diodes,[41] but as of late 2021 their products are not on the market. These emerging commercial applications represent an opportunity to incorporate safer and more sustainable practices into QD design.

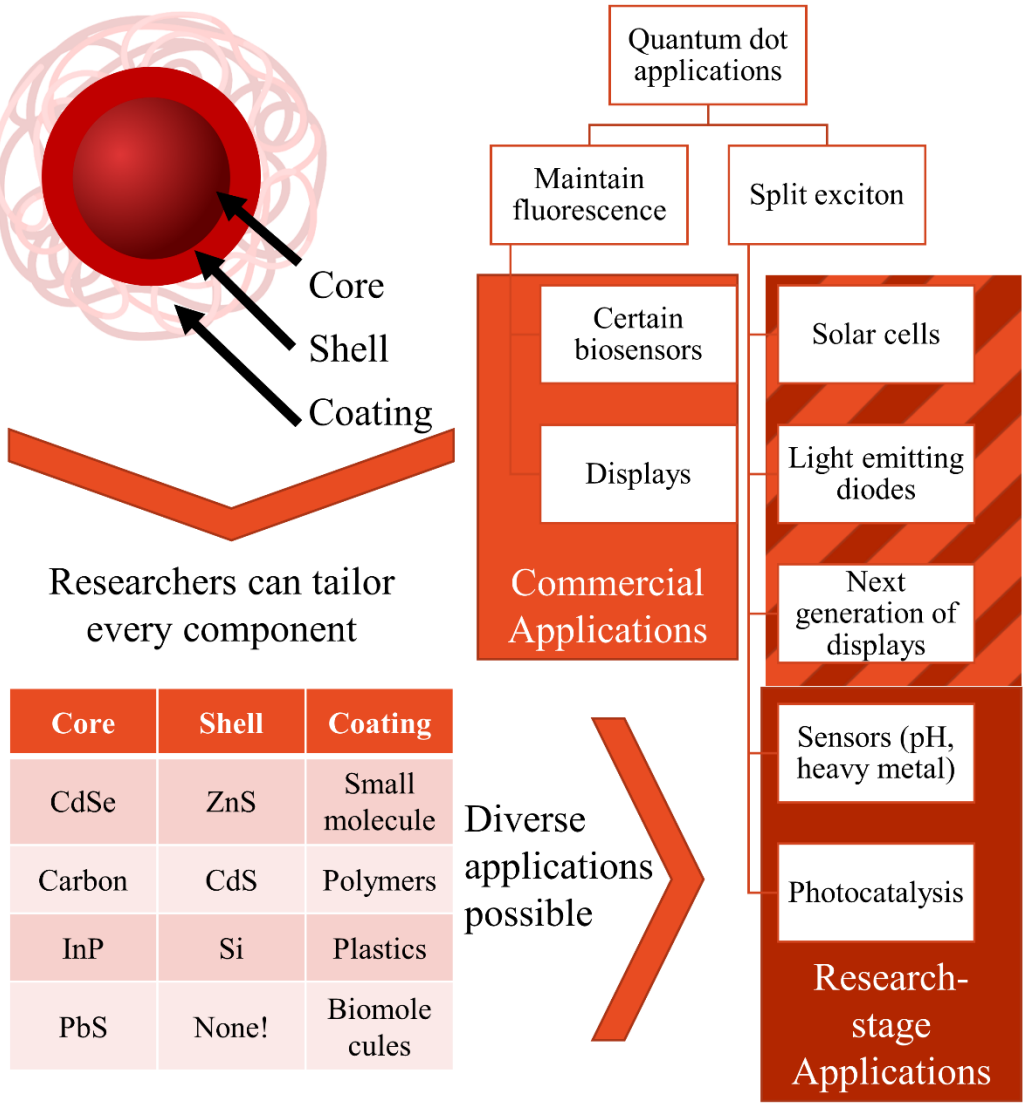

Figure 2-2: Summary of QD tunability and applications

2.2.6 Toxicological profile of quantum dots

QDs have been investigated in the literature because of two main areas of concern. First, QDs were developed with Cd (referred to as Cd-QD in the text) for biosensing and later commercial applications. Cd is a known carcinogenic and bio-accumulative heavy metal. Second, the small size of QDs could allow for nano-specific transport and toxicity concerns. We will first survey the common toxicity mechanism of QDs in the literature, followed by an exploration of how different QD components impact this toxicity.

2.2.7 Mechanisms of quantum dot toxicity

The main mechanisms through which quantum dot lead to cytotoxicity fall into two main categories: oxidative stress and ion release. These mechanisms rarely happen completely independently of each other, but for the sake of a clear explanation, we will examine each separately.

Oxidative stress is caused by an increase in reactive oxygen species (ROS). ROS are commonly accepted as a partially reduced form of oxygen, ozone (O_3), and singlet oxygen ($^1O_2$).[42] The partially reduced forms of oxygen include superoxide radical anion ($O_2^{\cdot -}$), hydrogen peroxide (H_2O_2), and hydroxyl radial ($OH^{\cdot}$).[42] Cells in aerobic organisms have evolved to tolerate and use a certain amount of oxygen and ROS. For example, the Krebs cycle in the mitochondria involves the reaction of molecular oxygen to water.[43] A small excess of ROS can be mediated by antioxidants and cellular processes that repair damaged biomolecules.[44] When the ROS is at a higher level than the corresponding antioxidants, the cell then goes into a state of oxidative stress.[44] At low levels of oxidative stress, a cell line may proliferate or adapt and upregulate their defense systems. [44] At higher levels of oxidative stress, a cell will experience oxidation of fatty acids, proteins, and other biomolecules, no longer divide, or have apoptosis triggered. [44]

Researchers have found evidence of reactive oxygen species once QDs are exposed to a variety of cell types.[45] ROS has been measured indirectly by the upregulation of certain enzymes[46] or the use of assays like 2,7-dichlorofluorescein diacetate (DCF).[47] One possible mechanism of QD-induced ROS generation is linked to the optical properties of the QDs.[48]

When QDs absorb light, their excited electrons can be transferred to O_2 while their holes can react with water to form hydroxyl radicals. Using electron spin resonance (EPR), Levy et al. have measured the UV-mediated generation of ROS from QDs.[49] This ROS generation was then used to kill multi-drug resistant pathogens.[49] ROS due to QD internalization has also been linked to inflammatory injury of cells.[50]

Cd ion release is another commonly studied QD toxicity mechanism. Cd ions bioaccumulate in humans (half life of 10-30 years) and other animals and have a high rate of soil-to-plant transfer.[51] Cd ions can replace Zn and Fe ions in key enzymes and bioprocesses.[51] In plants, Cd degenerates the mitochondria and produces ROS in tissues that are involved in photosynthesis.[52] Cd ions also cause DNA damage, and has been linked to liver, lung and kidney cancers. [53] A well-known effect of Cd toxicity is the generation of ROS in the cell. This ROS is not significantly different than the ROS mentioned above as a mechanism of QD toxicity. One well-known defense mechanism of cells again Cd toxicity is the generation of metallothionein, a protein whose upregulation is a sign of cellular Cd levels.[54]

It is a relatively simple mechanism to test for QDs– by comparing the amount of Cd in QDs to a soluble Cd salt, researchers can conclude whether there is a significant difference in toxicity. Some studies have linked all Cd-QD toxicity to the Cd present, while others have concluded that Cd-QD toxicity cannot be fully explained by Cd alone. [55,56,57] There is also a third group, which has found that Cd-QDs are less toxic than the equivalent amount of Cd.[58] Some reasons for these differing results will be elaborated on in the following section, which explores differences in Cd-QD structure. Another reason may be due to the different cell lines or mechanistic tests used. In short, there is no consensus in the field about how much Cd ion release contributes to Cd-QD toxicity.

2.2.8 Linking toxicity to QD structure

As discussed earlier, QDs have varied core, shell, and coating structures. The differences in possible QD structure have been acknowledged by researchers, who have then studied how changing certain components can lead to mediating the toxicity of the QD. These components can also mediate the toxicity mechanisms of QDs towards cells (Figure 2-3).

Before delving into specific studies, meta-analyses of QD toxicity have explored the impacts of different structures of QDs. Using Baysian networks based on 837 IC_{50} values (half maximum of the inhibitory concentration) from QD literature, Bilal et al. concluded that QD diameter was the most relevant for correlating IC_{50}.[59] A previous study focusing on just Cd-QDs found that the QD diameter, concentration, and surface ligands were the most important factors relating to IC_{50}.[60] These models are useful in comparing the entire field, but suffer from the limits of data availability (both in the combination of QDs and cell lines, but also in the characterization of QDs themselves).

Core: Although Bilal et al. found no apparent correlation between core composition of QD and cell viability, they noted that this could be due to the overwhelming amount of Cd-QDs examined (compared to In-QDs).[59] Others have explored the impact of replacing CdSe core of QDs.[59] Brunetti et al. compared the toxicity of CdSe/ZnS QDs to the toxicity of InP/ZnS QDs, with both QDs covered with mercaptopropionic acid (MPA).[61] They found that similar amounts of ions were released (<1% Cd and <1% In from QDs). However, the Cd-QDs were more toxic than the In-QDs (50% and 95% cell viability after 24h exposure at 5 nM) for human neuroblastoma cells.[61] InP QD toxicity was also compared to CdSe and CdTe QD toxicity in freshwater polyps (same ZnS shell, same penicillamine ligand). InP QDs induced 10% apoptotic nuclei compared to CdSe QD inducing 18% at 24h incubation with 50 nM QDs.[62]

Shell: There is consensus in the field that the presence of a ZnS shell can mitigate the toxicity of a CdSe core. This was demonstrated in 2004 by Derfus et al.,[63] and the result continues to be replicated in other cell lines.[64] This decrease in toxicity with the addition of the ZnS shell was also noted in the Cd-QDs metanalysis, where the presence of a shell was the third-most significant attribute to IC_{50}.[60] The prevailing theory is that the presence of a shell decreases the dissolution of Cd ions from the core, thus mitigating toxicity.

Charge of coating: Early on, positive charges were established as more toxic than negative or non-charged CdSe QDs.[65] This has been partly linked to the negative charges of most cell membrane models.[66] For example, Nagy et al. functionalized CdSe QDs with either a positive (mercaptopropionic acid) or negative (cysteamine) small molecule ligand. They found that both QDs exhibited genotoxicity, but that the positive cysteamine induced significantly higher

cytotoxicity. [46] Positively charged QD also translocate more efficiently through plants and roots than negatively charged particles.[67]

Amount of coating: Nagy et al. also explored the effect of CdSe with 'long' vs. 'short' ligands (11 vs 3 carbon atoms in chain) on toxicity, in the case of both positive and negative charges (carboxylic acid vs amines). They concluded that charges were more significant than ligand length, which was more significant than core size (3,5,10 nm CdSe examined).[68]

To the best of our knowledge, no group has probed whether the amount of polymer (innocuous or not) has impacts on toxicity of QDs. In fact, it seems relatively rare to report the amount of polymer used in toxicity studies for QDs, with just a few reports in the literature.[66] This is not a consequence of a lack of studies, as hydrophilic and amphiphilic polymers are the third and fourth-most popular coatings in the Cd-QD toxicity meta-analysis.[60] It is common practice to wash QDs and polymer mixtures in order to remove excess polymer,[69] which further complicates polymer estimates even if the preceding procedure is clear.

This factor may seem relatively trivial when considering QDs in bio-applications, where the coating will mostly likely be bio-compatible. However, in the case of commercial QDs in televisions, and their fate in the environment, these considerations may become important. Particles that are used in display applications are coated in a proprietary plastic.[38] Researchers who have mimicked this plastic coating (with well-known plastics) also report a limited toxicity to *S. oneidensis* MR-1 after exposure to the pristine QD-containing films.[70] To our knowledge, no researchers have mimicked a polymer coating for integration into plastics.

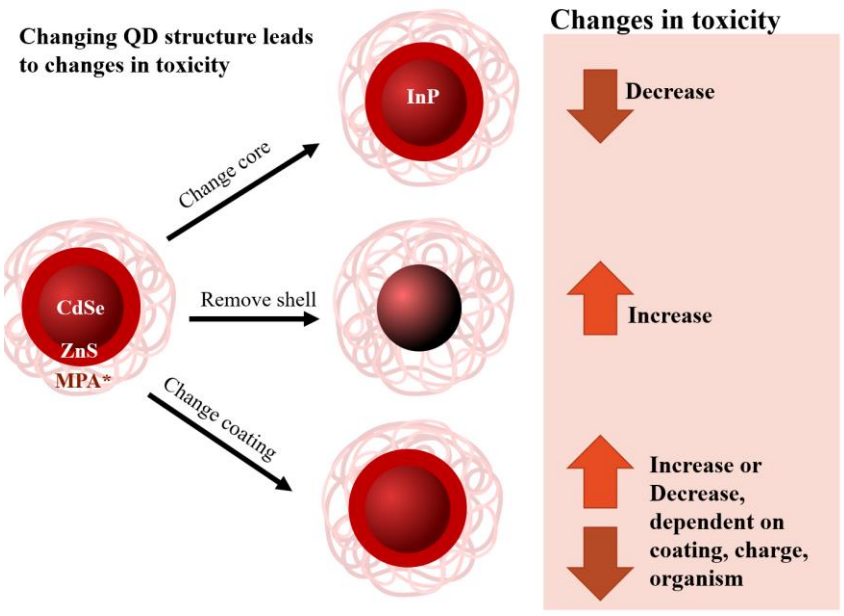

Figure 2-3: Components of QD structure that influence toxicity (including general trends)

2.2.9 Relevance of doses and particles chosen

Discussions on the changing structure of QDs has in this introduction have been qualitative – and have suggested that one component may increase or decrease toxicity. However, it would be more informative to relate quantum dot toxicity to absolute metrics to compare it to other compounds of known toxic substances. These comparisons can be done with the help of the Globally Harmonized System (GHS) which is the backbone of safety datasheets (SDS, Table 2-1). [71] GHS was developed and is maintained by the United Nations, with a new report released every two years. It has become a globally accepted metric for hazard classification of chemicals. The classifications are based on OECD testing guidelines and toxicity tests published in the literature.[72] A lower score for hazard indicates a higher hazard (1A being most hazardous).

Table 2-1: Comparison of Cd-QD to Cd toxicity using GHS benchmark tests,[71] where dark orange indicates a classification <1B, light orange of a classification of 2, and no coloring for missing of <2 categorizations. STOT RE represents specific target organ toxicity for repeat exposures. [71] The last two entires in this table are from SDS sheets and are not part of the published GHS database.

Compound Name	CAS	Carcinogenicity	Mutagenicity	Reproductive	Acute Toxicity	Aquatic acute	Aquatic chronic	STOT RE
Cadmium sulphide	215-147-8	1B	2	2	4	N/A	4	1
Cadmium compounds*	-	N/A	N/A	N/A	4	1	1	N/A
Cadmium chloride	10108-64-2	1B	1B	1B	2	1	1	1
Selenium compounds*	-	N/A	N/A	N/A	3	1	1	2
Cadmium Selenide	1306-24-7	1A	N/A	N/A	3	N/A	N/A	2
CdSe and CdSe/ZnS QDs in water[73]	-	1A	N/A	N/A	3	2	N/A	1
Qdot™ 655 ITK™ Carboxyl Quantum Dots[74]	-	N/A	N/A	N/A	N/A	N/A	N/A	N/A

* Does not include "cadmium sulphoselenide (xCdS.yCdSe), reaction mass of cadmium sulphide with zinc sulphide (xCdS.yZnS), reaction mass of cadmium sulphide with mercury sulphide (xCdS.yHgS), and those specified elsewhere in this Annex"[71]

At first glance, Cd-QDs seem to have less hazard than soluble Cd compounds such as cadmium chloride, and comparable hazard to less soluble CdS and CdSe (Table 2-1). However, there is a lack of standardized GHS tests done on Cd-QDs, even those that are marketed as labels for biomolecules,[74] resulting in many missing outputs in this table. There is also the question of dose, as the QDs dosed for aquatic GHS tests (1-100 mg/L)[71] is orders of magnitude higher than expected environmental concentrations QDs (< 10^{-6} ng/L).[75]

2.2.10 Toxicological concerns translate into regulation (sometimes)

Due to both the known carcinogenicity of Cd and the lack of values for Cd-QDs presented in Table 2-1, the introduction of Cd-QDs into display applications was a concern to regulators in the European Union. The amount of Cd present in the devices exceeded a limit set by the Restriction on Hazardous Substances.[76] The companies that planned on selling the Cd-QDs in displays in Europe then applied for an exemption to this regulation, based on the grounds that there was no viable alternative to this Cd-containing technology. This application was granted in 2011, but was later rescinded in 2019.[76] This was due to the emergence of InP and low-Cd alternative QDs in displays.[77]

In the US, QD-containing displays are allowed on the market. Researchers tested whether they released a hazardous concentration of metals with the Toxicity characteristics Leaching Procedure (TCLP) procedure developed by the EPA.[78] These tests did not reveal a significant amount of leached Cd above regulatory limits.

In conclusion, there are concerns regarding Cd-QD hazard in the literature, but regulators and manufacturers deemed the risk manageable (at least initially). Therefore, products containing these nanoparticles were (and maybe still are?) available on the market worldwide.

2.3 Transformations and resulting toxicity of nanoparticles

Thus far, the debate regarding the toxicity of nanoparticles has concerned the testing of pristine QDs. The changes in shell and coating of these pristine QDs had large impacts on their toxicity. Could the interaction of pristine QDs with environmental factors also change their toxicity? This became a relevant question with the introduction of QDs into products. With >80% of worldwide E-waste improperly disposed of (i.e. not recycled), we can assume that some QDs are being released into the environment.[79]

The interaction of nanoparticles with environmental factors can cause a host of transformations. These transformations can be categorized into chemical, physical, and biological. These transformations and their impacts on toxicity have been explored for other nanoparticles, which will form the basis of this discussion. These other engineered nanoparticles

(ENPs) have received particular attention because of their higher production volumes (up to 10^9 kg/year compared to QDs with 500-5000 kg/year).[35] Their applications include sunscreens, antimicrobials, catalysis, tire components.[35] For each transformation type, one of these common nanoparticles will be used as an example and their specific commercial uses outlined. Before delving into this discussion however, we will quickly explore why we will focus on one environment in particular – water.

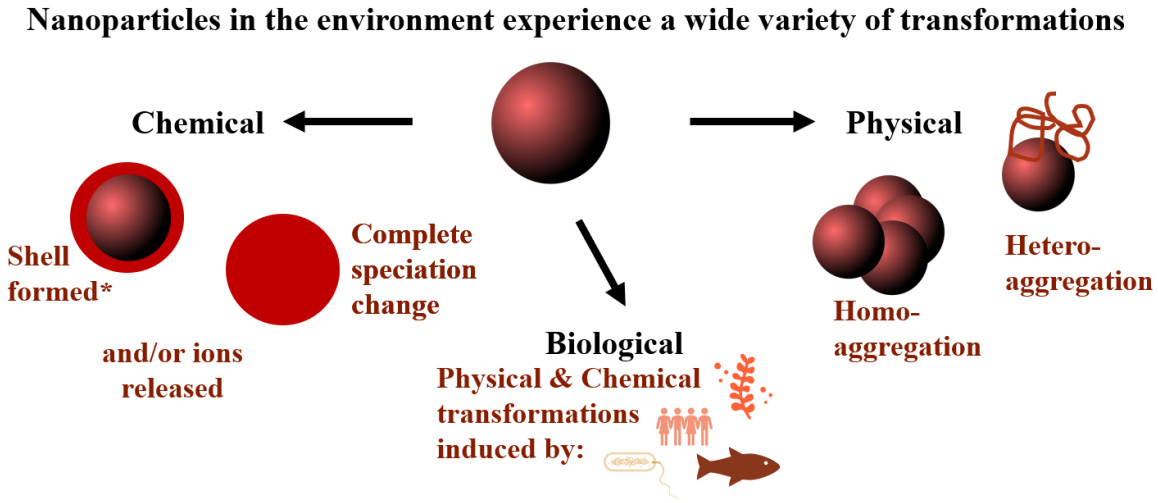

Figure 2-4: Brief overview of different nanoparticle transformations in the aquatic environment. *shell formation is not necessarily as uniform as displayed in the figure, the shell could be uneven or have incomplete NP core coverage.

2.3.1 Transformations: why we care so much about water

Water has long been a proxy for the environment in the GHS labelling system for two main reasons. First, water is the "final receiving environment for many harmful substances". Second, the organisms that inhabit water are particularly sensitive. For these reasons, environmental toxicity is measured by investigating the impacts of a substance on fish, crustacea, or aquatic plants. [72]

Many researchers have probed the environmental release of nanoparticles into different compartments (air, water, soil, landfills).[80] In most of these studies, there are non-negligible predicted environmental concentrations of nanoparticles in water and suspended sediments.

2.3.2 Physical Transformations

Physical transformations of nanoparticles involve adsorption, aggregation, deposition. These three transformations are not completely independent of one another. In fact, these may occur in a sequence: first and engineered nanoparticle (ENP) interacts with a natural colloid (adsorption) followed by the attachment of ENPs to these colloids (aggregation), which repeats until a large enough aggregate forms and sediments (deposition). [81]

Before we delve into a specific nanoparticle example, it is first necessary to establish a definition. These physical transformations can involve interactions between ENPs of the same substance, or ENPs with environmentally relevant colloids or minerals. We define homo-aggregation as between ENPs of the same substance. Hetero-aggregation has been used to describe either (1) associations between two different ENPs or (2) associations between ENPs and all other environmentally relevant colloids. For this work, we will use the second definition, which is more common in when discussing nanomaterials in the environment. [82–84]

The extensive work regarding the physical transformations of TiO_2 can serve as a basis for exploring other ENPs (such as Cd-QDs). TiO_2 consistently ranks as one of the top three nanoparticles produced and used in products.[35,85] It can be released into waterways after its use in sunscreens, cosmetics, paints and food. [83] Its high chemical stability allows for aggregation studies without the influence of chemical transformations (elaborated on below).[86] The primary particle size of TiO_2, usually determined by microscopy, are often much smaller than those reported via light scattering due to homo or hetero-aggregation.[86,87] For example, homo-aggregates are formed in solutions of solely TiO_2 nanoparticles, which decreases their UV light absorption and scattering properties.[88]

Physical transformations are primarily caused by two factors: inorganic ions in solution (i.e. ionic strength as well as pH) as well as organic components in solution. We will first quickly examine these separately before combining their effects. A commonly used metric for

aggregation is attachment efficiency (α) adapted form the Derjaguin-Landau-Verwey-Overbeek (DLVO) theory. Attachment efficiency is a ratio between 0 and unity which describes the probability of "sticking" after two nanoparticles collide.[89] Despite certain challenges in applying DLVO theory to nanoparticles,[89] the use of attachment efficiency remains relevant for quantitatively exploring factors that lead to nanoparticle aggregation.

The first key factor in TiO_2 aggregation is the ionic strength and pH of the solution. Low ionic strength imparts stability due to a larger electrostatic double layer.[90] Romanello et al. tested TiO_2 NPs without electrolyte and found that the rate of aggregation can be 0 across a wide range of pH values. Aggregation of TiO_2 reached a maximum ($\alpha=1$) in the presence of 10 mM NaCl or 0.5 mM $CaCl_2$ (pH 8). [91] The pH of the solution affects the electrostatic double layer of TiO_2 ENPs as well. This is especially evident near the point of zero charge of TiO_2, where particles will settle rapidly because of low repulsions.[92] Due to different crystal phases and manufacturing techniques, the initial point of zero charge of TiO_2 can vary from 2-8.9, with the average being pH 5.6.[93]

The second key factor to TiO_2 aggregation is the presence of environmentally relevant colloids. TiO_2 (much like other ENPs) will have both a high surface energy and a low concentration in comparison to other environmentally relevant colloids. The range of humic acid concentrations in surface water is 0.1-20 mg/L[94] while the concentration of TiO_2 is estimated at 10^{-3} to 10^{-6} mg/L.[80] Exposing TiO_2 to NOM can render the ENPs more stable due to the electrostatic repulsions introduced by the negatively-charged NOM. [91] For example, the presence of 2 mg/L extracellular polymeric substance (EPS, similar to NOM) changed the TiO_2 α from unity in 2 mM CaCl2 to $\alpha=0.1$, increasing colloidal stability. Humic acid (HA) also increased the stability of TiO_2 due to steric and electrostatic effects, and these effects were preserved in the presence of clay particles (which destabilized TiO_2 in the absence of HA).[81]

Due to the extreme variability in aggregation state, studies that seek to establish a link between aggregation and toxicity must be conducted with adequate nanoparticle characterization. Xia et al. tested TiO_2 aggregation, deposition, and toxicity in seawater at different pHs. They found that decreasing pH (from 8.20 to 7.47) would increase the amount of TiO_2 in solution (from 10% to 25%) and decrease the particle sizes of suspended NPs (from ~3000 nm to ~1000 nm after 72h). This decrease in pH (and aggregation) was then correlated to an increase in uptake

and toxicity to algae.[95] Lin et al. found that HA roughly halved the hydrodynamic radius of TiO_2 to 520 ±60 nm. The surface saturation of HA decreased TiO_2 toxicity to algae (~2.5-fold increase in EC_{50}).[96] NOM also causes a decrease in radical production of TiO_2 in the presence of UV light, decreasing TiO_2 toxicity. [97,98] Such studies have influenced models to describe the fate and toxicity thresholds of nanoparticles in the environment. One such calculation emphasized that including the effects of aggregation (especially hetero-aggregation) would decrease the comparative toxicity potential by 3-4 orders of magnitude.[99] In other words, the aggregation of TiO_2 is generally responsible for a decrease in toxicity.

2.3.3 Chemical Transformations

Chemical transformations of nanoparticles typically involve the reduction or oxidation of one or several nanoparticle components, as well as their dissolution and/or reprecipitation.

A nanoparticle with a variety of chemical transformations is Ag ENPs. Ag ENPs are Ag^0 coated with an organic capping layer (polymer or small molecule) and are commonly used as antimicrobials.[35] Once these particles enter the environment, it is thermodynamically favorable for Ag to oxidize and combine with chloride ions, sulfide ions or cysteine-containing biomolecules. Ag can oxidize fully or form an oxidized shell with a Ag^0 core. Ag ENPs can also fully dissolve into Ag ions, especially in the presence of low pH. In the presence of reducing agents (e.g. natural organic matter), these dissolved ions can also reprecipitate into Ag^0 NPs. This wide range of possible chemical transformations can be partly explained by Ag speciation models. Interestingly, the presence of traditional capping molecules or polymers on pristine Ag ENPs (citrate or polyvinylpyrrolidone) does not significantly affect the thermodynamics of these chemical transformations. However, polymers such as thiolated polyethylene glycol (PEG) and bovine serum albumin (BSA) could decrease dissolution rate of Ag ENPs.[100]

One last factor to consider for chemical transformations is light. Light can induce a NP size increase or induce particle formation because of the photo-reduction of Ag ions in solution.[101] Other researchers have used light in conjunction with natural organic matter (NOM, a known photo-reductant) to study the transformations of Ag ENPs as well. The photo-reduction of Ag in

solution by NOM in the presence of light has been shown to increase Ag NP size. This increase in size is not necessarily uniform, as Ag nanobridges have been observed.

These chemical transformations have been linked to changes in Ag toxicity. The surface oxidation of Ag NPs (i.e. presence of an AgO shell) has increased toxicity towards *E. coli*, which was partly attributed to the concurrent release of Ag ions.[102] The formation of AgCl causes increased toxicity in the presence of colloids (vs no colloids), which increase bioavailability.[103] After researchers accounted for the presence of AgCl colloids, the toxicity of Ag ENPs remains tied to ENP dissolution rate and the concentration of Ag^+ in solution.[104] Sulfidation of Ag ENPs overall decreases toxicity for two reasons. First, sulfidation causes decrease in released Ag^+ from nanoparticles. Second, sulfidated silver NPs are less bioavailable due to aggregation.[83,105] The effect of NOM and light on the toxicity of silver nanoparticles is more nuanced, as the type of NOM interaction with Ag dictates uptake into cells.[106] Photo-activation of Ag NPs (and other NPs) remains an understudied mechanism of toxicity.[107]

2.3.4 Biological transformations in the environment

The biological transformation of ENPs has a broad definition, as it encompasses any chemical or physical transformation that is caused by interaction with organisms or their biomacromolecules. Biomacromolecules are very large molecules (thousands of bonds) that originate from biological environments, such as proteins. Although NOM is considered a biomacromolecule by some researchers, we will not consider it for the sake of separation of NP transformation types. There is a wide range of biomacromolecules that have been studied in the context of nanoparticle transformation and toxicity, from proteins in blood (BSA) to biofilms from algae. There are biological transformations that can occur in the same freshwater environments as physical and chemical transformations examined above.

We will briefly survey a sample of biological transformations with zinc oxide nanoparticles, which have relatively high production volumes (top 5 of all ENPs).[35] The use of ZnO in sunscreens and cosmetics has led to the investigation of their transformations in media associated

with wastewater treatment plants or the human body (all biological fluids and hence leading to biological transformations). [108]

The association between ENPs and biomacromolecules in solution can form a corona (sometimes referred to as an eco-corona). Liu et al. tested ZnO thin film (a proxy for NPs) dissolution in different microbial growth media. [109] Peptides and amino acids complexed to ZnO and increased dissolution 10- to 30-fold compared to media without these biomolecules.[109] These dissolved Zn ions were also less likely to reprecipitate because of their association with biomolecules. [109] Briffa et al. tested the impact of proteins secreted by *D. magna* on the toxicity of ZnO ENPs towards *D. magna*.[110] If the proteins present aggregated the ZnS to a large size (200 nm rather than 15-20nm), then the *D. magna* would ingest these particles, which would then dissolve in their acidic gut and cause toxicity. However, as we saw with other physical transformations, this aggregation was time dependent – larger (more toxic) aggregates were formed after 12h ENP exposure to medium, but then smaller (less toxic) aggregates were formed after 24h. [110] Therefore, this biotransformation's impact on toxicity is highly dependent on aqueous chemistry conditions and organism (not all organisms will preferentially ingest large aggregates).

In contrast, other biomolecules can decrease uptake. For example, Ouyang et al. found that a EPS presence protected mature biofilms from ZnO toxicity.[111] This could be due to a variety of reasons, such as EPS increasing the integrity of biofilms and providing a barrier to nanoparticle interactions with cells, possibly by inducing nanoparticle aggregation.[111]

2.3.5 Biological transformations of ENPs in the body

In addition to the fresh and saltwater environments, biological transformations can occur inside of cells and organisms. The latter opens a staggering new range of ionic strength, pH, concentrations, and types of biomacromolecules. Researchers are tackling this problem by approaching biological environments that have a higher risk of nanoparticle exposure and therefore adverse effects. Li et al. recently investigated impacts of tear fluids (with and without proteins) on the microbial properties of ZnO.[112] The presence of proteins formed a protein corona, which protected ZnO from conversion into $Zn_5(CO_3)_2(OH)_6$. This protein corona also

slightly decreased the antimicrobial activity of the ZnO (compared to the pristine ZnO).[112] Quian et al. recently examined ZnO ENPs in simulated sweat, which contains L-histidine monohydrochloride monohydrate and lactic acid as well as orthophosphates. At pH 5.5 and 4.3, the presence of the phosphates caused a transition to zinc phosphate, which decreased the toxicity of ZnO towards *E. coli*. Although a test was not conducted without biomolecules present, the predominant effect on changes in bacterial survival seemed to come from the chemical transformation.

An environment that has recently gathered extensive research is the human intestinal system. This is partly due to the presence of ENPs in our diets, which serve to provide desirable textures or preserve our foods.[113] An added element of complexity is the presence of different foods in the human digestive system. This could change the coating of ENPs. Assessing changing toxicity (or subcellular impacts) is also difficult because of the gut microbial community and mucus barriers between intestinal fluids and intestinal epithelial cells.[114]

Nevertheless, transformations of ZnO ENPs have been assessed in simulated human digestive systems. Researchers have found that ZnO dissolved in the gastric phase, regardless of food type present.[115–117] However, ZnO reprecipitates in the intestinal phase, as pH is raised to 7.[117] Although the gastric phase of the intestinal system represents a low pH, not all metal oxide nanoparticles dissolves (TiO_2 for example is preserved).[115] There is also evidence that oils or protein powder could disrupt the ZnO dissolution and stabilize the particle size of TiO_2. This remains a relatively young interdisciplinary field of research, and more methodological development is needed before establishing links between transformation and toxicity (or subcellular effects). [118]

2.3.6 Transformation and resulting toxicity of quantum dots

Our survey of nanoparticle transformations and toxicity allows for the critical assessment of certain QD-related studies. But first an acknowledgement : QDs are not nearly as ubiquitous as TiO_2, Ag, or ZnO ENPs in consumer products.[119] QDs, especially Cd-QDs, are commonly used in displays where contact with consumers during the “use phase” is minimal.

However, the study of QDs transformations and toxicity remains an important course of study for a two main reasons. First, the use of QDs is only expanding as research-stage applications further tune QDs for more advanced applications. Point sources of QDs could be relevant in E-waste disposal locations, which are already plagued with high environmental concentrations of metals.[119] Learning lessons from the current QDs (and other nanoparticles) could decrease the unwanted toxicity of the next generation of QDs. Second, QDs make for interesting nanoparticle models.[120] Their fluorescence and heavy metal content make tracing these nanoparticles relatively simple, as compared to tracking abundant elements such as Zn, Ti, or carbon. Cd-QDs, which can be designed with robust shells, can serve as models for small persistent sulfidated nanoparticles. These small persistent nanoparticles have been shown to have higher toxicity potentials than larger aggregated structures,[121] so QDs can represent a "worst case" ENP scenario.

Just as with the discussion regarding QD toxicity mechanisms, the discussion regarding the transformation of QDs will be complicated by the various structures of QDs available to researchers. We will first examine the most popular QD structure studied for its environmental transformations; CdSe/ZnS with mercaptopropionic acid (MPA) as a ligand. Paydary et al. found that oxidative degradation occurred quickly for the ZnS shell (~1 week), but slower for the CdSe core.[122] The addition of ligand slowed dissolution by increasing the amount of MPA that is attached to the QD surface. Ethylenediaminetetraacetate (EDTA) increased dissolution by complexing with dissolved metals in solution.[122] Partially dissolved QDs had the same impact on *E. coli* as pristine QDs.[122]

Another popular QD is CdSe/ZnS covered with polymer. These QDs are most often purchased from companies by researchers and therefore a full characterization of the polymers is not available. Tests done on such polymer coated QDs in the presence of HA indicated that HA increased the hydrodynamic size but decreased sedimentation rate.[123] HA increased the dissolution of QDs in light.[123] Toxicity of aged QDs in these systems on mysids indicated that the main driver of toxicity was Cd metal dissolution.[123] Mahendra et al. tested the acid and base-mediated dissolution of similar QDs. This acid or base pre-treatment significantly increased QD toxicity to *E. coli*, but the presence of metal chelators mediated this (the most effective were HA

and BSA compared to small molecules like EDTA or citrate). [124] Another polymer used to coat CdSe/ZnS QDs was 5000-Da PEG-thiol. CdSe/ZnS-PEG thiol was then oxidatively degraded and tested on zebrafish embryos. These aged QDs had higher toxicity than pristine ones, with the keys to the enhanced toxicity being both the presence of Cd ions and the formation of amorphous selenium nanoparticles.[125]

There have also been investigations of QDs in plastics and their transformations. The Duncan group have embedded aliphatic-amine covered CdSe/ZnS QDs into plastics and found that particle dissolution was the main release route for Cd in Cd-QDs.[120] The group also found that the size of the particles (smaller dissolved faster) as well as the permeation extent of undissociated acids (rather than pH) were keys to increasing dissolution.[120,126] Gallagher et al. embedded CdSe/ZnS-TOPO QDs into a PMMA plastic. They found that only in the presence of light caused a significant decrease in *E. coli* viability after three weeks in a neutral solution. This was attributed not only to Cd^{2+} release but also the release of micron-sized plastic fragments.[70]

Regardless of coating (either small molecule, polymer, or plastic), the oxidative dissolution of QDs in light remains a key mechanism. This chemical transformation is spurred by the oxidation of Se or S in the QD. In the dark, dissolution slows.[127] The formation of an oxide shell to slow this dissolution has been theorized with the use of models,[122] but not yet observed experimentally. Reprecipitation of Se has only been reported once.[125]

Physical transformations, such as the increasingly impermeable QD coatings, serve to increase colloidal stability and decrease dissolution. These physical transformations, in essence, set the stage for the chemical transformations mentioned above. Physical transformations can also influence uptake of QDs by aquatic organisms.[119]

Biological transformations of QDs have focused on their possible dissolution or accumulation in the digestive tract of aquatic organisms and humans.[119] These observations have led to studies of the bioaccumulation of QDs across trophic levels, but the bioaccumulation factors can vary by orders of magnitude depending on the organisms and QDs used.[128,129]

Although certain broad statements regarding QD transformations can be made, there is a lack of systematic data in both QD transformation and the effect that this transformation has on the

bioavailability and mechanism of QD toxicity.[119] This hinders the application of models to anticipate the risk of low levels of QDs in the environment, either through release during manufacturing or after use in displays.

2.4 Pipeline for the study of transformation and toxicity of nanoparticles to inform decisions and design

Researchers run ENP transformation and toxicity tests for two reasons: inform the design of safer nanoparticle and/or decrease the current use of hazardous nanoparticles. One possible route of reaching these impacts is the use of these studies in models and assessments.

The alternative, where researchers do not consider the possible transformations and (many types of) toxicity and subcellular effects, lead to regrettable substitutions. Regrettable substitutions occur when a chemical is employed as a substitute without proper assessment of hazard or risk.[130] This leads to unintentional adverse effects. Assessments are a last line of defense to identify these regrettable substitutions before implementation.[131] Design principles (which will be discussed after assessments) are meant to engineer sustainability and safety from the start of material development to avoid regrettable substitution.

2.4.1 But first, translating studies to assessments

Before studies are translated into assessments, they must be translated into a format that an assessment can accept. The translation of toxicity (or other subcellular impacts) usually falls within two categories: (1) conducting a standardized test for hazard or (2) using models to estimate a standardized test result.

The former standardized tests could be in the Globally Harmonized System (GHS) which encompasses the hazards presented in Table 2-1. The result of these standardized tests can then fit into a certain scale (e.g. 1B for carcinogenicity). Other standardization methods include the Uniform system for the Evaluation of Substances (USES-LCA), which calculates human carcinogenic and noncarcinogenic effects for life cycle assessments (LCA, assessment explained

later). The units of these effects are different from GHS, for example ‘kg 1,4 DCB-eq’ (dichlorobenzene) represents ecotoxicity.

The second option is to model the results of a standardized test. This can be done through read-across approaches or by structure activity relationships, with the former being given a higher weight than the latter in the GHS system.[72] Read-across approaches require an expert to make decisions on predicted toxicity based on a chemicals structure and the toxicity of related chemical structures.[132] This approach has been criticized for its reliance on human expertise (which can be sometimes subjective) so structure activity relationships have also been developed.[133] Quantitative structure activity relationships (QSARs) serve to mathematically structure the prediction of toxicity. QSARs excel when supported by vast amounts of data and validation steps for QSAR models have been outlined by the OECD and REACH. [134]

QSARs for nanomaterials have been evolving for the last ten years, with a focus on metal oxide nanoparticles.[135,136] Although less data is available to ENP QSARs than traditional ones based on chemicals, other methods like a read-across based approach can be employed.[137] Despite this growth, not all nanomaterials are assessed with QSARs and the incorporation of fate considerations into these models remains a challenge.[138] Recent efforts, such as the modelling of mutagenicity of different polycyclic aromatic hydrocarbons, are accounting for the possible impacts of transformation products.[139]

These toxicity models do have the potential to inform assessment methodologies, but for now we will explore how certain assessments have had to make assumptions regarding nanomaterials.

2.4.2 Assessments and their use by regulators

There are many variations of safety and sustainability assessments, but a survey of the three popular assessments will be presented here (Figure 2-5).

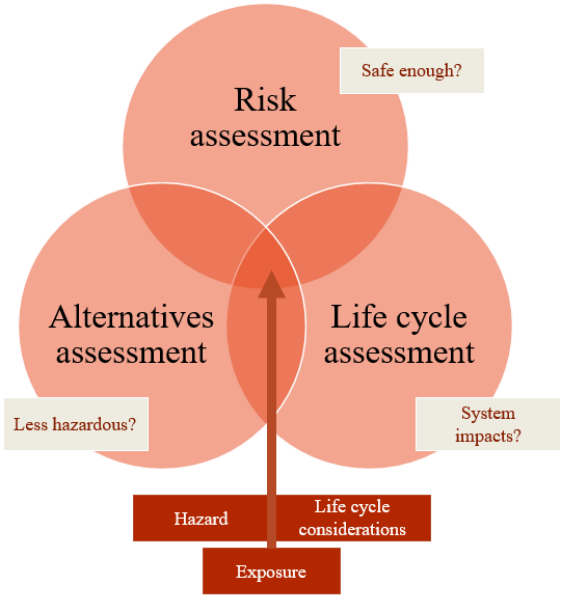

Figure 2-5: Safety and sustainability assessments (orange circles), with their inputs in dark red boxes, and their key questions in light grey boxes.

Risk assessment: Chemical risk assessment aims to determine whether a chemical or product is safe enough for its intended use case.[140] There are many methods for risk assessment, engrained into government processes due to legislation such as the Toxics Substances Control Act (US), Canadian Environmental Protection Act (Canada) and REACH (EU). The main steps of risk assessment include (1) identifying the hazards involved, (2) characterizing the hazards involved, (3) considering exposure to these hazards and (4) characterizing the risk by giving advice to decision makers.[140] These 4 steps can vary in their breadth and depth, but overall, a risk assessment calculates the "probability of suffering harm from a hazard". [140] Risk assessment is powerful because it can answer questions related to how much exposure is safe and prioritize dealing with different chemicals.[141] Risk assessment is hindered by a lack of available information (only partly addressed by QSARs) as well as the time commitment necessary to answer these difficult questions. Risk assessments are designed to be run on industrial scale processes, which hinders their adaptation to lab-scale scenarios.

Life cycle assessment: Life cycle assessment (LCA) tackles the environmental impacts of a product from cradle (resource extraction) to grave (disposal). It evaluates the environmental impacts of "a system of economic or industrial processes needed for a product to function." [141]

These impacts could be on climate change (greenhouse gas emissions), resource depletion, human toxicity, ecotoxicity etc. [142] The steps to an LCA involve (1) goal and scope formation, (2) inventory analysis and (3) impact assessment in a format laid out by the International Organization for Standardization 14040 series.[142] LCA is an apt method for weighing the impacts of a product during the manufacturing process compared to the use phase. It relies on large databases of industrial process data. For results, an LCA will present an impact (such as human toxicity) for an arbitrary functional unit, but that impact will not include a time component or a measure of whether that impact passes safety thresholds. A functional unit is the basis of an LCA and describes a function with specific bounds.[143] LCA is limited by data availability over an entire industrial process (which sometimes spans different geographic regions). Even though there is interest in including LCA into policy, to our knowledge it is not currently implemented as a decision-making tool. [144]

Alternatives assessment: Alternatives assessment is a hazard-focused assessment, aiming to answer the question as to which chemical or substance is less hazardous of all for a specific use. Although a younger field than risk assessment, alternatives assessments are being required in certain US state regulations and EU's REACH programme to address particularly hazardous chemicals.[130] This method's starting point is a certain hazardous chemical of concern. The problem is then scoped and potential alternatives identified.[141] After only certain alternatives are deemed feasible, the sub-assessments are run on these chemicals or substances: human health, ecotoxicity, and physiochemical (exposure can be added as well, but it is less commonly used). Then, life cycle thinking is applied with the use of an LCA, performance, and economic assessment.[145] From these assessments, the least hazardous substitute is identified, or (if not) more research is requested.[145] Alternatives assessment has the advantage of being possible to run relatively quickly before a chemical is used in a plant or by consumers (as exposure is not key). GHS provides a hazard database for this assessment. However, consistent data on cost, availability and performance of alternatives is sometimes difficult to obtain.[146] Lastly, similar to risk assessment, AA is used to inform decision making.

Specific challenges associated with nanoparticles: The analysis of nanomaterials with each of these assessments has been challenging due to a few reasons. First, the use of industrial scale nanomaterials is relatively new and small scale compared to the bulk chemicals usually

assessed.[147] This has introduced complications as to how to scale-up lab or pilot technologies. Second, the many transformations of nanomaterials in the environment complicates hazard estimations. This also complicates exposure estimations as well (for risk and LCA).[141] Third, there is an incredible diversity of nanomaterials on the market, some of which are not fully characterized. This calls for the development of new data tools to assess the fate, toxicity, and exposure of slightly different nanomaterials.[147]

In conclusion, risk assessment and alternatives assessment (and to a lesser extent LCA) are all tools used by decision-makers to decide whether nanomaterials are (1) a safe option and (2) the safest option of all available alternatives. Sometimes these decisions require a trade-off, or accepting an adverse impact as necessary for reducing another adverse impact.[131] For example, switching away from chlorinated solvents to aqueous detergents would decrease ozone creation, and human toxicity, but could harm aquatic environments.[148] Such trade-offs would need to be addressed and minimized before implementation.

2.4.3 Design: Approach of scientists

The same principles that dictate the assessment of substances can also dictate the design of the next generation of substances. With risk assessment in mind, Paul Anastas and John Warner designed the 12 principles of green chemistry in 1998 (Figure 2-6).[149] These principles can roughly be divided into 2 groups; efficiency and safety.

Efficiency is reflected in the principles that aim to reduce the use of derivatives (8) and unnecessary energy consumption (6). An efficient process at the molecular level (2) also prevents or reduces pollution (1,11). Catalysis can also render a process more efficient as well, reducing the need for stoichiometric reagents (9).

Safety principles cover the chemical itself (4), its synthesis (3), and how its synthesis is conducted (12), which includes the use of solvents and auxiliaries (5). A last piece of chemical safety to consider is a substance's end of life, where it should degrade into innocuous chemicals rather than persist and accumulate (10).

The last principle not yet mentioned (7) encourages the use of renewable feedstocks. This could be considered either efficient for the planet or making for a safer environment (due to the pollution associated with fossil fuel extraction and conversion).

1. **Prevention**. It is better to prevent waste than to treat or clean up waste after it is formed.
2. **Atom Economy**. Synthetic methods should be designed to maximize the incorporation of all materials used in the process into the final product.
3. **Less Hazardous Chemical Synthesis**. Whenever practicable, synthetic methodologies should be designed to use and generate substances that pose little or no toxicity to human health and the environment.
4. **Designing Safer Chemicals**. Chemical products should be designed to preserve efficacy of the function while reducing toxicity.
5. **Safer Solvents and Auxiliaries**. The use of auxiliary substances (e.g. solvents, separation agents, etc.) should be made unnecessary whenever possible and, when used, innocuous.
6. **Design for Energy Efficiency**. Energy requirements of chemical processes should be recognized for their environmental and economic impacts and should be minimized. If possible, synthetic methods should be conducted at ambient temperature and pressure.
7. **Use of Renewable Feedstocks**. A raw material or feedstock should be renewable rather than depleting whenever technically and economically practicable.
8. **Reduce Derivatives**. Unnecessary derivatization (use of blocking groups, protection/ deprotection, temporary modification of physical/chemical processes) should be minimized or avoided if possible, because such steps require additional reagents and can generate waste.
9. **Catalysis**. Catalytic reagents (as selective as possible) are superior to stoichiometric reagents.
10. **Design for Degradation**. Chemical products should be designed so that at the end of their function they break down into innocuous degradation products and do not persist in the environment.
11. **Real-Time Analysis for Pollution Prevention**. Analytical methodologies need to be further developed to allow for real-time, in-process monitoring and control prior to the formation of hazardous substances.
12. **Inherently Safer Chemistry for Accident Prevention**. Substances and the form of a substance used in a chemical process should be chosen to minimize the potential for chemical accidents, including releases, explosions, and fires.

Figure 2-6: The 12 principles of green chemistry, copied directly from reference[149]

These twelve principles echo the main ideas of the assessments discussed above: examine different life cycle stages, design products and process to reduce hazard, and employ a systematic approach. The advantage of these principles is that they are communicated in language that chemists understand and are not tied to specific benchmarks. For example, the 8th principle is ‘reduce derivatives’ which does not instruct chemists to eliminate all derivatives, but rather continue to strive for minimization. Chemists are not instructed to make a process safe, but

rather a safer one. The measurement of 'safe' would employ a risk assessment, which is not traditionally familiar or accessible to most chemists. The principles are meant to be used a cohesive system, rather than simply choosing one or two to justify a development. Just as in assessments, trade-offs should be acknowledged and (if possible) mediated.

Just as with different assessment methods, acknowledging the limits of the green chemistry principles is useful. Green chemistry, although often thought of as enabling cost-saving practices,[150] does not include any mention of a minimizing substance price in its principles. Common performance metrics are not included either, although one could argue that this is already engrained in chemist's development of substances. There is also a lack of acknowledgement of the current state of the art, which is often a basis for assessments (LCA and AA especially). Working from a need-based or broader systems perspective could introduce questions like 'Is this chemical necessary?' which could help to focus the application of the principles.

Common green chemistry metrics only measure efficiency: There are a few common methods to assess the use of green chemistry principles.[151] One of which is mentioned in the principles itself: atom economy (2). Atom economy measures how many atoms in the reactants remain in the desired final product. Carbon economy applies this same method but considers only the carbon atoms remaining. The E-factor is a waste-based metric, it measures the amount of waste divided by the total amount of product, using the weight of each. A metric can also be the number of steps in a reaction, as one-pot reactions are more desirable than multiple steps requiring purification.

The ease of measuring efficiency has led to its measurement in various contexts, such as material resource use. Increases in efficiencies in various sectors (12-50%) were applied to global resource use models for 2015-2050 by Krausmann et al. They found that despite these efficiencies, total resource extraction will continue to grow because of increases in wealth and population.[152] This reflects the trend of increasing the efficiency of fossil fuels leading to massive increases in consumption.[153] In short, increases in efficiency are tricky to implement without inadvertently using more resources as populations grow in size and wealth.

Therefore, green chemistry metrics that focus on the efficiency of a process should be complemented by metrics that evaluate the safety or hazard associated with a synthesis. This is

difficult to do in a simple manner. There are more complex tools available that do incorporate hazard.[154] LCA and alternatives assessment are among these 'more complex tools' but these must be tailored to use with all of the information available in a laboratory setting, where often hazard data must be estimated. Despite this challenge, there are many green chemistry solutions that have been assessed with LCA to evaluate impacts.[155,156] Editors of green and sustainable journals are increasingly calling for this sort of analysis as well.[157,158]

Challenges for nanoparticles: The challenges of applying green chemistry to the design of nanomaterials echo the challenges of assessing nanomaterials. These remains the challenge of effectively designing nanomaterials to maximise their potential use while minimizing their unwanted toxicity. To meet this need, various structure-property models have been developed.[159]

The principles of green chemistry can also be applied with increasing mechanistic understanding of syntheses. Using Cd-QDs as an example, the original syntheses used dimethyl cadmium and phosphine derivatives, which was quickly replaced by cadmium oxide and oleic acid after mechanisms were understood.[160] In-QDs and other QDs with less toxic cores soon followed. In short, the careful syntheses of nanomaterials is not a barrier to the full implementation of the principles, but it can slow the process.

Assessment and design are both needed: The three assessment strategies, as well as the design strategies surveyed here, are all necessary to employ in the search for safe and sustainable materials. They each excel in certain scenarios with specific problems, and therefore have limitations. A method that addressed all the situations discussed here would need an incredible amount of data and could be too inaccessible and complex for any one group of researchers. By exploring the limits of each of these strategies, we can effectively decide when an additional strategy is necessary to employ.

Both assessment and design are needed as well to avoid regrettable substitution. Causes of regrettable substitution include a lack of hazard data, a failure to consider the life cycle, endpoint trade-off, failure to consider exposure or functional use of a product.[131] Each of the assessments and design principles discussed above has certain characteristics that address some of the causes of regrettable substitution. For example, AA considers hazed, endpoint trade-offs, and functional use, but doesn't consider exposure or (depending on the assessment's depth) sometimes life

cycle. Design principles are necessary to decrease hazard in the initial product and simplify the synthesis, which would decrease risks from exposure and life cycle factors to consider during an LCA. In short, the strengths of each of these methods can be leveraged to avoid regrettable substitution, but using one method alone is not enough.

2.5 Conclusion:

This introduction began by assessing the development of quantum dots and surveying both the commercial and research-stage applications of these tunable nanoparticles. The complexity of these nanoparticles' structures initially complicated toxicity testing, but key pieces of their structure were then identified. Then, we considered the fate of nanomaterials in the environment, using other nanomaterials as examples of a wide variety of transformations. QD environmental fate literature is still evolving and has indicated that (like toxicity) the structure of these particles is key. Lastly, we surveyed how this information could be used to inform design and decisions. With both assessment methods and design principles, we identified knowledge gaps that still hinder the safer and more sustainable use and synthesis of nanomaterials.

Although the term "challenges" has been peppered throughout this review, they have served to identify 3 key opportunities:

(1) Researchers know that the current main commercial use of QDs in a plastic sheet in displays, although global production estimates and some life cycle considerations remain elusive. This should drive research into current QD toxicity and hazard estimation for assessments, despite the relatively small number of studies that probe QD structures like those in displays.

(2) In addition, QD development for different applications is ongoing. There is time (and motivation) to add safety and sustainability into their design before reaching commercial scale. Green chemistry design principles are excellent starting points, but the lack of hazard in their quick metrics calls for the use of other assessment strategies.

(3) QD researchers can leverage the extensive work done for other nanoparticles to uncover key levers of QD toxicity after transformation. There is also a robust understanding of pristine QD toxicity to help with this research as well. Combining existing literature with

more systematic studies can provide the missing link of estimating hazard of QDs (both current and future) for assessments and design.

2.6 References

(1) Bayda, S.; Adeel, M.; Tuccinardi, T.; Cordani, M.; Rizzolio, F. The History of Nanoscience and Nanotechnology: From Chemical–Physical Applications to Nanomedicine. *Molecules* **2019**, *25* (1), 112. https://doi.org/10.3390/molecules25010112.

(2) *Nanotechnology*; Schmid, G., Ed.; Wiley-VCH: Weinheim, 2008.

(3) Yoffe, A. D. Semiconductor Quantum Dots and Related Systems: Electronic, Optical, Luminescence and Related Properties of Low Dimensional Systems. *Advances in Physics* **2001**, *50* (1), 1–208. https://doi.org/10.1080/00018730010006608.

(4) The Many Aspects of Quantum Dots. *Nature Nanotech* **2010**, *5* (6), 381–381. https://doi.org/10.1038/nnano.2010.127.

(5) Konstantatos, G.; Sargent, E. H. Nanostructured Materials for Photon Detection. *Nature Nanotech* **2010**, *5* (6), 391–400. https://doi.org/10.1038/nnano.2010.78.

(6) Vanmaekelbergh, D.; Liljeroth, P. Electron-Conducting Quantum Dot Solids: Novel Materials Based on Colloidal Semiconductor Nanocrystals. *Chem. Soc. Rev.* **2005**, *34* (4), 299–312. https://doi.org/10.1039/B314945P.

(7) Lim, S. Y.; Shen, W.; Gao, Z. Carbon Quantum Dots and Their Applications. *Chem. Soc. Rev.* **2014**, *44* (1), 362–381. https://doi.org/10.1039/C4CS00269E.

(8) Gaponenko, S. V.; Demir, H. V. *Applied Nanophotonics*; Cambridge University Press: Cambridge, 2018. https://doi.org/10.1017/9781316535868.

(9) Fomenko, V.; Nesbitt, D. J. Solution Control of Radiative and Nonradiative Lifetimes: A Novel Contribution to Quantum Dot Blinking Suppression. *Nano Lett.* **2008**, *8* (1), 287–293. https://doi.org/10.1021/nl0726609.

(10) Hines, M. A.; Guyot-Sionnest, P. Synthesis and Characterization of Strongly Luminescing ZnS-Capped CdSe Nanocrystals. *J. Phys. Chem.* **1996**, *100* (2), 468–471. https://doi.org/10.1021/jp9530562.

(11) Peng, X.; Schlamp, M. C.; Kadavanich, A. V.; Alivisatos, A. P. Epitaxial Growth of Highly Luminescent CdSe/CdS Core/Shell Nanocrystals with Photostability and Electronic Accessibility. *J. Am. Chem. Soc.* **1997**, *119* (30), 7019–7029. https://doi.org/10.1021/ja970754m.

(12) Talapin, D. V.; Mekis, I.; Götzinger, S.; Kornowski, A.; Benson, O.; Weller, H. CdSe/CdS/ZnS and CdSe/ZnSe/ZnS Core−Shell−Shell Nanocrystals. *J. Phys. Chem. B* **2004**, *108* (49), 18826–18831. https://doi.org/10.1021/jp046481g.

(13) Xie, R.; Kolb, U.; Li, J.; Basché, T.; Mews, A. Synthesis and Characterization of Highly Luminescent CdSe−Core CdS/Zn 0.5 Cd 0.5 S/ZnS Multishell Nanocrystals. *J. Am. Chem. Soc.* **2005**, *127* (20), 7480–7488. https://doi.org/10.1021/ja042939g.

(14) McBride, J.; Treadway, J.; Feldman, L. C.; Pennycook, S. J.; Rosenthal, S. J. Structural Basis for Near Unity Quantum Yield Core/Shell Nanostructures. *Nano Lett.* **2006**, *6* (7), 1496–1501. https://doi.org/10.1021/nl060993k.

(15) Wang, X.-S.; Dykstra, T. E.; Salvador, M. R.; Manners, I.; Scholes, G. D.; Winnik, M. A. Surface Passivation of Luminescent Colloidal Quantum Dots with Poly(Dimethylaminoethyl Methacrylate) through a Ligand Exchange Process. *J. Am. Chem. Soc.* **2004**, *126* (25), 7784–7785. https://doi.org/10.1021/ja0489339.
(16) Kim, S.; Bawendi, M. G. Oligomeric Ligands for Luminescent and Stable Nanocrystal Quantum Dots. *J. Am. Chem. Soc.* **2003**, *125* (48), 14652–14653. https://doi.org/10.1021/ja0368094.
(17) Chan, W. C. W.; Nie, S. Quantum Dot Bioconjugates for Ultrasensitive Nonisotopic Detection. *Science* **1998**, *281* (5385), 2016–2018. https://doi.org/10.1126/science.281.5385.2016.
(18) Veinot, J. G. C.; Galloro, J.; Pugliese, L.; Pestrin, R.; Pietro, W. J. Surface Functionalization of Cadmium Sulfide Quantum-Confined Nanoclusters. 5. Evidence of Facile Surface-Core Electronic Communication in the Photodecomposition Mechanism of Functionalized Quantum Dots. *Chem. Mater.* **1999**, *11* (3), 642–648. https://doi.org/10.1021/cm980513t.
(19) Munro, A. M.; Ginger, D. S. Photoluminescence Quenching of Single CdSe Nanocrystals by Ligand Adsorption. *Nano Lett.* **2008**, *8* (8), 2585–2590. https://doi.org/10.1021/nl801132t.
(20) Green, M. The Nature of Quantum Dot Capping Ligands. *Journal of Materials Chemistry* **2010**, *20* (28), 5797–5809. https://doi.org/10.1039/C0JM00007H.
(21) Zhuang, Z.; Peng, Q.; Li, Y. Controlled Synthesis of Semiconductor Nanostructures in the Liquid Phase. *Chem. Soc. Rev.* **2011**, *40* (11), 5492–5513. https://doi.org/10.1039/C1CS15095B.
(22) Cotta, M. A. Quantum Dots and Their Applications: What Lies Ahead? *ACS Appl. Nano Mater.* **2020**, *3* (6), 4920–4924. https://doi.org/10.1021/acsanm.0c01386.
(23) Biju, V.; Itoh, T.; Ishikawa, M. Delivering Quantum Dots to Cells: Bioconjugated Quantum Dots for Targeted and Nonspecific Extracellular and Intracellular Imaging. *Chem. Soc. Rev.* **2010**, *39* (8), 3031. https://doi.org/10.1039/b926512k.
(24) Bentzen, E. L.; Tomlinson, I. D.; Mason, J.; Gresch, P.; Warnement, M. R.; Wright, D.; Sanders-Bush, E.; Blakely, R.; Rosenthal, S. J. Surface Modification To Reduce Nonspecific Binding of Quantum Dots in Live Cell Assays. *Bioconjugate Chem.* **2005**, *16* (6), 1488–1494. https://doi.org/10.1021/bc0502006.
(25) Murcia, M. J.; Minner, Daniel. E.; Mustata, G.-M.; Ritchie, K.; Naumann, C. A. Design of Quantum Dot-Conjugated Lipids for Long-Term, High-Speed Tracking Experiments on Cell Surfaces. *J. Am. Chem. Soc.* **2008**, *130* (45), 15054–15062. https://doi.org/10.1021/ja803325b.
(26) Rodrigues, M.; Richards, N.; Ning, B.; Lyon, C. J.; Hu, T. Y. Rapid Lipid-Based Approach for Normalization of Quantum-Dot-Detected Biomarker Expression on Extracellular Vesicles in Complex Biological Samples. *Nano Lett.* **2019**, *19* (11), 7623–7631. https://doi.org/10.1021/acs.nanolett.9b02232.
(27) Gao, X.; Wang, T.; Wu, B.; Chen, J.; Chen, J.; Yue, Y.; Dai, N.; Chen, H.; Jiang, X. Quantum Dots for Tracking Cellular Transport of Lectin-Functionalized Nanoparticles. *Biochemical and Biophysical Research Communications* **2008**, *377* (1), 35–40. https://doi.org/10.1016/j.bbrc.2008.09.077.

(28) Kikkeri, R.; Lepenies, B.; Adibekian, A.; Laurino, P.; Seeberger, P. H. In Vitro Imaging and in Vivo Liver Targeting with Carbohydrate Capped Quantum Dots. *J. Am. Chem. Soc.* **2009**, *131* (6), 2110–2112. https://doi.org/10.1021/ja807711w.
(29) Silvi, S.; Credi, A. Luminescent Sensors Based on Quantum Dot–Molecule Conjugates. *Chemical Society Reviews* **2015**, *44* (13), 4275–4289. https://doi.org/10.1039/C4CS00400K.
(30) Avellini, T.; Lincheneau, C.; Vera, F.; Silvi, S.; Credi, A. Hybrids of Semiconductor Quantum Dot and Molecular Species for Photoinduced Functions. *Coordination Chemistry Reviews* **2014**, *263–264*, 151–160. https://doi.org/10.1016/j.ccr.2013.07.014.
(31) Dennis, A. M.; Rhee, W. J.; Sotto, D.; Dublin, S. N.; Bao, G. Quantum Dot–Fluorescent Protein FRET Probes for Sensing Intracellular PH. *ACS Nano* **2012**, *6* (4), 2917–2924. https://doi.org/10.1021/nn2038077.
(32) Pan, Z.; Rao, H.; Mora-Seró, I.; Bisquert, J.; Zhong, X. Quantum Dot-Sensitized Solar Cells. *Chem. Soc. Rev.* **2018**, *47* (20), 7659–7702. https://doi.org/10.1039/C8CS00431E.
(33) Yuan, Y.; Jin, N.; Saghy, P.; Dube, L.; Zhu, H.; Chen, O. Quantum Dot Photocatalysts for Organic Transformations. *J. Phys. Chem. Lett.* **2021**, *12* (30), 7180–7193. https://doi.org/10.1021/acs.jpclett.1c01717.
(34) Kim, T.; Kim, K.-H.; Kim, S.; Choi, S.-M.; Jang, H.; Seo, H.-K.; Lee, H.; Chung, D.-Y.; Jang, E. Efficient and Stable Blue Quantum Dot Light-Emitting Diode. *Nature* **2020**, *586* (7829), 385–389. https://doi.org/10.1038/s41586-020-2791-x.
(35) Janković, N. Z.; Plata, D. L. Engineered Nanomaterials in the Context of Global Element Cycles. *Environ. Sci.: Nano* **2019**, *6* (9), 2697–2711. https://doi.org/10.1039/C9EN00322C.
(36) Quantum Dot Industry Trends, Opportunities | Global Quantum Dot Market Forecast to 2026 | MarketsandMarkets™ https://www.marketsandmarkets.com/ResearchInsight/quantum-dots-qd-market.asp (accessed 2021 -11 -29).
(37) Jang, E. Environmentally Friendly Quantum Dots for Display Applications. In *2018 IEEE International Electron Devices Meeting (IEDM)*; 2018; p 38.2.1-38.2.4. https://doi.org/10.1109/IEDM.2018.8614647.
(38) Dubrow, R. S.; Freeman, W. P.; Lee, E.; Furuta, P. Quantum Dot Films, Lighting Devices, and Lighting Methods. US9199842B2, December 1, 2015.
(39) DSCC Releases New Annual Quantum Dot Display Technology and Market Outlook Report - Display Supply Chain Consultants https://www.displaysupplychain.com/blog/dscc-releases-new-annual-quantum-dot-display-technology-and-market-outlook-report (accessed 2021 -11 -29).
(40) QD Solar Inc. *About QD Solar*, 2021.
(41) Quantum Dots from Osram make LEDs even more efficient | OSRAM https://www.osram.com/os/press/press-releases/quantum-dots-from-osram-make-leds-even-more-efficient-osconiq-s-3030-qd.jsp (accessed 2021 -12 -10).
(42) Krumova, K.; Cosa, G. Chapter 1 Overview of Reactive Oxygen Species. **2016**, 1–21. https://doi.org/10.1039/9781782622208-00001.
(43) Halliwell, B.; Gutteridge, J. M. C. Oxygen: Boon yet Bane—Introducing Oxygen Toxicity and Reactive Species. In *Free Radicals in Biology and Medicine*; Oxford University Press: Oxford, 2015. https://doi.org/10.1093/acprof:oso/9780198717478.003.0001.

(44) Halliwell, B.; Gutteridge, J. M. C. Oxidative Stress and Redox Regulation: Adaptation, Damage, Repair, Senescence, and Death. In *Free Radicals in Biology and Medicine*; Oxford University Press: Oxford, 2015. https://doi.org/10.1093/acprof:oso/9780198717478.003.0005.
(45) Hu, L.; Zhong, H.; He, Z. Toxicity Evaluation of Cadmium-Containing Quantum Dots: A Review of Optimizing Physicochemical Properties to Diminish Toxicity. *Colloids and Surfaces B: Biointerfaces* **2021**, *200*, 111609. https://doi.org/10.1016/j.colsurfb.2021.111609.
(46) Nagy, A.; Hollingsworth, J. A.; Hu, B.; Steinbrück, A.; Stark, P. C.; Rios Valdez, C.; Vuyisich, M.; Stewart, M. H.; Atha, D. H.; Nelson, B. C.; Iyer, R. Functionalization-Dependent Induction of Cellular Survival Pathways by CdSe Quantum Dots in Primary Normal Human Bronchial Epithelial Cells. *ACS Nano* **2013**, *7* (10), 8397–8411. https://doi.org/10.1021/nn305532k.
(47) Luo, Y.-H.; Wu, S.-B.; Wei, Y.-H.; Chen, Y.-C.; Tsai, M.-H.; Ho, C.-C.; Lin, S.-Y.; Yang, C.-S.; Lin, P. Cadmium-Based Quantum Dot Induced Autophagy Formation for Cell Survival via Oxidative Stress. *Chem. Res. Toxicol.* **2013**, *26* (5), 662–673. https://doi.org/10.1021/tx300455k.
(48) Bottrill, M.; Green, M. Some Aspects of Quantum Dot Toxicity. *Chemical Communications* **2011**, *47* (25), 7039–7050. https://doi.org/10.1039/C1CC10692A.
(49) Levy, M.; Courtney, C. M.; Chowdhury, P. P.; Ding, Y.; Grey, E. L.; Goodman, S. M.; Chatterjee, A.; Nagpal, P. Assessing Different Reactive Oxygen Species as Potential Antibiotics: Selectivity of Intracellular Superoxide Generation Using Quantum Dots. *ACS Appl. Bio Mater.* **2018**, *1* (2), 529–537. https://doi.org/10.1021/acsabm.8b00292.
(50) Wang, Y.; Tang, M. Review of in Vitro Toxicological Research of Quantum Dot and Potentially Involved Mechanisms. *Science of The Total Environment* **2018**, *625*, 940–962. https://doi.org/10.1016/j.scitotenv.2017.12.334.
(51) Jaishankar, M.; Tseten, T.; Anbalagan, N.; Mathew, B. B.; Beeregowda, K. N. Toxicity, Mechanism and Health Effects of Some Heavy Metals. *Interdiscip Toxicol* **2014**, *7* (2), 60–72. https://doi.org/10.2478/intox-2014-0009.
(52) Lin, Y.-F.; Aarts, M. G. M. The Molecular Mechanism of Zinc and Cadmium Stress Response in Plants. *Cell. Mol. Life Sci.* **2012**, *69* (19), 3187–3206. https://doi.org/10.1007/s00018-012-1089-z.
(53) Rafati Rahimzadeh, M.; Rafati Rahimzadeh, M.; Kazemi, S.; Moghadamnia, A. Cadmium Toxicity and Treatment: An Update. *Caspian J Intern Med* **2017**, *8* (3), 135–145. https://doi.org/10.22088/cjim.8.3.135.
(54) Leber, A. P.; Miya, T. S. A Mechanism for Cadmium- and Zinc-Induced Tolerance to Cadmium Toxicity: Involvement of Metallothionein. *Toxicology and Applied Pharmacology* **1976**, *37* (3), 403–414. https://doi.org/10.1016/0041-008X(76)90202-7.
(55) Priester, J. H.; Stoimenov, P. K.; Mielke, R. E.; Webb, S. M.; Ehrhardt, C.; Zhang, J. P.; Stucky, G. D.; Holden, P. A. Effects of Soluble Cadmium Salts Versus CdSe Quantum Dots on the Growth of Planktonic Pseudomonas Aeruginosa. *Environ. Sci. Technol.* **2009**, *43* (7), 2589–2594. https://doi.org/10.1021/es802806n.
(56) Majumdar, S.; Pagano, L.; A. Wohlschlegel, J.; Villani, M.; Zappettini, A.; C. White, J.; A. Keller, A. Proteomic, Gene and Metabolite Characterization Reveal the Uptake and Toxicity Mechanisms of Cadmium Sulfide Quantum Dots in Soybean Plants.

Environmental Science: Nano **2019**, *6* (10), 3010–3026. https://doi.org/10.1039/C9EN00599D.

(57) King-Heiden, T. C.; Wiecinski, P. N.; Mangham, A. N.; Metz, K. M.; Nesbit, D.; Pedersen, J. A.; Hamers, R. J.; Heideman, W.; Peterson, R. E. Quantum Dot Nanotoxicity Assessment Using the Zebrafish Embryo. *Environmental Science & Technology* **2009**, *43* (5), 1605–1611. https://doi.org/10.1021/es801925c.

(58) Zarco-Fernández, S.; Coto-García, A. M.; Muñoz-Olivas, R.; Sanz-Landaluze, J.; Rainieri, S.; Cámara, C. Bioconcentration of Ionic Cadmium and Cadmium Selenide Quantum Dots in Zebrafish Larvae. *Chemosphere* **2016**, *148*, 328–335. https://doi.org/10.1016/j.chemosphere.2015.12.077.

(59) Bilal, M.; Oh, E.; Liu, R.; Breger, J. C.; Medintz, I. L.; Cohen, Y. Bayesian Network Resource for Meta-Analysis: Cellular Toxicity of Quantum Dots. *Small* **2019**, *15* (34), 1900510. https://doi.org/10.1002/smll.201900510.

(60) Oh, E.; Liu, R.; Nel, A.; Gemill, K. B.; Bilal, M.; Cohen, Y.; Medintz, I. L. Meta-Analysis of Cellular Toxicity for Cadmium-Containing Quantum Dots. *Nature Nanotechnology* **2016**, *11* (5), 479–486. https://doi.org/10.1038/nnano.2015.338.

(61) Brunetti, V.; Chibli, H.; Fiammengo, R.; Galeone, A.; Ada Malvindi, M.; Vecchio, G.; Cingolani, R.; L. Nadeau, J.; Paolo Pompa, P. InP/ZnS as a Safer Alternative to CdSe/ZnS Core/Shell Quantum Dots : In Vitro and in Vivo Toxicity Assessment. *Nanoscale* **2013**, *5* (1), 307–317. https://doi.org/10.1039/C2NR33024E.

(62) Allocca, M.; Mattera, L.; Bauduin, A.; Miedziak, B.; Moros, M.; De Trizio, L.; Tino, A.; Reiss, P.; Ambrosone, A.; Tortiglione, C. An Integrated Multilevel Analysis Profiling Biosafety and Toxicity Induced by Indium- and Cadmium-Based Quantum Dots in Vivo. *Environ. Sci. Technol.* **2019**, *53* (7), 3938–3947. https://doi.org/10.1021/acs.est.9b00373.

(63) Derfus, A. M.; Chan, W. C. W.; Bhatia, S. N. Probing the Cytotoxicity of Semiconductor Quantum Dots. *Nano Lett.* **2004**, *4* (1), 11–18. https://doi.org/10.1021/nl0347334.

(64) Pramanik, S.; Hill, S. K. E.; Zhi, B.; Hudson-Smith, N. V.; Wu, J. J.; White, J. N.; McIntire, E. A.; Kondeti, V. S. S. K.; Lee, A. L.; Bruggeman, P. J.; Kortshagen, U. R.; Haynes, C. L. Comparative Toxicity Assessment of Novel Si Quantum Dots and Their Traditional Cd-Based Counterparts Using Bacteria Models Shewanella Oneidensis and Bacillus Subtilis. *Environ. Sci.: Nano* **2018**, *5* (8), 1890–1901. https://doi.org/10.1039/C8EN00332G.

(65) Guo, G.; Liu, W.; Liang, J.; He, Z.; Xu, H.; Yang, X. Probing the Cytotoxicity of CdSe Quantum Dots with Surface Modification. *Materials Letters* **2007**, *61* (8), 1641–1644. https://doi.org/10.1016/j.matlet.2006.07.105.

(66) Mensch, A. C.; Buchman, J. T.; Haynes, C. L.; Pedersen, J. A.; Hamers, R. J. Quaternary Amine-Terminated Quantum Dots Induce Structural Changes to Supported Lipid Bilayers. *Langmuir* **2018**, *34* (41), 12369–12378. https://doi.org/10.1021/acs.langmuir.8b02047.

(67) Pang, C.; Gong, Y. Current Status and Future Prospects of Semiconductor Quantum Dots in Botany. *J. Agric. Food Chem.* **2019**, *67* (27), 7561–7568. https://doi.org/10.1021/acs.jafc.9b00730.

(68) Nagy, A.; Steinbrück, A.; Gao, J.; Doggett, N.; Hollingsworth, J. A.; Iyer, R. Comprehensive Analysis of the Effects of CdSe Quantum Dot Size, Surface Charge, and Functionalization on Primary Human Lung Cells. *ACS Nano* **2012**, *6* (6), 4748–4762. https://doi.org/10.1021/nn204886b.

(69) Park, J.; Lee, J.; Kwag, J.; Baek, Y.; Kim, B.; Yoon, C. J.; Bok, S.; Cho, S.-H.; Kim, K. H.; Ahn, G.-O.; Kim, S. Quantum Dots in an Amphiphilic Polyethyleneimine Derivative Platform for Cellular Labeling, Targeting, Gene Delivery, and Ratiometric Oxygen Sensing https://pubs.acs.org/doi/abs/10.1021/acsnano.5b02357 (accessed 2021 -11 -30). https://doi.org/10.1021/acsnano.5b02357.
(70) Gallagher, M. J.; Buchman, J. T.; Qiu, T. A.; Zhi, B.; Lyons, T. Y.; Landy, K. M.; Rosenzweig, Z.; Haynes, C. L.; Fairbrother, D. H. Release, Detection and Toxicity of Fragments Generated during Artificial Accelerated Weathering of CdSe/ZnS and CdSe Quantum Dot Polymer Composites. *Environ. Sci.: Nano* **2018**, *5* (7), 1694–1710. https://doi.org/10.1039/C8EN00249E.
(71) EUR-Lex - 02008R1272-20200101 - EN - EUR-Lex https://eur-lex.europa.eu/eli/reg/2008/1272/2020-01-01 (accessed 2021 -12 -01).
(72) *Globally Harmonized System of Classification and Labelling of Chemicals (GHS)*; Vereinte Nationen, Ed.; United Nations publication; United Nations: New York Geneva, 2021.
(73) NNCrystal US Corporation. SDS SHEET: Cadmium Selenide / Zinc Sulfide Nanocrystals in Water. 2017.
(74) Qdot™ 655 ITK™ Carboxyl Quantum Dots https://www.thermofisher.com/order/catalog/product/Q21321MP (accessed 2021 -12 -01).
(75) Supiandi, N. I.; Charron, G.; Tharaud, M.; Cordier, L.; Guigner, J.-M.; Benedetti, M. F.; Sivry, Y. Isotopically Labeled Nanoparticles at Relevant Concentrations: How Low Can We Go? The Case of CdSe/ZnS QDs in Surface Waters. *Environmental Science & Technology* **2019**, *53* (5), 2586–2594. https://doi.org/10.1021/acs.est.8b04096.
(76) ROHS - Exemptions from Article 4(1) Restrictions, Annexes III & IV - exemptions-art-4-restrictions-rohs - ECHA https://echa.europa.eu/exemptions-art-4-restrictions-rohs?p_p_id=eucleflegislationlist_WAR_euclefportlet&p_p_lifecycle=0&p_p_col_id=column-1&p_p_col_count=1 (accessed 2021 -05 -14).
(77) Markets, R. and. The Worldwide Quantum Dot Industry is Expected to Reach $8.6 Billion by 2026 https://www.prnewswire.com/news-releases/the-worldwide-quantum-dot-industry-is-expected-to-reach-8-6-billion-by-2026--301399021.html (accessed 2021 -12 -01).
(78) Brown, F. C.; Bi, Y.; Chopra, S. S.; Hristovski, K. D.; Westerhoff, P.; Theis, T. L. End-of-Life Heavy Metal Releases from Photovoltaic Panels and Quantum Dot Films: Hazardous Waste Concerns or Not? *ACS Sustainable Chem. Eng.* **2018**, *6* (7), 9369–9374. https://doi.org/10.1021/acssuschemeng.8b01705.
(79) Forti, V.; Balde, C. P.; Kuehr, R.; Bel, G. *The Global E-Waste Monitor 2020: Quantities, Flows and the Circular Economy Potential.*; United Nations University (UNU)/United Nations Institute for Training and Research (UNITAR) – co-hosted SCYCLE Programme, International Telecommunication Union (ITU) & International Solid Waste Association (ISWA),: Bonn/Geneva/Rotterdam, 2020; pp 1–15.
(80) Garner, K. L.; Suh, S.; Keller, A. A. Assessing the Risk of Engineered Nanomaterials in the Environment: Development and Application of the NanoFate Model. *Environ. Sci. Technol.* **2017**, *51* (10), 5541–5551. https://doi.org/10.1021/acs.est.6b05279.

(81) Tang, Z.; Cheng, T. Stability and Aggregation of Nanoscale Titanium Dioxide Particle (NTiO2): Effect of Cation Valence, Humic Acid, and Clay Colloids. *Chemosphere* **2018**, *192*, 51–58. https://doi.org/10.1016/j.chemosphere.2017.10.105.
(82) Praetorius, A.; Badetti, E.; Brunelli, A.; Clavier, A.; Alberto Gallego-Urrea, J.; Gondikas, A.; Hassellöv, M.; Hofmann, T.; Mackevica, A.; Marcomini, A.; Peijnenburg, W.; K. Quik, J. T.; Seijo, M.; Stoll, S.; Tepe, N.; Walch, H.; Kammer, F. von der. Strategies for Determining Heteroaggregation Attachment Efficiencies of Engineered Nanoparticles in Aquatic Environments. *Environmental Science: Nano* **2020**, *7* (2), 351–367. https://doi.org/10.1039/C9EN01016E.
(83) Ahamed, A.; Liang, L.; Lee, M. Y.; Bobacka, J.; Lisak, G. Too Small to Matter? Physicochemical Transformation and Toxicity of Engineered NTiO2, NSiO2, NZnO, Carbon Nanotubes, and NAg. *Journal of Hazardous Materials* **2021**, *404*, 124107. https://doi.org/10.1016/j.jhazmat.2020.124107.
(84) Lowry, G. V.; Gregory, K. B.; Apte, S. C.; Lead, J. R. Transformations of Nanomaterials in the Environment. *Environ. Sci. Technol.* **2012**, *46* (13), 6893–6899. https://doi.org/10.1021/es300839e.
(85) Piccinno, F.; Gottschalk, F.; Seeger, S.; Nowack, B. Industrial Production Quantities and Uses of Ten Engineered Nanomaterials in Europe and the World. *J Nanopart Res* **2012**, *14* (9), 1109. https://doi.org/10.1007/s11051-012-1109-9.
(86) Sun, J.; Guo, L.-H.; Zhang, H.; Zhao, L. UV Irradiation Induced Transformation of TiO2 Nanoparticles in Water: Aggregation and Photoreactivity. *Environ. Sci. Technol.* **2014**, *48* (20), 11962–11968. https://doi.org/10.1021/es502360c.
(87) Jassby, D.; Farner Budarz, J.; Wiesner, M. Impact of Aggregate Size and Structure on the Photocatalytic Properties of TiO2 and ZnO Nanoparticles. *Environ. Sci. Technol.* **2012**, *46* (13), 6934–6941. https://doi.org/10.1021/es202009h.
(88) Pellegrino, F.; Pellutiè, L.; Sordello, F.; Minero, C.; Ortel, E.; Hodoroaba, V.-D.; Maurino, V. Influence of Agglomeration and Aggregation on the Photocatalytic Activity of TiO2 Nanoparticles. *Applied Catalysis B: Environmental* **2017**, *216*, 80–87. https://doi.org/10.1016/j.apcatb.2017.05.046.
(89) Hotze, E. M.; Phenrat, T.; Lowry, G. V. Nanoparticle Aggregation: Challenges to Understanding Transport and Reactivity in the Environment. *Journal of Environmental Quality* **2010**, *39* (6), 1909–1924. https://doi.org/10.2134/jeq2009.0462.
(90) Lin, D.; Drew Story, S.; Walker, S. L.; Huang, Q.; Cai, P. Influence of Extracellular Polymeric Substances on the Aggregation Kinetics of TiO2 Nanoparticles. *Water Research* **2016**, *104*, 381–388. https://doi.org/10.1016/j.watres.2016.08.044.
(91) Romanello, M. B.; Fidalgo de Cortalezzi, M. M. An Experimental Study on the Aggregation of TiO2 Nanoparticles under Environmentally Relevant Conditions. *Water Research* **2013**, *47* (12), 3887–3898. https://doi.org/10.1016/j.watres.2012.11.061.
(92) Hsiung, C.-E.; Lien, H.-L.; Galliano, A. E.; Yeh, C.-S.; Shih, Y. Effects of Water Chemistry on the Destabilization and Sedimentation of Commercial TiO2 Nanoparticles: Role of Double-Layer Compression and Charge Neutralization. *Chemosphere* **2016**, *151*, 145–151. https://doi.org/10.1016/j.chemosphere.2016.02.046.
(93) Kosmulski, M. The Significance of the Difference in the Point of Zero Charge between Rutile and Anatase. *Advances in Colloid and Interface Science* **2002**, *99* (3), 255–264. https://doi.org/10.1016/S0001-8686(02)00080-5.

(94) Rodrigues, A.; Brito, A.; Janknecht, P.; Proença, M. F.; Nogueira, R. Quantification of Humic Acids in Surface Water: Effects of Divalent Cations, PH, and Filtration. *J. Environ. Monit.* **2009**, *11* (2), 377–382. https://doi.org/10.1039/B811942B.
(95) Xia, B.; Sui, Q.; Sun, X.; Han, Q.; Chen, B.; Zhu, L.; Qu, K. Ocean Acidification Increases the Toxic Effects of TiO2 Nanoparticles on the Marine Microalga Chlorella Vulgaris. *Journal of Hazardous Materials* **2018**, *346*, 1–9. https://doi.org/10.1016/j.jhazmat.2017.12.017.
(96) Lin, D.; Ji, J.; Long, Z.; Yang, K.; Wu, F. The Influence of Dissolved and Surface-Bound Humic Acid on the Toxicity of TiO2 Nanoparticles to Chlorella Sp. *Water Research* **2012**, *46* (14), 4477–4487. https://doi.org/10.1016/j.watres.2012.05.035.
(97) Coral, J. A.; Kitchens, C. L.; Brumaghim, J. L.; Klaine, S. J. Correlating Quantitative Measurements of Radical Production by Photocatalytic TiO2 with Daphnia Magna Toxicity. *Environmental Toxicology and Chemistry* **2021**, *40* (5), 1322–1334. https://doi.org/10.1002/etc.4982.
(98) Tong, T.; Binh, C. T. T.; Kelly, J. J.; Gaillard, J.-F.; Gray, K. A. Cytotoxicity of Commercial Nano-TiO2 to Escherichia Coli Assessed by High-Throughput Screening: Effects of Environmental Factors. *Water Research* **2013**, *47* (7), 2352–2362. https://doi.org/10.1016/j.watres.2013.02.008.
(99) Ettrup, K.; Kounina, A.; Hansen, S. F.; Meesters, J. A. J.; Vea, E. B.; Laurent, A. Development of Comparative Toxicity Potentials of TiO2 Nanoparticles for Use in Life Cycle Assessment. *Environ. Sci. Technol.* **2017**, *51* (7), 4027–4037. https://doi.org/10.1021/acs.est.6b05049.
(100) Liu, C.; Leng, W.; Vikesland, P. J. Controlled Evaluation of the Impacts of Surface Coatings on Silver Nanoparticle Dissolution Rates. *Environ. Sci. Technol.* **2018**, *52* (5), 2726–2734. https://doi.org/10.1021/acs.est.7b05622.
(101) Gorham, J. M.; Rohlfing, A. B.; Lippa, K. A.; MacCuspie, R. I.; Hemmati, A.; David Holbrook, R. Storage Wars: How Citrate-Capped Silver Nanoparticle Suspensions Are Affected by Not-so-Trivial Decisions. *J Nanopart Res* **2014**, *16* (4), 2339. https://doi.org/10.1007/s11051-014-2339-9.
(102) Gunawan, C.; Teoh, W. Y.; Marquis, C. P.; Lifia, J.; Amal, R. Reversible Antimicrobial Photoswitching in Nanosilver. *Small* **2009**, *5* (3), 341–344. https://doi.org/10.1002/smll.200801202.
(103) Engelke, M.; Köser, J.; Hackmann, S.; Zhang, H.; Mädler, L.; Filser, J. A Miniaturized Solid Contact Test with Arthrobacter Globiformis for the Assessment of the Environmental Impact of Silver Nanoparticles. *Environmental Toxicology and Chemistry* **2014**, *33* (5), 1142–1147. https://doi.org/10.1002/etc.2542.
(104) Köser, J.; Engelke, M.; Hoppe, M.; Nogowski, A.; Filser, J.; Thöming, J. Predictability of Silver Nanoparticle Speciation and Toxicity in Ecotoxicological Media. *Environmental Science: Nano* **2017**, *4* (7), 1470–1483. https://doi.org/10.1039/C7EN00026J.
(105) Schultz, C. L.; Adams, J.; Jurkschat, K.; Lofts, S.; Spurgeon, D. J. Chemical Transformation and Surface Functionalisation Affect the Potential to Group Nanoparticles for Risk Assessment. *Environ. Sci.: Nano* **2020**, *7* (10), 3100–3107. https://doi.org/10.1039/D0EN00578A.
(106) Zhong, L.; Chen, S.; Tang, Z.; Guo, X.; Hu, X.; Zheng, W.; Lian, H. Transport of Environmental Natural Organic Matter Coated Silver Nanoparticle across Cell Membrane

Based on Membrane Etching Treatment and Inhibitors. *Sci Rep* **2021**, *11* (1), 507. https://doi.org/10.1038/s41598-020-79901-y.
(107) Albalghiti, E.; M. Stabryla, L.; M. Gilbertson, L.; B. Zimmerman, J. Towards Resolution of Antibacterial Mechanisms in Metal and Metal Oxide Nanomaterials: A Meta-Analysis of the Influence of Study Design on Mechanistic Conclusions. *Environmental Science: Nano* **2021**, *8* (1), 37–66. https://doi.org/10.1039/D0EN00949K.
(108) Joo, S. H.; Zhao, D. Environmental Dynamics of Metal Oxide Nanoparticles in Heterogeneous Systems: A Review. *Journal of Hazardous Materials* **2017**, *322*, 29–47. https://doi.org/10.1016/j.jhazmat.2016.02.068.
(109) Liu, S.; Killen, E.; Lim, M.; Gunawan, C.; Amal, R. The Effect of Common Bacterial Growth Media on Zinc Oxide Thin Films: Identification of Reaction Products and Implications for the Toxicology of ZnO. *RSC Adv.* **2013**, *4* (9), 4363–4370. https://doi.org/10.1039/C3RA46177G.
(110) M. Briffa, S.; Nasser, F.; Valsami-Jones, E.; Lynch, I. Uptake and Impacts of Polyvinylpyrrolidone (PVP) Capped Metal Oxide Nanoparticles on Daphnia Magna : Role of Core Composition and Acquired Corona. *Environmental Science: Nano* **2018**, *5* (7), 1745–1756. https://doi.org/10.1039/C8EN00063H.
(111) Ouyang, K.; Yu, X.-Y.; Zhu, Y.; Gao, C.; Huang, Q.; Cai, P. Effects of Humic Acid on the Interactions between Zinc Oxide Nanoparticles and Bacterial Biofilms. *Environmental Pollution* **2017**, *231*, 1104–1111. https://doi.org/10.1016/j.envpol.2017.07.003.
(112) Li, L.; Ubaid Khan, A.; Zhang, X.; Qian, X.; Wang, Y. Emerging Investigator Series: Chemical Transformation of Silver and Zinc Oxide Nanoparticles in Simulated Human Tear Fluids: Influence of Biocoronae. *Environmental Science: Nano* **2021**, *8* (9), 2430–2440. https://doi.org/10.1039/D1EN00566A.
(113) McClements, D. J.; Xiao, H. Is Nano Safe in Foods? Establishing the Factors Impacting the Gastrointestinal Fate and Toxicity of Organic and Inorganic Food-Grade Nanoparticles. *npj Sci Food* **2017**, *1* (1), 6. https://doi.org/10.1038/s41538-017-0005-1.
(114) Huang, X.; Tang, M. Review of Gut Nanotoxicology in Mammals: Exposure, Transformation, Distribution and Toxicity. *Science of The Total Environment* **2021**, *773*, 145078. https://doi.org/10.1016/j.scitotenv.2021.145078.
(115) Sohal, I. S.; Cho, Y. K.; O'Fallon, K. S.; Gaines, P.; Demokritou, P.; Bello, D. Dissolution Behavior and Biodurability of Ingested Engineered Nanomaterials in the Gastrointestinal Environment. *ACS Nano* **2018**, *12* (8), 8115–8128. https://doi.org/10.1021/acsnano.8b02978.
(116) He, X.; Zhang, H.; Shi, H.; Liu, W.; Sahle-Demessie, E. Fates of Au, Ag, ZnO, and CeO2 Nanoparticles in Simulated Gastric Fluid Studied Using Single-Particle-Inductively Coupled Plasma-Mass Spectrometry. *J. Am. Soc. Mass Spectrom.* **2020**, *31* (10), 2180–2190. https://doi.org/10.1021/jasms.0c00278.
(117) Voss, L.; Saloga, P. E. J.; Stock, V.; Böhmert, L.; Braeuning, A.; Thünemann, A. F.; Lampen, A.; Sieg, H. Environmental Impact of ZnO Nanoparticles Evaluated by in Vitro Simulated Digestion. *ACS Appl. Nano Mater.* **2020**, *3* (1), 724–733. https://doi.org/10.1021/acsanm.9b02236.
(118) Committee, E. S.; More, S.; Bampidis, V.; Benford, D.; Bragard, C.; Halldorsson, T.; Hernández-Jerez, A.; Hougaard Bennekou, S.; Koutsoumanis, K.; Lambré, C.; Machera, K.; Naegeli, H.; Nielsen, S.; Schlatter, J.; Schrenk, D.; Silano (deceased), V.; Turck, D.;

Younes, M.; Castenmiller, J.; Chaudhry, Q.; Cubadda, F.; Franz, R.; Gott, D.; Mast, J.; Mortensen, A.; Oomen, A. G.; Weigel, S.; Barthelemy, E.; Rincon, A.; Tarazona, J.; Schoonjans, R. Guidance on Risk Assessment of Nanomaterials to Be Applied in the Food and Feed Chain: Human and Animal Health. *EFSA Journal* **2021**, *19* (8), e06768. https://doi.org/10.2903/j.efsa.2021.6768.

(119) S. Giroux, M.; Zahra, Z.; A. Salawu, O.; M. Burgess, R.; T. Ho, K.; S. Adeleye, A. Assessing the Environmental Effects Related to Quantum Dot Structure, Function, Synthesis and Exposure. *Environmental Science: Nano* **2022**. https://doi.org/10.1039/D1EN00712B.

(120) Pillai, K. V.; Gray, P. J.; Tien, C.-C.; Bleher, R.; Sung, L.-P.; Duncan, T. V. Environmental Release of Core–Shell Semiconductor Nanocrystals from Free-Standing Polymer Nanocomposite Films. *Environ. Sci.: Nano* **2016**, *3* (3), 657–669. https://doi.org/10.1039/C6EN00064A.

(121) Shang, L.; Nienhaus, K.; Nienhaus, G. U. Engineered Nanoparticles Interacting with Cells: Size Matters. *Journal of Nanobiotechnology* **2014**, *12* (1), 5. https://doi.org/10.1186/1477-3155-12-5.

(122) Paydary, P.; Larese-Casanova, P. Water Chemistry Influences on Long-Term Dissolution Kinetics of CdSe/ZnS Quantum Dots. *Journal of Environmental Sciences* **2020**, *90*, 216–233. https://doi.org/10.1016/j.jes.2019.11.011.

(123) Xiao, Y.; Ho, K. T.; Burgess, R. M.; Cashman, M. Aggregation, Sedimentation, Dissolution, and Bioavailability of Quantum Dots in Estuarine Systems. *Environ. Sci. Technol.* **2017**, *51* (3), 1357–1363. https://doi.org/10.1021/acs.est.6b04475.

(124) Mahendra, S.; Zhu, H.; Colvin, V. L.; Alvarez, P. J. Quantum Dot Weathering Results in Microbial Toxicity. *Environ. Sci. Technol.* **2008**, *42* (24), 9424–9430. https://doi.org/10.1021/es8023385.

(125) Wiecinski, P. N.; Metz, K. M.; King Heiden, T. C.; Louis, K. M.; Mangham, A. N.; Hamers, R. J.; Heideman, W.; Peterson, R. E.; Pedersen, J. A. Toxicity of Oxidatively Degraded Quantum Dots to Developing Zebrafish (Danio Rerio). *Environmental Science & Technology* **2013**, *47* (16), 9132–9139. https://doi.org/10.1021/es304987r.

(126) Gray, P. J.; Hornick, J. E.; Sharma, A.; Weiner, R. G.; Koontz, J. L.; Duncan, T. V. Influence of Different Acids on the Transport of CdSe Quantum Dots from Polymer Nanocomposites to Food Simulants. *Environmental Science & Technology* **2018**, *52* (16), 9468–9477. https://doi.org/10.1021/acs.est.8b02585.

(127) Zhang, S.; Jiang, Y.; Chen, C.-S.; Spurgin, J.; Schwehr, K. A.; Quigg, A.; Chin, W.-C.; Santschi, P. H. Aggregation, Dissolution, and Stability of Quantum Dots in Marine Environments: Importance of Extracellular Polymeric Substances. *Environ. Sci. Technol.* **2012**, *46* (16), 8764–8772. https://doi.org/10.1021/es301000m.

(128) Modlitbová, P.; Novotný, K.; Pořízka, P.; Klus, J.; Lubal, P.; Zlámalová-Gargošová, H.; Kaiser, J. Comparative Investigation of Toxicity and Bioaccumulation of Cd-Based Quantum Dots and Cd Salt in Freshwater Plant Lemna Minor L. *Ecotoxicology and Environmental Safety* **2018**, *147*, 334–341. https://doi.org/10.1016/j.ecoenv.2017.08.053.

(129) Gupta, G. S.; Kumar, A.; Senapati, V. A.; Pandey, A. K.; Shanker, R.; Dhawan, A. Laboratory Scale Microbial Food Chain To Study Bioaccumulation, Biomagnification, and Ecotoxicity of Cadmium Telluride Quantum Dots. *Environ. Sci. Technol.* **2017**, *51* (3), 1695–1706. https://doi.org/10.1021/acs.est.6b03950.

(130) Tickner, J.; Jacobs, M.; Malloy, T.; Buck, T.; Stone, A.; Blake, A.; Edwards, S. Advancing Alternatives Assessment for Safer Chemical Substitution: A Research and Practice Agenda. *Integrated Environmental Assessment and Management* **2019**, *15* (6), 855–866. https://doi.org/10.1002/ieam.4094.
(131) Maertens, A.; Golden, E.; Hartung, T. Avoiding Regrettable Substitutions: Green Toxicology for Sustainable Chemistry. *ACS Sustainable Chem. Eng.* **2021**. https://doi.org/10.1021/acssuschemeng.0c09435.
(132) Schultz, T. W.; Amcoff, P.; Berggren, E.; Gautier, F.; Klaric, M.; Knight, D. J.; Mahony, C.; Schwarz, M.; White, A.; Cronin, M. T. D. A Strategy for Structuring and Reporting a Read-across Prediction of Toxicity. *Regulatory Toxicology and Pharmacology* **2015**, *72* (3), 586–601. https://doi.org/10.1016/j.yrtph.2015.05.016.
(133) Gajewicz, A. How to Judge Whether QSAR/Read-across Predictions Can Be Trusted: A Novel Approach for Establishing a Model's Applicability Domain. *Environmental Science: Nano* **2018**, *5* (2), 408–421. https://doi.org/10.1039/C7EN00774D.
(134) European Chemicals Agency. *How to Use and Report (Q)SARs: Version 3.0. Practical Guide 5. Practical Guide 5.*; ECHA: Helsinki, 2016.
(135) Mikolajczyk, A.; Gajewicz, A.; Mulkiewicz, E.; Rasulev, B.; Marchelek, M.; Diak, M.; Hirano, S.; Zaleska-Medynska, A.; Puzyn, T. Nano-QSAR Modeling for Ecosafe Design of Heterogeneous TiO 2 -Based Nano-Photocatalysts. *Environmental Science: Nano* **2018**, *5* (5), 1150–1160. https://doi.org/10.1039/C8EN00085A.
(136) Puzyn, T.; Rasulev, B.; Gajewicz, A.; Hu, X.; Dasari, T. P.; Michalkova, A.; Hwang, H.-M.; Toropov, A.; Leszczynska, D.; Leszczynski, J. Using Nano-QSAR to Predict the Cytotoxicity of Metal Oxide Nanoparticles. *Nature Nanotech* **2011**, *6* (3), 175–178. https://doi.org/10.1038/nnano.2011.10.
(137) Gajewicz, A. What If the Number of Nanotoxicity Data Is Too Small for Developing Predictive Nano-QSAR Models? An Alternative Read-across Based Approach for Filling Data Gaps. *Nanoscale* **2017**, *9* (24), 8435–8448. https://doi.org/10.1039/C7NR02211E.
(138) Xiarchos, I.; Morozinis, A. K.; Kavouras, P.; Charitidis, C. A. Nanocharacterization, Materials Modeling, and Research Integrity as Enablers of Sound Risk Assessment: Designing Responsible Nanotechnology. *Small* **2020**, *16* (36), 2001590. https://doi.org/10.1002/smll.202001590.
(139) Sleight, T. W.; Sexton, C. N.; Mpourmpakis, G.; Gilbertson, L. M.; Ng, C. A. A Classification Model to Identify Direct-Acting Mutagenic Polycyclic Aromatic Hydrocarbon Transformation Products. *Chem. Res. Toxicol.* **2021**, *34* (11), 2273–2286. https://doi.org/10.1021/acs.chemrestox.1c00187.
(140) Whittaker, M. H. Risk Assessment and Alternatives Assessment: Comparing Two Methodologies. *Risk Analysis* **2015**, *35* (12), 2129–2136. https://doi.org/10.1111/risa.12549.
(141) Guinée, J. B.; Heijungs, R.; Vijver, M. G.; Peijnenburg, W. J. G. M. Setting the Stage for Debating the Roles of Risk Assessment and Life-Cycle Assessment of Engineered Nanomaterials. *Nature Nanotech* **2017**, *12* (8), 727–733. https://doi.org/10.1038/nnano.2017.135.
(142) 14:00-17:00. ISO 14044:2006 https://www.iso.org/cms/render/live/en/sites/isoorg/contents/data/standard/03/84/38498.html (accessed 2021 -09 -03).

(143) Olsen, S. I.; Christensen, F. M.; Hauschild, M.; Pedersen, F.; Larsen, H. F.; Tørsløv, J. Life Cycle Impact Assessment and Risk Assessment of Chemicals — a Methodological Comparison. *Environmental Impact Assessment Review* **2001**, *21* (4), 385–404. https://doi.org/10.1016/S0195-9255(01)00075-0.
(144) Sala, S.; Amadei, A. M.; Beylot, A.; Ardente, F. The Evolution of Life Cycle Assessment in European Policies over Three Decades. *Int J Life Cycle Assess* **2021**. https://doi.org/10.1007/s11367-021-01893-2.
(145) Council, N. R.; Studies, D. on E. and L.; Toxicology, B. on E. S. and; Technology, B. on C. S. and; Decisions, C. on the D. and E. of S. C. S. A. F. to I. G. and I. *A Framework to Guide Selection of Chemical Alternatives*; National Academies Press, 2014.
(146) Geiser, K.; Tickner, J.; Edwards, S.; Rossi, M. The Architecture of Chemical Alternatives Assessment. *Risk Analysis* **2015**, *35* (12), 2152–2161. https://doi.org/10.1111/risa.12507.
(147) Hjorth, R.; Hansen, S. F.; Jacobs, M.; Tickner, J.; Ellenbecker, M.; Baun, A. The Applicability of Chemical Alternatives Assessment for Engineered Nanomaterials. *Integrated Environmental Assessment and Management* **2017**, *13* (1), 177–187. https://doi.org/10.1002/ieam.1762.
(148) Kikuchi, E.; Kikuchi, Y.; Hirao, M. Analysis of Risk Trade-off Relationships between Organic Solvents and Aqueous Agents: Case Study of Metal Cleaning Processes. *Journal of Cleaner Production* **2011**, *19* (5), 414–423. https://doi.org/10.1016/j.jclepro.2010.05.021.
(149) Anastas, P.; Eghbali, N. Green Chemistry: Principles and Practice. *Chemical Society Reviews* **2010**, *39* (1), 301–312. https://doi.org/10.1039/B918763B.
(150) Sheldon, R. A. Metrics of Green Chemistry and Sustainability: Past, Present, and Future. *ACS Sustainable Chem. Eng.* **2018**, *6* (1), 32–48. https://doi.org/10.1021/acssuschemeng.7b03505.
(151) *Handbook of Green Chemistry. Volume 11: Green Metrics / Edited by David J. Constable and Concepción Jiménez-González*; Constable, D., Jiménez-González, C., Eds.; Wiley-VCH Verlag GmbH & KGaA: Weinheim, 2018.
(152) Krausmann, F.; Lauk, C.; Haas, W.; Wiedenhofer, D. From Resource Extraction to Outflows of Wastes and Emissions: The Socioeconomic Metabolism of the Global Economy, 1900–2015. *Global Environmental Change* **2018**, *52*, 131–140. https://doi.org/10.1016/j.gloenvcha.2018.07.003.
(153) Hallett, S. *The Efficiency Trap: Finding a Better Way to Achieve a Sustainable Energy Future*; Prometheus Books, 2013.
(154) Subramaniam, B.; Licence, P.; Moores, A.; Allen, D. T. Shaping Effective Practices for Incorporating Sustainability Assessment in Manuscripts Submitted to ACS Sustainable Chemistry & Engineering: An Initiative by the Editors. *ACS Sustainable Chem. Eng.* **2021**, *9* (11), 3977–3978. https://doi.org/10.1021/acssuschemeng.1c01511.
(155) Kralisch, D.; Ott, D.; Gericke, D. Rules and Benefits of Life Cycle Assessment in Green Chemical Process and Synthesis Design: A Tutorial Review. *Green Chem.* **2014**, *17* (1), 123–145. https://doi.org/10.1039/C4GC01153H.
(156) G. Davidson, M.; Elgie, S.; Parsons, S.; J. Young, T. Production of HMF, FDCA and Their Derived Products: A Review of Life Cycle Assessment (LCA) and Techno-Economic Analysis (TEA) Studies. *Green Chemistry* **2021**, *23* (9), 3154–3171. https://doi.org/10.1039/D1GC00721A.

(157) Jessop, P. Editorial: Evidence of a Significant Advance in Green Chemistry. *Green Chemistry* **2020**, *22* (1), 13–15. https://doi.org/10.1039/C9GC90119A.
(158) Advancing the Use of Sustainability Metrics in ACS Sustainable Chemistry & Engineering. *ACS Sustainable Chem. Eng.* **2018**, *6* (1), 1–1. https://doi.org/10.1021/acssuschemeng.7b04700.
(159) M. Gilbertson, L.; B. Zimmerman, J.; L. Plata, D.; E. Hutchison, J.; T. Anastas, P. Designing Nanomaterials to Maximize Performance and Minimize Undesirable Implications Guided by the Principles of Green Chemistry. *Chemical Society Reviews* **2015**, *44* (16), 5758–5777. https://doi.org/10.1039/C4CS00445K.
(160) H. r, C.; Schiffman, J. D.; Balakrishna, R. G. Quantum Dots as Fluorescent Probes: Synthesis, Surface Chemistry, Energy Transfer Mechanisms, and Applications. *Sensors and Actuators B: Chemical* **2018**, *258*, 1191–1214. https://doi.org/10.1016/j.snb.2017.11.189.

3 Cadmium-Containing Quantum Dots Used in Electronic Displays: Implications for Toxicity and Environmental Transformations

Bechu, A.; Liao, J.; Huang, C.; Ahn, C.; McKeague, M.; Ghoshal, S.; Moores, A. Cadmium-Containing Quantum Dots Used in Electronic Displays: Implications for Toxicity and Environmental Transformations. *ACS Appl. Nano Mater.* **2021**, *4* (8), 8417–8428. https://doi.org/10.1021/acsanm.1c01659.

Also available on ChemRxiv: https://doi.org/10.26434/chemrxiv-2021-n3c99

3.1 Connecting text

The fields of QD development, ENP transformation, ENP toxicity, and assessments are each faced with difficult research questions. It is also challenging to connect these fields under the goal of implementing safer and more sustainable substances. The next chapter explores of these questions by developing a QD model that reflects the QDs that are currently in displays. As well, we systematically test certain environmental conditions and probe whether toxicity is due to the transformed QD or its released ions.

3.2 Abstract:

Cadmium-containing quantum dot nanoparticles (QDs) are integrated into electronic displays because of their ability to efficiently convert colors. There are conflicting accounts as to whether these particles present a hazard to the environment, as they have been studied either as (1) embedded QDs in display screen films or (2) as model QDs with small, hydrophilic ligands. Both approaches have limitations that we addressed by synthesizing QDs featuring the core-shell structure and the thick polymer coating present in commercial devices, to probe the dissolution of QDs in response to two environmental factors (pH, dissolved oxygen) over 1 day and 6 months.

Results show that QDs were chemically stable at circumneutral pH (0% Cd dissolution after 6 months), but low pH initiated rapid dissolution under both aerobic and anaerobic conditions (up to 100% Cd dissolution after 6 months). In addition to the presence of a capping polymer, the QDs shell structure led to more chemically stable nanoparticles compared to non-shelled QDs, as the presence of ZnS shells decreased Cd dissolution by 75%. The dense aggregation of QDs into structures of ~100 nm in diameter over time was observed as well, which could lead to decreased bioavailability. To test this, we used liver cells to compare the toxicity of pristine QDs to those subjected to acid dissolution. Our results reveal that low-pH exposed QDs separated from dissolved ions are less toxic than pristine QDs (IC_{50} of 290 and 150 mg/L, respectively) and suggest a key role of dissolved ions and capping polymers for QD toxicity. These findings highlight the use of a commercially-relevant nanoparticle structure to demonstrate fate and toxicity.

3.3 Introduction:

Quantum dots (QDs) are versatile nanoparticles whose excitons are confined in three dimensions, creating a distinct bandgap and narrow emission.[1,2] With innovations in synthesis and measurement techniques, the quantum yield of certain QDs approaches unity.[3] Such nanomaterials are used in electronic displays as they can enhance color, durability, and efficiency for both green and red pixels.[4] High-performance electronic displays containing QDs have been available since 2013, with sales increasing every year.[5]

Commercial QDs are complex nanostructures containing several essential parts, important for both their function and their formulation, namely a core, a shell, a ligand, and possibly a capping polymer. The core is responsible for the desired optical properties and commonly made of a semiconductor. The wavelength of emitted light is dependent on the easily tunable QD core size.[6] Cadmium selenide (CdSe) initially emerged as a preferable core material because of its emission in visible wavelengths and its simple synthesis that has cheap and air stable precursors.[7,8] Although many materials are cited in patents as good for QD use in electronics, CdSe is highlighted because of "the relative maturity of the synthesis".[9] These cores are then covered by an inorganic shell to shield them from oxidation and further increase quantum yield.[10] CdSe QD cores can be protected by layers, i.e., shells of CdS, ZnSe, ZnS, silica, or a combination of these materials which inhibit

non-radiative recombination by providing distance between the core and possible surface defects.[10,11] Next, these layers or shells are often stabilized by an organic ligand and/or a capping polymer. The organic ligand plays a role in the core and shell synthesis in order to control the size as well as optical properties and the capping polymer helps with QDs stability and formulation in a desired media (water, plastics precursors, organic solvents, etc.).[12] In the case of commercial QDs for display applications, both a small molecule organic ligand and a capping polymer are used.[9] The tunability and complexity of possible QD structures is a reason for their successful integration into electronics, but their varied and complex structures and proprietary synthesis protocols makes them difficult (if not impossible) to completely reproduce commercially-relevant QDs for academic purposes.

With only 20% of electronic waste properly recycled,[13] QDs are likely to be released into the environment through either (1) leakages and discharges from engineered landfills or unregulated waste dumps to soil and groundwater, or (2) unregulated recycling in unsafe conditions. A significant number of displays manufactured have QD cores containing Cd, which is a known carcinogenic and bio-accumulative heavy metal, with recommended drinking water limits of 0.003 mg/L.[14] Therefore, the potential release of Cd through aged quantum dots is a concern. Ageing QDs – i.e. exposing them in a prolonged fashion to the environment or to specific environmental conditions (e.g. a range of pH, dissolved oxygen, natural organic matter) in model systems – [15] can lead to nanoparticle dissolution, aggregation, among other transformations. The ageing of QDs has been studied by using both aged (1) model QD structures dispersed in solution and (2) proprietary complex QD-containing structures embedded in commercial products.

Model QDs (1) are commonly CdSe cores with ZnS shells which are designed to be initially colloidally stable, are easily tracked (through fluorescence or isotopes present) and usually contain either small molecules as ligands, or innocuous polymers used for toxicity tests.[16–18] The study of (1) model QDs suggests a high potential for rapid dissolution in response to low or high pH. For example, Paydary et al. noted that Cd and Zn dissolution at pH 7 reached equilibrium after either 8 days (Zn) or 80 days (Cd) from CdSe/ZnS-mercaptopropionic acid QDs.[16] Lowering the pH to 4 increased those rates.16 Mahendra et al. demonstrated a 100× increase in soluble Cd and Se from CdSe/ZnS (with unknown polymer ligand) QDs at pH of 2 and 12 compared to pH 7 after only 30 min.[19] These studies do not decouple the roles of low pH and

oxygen, both of which could be key to initiating the dissolution of sulfides and selenides. Aggregation is another alternative fate of QDs under environmentally representative conditions. The stable hydrodynamic radius of polymer-coated CdSe/ZnS QDs in seawater has been noted[20] and increased concentration of solutions spurred aggregation (at 20 ppm CdSe/ZnS-mercaptopropionic acid QDs).[16] Different ligands, thioglycolic acid and poly(maleic anhydride-alt-1-octadecene), initiated different amounts of aggregation and dissolution in soil column experiments.[21] However, the model QDs used in such fate studies are often coated with ligands selected for their ability to disperse QDs in water, for use as innocuous biosensors or in other medical applications, or as a benign coating for toxicity tests. Their structure greatly differ from the ones of QDs in real devices, which are designed for formulation and long-lasting fluorescence when incorporated into a product, usually through encapsulation into a polymer.9 These proprietary QDs are therefore designed with different shell structures, ligands and capping polymers than previously studied model QDs.

In contrast, other groups have decided to study QDs already embedded in products (2) and in these cases have found that the particles are relatively chemically stable. For example, a study on QD-containing polymer prototype for LEDs (QD Vision) indicated that, after 30 days, 7% Cd leaching under near-neutral conditions (pH 5 or 1mM H_2O_2).[22] A QD-containing Kindle (Amazon) film leached only 10% of its Cd after the waste extraction test (WET) using citric acid at pH 5.[23] However, these studies provide limited information on how QDs are transformed because they assess an entire product, in which QDs cannot be separated from the encapsulating solid matrix and do not allow for extraction of QD materials necessary for in-depth characterization and fate analysis. Additionally, limited effort was devoted to low pH exposures, despite their environmental and biological relevance. Furthermore, the impacts of certain environmental conditions on QD transformations could be suppressed. For example, the dissolution of QDs could be altered by the absorption of ions on another component of the product (e.g., the encapsulating solid matrix).

In addition to the dissolution of QDs in the environment, it is necessary to determine the toxicity trends associated with commercially-relevant QDs and how the toxicity changes with environmental ageing. When comparing different pristine Cd-containing QDs, it has been reported that toxicity is mediated by surface components (i.e. ligand and metal sulfide shell),[24] but such surface components change after particle ageing. Several studies have demonstrated that certain

model QDs become more toxic as they age.[18,19] As an example, CdSe/ZnS QDs capped with polyethylene glycol transformed into Cd ion and Se nanoparticles after exposure to oxidative conditions, resulting in increased toxicity to zebrafish embryos (LC_{50} of 50 μM Cd equivalents prior to oxidative conditions versus 10 μM Cd equivalents after exposure).[18] The exposure of QDs to non-physiological pH increased toxicity as well, but the toxicity of constituent ions dosed together could not explain the aged QD toxicity increase to bacteria.[16] These studies lay an important and extensive groundwork for the toxicity study of aged QDs, but certain aspects of these QDs studies hinder the prediction of toxicity of QDs in electronics. In short, aged QD toxicity studies suffer from a similar constraint as QDs transformed by the environment: the starting QD does not model the complexities of QDs used in products. In addition, they do not address the possible toxicity of aged QDs alone, separate from their ionic constituents

As toxicity is closely linked to both QD surface coating and QD ageing, the gap between the environmentally-mediated transformation of model particles and QD-containing products must be addressed. There is a disconnect between the high dissolution of uncoated or simplified composition model QDs compared to the low release of ions from QD-containing products. This contradiction merits the use of better QD models that are representative of the more chemically stable QDs in products, both for ageing and subsequent toxicity studies. The assessment of the combination of environmental aging and subsequent toxicity of a QD model that is relevant to the industry is an innovative approach to the assessment of possible end-of-life nanoparticle hazard.

To bridge the gap, we synthesized a representative commercial QD, and assessed it dissolution, aggregation, and toxicity in aqueous media. While it is unknown to what extent commercially relevant QDs released from disposed products in landfills or during recycling would compare to the pristine forms of those QDs added into products, the assessment of the environmental transformations and toxicity of the pristine QDs could serve as a 'worst case' scenario. We synthesized and used the 'most preferable' capping polymer[9] mentioned in the patent outlining QDs for display use. To further mimic conditions in display screens, we used an excess of this capping polymer compared to QDs. We examined the effect of exposing QDs to two environmental factors: pH and dissolved oxygen with short (1 day) and long term (6 months) ageing. The impact of pH on the chemical stability of the different shells and the core that constitute the commercially relevant QDs were assessed. We then compared the toxicity of a

commercial model of pristine QDs and aged QDs in a human cell line. Furthermore, we examined QD cytotoxicity on a common model for the liver, HepG2 cells, to specifically address the impact of commercially-relevant ligands on fate and toxicity. This study brings attention to the importance of the role of an abundant, relevant ligand designed for use in displays. This approach considers a chemist's interest in nanoparticle design, an environmental engineers' assessment of important natural ageing triggers, and a toxicologist's rigor in assessing the different parts of this complex nanoparticle. Given that these QDs that could be released into the environment, the knowledge of relevant transformation reactions and toxicity trends can ultimately inform the design and assessment of safer QDs in the future.

3.4 Results and Discussion:

3.4.1 CdSe/ZnS-PEI&E3P synthesis:

Following our goal to access QDs that are relevant to QD in existing devices, we designed them according to the Quantum Dot Emission Film (QDEF) patent.[9] This patent is assigned to Nanosys Inc, a major manufacturer in the QD display industry. Both cadmium and zinc have been found in QD-containing display films in previous studies and we confirmed the presence of both of these elements in a QD display film (see Figure S3-6).[23] While the patent was not explicit on the QD core/shell synthesis, it did mention that CdSe was an exemplary material for QDs, preferably with the presence of both CdS and ZnS shells.[9] We hypothesize that these QDs possess a cadmium selenide (CdSe) core for narrow emission, an alloyed cadmium sulfide zinc sulfide (CdS/ZnS) shell for enhancement of quantum yield and stability.[25] The QDs are capped by a polymer, i.e. polyethyleneimine reacted with an epoxide (PEI&E3P), also mentioned by the patent.[9] We confirmed the presence of key functional groups of PEI&E3P in QD-containing films extracted from a commercial display using ^{13}C solid state carbon nuclear magnetic resonance (^{13}C-ssNMR, see Figure S3-7). With this information, we designed a synthesis for CdSe//ZnS-PEI&E3P QDs (see Scheme 3-1).

Scheme 3-1: Outline of CdSe/ZnS-PEI&E3P synthesis. The process begins with the hot-injection synthesis of CdSe QDs, followed by the addition of alloyed CdS/ZnS shells using the SILAR method (alloyed shells from 3 subsequent precursor additions without purification;

CdS/$Cd_{0.5}Zn_{0.5}S$/ZnS). On the bottom left is the reaction between polyethyleneimine (PEI) and 1,2 epoxy-3-phenoxypropane (E3P) to yield the product of PEI&E3P. CdSe/ZnS QDs were then integrated into the PEI&E3P. This procedure is adapted from a patent outlining the use of QDs in display applications.[9]

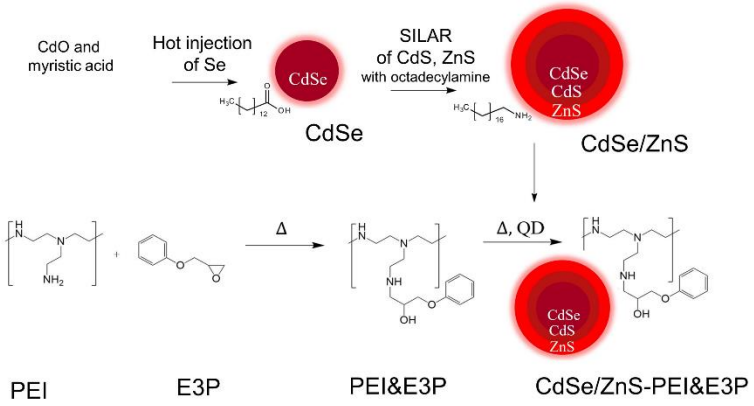

Because no specific core/shell synthesis was mentioned in the patent, we chose to synthesize a CdSe core QD with a graded shell of CdS/ZnS based on a previously published synthesis.[26,27] Specifically, myristic acid stabilized CdSe nanoparticles were synthesized as cores.[26] The emission peak of the cores was 595 nm with a full width at half max (FWHM) of 34 nm (see Figure S3-8, Table S3-1). The transmission electron microscopy (TEM) analysis of these spherical particles indicated that their average diameter was 3.2 ± 0.4 nm (n=50, Figure S3-9). These particles were also crystalline, as demonstrated by lattice lines on the TEM and peaks on powder X-Ray diffraction (pXRD, Figure S3-10).

Next, inorganic shells were added onto the core using successive ion layer absorption and reaction (SILAR) method that uses octadecylamine as a ligand.[27] We chose to add 3 different layers to the shell, from CdS to $Cd_{0.5}Zn_{0.5}S$, to ZnS for all QDs because this procedure has proven to decrease the lattice mismatch between shells and enhance photostability.[25] These shells were added sequentially to the reaction mixture (i.e. no purification between their additions). There was a 10 minute gap between additions of the shell elements (either Cd, $Cd_{0.5}Zn_{0.5}$, Zn, or S), which had been previously established because after this time period the optical properties displayed no further changes.[27] These inorganic sulfide shells will be referred to as "alloyed" shells. QD particles increased in diameter from 3.2 ± 0.4 nm (cores) to 4.8 ± 0.8 nm when the shells were

added (Figure 3-1A). The shape variation of the shelled QDs indicates that the addition of different layers to (i.e. shelling) the spherical core is not completely uniform. However, these size ranges and shapes align with those previously reported in the literature for the shelling of synthesized and purchased quantum dots.[27,28,16,29] The crystallinity of the samples is observed via pXRD measurements, which indicate a cubic structure of CdSe core, CdS, and ZnS alloyed shells present in the QDs (Figure 3-1B). Three reflections of the cubic phase are indicated in the figure, where broad peaks are a result of the mix of CdS, ZnS and CdSe present.[30,31] Both TEM and pXRD spectra were taken without the addition of the capping polymer (see procedure below) because the large quantity of organic molecules in that polymer could obscure the bulk and particulate crystallinity observations. The addition of alloyed shells, CdS to $Cd_{0.5}Zn_{0.5}S$, to ZnS (with each layer added sequentially without purification in between), for all CdSe QDs, is key to designing stable, commercially relevant QDs. This alloyed shell structure is important to keep in mind as these particles are aged later in the paper.

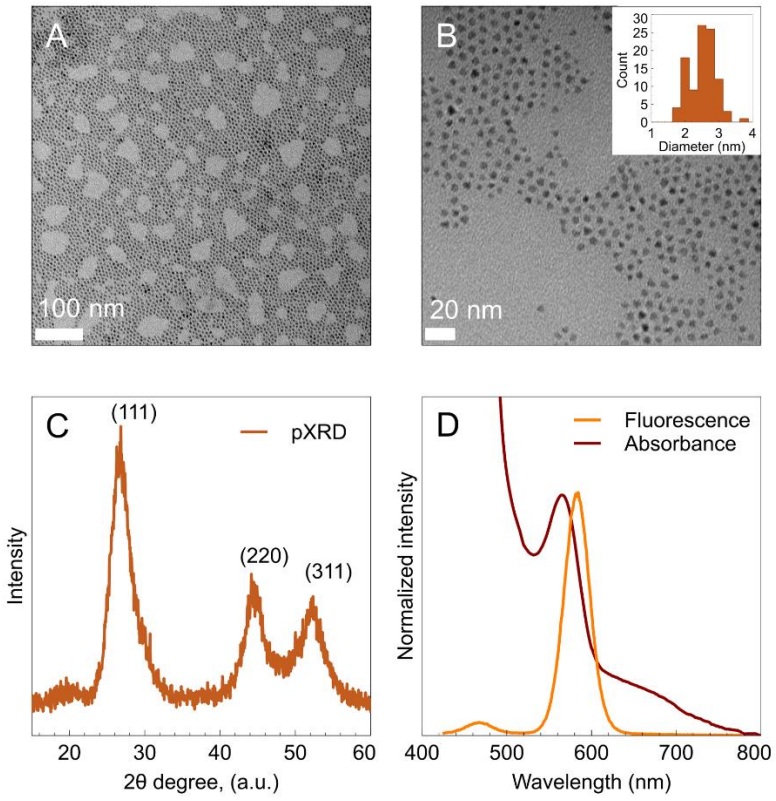

Figure 3-1: (A,B) Representative TEM image of CdSe/ZnS-octadecylamine QDs with inset demonstrating size range of CdSe/ZnS QDs by TEM (n=200) (C) pXRD CdSe/ZnS-octadecylamine QDs and (D) Absorbance (red) and fluorescence (orange) of CdSe/ZnS – PEI&E3P in toluene (excitation at 400 nm).

After the addition of inorganic shells to the CdSe core, the ligand present on the surface of these QDs is octadecylamine because of the synthesis. We then coated these QDs in an additional capping polymer layer.[9] Polyethyleneimine (PEI) and 1,2-epoxy-3-phenoxypropane (E3P) were combined under argon in an addition reaction which formed a C-N bond (see Scheme 3-1). The synthesized polymer was characterized by ^{1}H-NMR (see Figure S3-11). The characteristic sharp peaks of the epoxide at 4.25, 3.95, and 2.92 ppm broadened and shifted as they were incorporated in the broad peak of the polymer network from 2.4 to 2.8 ppm and 3.8 to 4.2 ppm (see Figure S3-11). Importantly, the hydrogen directly bonded to the secondary carbon on the epoxide ring in E3P at 3.38 ppm is no longer apparent, indicating that no epoxide rings could react with QDs (Scheme 3-1).

In Scheme 3-1, QDs were added to the as-synthesized capping polymer at 100°C. To ensure that the same amount of QD was added to this polymer in each synthesis, thermogravimetric analysis (TGA) was done on every CdSe/ZnS-octadecylamine sample to evaluate the ratio of inorganic/organic contents (Figure S3-12). The organic content (octadecylamine) varied from 30-40% depending on the QD sample. With the ratio known for each sample, the amount of QDs added to the 450 mg of the polymer was adjusted so that the total inorganic weight added for every synthesis would be the same (20 mg). These synthesized QDs were labeled as CdSe/ZnS-PEI&E3P, which were approximately 4 wt% inorganic QD. This translates to 2 wt% Cd and 1 wt% Zn, which was later confirmed via acid/H_2O_2 digestion and measurement in the ICP-OES. This low amount of QD reflects the amounts of QDs used in the QD film in display applications, which is approximately 0.01% Cd.[32]

After the addition of a capping polymer, we checked that the desired QD properties were still intact. The preservation of the QD fluorescence was demonstrated by the preserved emission of the QDs at 584 nm with a full width at half max (FWHM) of 34 nm (Figure 3-1D, Table S3-1). This correlates well to the fluorescence of the CdSe core (peak emission of 595 nm and FWHM of 37 nm). The fluorescence changes with coating of ZnS-PEI&E3P represent a slight decrease in core size, but a slight increase in core uniformity.[33] The ^{1}H-NMR analysis also revealed octadecylamine ligands were still present (1-2 ppm peaks, Figure S3-13).

In short, this construction of CdSe/ZnS-PEI&E3P is focused on replicating the QDs found in displays (alloyed shell and polymer coating) while also maintaining the ability to fully synthesize and characterize a nanoparticle free of a plastic coating.

3.4.2 CdSe/ZnS-PEI&E3P dissolution in response to pH and oxygen

After the CdSe/ZnS-PEI&E3P was synthesized, it was subject to dissolution tests to determine the amount of solubilized ions after exposure to pH 2-8 as well as atmospheric O_2 and anoxic (N_2 atmosphere) system (Figure 3-2). Initial sample preparation involved a pH adjustment with acetic acid because the solution of 100 mg/L of CdSe/ZnS-PEI&E3P had an initial pH of 10. We chose acetic acid because of its use in the Toxicity Characteristic Leaching Procedure[34] to measure metal

release from waste and because acetic acid prompted more dissolution of QDs from LDPE (compared to hydrochloric acid and citric acid) in a study by Duncan et al.[35]

The initial Cd and Zn concentrations in these dissolution tests were 3 and 1.5 mg/L, respectively, all in nanoparticle form. After the exposure tests to specific environmental conditions were completed (dark conditions for either 24h or 6 months), we separated the fraction of the sample containing <3 kDa species from any remaining nanoparticle matter (>3 kDa) using filtration with ultracentrifugation filters (see SI for method validation). Solubilized ion and nanoparticle fractions were digested separately with both nitric acid and hydrogen peroxide to release all metals present into solution and break down PEI&E3P.[36] Finally, the concentrations of Zn and Cd in the dissolved and nanoparticle solutions were measured using inductively-coupled plasma optical emission spectroscopy (ICP-OES). The results of the dissolution are presented as a percentage of the total metal content in the QDs which was found dissolved, i.e. which passed through a 3 kDa filter. Specifically, 100% indicates that all metal was dissolved and none remained as components of a QD. These results in aerobic conditions (Figure 3-2A and B) were then compared to anaerobic conditions (Figure 3-2C and 2D).

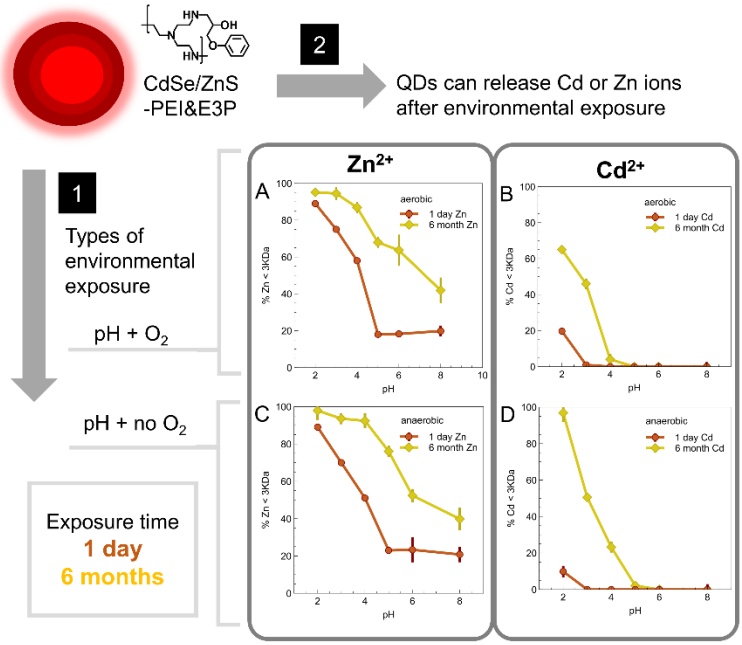

Figure 3-2: Dissolution of (A) Zn and (B) Cd after exposure to waters at varying pH for 1 day (orange circles) and 6 months (yellow diamonds) in a dark aerobic environment. (C) Zn and (D) Cd dissolution under an anaerobic environment kept all other conditions the same. Error bars represent the standard deviation of duplicate samples, each of which yielded three ICP-OES measurements (total six values used for each data point).

This analysis of CdSe/ZnS-PEI&E3P QDs ageing at pH 2-8 indicated that the free ion concentrations increased as pH decreased under both aerobic and anaerobic conditions. The Zn content of the QDs was almost completely dissolved as $Zn^{2+}_{(aq)}$ after 1 day at pH 2, while only 5-10% of their Cd content was present as aqueous ions under the same conditions. After 6 months, the dissolution of Zn was complete for pHs below 4, while at pHs above 4 Zn remained partially undissolved with the QD shells. Even after 6 months at pHs above 4, Cd overall remained undissolved. Only at pH 2 did we observe modest dissolution of Cd.

This lack of dissolution at circumneutral pH is in agreement with studies on QDs embedded in plastics or display films, but differs from results with model QDs. This result offers a validation

of our synthetic design, in the sense that it affords a fully characterized model of a slow metals release particle, similar to the real ones found in devices. The CdSe/ZnS-PEI&E3P QDs in this study released fewer metal ions than comparable CdSe/ZnS -mercaptopropionic acid QDs from another study at lower concentrations (1 ppm QD) under similar conditions (dark, circa 1 day dissolution time).[14] After 24h at pH 7, CdSe/ZnS-mercaptopropionic acid QDs released 30% of their Cd and 90% of their Zn,[14] while in this work CdSe/ZnS-PEI&E3P released 0% of their Cd and 20% of their Zn.

Ligand functional groups and their quantity may play a role in this limited dissolution.[16,37] In fact, it is not common to report the amount of ligand or capping polymer used for dissolution tests.[19,20,38] In this study, the amount of capping polymer may have influenced the robustness QDs at circumneutral pHs such that our model behaves more like QDs in displays.

Our studies indicated a significant difference in aerobic vs anaerobic conditions occurred after 6 months at pH 2 for Cd, where roughly 65% of Cd was dissolved in aerobic conditions, but 100% was dissolved in anaerobic conditions. In addition, the pH range for Cd dissolution increased from pH 2 in aerobic conditions to pH 2-4 in anaerobic waters. For Zn dissolution, aerobic conditions caused higher dissolution for pH 3-4 after 1 day compared to anaerobic conditions, but after 6 months there was no significant difference between in aerobic vs anaerobic conditions for Zn dissolution of all pH studied ($p<0.02$ is significance benchmark for all comparisons).

The two variations of conditions were chosen in order to decipher the role of oxygen in low pH metal sulfides (MS) dissolution experiments pH. This dissolution reaction has been proposed before to proceed via either an anaerobic pathway (eq.1) or an aerobic one (eq. 2).[39]

$$MS_{(s)} + 2H^{+}_{(aq)} \rightarrow H_2S_{(aq)} + M^{2+}_{(aq)} \qquad \text{eq. 1}$$

$$MS_{(s)} + 2H^{+}_{(aq)} + H_2O + 2O_2 \rightarrow SO_4^{2-}{}_{(aq)} + M^{2+}_{(aq)} + 2H^{+}_{(aq)} + H_2O \qquad \text{eq. 2}$$

Eq. 1 describes a well-known mechanism for the dissolution of acid-soluble metal sulfides. [40] In Eq. 2, oxygen plays a role in further oxidizing sulfur-containing reaction by-products, but it may also participate in the dissolution itself, via sorption of $O_{2\ (aq)}$ onto a metal sulfide so as to release sulfates and metal ions from the QD surface. [29,39] Eq 2 may also proceed in another manner: Eq 1

followed by the oxidation of hydrogen sulfide to sulfate in solution. In this study, both aerobic and anaerobic dissolution rates for ZnS and CdS increased steadily as the pH was decreased, which is consistent with both equations 1 and 2 (Figure 3-2).

Yet, for Cd, the anaerobic conditions afforded faster dissolution than the aerobic ones, the difference being more pronounced after 6 months than 1 day.[41] This point strongly suggests that indeed O_2 must actively participate mechanistically to the aerobic dissolution of the metal sulfide itself and thus slow down the reaction in this case. For instance, the presence of O_2 may trigger the formation of a passivating CdO layer locally. This explanation is consistent with the difference being more pronounced after a longer reaction time.

To test whether the persistence of the CdSe/ZnS-PEI&E3P in response to pH and oxygen was a result of the alloyed shell, we synthesized two other model particles. First, we synthesized ZnS-PEI&E3P to mimic the shell material (see SI for synthesis, Figure S3-14 for characterization). ZnS particles were 4.0 ± 0.6 nm (n=100) in diameter capped with oleylamine because of the synthesis (compared to 4.8 ± 0.8 nm diameter CdSe/ZnS synthesized with octadecylamine). Then, these ZnS QDs were stabilized by same capping polymer (PEI&E3P) in the same procedure as CdSe/ZnS QDs. We measured the Zn ion dissolution from ZnS QDs at pH 2 and 4. The dissolution extent matched those of Zn in CdSe/ZnS QDs at pH 2 over 24h dissolution time, but at pH 4 there was less dissolution for ZnS compared to CdSe/ZnS QDs (Figure 3-3A). The fact ZnS dissolved preferably when it is shelled over CdSe/CdS than when it is the sole constituent of a nanoparticle can arise from the fact ZnS is likely to have more defects if it is grown over materials with different epitaxies (CdSe and CdS), as it has been shown by others.[42] However, the difference between CdSe and ZnS is greater than that between CdS and ZnS. Therefore, the alloyed shells may decrease dissolution. This alloying is not mentioned in comparable QD dissolution studies with model QDs,[16] which may be a reason for their QDs relative lower stability.

Also, we synthesized CdSe-PEI&E3P with no CdS or ZnS shells, with the same CdSe and PEI&E3P methods used for CdSe/ZnS-PEI&E3P. CdSe-PEI&E3P QDs did not contain a long chain amine similar to CdSe/ZnS-PEI&E3P and ZnS-PEI&E3P, but instead myristic acid as a result of the synthesis. The dissolution of CdSe-PEI&E3P after 24 h at pH 2 and 4 is almost complete (>75%, Figure 3-3). Cd dissolution from CdSe-PEI&E3P was much higher than in the

sulfide-shelled CdSe/ZnS-PEI&E3P, confirming the anticipated protective function of the shell in this context.

Specifically, Cd ions can only be released from CdSe/ZnS-PEI&E3P after complete dissolution of the ZnS shell, at which point the mixed Cd/Zn sulfide shell is exposed. After 24 h, Cd dissolution at pH 2 in aerobic conditions indicates that the Cd contained in this $Cd_{0.5}Zn_{0.5}S$ layer is partially dissolved (~22% of all Cd, Figure 3-2B), however, the remaining CdSe core is intact. This protection of CdSe core however, is only temporary. The dissolution results for Cd after 6 months (60-100% of Cd is dissolved at pH 2, Figure 3-2) points to the fact that CdSe and CdS are not stable in the long term under low pH. This long-term outlook on the potential dissolution of CdSe/ZnS-PEI&E3P is necessary to determine the possible results of QD dissolution.

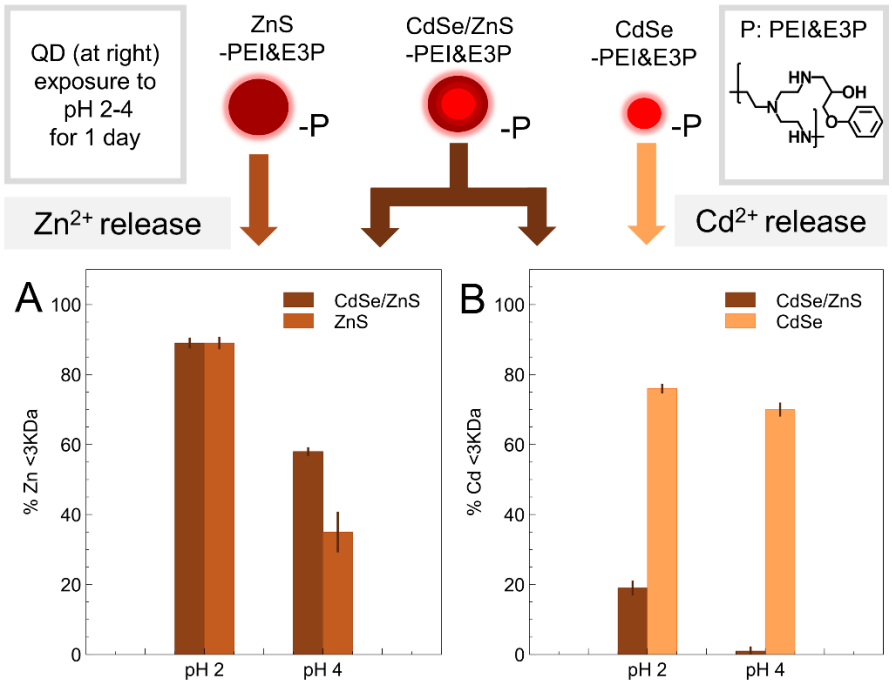

Figure 3-3: (A) Dissolution of Zn from CdSe/ZnS-PEI&E3P and ZnS-PEI&E3P and (B) dissolution of Cd from CdSe-PEI&E3P and CdSe/ZnS-PEI&E3P. Dissolution was measured after 24 h in the dark in aerobic conditions at pH 2 and 4 regulated by acetic acid.

3.4.3 Aggregation of CdSe/ZnS-PEI&E3P

Besides dissolution, CdSe/ZnS-PEI&E3P particles may undergo transformations, namely their ability to aggregate. To gain insight into the structural evolution of these nanoparticles, we investigated them after different ageing events with dynamic light scattering (DLS) and ζ-potential measurements. At 0.3 mg/mL at neutral pH, the ζ-potential of CdSe/ZnS-PEI&E3P was on par with the ζ-potential of PEI&E3P alone at +35-45 mV, which confirms the surface charge of CdSe/ZnS-PEI&E3P are stemming entirely from their capping polymer. With decreasing pH to 8, the ζ-potential decreases slightly (to 26-28 mV), indicating that the protonation extent of the capping polymer is only slightly decreased (Figure S3-15). Over pH 2-8, the hydrodynamic size of CdSe/ZnS-PEI&E3P in solution after 1h is slightly larger than polymer alone (hydrodynamic radius is stable at 100-130 nm over pH 3-9). This large hydrodynamic size of the CdSe/ZnS-PEI&E3P was maintained after 24h as well (Figure S3-15). These hydrodynamic sizes and zeta potentials are relatively stable over the pHs measured, compared to CdSe/ZnS QDs coated with octylamine-modified poly(acrylic acid).[43]

The fluorescence of QDs has also been linked to the aggregation state of the particles. The fluorescence of CdSe/ZnS-PEI&E3P was measured after 1 hour, 1 day, and three weeks (Figure S3-16 and Figure S3-17). After 1 day, fluorescence peak intensity from pH 6 and 8 decreased, while intensity at pH 4 increased to 170% of initial intensity (taken after 1h). A similar increase in fluorescence intensity has been well documented for thiol-based ligands,[44] but in this case amines may be temporarily passivating surface traps with protons. These spectra indicate that after 3 weeks, there is a complete loss of fluorescence of QDs in solution. This could partly be due to degradation of the QD structure, via shell dissolution at low pHs, or due to aggregation. Aggregation proved to be influential because the vortexing of solutions for 30 min increased the fluorescent signal intensity to 35% of the initial fluorescence intensity. This technique indicated that QDs were aggregating over time.

To gain more insight in the structure of nanoparticle aggregates, we performed a complementary study by TEM and EDS. CdSe/ZnS-PEI&E3P was initially suspended at pH 4 and drop cast onto a TEM grid (Figure 3-4), demonstrating particles that are discrete and not stacked on one another. While TEM analysis does not allow direct visualization of ligand or capping polymer (or both) at

the QDs surface, it is realistic to assume that these dispersed particles are initially stabilized by organics.

After ageing CdSe/ZnS-PEI&E3P for 1 day in pH 4, we filtered the sample and retained the >3kDa fraction (i.e. particles larger than ~1.5 nm). These QDs demonstrated larger loose aggregates than the QDs originally studied (Figure 3-4C,D) indicating that the coating separating the QDs may be less effective at separating QDs over time. These structures are similar to those noted by Mukherjee et al, who demonstrated via TEM the loose aggregation of carboxyl- and amine-capped CdSe/ZnS (polymer unknown) in the presence of algal exudate.[45]

However, on the same TEM grids of >3 kDa fraction (i.e. particles larger than ~1.5 nm) after 6 months of ageing, we observed large tight aggregates of discrete nanoparticles (Figure 3-4E,F) that are of similar size and shape to the original QDs used for dissolution studies (Figure 3-1A,B). Other studies have noted aggregation of hydrophobic QDs in response to increasing electrolyte concentration, humic acid presence, or oxidants as well.[46–48] However, the tight aggregates reported here are smaller in size and induced solely with a long period of time and low pH. Aggregation typically decreases the toxicity of nanoparticles, but a link between bioavailability and aggregation has not yet been established for such small QD aggregates with a commercially relevant capping polymer.

At all time frames, we found no evidence of reprecipitated species, which would have been particles of Cd or Zn-containing oxides or sulfides retained by the 3 kDa filter. These reprecipitated species would have been either (1) a result or Cd or Zn ions in solution complexing with Se or S in solution forming crystals or amorphous solids or (2) elemental Se or S, such as those observed by Pedersen et al[48] and Carrière et al.[49] The stability of ions in our system could be due their chelation by amines in PEI&E3P or simply due to a lack of other oxidizing or reducing species.

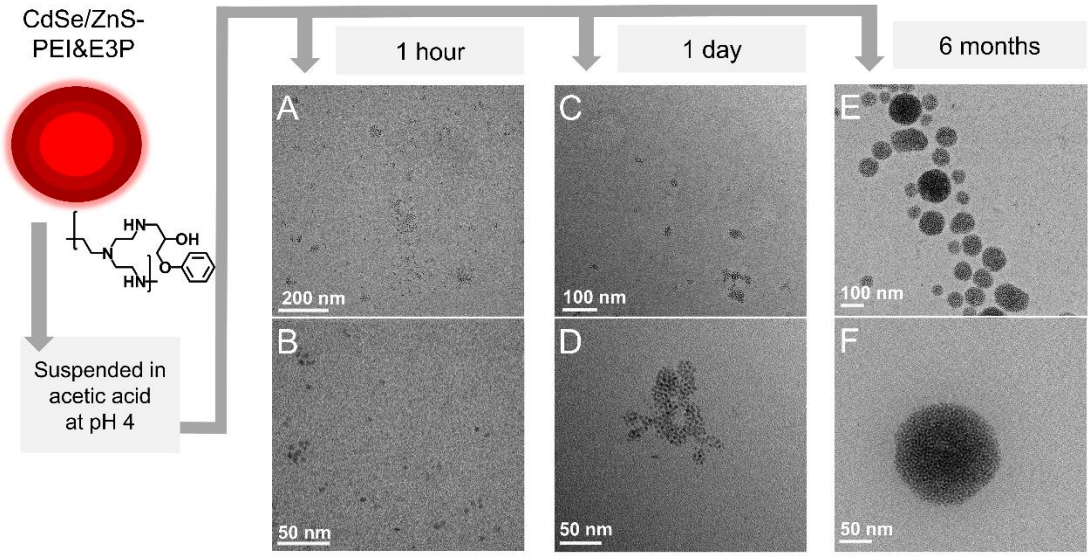

Figure 3-4: (A,B) TEM images of pristine CdSe/ZnS-PEI&E3P and CdSe/ZnS-PEI&E3P after 24h (C,D) and 6 months (E,F) of dissolution in aerobic conditions at pH 4.

3.4.4 Toxicity of CdSe/ZnS-PEI&E3P to HepG2 Cells

From the fate experiments conducted above, we turned to toxicity measurements to better understand how sample ageing, and specifically the components emerging from it, are impacting the toxicity of the ensemble. We chose to use HepG2 liver cells because the number of metabolizing enzymes within hepatocytes makes the liver the primary susceptible organ to xenobiotics.[50]

We first validated a CellTiter-Glo Luminescence assay as a suitable cell viability assay for the HepG2 cell model by measuring cytotoxicity resulting from exposure to Cd^{2+} ions for 1 day, the component in Cd-containing QDs most commonly associated with toxicity.[51] The impact of Cd^{2+} on HepG2 cell viability has been intensively studied (IC_{50} = 1.7 mg/L[52] and IC_{50} = 1.1 mg/L[53]), and we observed a similarly high sensitivity of HepG2 cells. Toxicity was independent of counter ions present ($CdCl_2$ IC_{50} = 0.64 ± 0.08 mg/L and $Cd(NO_3)_2$ IC_{50} = 0.5 ± 0.2 mg/L; detailed results Figure S3-18).

Having validated the luminescence assay, we next determined cytotoxicity resulting from other components in CdSe/ZnS-PEI&E3P including Zn^{2+} and the PEI&E3P ligand. Our results confirm

that Zn^{2+} is much less toxic than Cd^{2+}, independent of the counter ion ($ZnSO_4$ IC_{50} = 30 ± 12 mg/L and $Zn(OAc)_2$ IC_{50} = 26 ± 7 mg/L): viability results in Figure S3-19. Our results are in line with previous experiments in zebrafish *Danio rerio* liver cells after a 24h incubation period ($ZnSO_4$ IC_{50} = 67 mg/L).[54] In contrast, PEI&E3P has not been previously tested in terms of toxicity on HepG2 cells. PEI&E3P ligand however, while not as toxic as Cd^{2+} to HepG2 cells, featured significant toxicity with a measured IC_{50} value of 220 ± 50 mg/L (viability results in Figure S3-20). This toxicity of PEI&E3P is particularly relevant considering the high ratio of this ligand present in QDs compared to Cd^{2+} and Zn^{2+} (i.e. Cd^{2+}: Zn^{2+}: PEI&E3P which is 2:1:100).

A rough comparison of PEI&E3P to polyethylene glycol (PEG) capped TiO2 NPs[55] (analyzed with the same cells and assays used here) indicates that PEI&E3P is more toxic than PEG. When QDs capped with PEI are compared to QDs capped with negatively-charged or neutral ligands, the PEI-capped QDs are consistently more toxic.[56,57] Although the hydrodynamic radius is reported in these studies, there is no clear indication of the mass of capping polymer used for those toxicity tests. Just as in environmental fate studies, reporting the mass of ligand used in toxicity tests is crucial.

We determined the toxicity of pristine CdSe/ZnS-PEI&E3P (IC_{50} = 150 ± 20 mg/L, Figure S3-21). Additionally, we confirmed the presence of QDs inside or strongly adhered to cells by washing the QD-exposed cells with fresh PBS and then observing the cells with confocal microscopy (Figure S3-22). Despite clear interactions between the QDs and cell, QD-induced toxicity is difficult to compare to previous literature. Molarity of QDs is difficult to replicate between studies,[51] and in this case molarity of QDs is skewed by the presence of a capping polymer (which makes up ~96 wt%). Comparisons based on molarity of QDs alone would indicate that CdSe/ZnS-PEI&E3P (IC_{50} = 90 ± 10 nM) are much more toxic than previously studied CdSe/ZnS-PEG exposed to HepG2 cells (no cell toxicity observed at 100 nM).[58]

3.4.5 Exposing CdSe/ZnS-PEI&E3P to low pH reduces the toxicity of the residual QD particles

We next applied the same 24h incubation viability assay to study how the toxicity changes following one case of environmentally-mimicked ageing (in this case 24h at pH=2 in aerobic conditions). We chose to study CdSe/ZnS-PEI&E3P aged at pH 2 for 24h in aerobic conditions

because this condition offered complete dissolution of the ZnS shell and partial dissolution of the CdS shells. However, to both mimic the ageing conditions in Figure 3-2 and allow for the calculation of IC_{50}, samples were concentrated with ultrafiltration with 3 kDa filters. Additionally, this concentration procedure reduces the acetic acid present and the amount of sodium hydroxide needed to neutralize it, while preserving the polymer concentration (Figure S3-23).

We developed three model systems to specifically distinguish toxicity arising from the aged particles and the released ions (Figure 3-5A). These models include: 1) aged CdSe/ZnS-PEI&E3P which were filtered (3 kDa) from the solution in which they were aged (called aged QDs alone) thus removing all dissolved $Cd^{2+}$and Zn^{2+} (20% of Cd in pristine QD and 100% of initial Zn in pristine QD) and neutralized with sodium hydroxide.; 2) concentrations of freshly prepared PEI&E3P, $Cd^{2+}$and Zn^{2+} equivalent to what is measured in solution following ageing of 2 g/L of CdSe/ZnS-PEI&E3P (called ions and ligands); 3) the full model of aged CdSe/ZnS-PEI&E3P, consisting of the aged QDs with $Cd^{2+}$and Zn^{2+} in solution due to ageing along with the remaining weathered particles themselves (Figure S3-24-27,Table S3-3).

Our results confirm that the aged CdSe/ZnS-PEI&E3P, after removing dissolved ions (20% of total Cd and 100% of Zn), are significantly less toxic than pristine CdSe/ZnS-PEI&E3P (aged IC_{50} = 290 ± 60 mg/L vs pristine IC_{50} = 150 ± 20 mg/L; p = 0.005, Figure 5). Interestingly, there is no significant difference in comparing the toxicity of the fully aged CdSe/ZnS-PEI&E3P model as well the model containing the relevant concentrations of dissolved Cd^{2+}, Zn^{2+}, and PEI&E3P arising from weathering of the pristine QDs (Cd, Zn, PEI&E3P model IC_{50} = 170 ± 30 mg/L; fully aged QD model IC_{50} = 190 ± 40 mg/L, Figure 3-5). This suggests that dissolved ions from QDs are the major source of toxicity to human cells.

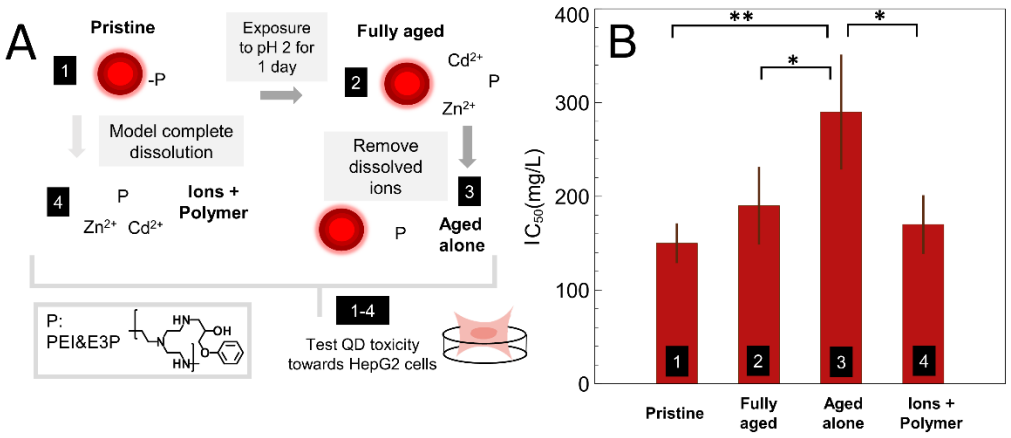

Figure 3-5:Ageing of CdSe/ZnS-PEI&E3P reduces toxicity in human liver cells. (A) Models used to test for impact of ageing on QD toxicity. (B) Comparison of IC_{50} values of pristine QDs with aged QD models in HepG2 cells. Each value is the mean and standard deviation from three biological experiments. *= $p < 0.05$ ** = $p < 0.01$.

Our findings support our hypothesis that leached components, including $Cd^{2+}$and PEI&E3P, and less so Zn^{2+} are a major source of toxicity. Importantly, because these components are leached from QDs upon environmental weathering, the remaining aged QD particles are significantly less toxic compared to these components and pristine QDs. Additionally, the aged CdSe/ZnS-PEI&E3P could be more aggregated or have a different colloidal stability in media than pristine QDs. Whether the Cd^{2+}, Zn^{2+}, PEI&E3P, or QDs will pose a significant risk to humans depends on mainly two factors: relevant doses and physiological conditions. In terms of relevant dose, further studies are needed to determine the possible amounts of QDs that will leak out from damaged electronic displays. Once determined, the amount of QDs that could have contact with liver cells also needs to be investigated. Finally, different physiological conditions such as bloodstream conditions or gastric conditions can also possibly alter the QDs cytotoxicity via changing its structural stability and biological solubility.

3.5 Conclusions

CdSe/ZnS-PEI&E3P were synthesized with a commercially-relevant capping polymer to close the knowledge gap between products embedded with QDs and model QDs with small mobile ligands. Dissolution results indicated that the CdSe core of CdSe/ZnS-PEI&E3P does not dissolve at circumneutral pH, even after 6 months. At low pH, dissolution of the CdSe core is temporarily hindered by the presence of ZnS and CdS shells (75% decrease in Cd dissolution after 1 day compared to unshelled CdSe). The presence of oxygen in the dark did not facilitate the dissolution of the QD. Aggregation of the QDs in solution was documented at pH 4, forming loose (after 24h) and eventually dense ~100 nm aggregates (after 6 months). These relatively robust QDs can serve as a platform to further investigate QDs from display applications because of their limited dissolution and complex coating.

Subsequent toxicity tests pointed out the relatively high toxicity of the encapsulating polymer alone, highlighting the fact that the organic portion of quantum dots must be considered to fully account for toxicity of the complex nanomaterial. When adding environmental transformations to toxicity tests, QDs exposed to an environmentally relevant conditions are significantly less toxic compared to intact pristine QDs (IC_{50} of 150 and 290mg/L, respectively). Our results suggest that this reduction in toxicity to human cells is a result of the lower concentration of toxic components, Cd^{2+} and Zn^{2+} available following their dissolution (10% and 100% present as ions, respectively). As such, QDs that are left in the environment for long periods (6 months) will likely release higher concentrations of toxic ions and polymer components, thus the surrounding aqueous phase could result in more serious toxicological effects whereas the QD itself would have diminished toxicity.

In conclusion, this paper highlights the need for studies on the environmental implications of industrially relevant QDs to investigate the complex interactions with capping polymers.

3.6 Methods

3.6.1 Synthesis of CdSe/ZnS QDs

The synthesis of the CdSe quantum dots was based on the methods utilized by J. Zhou et al. and R. Xie et al. (see SI for step-by-step procedure and modifications).[26,27] The synthesis

produced CdSe/CdS/$Cd_{0.5}Zn_{0.5}S$/ZnS QDs with octadecylamine ligands, which will be referred to as CdSe/ZnS.

3.6.2 Octadecylamine and PEI & E3P Ligand Exchange

Branched polyethyleneimine (PEI) as a 50% w/w solution and 1,3-epoxy-3-phenoxypropane were purchased from Sigma Aldrich. Before use, the PEI solution was frozen and lyophilized overnight to remove the water content (checked with ^{1}H-NMR, see SI).

To synthesize the polymer, 0.300 g of PEI was added to a two-neck 25mL round bottom flask. The flask was set up under a reflux system and heated to 100ºC. N_2 was flushed through the system so that no air was present during the reaction. The 1,2-epoxy-3-phenoxypropane (E3P) precursor was prepared by adding 0.150 g of E3P into a 0.5 Dram vial. Once the reaction flask reached 100ºC, the E3P precursor was injected into the solution, and the monomers were left to react for 30 min under nitrogen and stirring at 200 rpm.

To add the capping polymer on the surface of the nanoparticles, 20 mg of the previously prepared, shelled quantum dots was dissolved in 2 mL of toluene. After the polymer synthesis was conducted for 30 minutes, the quantum dot solution was injected directly into the reaction flask. The solution was left stirring under N_2 for an additional 30 min. Once the ligand exchange was completed, the solution was cooled to room temperature, while the precipitate settled to the bottom of the flask. The excess toluene was removed using a rotary evaporator and the product was dried in a vacuum oven at <50ºC overnight. The final dried product was stored in a desiccator.

3.6.3 Dissolution Tests

CdSe/ZnS-PEI&E3P was added to solutions of different pH at the same concentration (150 mg/L). We had previously confirmed none of the Cd and Zn were present as ions in this initial solution (see Table S3-2). The pH of solutions was adjusted with acetic acid to be either 2, 4, 6, or 8. Once the QD-containing solutions in glass vials were prepared, they were left to sit for 24h or 6 months in the dark while stirring at 100 rpm at ambient lab temperature (20-22 °C). Then each of these solutions was passed through a 3 kDa Amicon Ultra-4 Centrifugal Filter Unit for 45 minutes at 4500 rpm (Sorvall Legend XF).

The method used to separate intact QDs from dissolved ions relied on the use of 3 kDa centrifugal filters (see SI for details). The retentate was recovered from the filter by adding 1 mL of 30% H_2O_2. After 10 min, this solution was pipetted into a digestion tube and heated for 30 minutes at 95°C. Twenty minutes into this digestion, 1 mL of 70% nitric acid (Trace metal grade) was added to the retentate. At the end of the thirty minutes of the H_2O_2 digestion, the 1 mL of nitric acid from the retentate was added to the H_2O_2 - containing solution. Then this solution was heated to 95°C for 60 minutes to complete the digestion. The solution was then diluted to 15 mL with deionized water and measured in the ICP-OES (see SI for conditions).

The filtrate was divided into two aliquots of 1.5 mL into digestion tubes and digested with a similar procedure. First, 1 mL of hydrogen peroxide was added and heated to 95°C for 30 minutes. Second, nitric acid was added to the solutions and heated to 95°C for 30 minutes. The solution was then diluted to 15 mL with deionized water and measured in the ICP-OES.

3.6.4 Cell culture and quantum dot model components

HepG2 cells (ATCC® HB-8065) were cultured at 37 ℃ with 5% CO_2 in Dulbecco's modified Eagle's media (DMEM) with phenol red (Gibco) supplemented with 10% (v/v) fetal bovine serum (Gibco) and 1% (v/v) antibiotics/antimycotics (Gibco). Cells were maintained in 10 cm petri dishes and passaged using 0.25% (w/v) Trypsin- 0.53 mM EDTA prior to reaching 70-80% confluency.

All individual QD components and QD model systems were prepared immediately prior to use. Individual QD components for testing including Cadmium chloride (Sigma), Cadmium nitrate tetrahydrate (Sigma), Zinc sulfate heptahydrate (Sigma), Zinc acetate (Sigma), and PEI&E3P (synthesized according to Scheme 3-1) were suspended in the supplemented DMEM. All QD models were prepared individually as stock solutions in supplemented DMEM at 2 g/L. Specifically, the pristine QD model was synthesized as described in 'QD synthesis' section and the 24h-aged model was synthesized and aged as described above in section 'Dissolution Tests'. A QD model called "ions and capping polymer" was prepared with Cd^{2+} and Zn^{2+} ions as well as the PEI&E3P ligand representing the total dissolved components from 2 g/L of 24-h aged QDs as

described in Figure 3-2. Finally, the full aged QD model was prepared by combining the 2 g/L 24h-aged and filtered QDs with the total dissolved components.

3.6.5 In vitro cell viability assay

For each assay, HepG2 cells were seeded in a clear 96-well microplate at a density of 6000 cells/well and incubated for 24h. The media was then carefully replaced with serial dilutions of the QD components or QD model solution and incubated for 24h. Cell viability was then assessed using the CellTiter-Glo® luminescence assay (Promega) as per manufacturer instructions. Specifically, the CellTiter-Glo reagent was added to each well, gently mixed for 2 min and incubated in the dark for 10 minutes at room temperature. 80 µL of the mixture from each well was transfer to a white 96-well plate and measured on a Spark® multimode plate reader (Tecan Life Sciences). Luminescence was recorded at 25 °C (Attenuation automatic, integration time 1000 ms). Cell viability was plotted as the mean and standard deviation of relative luminescence units (RLU). IC_{50} values were derived using nonlinear regression (Inhibitor vs. response - Variable slope four parameters) using GraphPad Prism (GraphPad Software, Inc., La Jolla, CA, USA). Statistical comparisons were performed using a one-way ANOVA followed by Tukey's multiple comparisons test.

3.6.6 Characterization instruments and methods

The formation of CdSe and CdSe/ZnS nanoparticles was monitored by measuring their photoluminescence and UV-Vis spectra using a Cary Eclipse Fluorescence Spectrophotometer and a Jasco V-670 Spectrophotometer, respectively. To prepare for the measurements, the CdSe cores were suspended in toluene, and the shelled CdSe/ZnS nanoparticles and monolayer aliquots were suspended in hexanes. The excitation wavelength was set at 400 nm when conducting the fluorescence measurements. The spectrum was taken over a range of 425 – 775 nm. The UV-Vis spectrophotometer was set at a scanning rate of 200 nm/min, and the spectrum was taken over a range of 400 – 800 nm.

Transmission Electron Microscopy (TEM) was done with an FEI Technai G^2 F20 200 kV Cryo-STEM to visualize the nanoparticles. Samples were deposited onto a Cu grid with carbon backing (from Electron Microscopy Sciences).

PerkinElmer Optima 8300 ICP-OES was used to measure Zn and Cd concentrations at wavelengths 206.20 nm and 228.80 nm, respectively.

Bruker D8 Advantage X-Ray Diffractometer using a Cu-Kα (λ = 1.5418 Å) source acquired pXRD spectra. The instrument operated at 30 kV and 10 mA and was equipped with a LinxEye detector and a Ni filter.

^{1}H-NMR samples were prepared by dispersing 1 mg of samples into 0.5 mL of deuterated chloroform. Samples were run on Bruker AVIIIHD 500 MHz NMR spectrometer.

3.7 References

(1) Pan, Z.; Rao, H.; Mora-Seró, I.; Bisquert, J.; Zhong, X. Quantum Dot-Sensitized Solar Cells. *Chem. Soc. Rev.* **2018**, *47* (20), 7659–7702. https://doi.org/10.1039/C8CS00431E.

(2) Filali, S.; Pirot, F.; Miossec, P. Biological Applications and Toxicity Minimization of Semiconductor Quantum Dots. *Trends Biotechnol.* **2020**, *38* (2), 163–177. https://doi.org/10.1016/j.tibtech.2019.07.013.

(3) Hanifi, D. A.; Bronstein, N. D.; Koscher, B. A.; Nett, Z.; Swabeck, J. K.; Takano, K.; Schwartzberg, A. M.; Maserati, L.; Vandewal, K.; Burgt, Y. van de; Salleo, A.; Alivisatos, A. P. Redefining Near-Unity Luminescence in Quantum Dots with Photothermal Threshold Quantum Yield. *Science* **2019**, *363* (6432), 1199–1202. https://doi.org/10.1126/science.aat3803.

(4) McCoy, M. A Quantum Leap In Display Quality From Quantum Dots https://cen.acs.org/articles/odsmeter.html (accessed 2019 -08 -28).

(5) Nanosys. Nanosys on track for record shipments of Quantum Dots for displays in 2019 https://www.prnewswire.com/news-releases/nanosys-on-track-for-record-shipments-of-quantum-dots-for-displays-in-2019-300937397.html (accessed 2020 -01 -29).

(6) Zhu, R.; Luo, Z.; Chen, H.; Dong, Y.; Wu, S.-T. Realizing Rec. 2020 Color Gamut with Quantum Dot Displays. *Opt. Express* **2015**, *23* (18), 23680–23693. https://doi.org/10.1364/OE.23.023680.

(7) Bodnarchuk, M. I.; Kovalenko, M. V. Engineering Colloidal Quantum Dots. In *Colloidal Quantum Dot Optoelectronics and Photovoltaics*; Konstantatos, G., Sargent, E. H., Eds.; Cambridge University Press: Cambridge, 2013; pp 1–29. https://doi.org/10.1017/CBO9781139022750.002.

(8) Rzigalinski, B. A.; Strobl, J. S. Cadmium-Containing Nanoparticles: Perspectives on Pharmacology and Toxicology of Quantum Dots. *Toxicol. Appl. Pharmacol.* **2009**, *238* (3), 280–288. https://doi.org/10.1016/j.taap.2009.04.010.

(9) Dubrow, R. S.; Freeman, W. P.; Lee, E.; Furuta, P. Quantum Dot Films, Lighting Devices, and Lighting Methods. US9199842B2, December 1, 2015.

(10) McBride, J.; Treadway, J.; Feldman, L. C.; Pennycook, S. J.; Rosenthal, S. J. Structural Basis for Near Unity Quantum Yield Core/Shell Nanostructures. *Nano Lett.* **2006**, *6* (7), 1496–1501. https://doi.org/10.1021/nl060993k.
(11) Gerion, D.; Pinaud, F.; Williams, S. C.; Parak, W. J.; Zanchet, D.; Weiss, S.; Alivisatos, A. P. Synthesis and Properties of Biocompatible Water-Soluble Silica-Coated CdSe/ZnS Semiconductor Quantum Dots †. *J. Phys. Chem. B* **2001**, *105* (37), 8861–8871. https://doi.org/10.1021/jp0105488.
(12) Dubois, F.; Mahler, B.; Dubertret, B.; Doris, E.; Mioskowski, C. A Versatile Strategy for Quantum Dot Ligand Exchange. *J. Am. Chem. Soc.* **2007**, *129* (3), 482–483. https://doi.org/10.1021/ja067742y.
(13) Balde, C. P.; Forti, V.; Gray, V.; Kuehr, R.; Stegmann, P. *The Global E-Waste Monitor – 2017*; United Nations University (UNU), International Telecommunication Union (ITU) & International Solid Waste Association (ISWA),: Bonn/Geneva/Vienne, 2017; pp 1–116.
(14) Fawell, J. *Cadmium in Drinking-Water*; Background document for development of WHO Guidelines for Drinking-water Quality; WHO/SDE/WSH/03.04/80/Rev/1; World Health Organization: Geneva, 2011; pp 1–16.
(15) Nowack, B.; Mitrano, D. M. Procedures for the Production and Use of Synthetically Aged and Product Released Nanomaterials for Further Environmental and Ecotoxicity Testing. *NanoImpact* **2018**, *10*, 70–80. https://doi.org/10.1016/j.impact.2017.12.001.
(16) Paydary, P.; Larese-Casanova, P. Water Chemistry Influences on Long-Term Dissolution Kinetics of CdSe/ZnS Quantum Dots. *J. Environ. Sci.* **2020**, *90*, 216–233. https://doi.org/10.1016/j.jes.2019.11.011.
(17) Supiandi, N. I.; Charron, G.; Tharaud, M.; Benedetti, M. F.; Sivry, Y. Tracing Multi-Isotopically Labelled CdSe/ZnS Quantum Dots in Biological Media. *Sci. Rep.* **2020**, *10* (1), 2866. https://doi.org/10.1038/s41598-020-59206-w.
(18) Wiecinski, P. N.; Metz, K. M.; King Heiden, T. C.; Louis, K. M.; Mangham, A. N.; Hamers, R. J.; Heideman, W.; Peterson, R. E.; Pedersen, J. A. Toxicity of Oxidatively Degraded Quantum Dots to Developing Zebrafish (Danio Rerio). *Environ. Sci. Technol.* **2013**, *47* (16), 9132–9139. https://doi.org/10.1021/es304987r.
(19) Mahendra, S.; Zhu, H.; Colvin, V. L.; Alvarez, P. J. Quantum Dot Weathering Results in Microbial Toxicity. *Environ. Sci. Technol.* **2008**, *42* (24), 9424–9430. https://doi.org/10.1021/es8023385.
(20) Xiao, Y.; Ho, K. T.; Burgess, R. M.; Cashman, M. Aggregation, Sedimentation, Dissolution, and Bioavailability of Quantum Dots in Estuarine Systems. *Environ. Sci. Technol.* **2017**, *51* (3), 1357–1363. https://doi.org/10.1021/acs.est.6b04475.
(21) Carboni, A.; Gelabert, A.; Charron, G.; Faucher, S.; Lespes, G.; Sivry, Y.; Benedetti, M. F. Mobility and Transformation of CdSe/ZnS Quantum Dots in Soil: Role of the Capping Ligands and Ageing Effect. *Chemosphere* **2020**, *254*, 126868. https://doi.org/10.1016/j.chemosphere.2020.126868.
(22) Liu, J.; Katahara, J.; Li, G.; Coe-Sullivan, S.; Hurt, R. H. Degradation Products from Consumer Nanocomposites: A Case Study on Quantum Dot Lighting. *Environ. Sci. Technol.* **2012**, *46* (6), 3220–3227. https://doi.org/10.1021/es204430f.
(23) Brown, F. C.; Bi, Y.; Chopra, S. S.; Hristovski, K. D.; Westerhoff, P.; Theis, T. L. End-of-Life Heavy Metal Releases from Photovoltaic Panels and Quantum Dot Films: Hazardous

Waste Concerns or Not? *ACS Sustain. Chem. Eng.* **2018**, *6* (7), 9369–9374. https://doi.org/10.1021/acssuschemeng.8b01705.
(24) Oh, E.; Liu, R.; Nel, A.; Gemill, K. B.; Bilal, M.; Cohen, Y.; Medintz, I. L. Meta-Analysis of Cellular Toxicity for Cadmium-Containing Quantum Dots. *Nat. Nanotechnol.* **2016**, *11* (5), 479–486. https://doi.org/10.1038/nnano.2015.338.
(25) Talapin, D. V.; Mekis, I.; Götzinger, S.; Kornowski, A.; Benson, O.; Weller, H. CdSe/CdS/ZnS and CdSe/ZnSe/ZnS Core−Shell−Shell Nanocrystals. *J. Phys. Chem. B* **2004**, *108* (49), 18826–18831. https://doi.org/10.1021/jp046481g.
(26) Zhou, J.; Zhu, M.; Meng, R.; Qin, H.; Peng, X. Ideal CdSe/CdS Core/Shell Nanocrystals Enabled by Entropic Ligands and Their Core Size-, Shell Thickness-, and Ligand-Dependent Photoluminescence Properties. *J. Am. Chem. Soc.* **2017**, *139* (46), 16556–16567. https://doi.org/10.1021/jacs.7b07434.
(27) Xie, R.; Kolb, U.; Li, J.; Basché, T.; Mews, A. Synthesis and Characterization of Highly Luminescent CdSe−Core CdS/Zn $_{0.5}$ Cd $_{0.5}$ S/ZnS Multishell Nanocrystals. *J. Am. Chem. Soc.* **2005**, *127* (20), 7480–7488. https://doi.org/10.1021/ja042939g.
(28) Supiandi, N. I.; Charron, G.; Tharaud, M.; Cordier, L.; Guigner, J.-M.; Benedetti, M. F.; Sivry, Y. Isotopically Labeled Nanoparticles at Relevant Concentrations: How Low Can We Go? The Case of CdSe/ZnS QDs in Surface Waters. *Environ. Sci. Technol.* **2019**, *53* (5), 2586–2594. https://doi.org/10.1021/acs.est.8b04096.
(29) Durisic, N.; Godin, A. G.; Walters, D.; Grütter, P.; Wiseman, P. W.; Heyes, C. D. Probing the "Dark" Fraction of Core–Shell Quantum Dots by Ensemble and Single Particle PH-Dependent Spectroscopy. *ACS Nano* **2011**, *5* (11), 9062–9073. https://doi.org/10.1021/nn203272p.
(30) Wang, W.; Germanenko, I.; El-Shall, M. S. Room-Temperature Synthesis and Characterization of Nanocrystalline CdS, ZnS, and CdxZn1-XS. *Chem. Mater.* **2002**, *14* (7), 3028–3033. https://doi.org/10.1021/cm020040x.
(31) Surana, K.; Salisu, I. T.; Mehra, R. M.; Bhattacharya, B. A Simple Synthesis Route of Low Temperature CdSe-CdS Core-Shell Quantum Dots and Its Application in Solar Cell. *Opt. Mater.* **2018**, *82*, 135–140. https://doi.org/10.1016/j.optmat.2018.05.060.
(32) S. Chopra, S.; Bi, Y.; C. Brown, F.; L. Theis, T.; D. Hristovski, K.; Westerhoff, P. Interdisciplinary Collaborations to Address the Uncertainty Problem in Life Cycle Assessment of Nano-Enabled Products: Case of the Quantum Dot-Enabled Display. *Environ. Sci. Nano* **2019**, *6* (11), 3256–3267. https://doi.org/10.1039/C9EN00603F.
(33) Yu, W. W.; Peng, X. Formation of High-Quality CdS and Other II–VI Semiconductor Nanocrystals in Noncoordinating Solvents: Tunable Reactivity of Monomers. *Angew. Chem. Int. Ed.* **2002**, *41* (13), 2368–2371. https://doi.org/10.1002/1521-3773(20020703)41:13<2368::AID-ANIE2368>3.0.CO;2-G.
(34) US EPA, O. SW-846 Test Method 1311: Toxicity Characteristic Leaching Procedure https://www.epa.gov/hw-sw846/sw-846-test-method-1311-toxicity-characteristic-leaching-procedure (accessed 2019 -07 -12).
(35) Gray, P. J.; Hornick, J. E.; Sharma, A.; Weiner, R. G.; Koontz, J. L.; Duncan, T. V. Influence of Different Acids on the Transport of CdSe Quantum Dots from Polymer Nanocomposites to Food Simulants. *Environ. Sci. Technol.* **2018**, *52* (16), 9468–9477. https://doi.org/10.1021/acs.est.8b02585.

(36) Seow, W. Y.; Liang, K.; Kurisawa, M.; Hauser, C. A. E. Oxidation as a Facile Strategy To Reduce the Surface Charge and Toxicity of Polyethyleneimine Gene Carriers. *Biomacromolecules* **2013**, *14* (7), 2340–2346. https://doi.org/10.1021/bm4004628.
(37) Aldana, J.; Wang, Y. A.; Peng, X. Photochemical Instability of CdSe Nanocrystals Coated by Hydrophilic Thiols. *J. Am. Chem. Soc.* **2001**, *123* (36), 8844–8850. https://doi.org/10.1021/ja016424q.
(38) Li, Y.; Zhang, W.; Li, K.; Yao, Y.; Niu, J.; Chen, Y. Oxidative Dissolution of Polymer-Coated CdSe/ZnS Quantum Dots under UV Irradiation: Mechanisms and Kinetics. *Environ. Pollut.* **2012**, *164*, 259–266. https://doi.org/10.1016/j.envpol.2012.01.047.
(39) Hsieh, Y. H.; Huang, C. P. Photooxidative Dissolution of CdS(s) Part I. Important Factors and Mechanistic Aspects. *Colloids Surf.* **1991**, *53* (2), 275–295. https://doi.org/10.1016/0166-6622(91)80142-B.
(40) Schippers, A. Biogeochemistry of Metal Sulfide Oxidation in Mining Environments, Sediments, and Soils. In *Sulfur Biogeochemistry - Past and Present*; Geological Society of America, 2004. https://doi.org/10.1130/0-8137-2379-5.49.
(41) Wilmot, P. D.; Cadee, K.; Katinic, J. J.; Kavanagh, B. V. Kinetics of Sulfide Oxidation by Dissolved Oxygen. *J. Water Pollut. Control Fed.* **1988**, *60* (7), 1264–1270.
(42) Eskelsen, J. R.; Xu, J.; Chiu, M.; Moon, J.-W.; Wilkins, B.; Graham, D. E.; Gu, B.; Pierce, E. M. Influence of Structural Defects on Biomineralized ZnS Nanoparticle Dissolution: An in-Situ Electron Microscopy Study. *Environ. Sci. Technol.* **2018**, *52* (3), 1139–1149. https://doi.org/10.1021/acs.est.7b04343.
(43) Li, C.; Hassan, A.; Palmai, M.; Snee, P. T.; Baveye, P. C.; Darnault, C. J. G. Colloidal Stability and Aggregation Kinetics of Nanocrystal CdSe/ZnS Quantum Dots in Aqueous Systems: Effects of PH and Organic Ligands. *J. Nanoparticle Res.* **2020**, *22* (11), 349. https://doi.org/10.1007/s11051-020-05080-6.
(44) Green, M. The Nature of Quantum Dot Capping Ligands. *J. Mater. Chem.* **2010**, *20* (28), 5797–5809. https://doi.org/10.1039/C0JM00007H.
(45) Chakraborty, D.; Ethiraj, K. R.; Chandrasekaran, N.; Mukherjee, A. Mitigating the Toxic Effects of CdSe Quantum Dots towards Freshwater Alga Scenedesmus Obliquus: Role of Eco-Corona. *Environ. Pollut.* **2021**, *270*, 116049. https://doi.org/10.1016/j.envpol.2020.116049.
(46) Marşan, D.; Şengül, H.; Özdil, A. M. A. Comparative Assessment of the Phase Transfer Behaviour of InP/ZnS and CuInS/ZnS Quantum Dots and CdSe/ZnS Quantum Dots under Varying Environmental Conditions. *Environ. Sci. Nano* **2019**, *6* (3), 879–891. https://doi.org/10.1039/C8EN01073K.
(47) Noh, M.; Kim, T.; Lee, H.; Kim, C.-K.; Joo, S.-W.; Lee, K. Fluorescence Quenching Caused by Aggregation of Water-Soluble CdSe Quantum Dots. *Colloids Surf. Physicochem. Eng. Asp.* **2010**, *359* (1), 39–44. https://doi.org/10.1016/j.colsurfa.2010.01.059.
(48) Metz, K. M.; Mangham, A. N.; Bierman, M. J.; Jin, S.; Hamers, R. J.; Pedersen, J. A. Engineered Nanomaterial Transformation under Oxidative Environmental Conditions: Development of an in Vitro Biomimetic Assay. *Environ. Sci. Technol.* **2009**, *43* (5), 1598–1604. https://doi.org/10.1021/es802217y.
(49) Tarantini, A.; Wegner, K. D.; Dussert, F.; Sarret, G.; Beal, D.; Mattera, L.; Lincheneau, C.; Proux, O.; Truffier-Boutry, D.; Moriscot, C.; Gallet, B.; Jouneau, P.-H.; Reiss, P.;

Carrière, M. Physicochemical Alterations and Toxicity of InP Alloyed Quantum Dots Aged in Environmental Conditions: A Safer by Design Evaluation. *NanoImpact* **2019**, *14*, 100168. https://doi.org/10.1016/j.impact.2019.100168.

(50) Sturgill, M. G.; Lambert, G. H. Xenobiotic-Induced Hepatotoxicity: Mechanisms of Liver Injury and Methods of Monitoring Hepatic Function. *Clin. Chem.* **1997**, *43* (8), 1512–1526. https://doi.org/10.1093/clinchem/43.8.1512.

(51) Yong, K.-T.; Law, W.-C.; Hu, R.; Ye, L.; Liu, L.; Swihart, M. T.; Prasad, P. N. Nanotoxicity Assessment of Quantum Dots: From Cellular to Primate Studies. *Chem. Soc. Rev.* **2013**, *42* (3), 1236–1250. https://doi.org/10.1039/C2CS35392J.

(52) Fotakis, G.; Timbrell, J. A. In Vitro Cytotoxicity Assays: Comparison of LDH, Neutral Red, MTT and Protein Assay in Hepatoma Cell Lines Following Exposure to Cadmium Chloride. *Toxicol. Lett.* **2006**, *160* (2), 171–177. https://doi.org/10.1016/j.toxlet.2005.07.001.

(53) Lawal, A. O.; Ellis, E. Differential Sensitivity and Responsiveness of Three Human Cell Lines HepG2, 1321N1 and HEK 293 to Cadmium. *J. Toxicol. Sci.* **2010**, *35* (4), 465–478. https://doi.org/10.2131/jts.35.465.

(54) Tang, S.; Allagadda, V.; Chibli, H.; Nadeau, J. L.; Mayer, G. D. Comparison of Cytotoxicity and Expression of Metal Regulatory Genes in Zebrafish (Danio Rerio) Liver Cells Exposed to Cadmium Sulfate, Zinc Sulfate and Quantum Dots. *Metallomics* **2013**, *5* (10), 1411–1422.

(55) Mano, S. S.; Kanehira, K.; Sonezaki, S.; Taniguchi, A. Effect of Polyethylene Glycol Modification of TiO2 Nanoparticles on Cytotoxicity and Gene Expressions in Human Cell Lines. *Int. J. Mol. Sci.* **2012**, *13* (3), 3703–3717. https://doi.org/10.3390/ijms13033703.

(56) Zheng, H.; Mortensen, L. J.; DeLouise, L. A. Thiol Antioxidant-Functionalized CdSe/ZnS Quantum Dots: Synthesis, Characterization, Cytotoxicity. *J. Biomed. Nanotechnol.* **2013**, *9* (3), 382–392. https://doi.org/10.1166/jbn.2013.1561.

(57) Pathakoti, K.; Hwang, H.-M.; Xu, H.; Aguilar, Z. P.; Wang, A. In Vitro Cytotoxicity of CdSe/ZnS Quantum Dots with Different Surface Coatings to Human Keratinocytes HaCaT Cells. *J. Environ. Sci.* **2013**, *25* (1), 163–171. https://doi.org/10.1016/S1001-0742(12)60015-1.

(58) Peng, L.; He, M.; Chen, B.; Wu, Q.; Zhang, Z.; Pang, D.; Zhu, Y.; Hu, B. Cellular Uptake, Elimination and Toxicity of CdSe/ZnS Quantum Dots in HepG2 Cells. *Biomaterials* **2013**, *34* (37), 9545–9558. https://doi.org/10.1016/j.biomaterials.2013.08.038.

3.8 Supporting Information

3.8.1 Analysis of pristine display film containing quantum dots

QD film samples in a display were identified with fluorescence measurements (not shown) and extracted. The two clear outer films were separated from the colored QD-containing inner film, and the latter was used for analysis. Then 0.05g of films were digested with wet ashing using 2 mL of sulfuric acid (Fisher Chemical Trace Metal Grade) and microwave irradiation (CEM Mars 6). The samples were digested by ramping the temperature to 180 °C (15 minutes) and then holding that temperature for 15 minutes. The samples were then digested with 3 mL nitric acid and 2 mL hydrogen peroxide (Fisher Chemical Trace Metal Grade) at 100°C for an hour. The samples were diluted and measured in an ICP-OES (Thermo iCAP 6500 Duo) using lines at 206.20 nm and 228.80 nm for Zn and Cd, respectively. Error bars represent the standard deviation of three measurements.

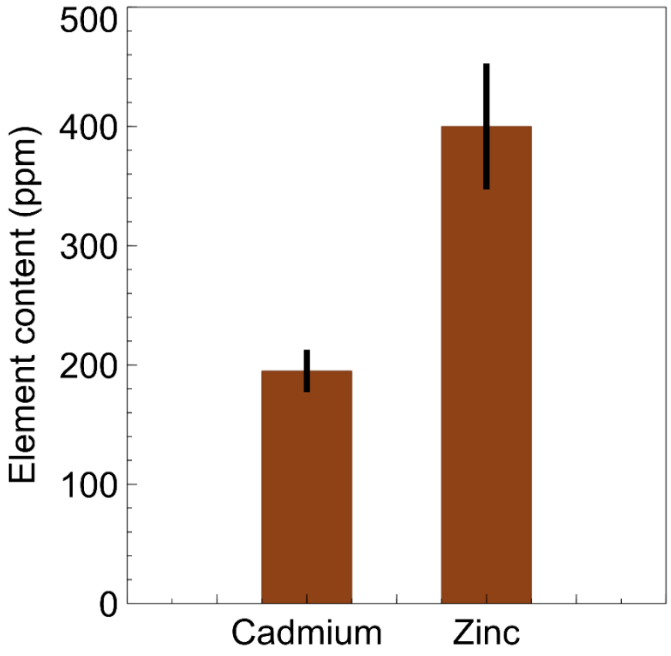

Figure S3-6: Elements present in QD display inner film, measured with ICP-OES.

The inner film was then cut into small (0.5 cm x 0.5 cm) pieces and loaded a teflon rotor. The rotor was then loaded into a solid-state NMR (Varian VNMRS 400 MHz, now Agilent, Santa Clara, CA, USA) and ^{13}C was measured. The spectrometer operated at 100.5 MHz for ^{13}C

using a 4 mm double-resonance Varian Chemagnetics T3 probe. The sample was spun at 13 kHz and the sequence used was a cross-polarization (CP) magic angle spinning (tanquantcpxecho).[1] Other parameters include: the number of scans was 64, recycle delay was 3s, acquisition time was 15 ms, CP contact time of 1000 ms, number of CP periods was 11, and time between CP periods was 1s.

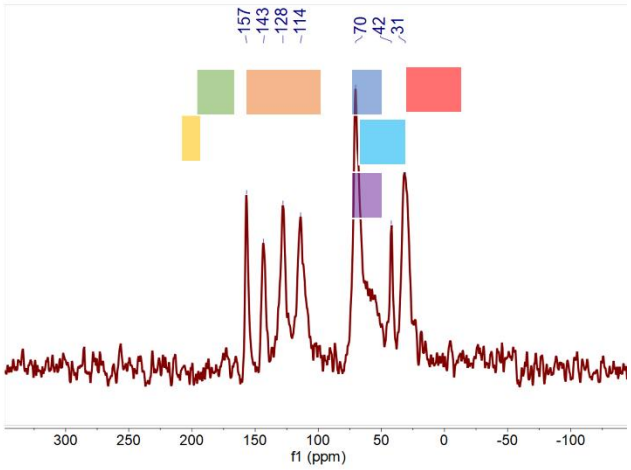

Figure S3-7: Solid State ^{13}C-NMR of inner display film, from a commercial TV display, with functional groups highlighted that are also present in PEI&E3P.

Figure S2 demonstrates the presence of aromatics, C-H, C-OH, and C-N bonds, whose shifts are well-outlined in the literature, in the inner display film from a commercial TV display.[2,3] These functional groups are also present in PEI&E3P (see structure in Scheme 3-1). Therefore, although we could not confirm the presence of PEI&E3P in the TV display without doubt, the presence of such functional groups, and the patent describing the manufacture of PEI&E3P covered QDs for display indicate that a similar polymer is present in the plastic matrix surrounding the QDs.

3.8.2 Synthesis of CdSe/ZnS

All the reagents were purchased through Sigma-Aldrich, and all the solvents (ACS reagent grade) were purchased through Fischer Scientific. The purity of the both the CdO and the Se were ≥ 99.9%; both compounds were purchased from Sigma- Aldrich. The Se was stored in a desiccator. All chemicals were used as purchased.

These syntheses were based on previously published CdSe core and CdS/ZnS shelling syntheses.[4,5] We modified the washing procedures of these syntheses. Below is a step-by-step procedure.

The Cd precursor was prepared in a 50 mL, 2-neck round bottom flask by combining 0.0256 g (0.0002 mol) of CdO and 0.114 g (0.0005 mol) of myristic acid in 4 mL of ODE. The mixture was stirred and heated to 290ºC, while N_2 was bubbled into the solution. The Se precursor was prepared by sonicating 0.0237 g (0.0003 mol) of elemental Se powder in 3 mL of ODE for ~10 min; this was done to uniformly suspend the Se in the ODE.

After ~30 min of heating, the CdO and myristic acid to form a Cd-myristate precursor which resulted into a colourless and transparent solution. The temperature was reduced to 250ºC, and 1 mL of the Se precursor was injected into the reaction mixture. After ~5 min of growth, 0.1 mL of the Se precursor was injected into the reaction mixture, and the reaction proceeded for an additional 3 min. After the 3 min reaction period, the previous injection was conducted once more, and the reaction proceeded for an additional 3 min. Because the Se precursor was only stable ~5 min after sonication, the Se precursor was sonicated between each injection to ensure a uniform suspension.

The resulting quantum dot solution was split equally between two centrifuge tubes and quenched with 10 mL of toluene. ~5 mL of acetonitrile was added to the centrifuge tubes to crash out the nanoparticles, and the mixture was centrifuged at 10000 rpm for 5 minutes. This washing procedure was conducted three times. To store the nanoparticles, they were suspended in ~10 mL of toluene.

After the 0.0383 g (0.0002 mol) of synthesized CdSe was dissolved in minimal amounts of toluene, the solution was added to a 50 mL, 2-neck round bottom flask, along with 6 mL of

ODE and 1 g of octadecylamine. The mixture was heated to 235ºC, and the toluene was boiled out of the solution for ~30 minutes. Once the mixture stopped boiling, the flask was capped, and N_2 was bubbled into the solution for the rest of the reaction. Three solutions were prepared for the shelling of the CdSe nanoparticles – Cd, Zn, and S precursors. To prepare the Cd and Zn precursors, 3.09 g of oleic acid and 9 mL of ODE were added into two vials. The vials were stirred and heated to 250ºC while N_2 was bubbled through both solutions. Once the solutions were yellow and transparent, the temperature was dropped to 80ºC, and the solutions were maintained at that temperature throughout the synthesis. The S precursor was prepared by adding 0.032 g of S into a vial with 10 mL of ODE and was sonicated for ~10 min.

Once the CdSe solution became transparent each of the specified additions were injected, dropwise, into the solution, where 10 min of growth was allowed after each addition – unless otherwise specified. This resulted in four separate monolayers on the surface of the CdSe nanoparticles. First monolayer: 0.75 mL of Cd precursor, and 1.5 mL of S precursor. Second monolayer: 0.9 mL of Cd precursor immediately followed by 0.9 mL of Zn precursor, and 1.9 mL of S precursor. Third monolayer: 1.1 mL of Cd precursor immediately followed by 1.1 mL of Zn precursor, and 2.3 mL of S precursor. Fourth monolayer: 2.7 mL of Zn precursor and 2.7 mL of S precursor.

Once the shelling was complete, the quantum dot solution was split into four separate centrifuge tubes, and each fraction was quenched with 5 mL of hexanes. As the solution cooled, excess octadecylamine would precipitate out of the solution, so, once the mixture was at room temperature, the mixture was centrifuged at 10,000 rpm for 5 min. The resulting solution, which contained the colloidal nanoparticles, was decanted into separate centrifuge tubes. 10 mL of isopropanol (iPrOH) was added to each tube, and the mixtures were centrifuged at 10,000 rpm for 5 min. After disposing the washing solution, the precipitate was resuspended in 5 mL of hexanes. 10 mL of acetone was added to the quantum dot solution, and the mixture was centrifuged at 10,000 rpm for 5 min; this process was conducted twice. The final precipitate was stored under a vacuum to dry.

3.8.3 Analysis of pristine CdSe/ZnS

Thermal Gravimetric Analysis (TGA) was conducted with a Mettler and Toledo TGA/DSC Stare System to monitor the amount of ligand attached to the surface of the nanoparticles. The method utilized a temperature range of 30 – 700 ºC under air, which was at a flow rate of 40 mL/min, and the sample was heated at a rate of 10ºC/min.

Powder X-Ray Diffraction (pXRD) was conducted using the Bruker D8 Advance to monitor lattice structure. The recorded 2θ range was 10º - 80º, and the sample was rotated at a rate of 15 rot/min. The step rate was set at 5985 steps/s. The primary and secondary slit widths were set at 0.600 mm and 2.500 mm, respectively.

A Bruker AVIIIHD 500 MHz was used to find the NMR spectrum of the final product. To measure the NMR spectrum, the final product was dissolved in chloroform-d.

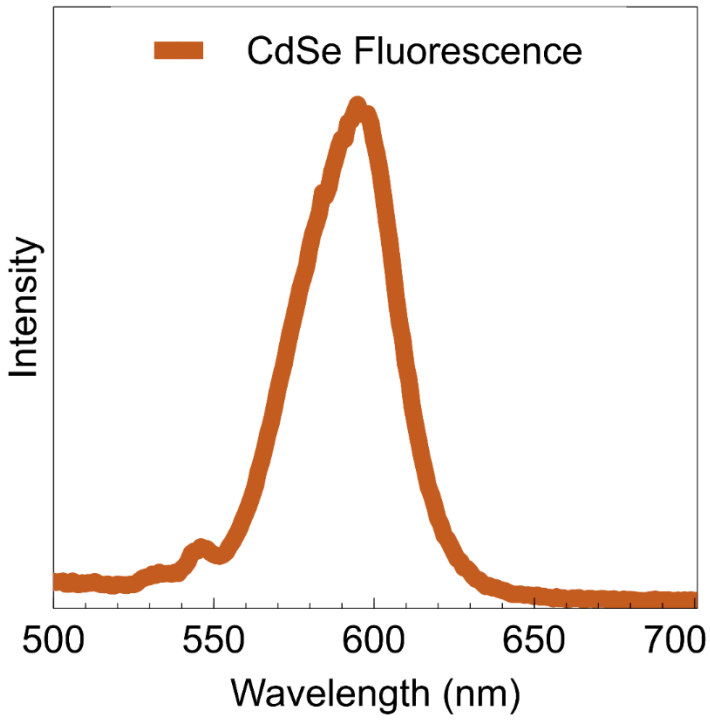

Figure S3-8: CdSe fluorescence with excitation at 400nm, emission from 500-700nm

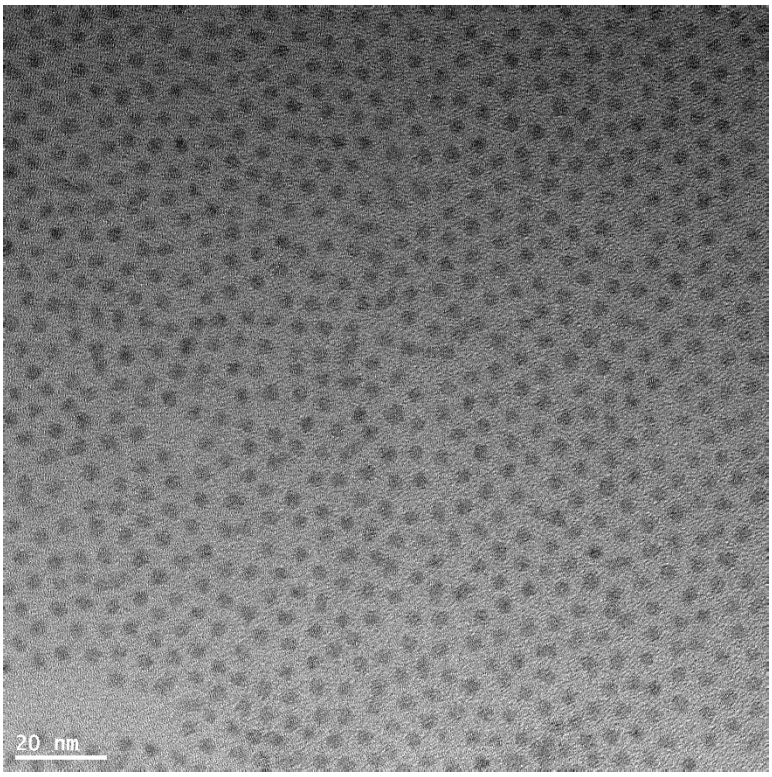

Figure S3-9: TEM of CdSe core used for size estimations (n=50)

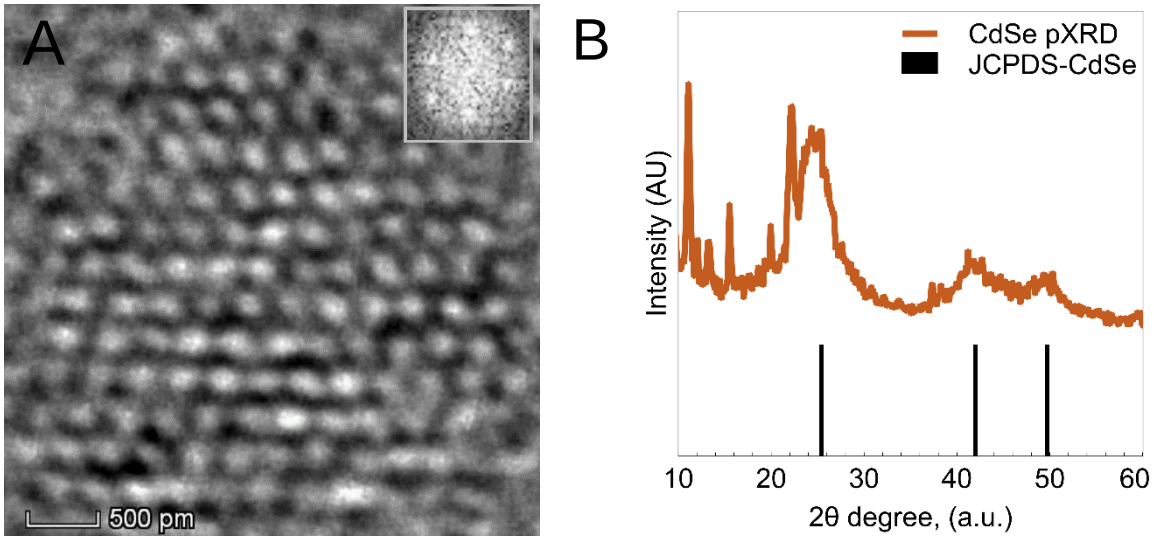

Figure S3-10: (A) TEM image of CdSe QD displaying crystallinity (B) pXRD of CdSe QDs (orange) with expected peaks represented as black bars.[6] Other peaks < 20° correspond to the presence of myristic acid ligand, as the intensity of these peaks decreased after washing.

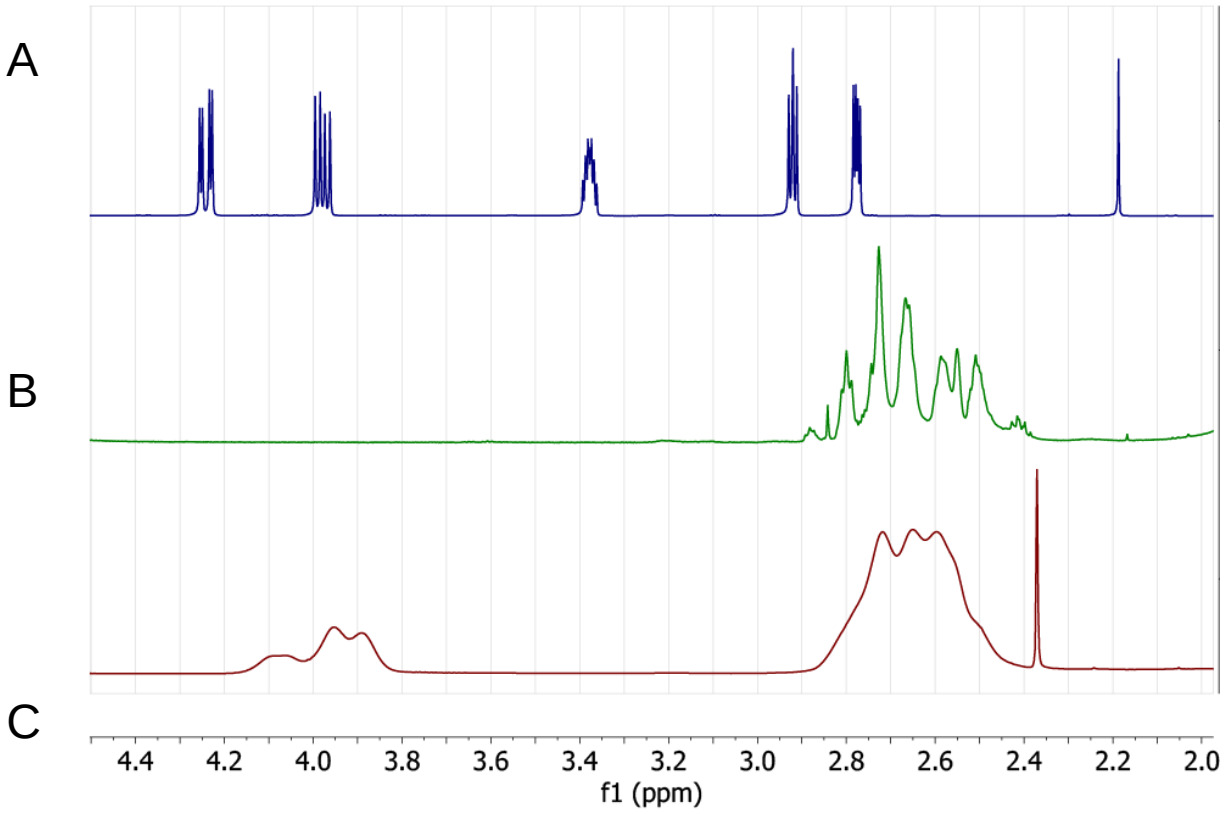

Figure S3-11: ^{1}H-NMR of (A) 1,2-epoxy-3-phenoxypropane (E3P), (B) polyethylene imine (PEI) and (C) the polymer PEI&E3P.

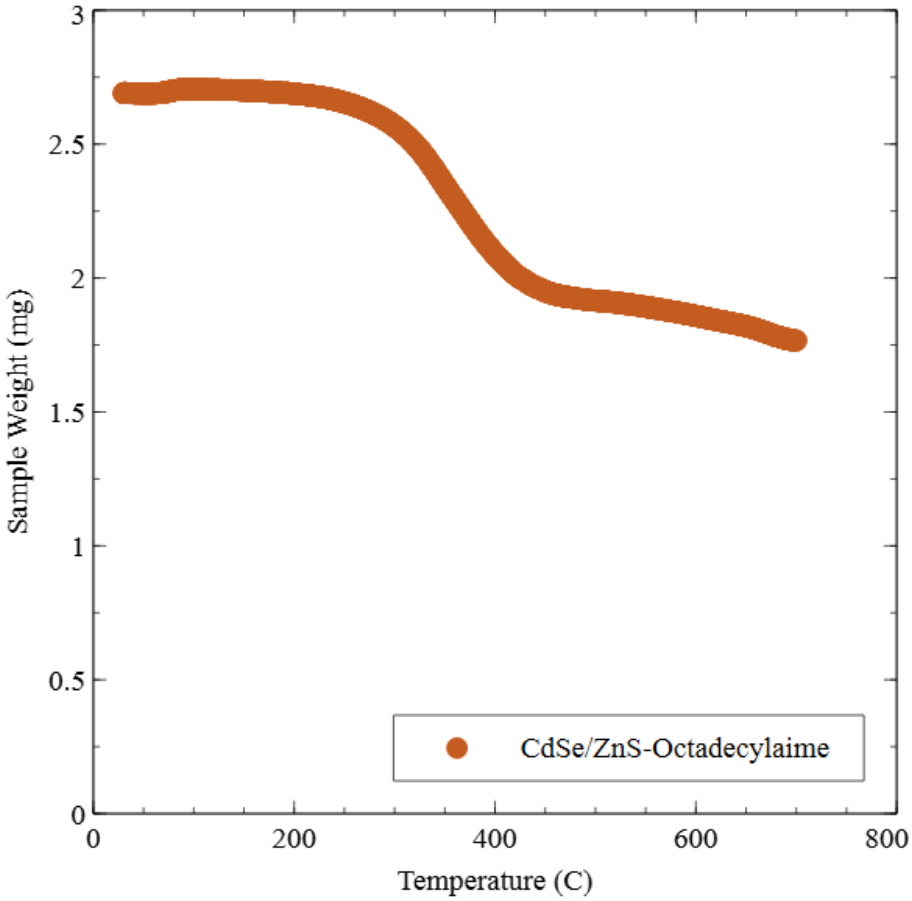

Figure S3-12: TGA of CdSe/ZnS-Octadecylamine.

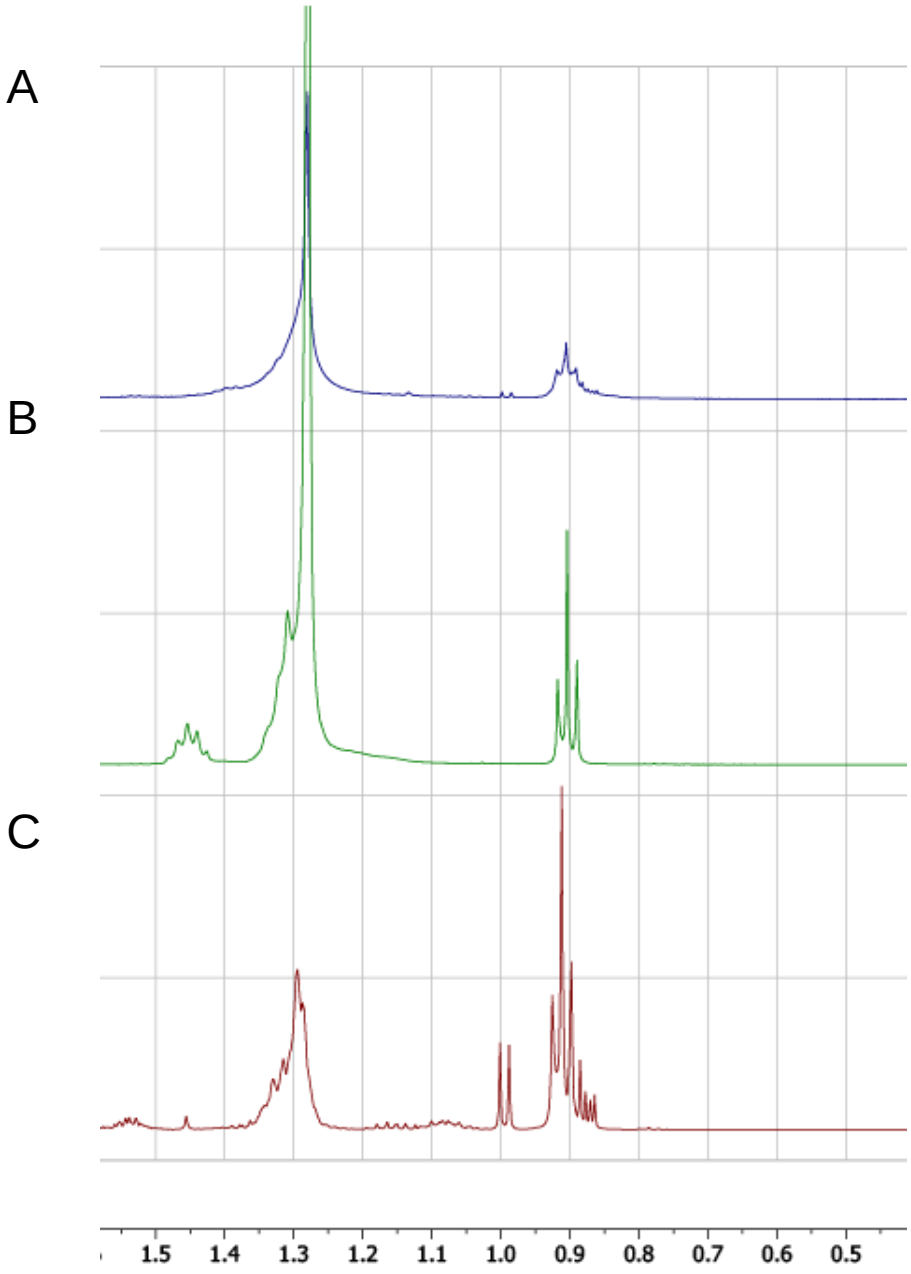

Figure S3-13: ^{1}H-NMR of (A) octadecylamine, (B) CdSe/ZnS-octadecylamine, (C) CdSe/ZnS-PEI&E3P with traces of octadecylamine.

Table S3-1:Effect of coating CdSe particles with ZnS-PEI&E3P on the fluorescent properties of the samples.

QD sample	Peak Wavelength (nm)	FWHM (nm)
CdSe	595	37
CdSe/ZnS-PEI&E3P	584	34

3.8.4 Blanks of dissolution tests

The following blanks were performed for the dissolution tests (Table S3-2). These demonstrate that the filtration method is effective at recovering >90% of the ions in solution and in QDs, even in the presence of the QD ligand (PEI&E3P) or a proxy for that ligand (PEI).

Table S3-2: Recovery of ions and QDs from 3 kDa filters after 24h for ions, and after 0h for the QDs.

Description of tested solution	Cd recovery	Zn recovery
pH 4, 3000 ppb Cd, Zn, S, Se, 250 mg/L PEI	95%	100%
pH 4, QDs at 4 mg/L Cd	90%	94%

In addition to these tests, for every dissolution test the stock solution of QDs was digested to determine the initial concertation of QDs in solution. This was matched to the total ions recovered (both in the retentate and the filtrate) and the missing ion fraction (<10%) was attributed to QDs. This method aligns with previous studies that have used 3 kDa filters to separate QDs from their ionic constituents.[7–9] Lastly, in the QD sample, all of the Zn and Cd were recovered in the >3 kDa fraction, indicating that these elements are present in a QD particle, rather than as ions.

3.8.5 Synthesis of ZnS QDs

The synthesis of ZnS QDs was an adaptation from Trimmel et al.[10] A mixture of ZnCl2 (272.6 mg, 2.00 mmol, 1.0 eq.) and oleylamine (10 mL, 30.3 mmol, 15.1 eq.) were heated to 170

°C for 30 min. Then the solution was allowed to cool to room temperature while stirring continued. A solution of sulfur (192.4 mg, 6.00 mmol, 3 eq.) in oleylamine (3 mL, 9.08 mmol, 4.5 eq.) was then added to this mixture at room temperature. This sulfur solution, if made >10min before its addition to the zinc solution, would turn a dark red color. This color change did not impact the final state of the QDs. The solution of sulfur and zinc in oleylamine at room temperature was then heated to 210 °C for 1h. After the solution was cooled to room temperature, the solution was transferred to centrifuge tubes. Methanol was added to the centrifuge tubes and the ZnS QDs precipitated after centrifugation at 10000 rpm for 5 min. These particles were then dried with a rotary evaporator and stored in vacuum until use.

The particles were characterized to ensure their size and their crystallinity. The size of these QDs was 4.0 ± 0.6 nm (n=100) and the crystallinity, observed on both the nano-scale and over the entire sample, indicated a cubic structure.

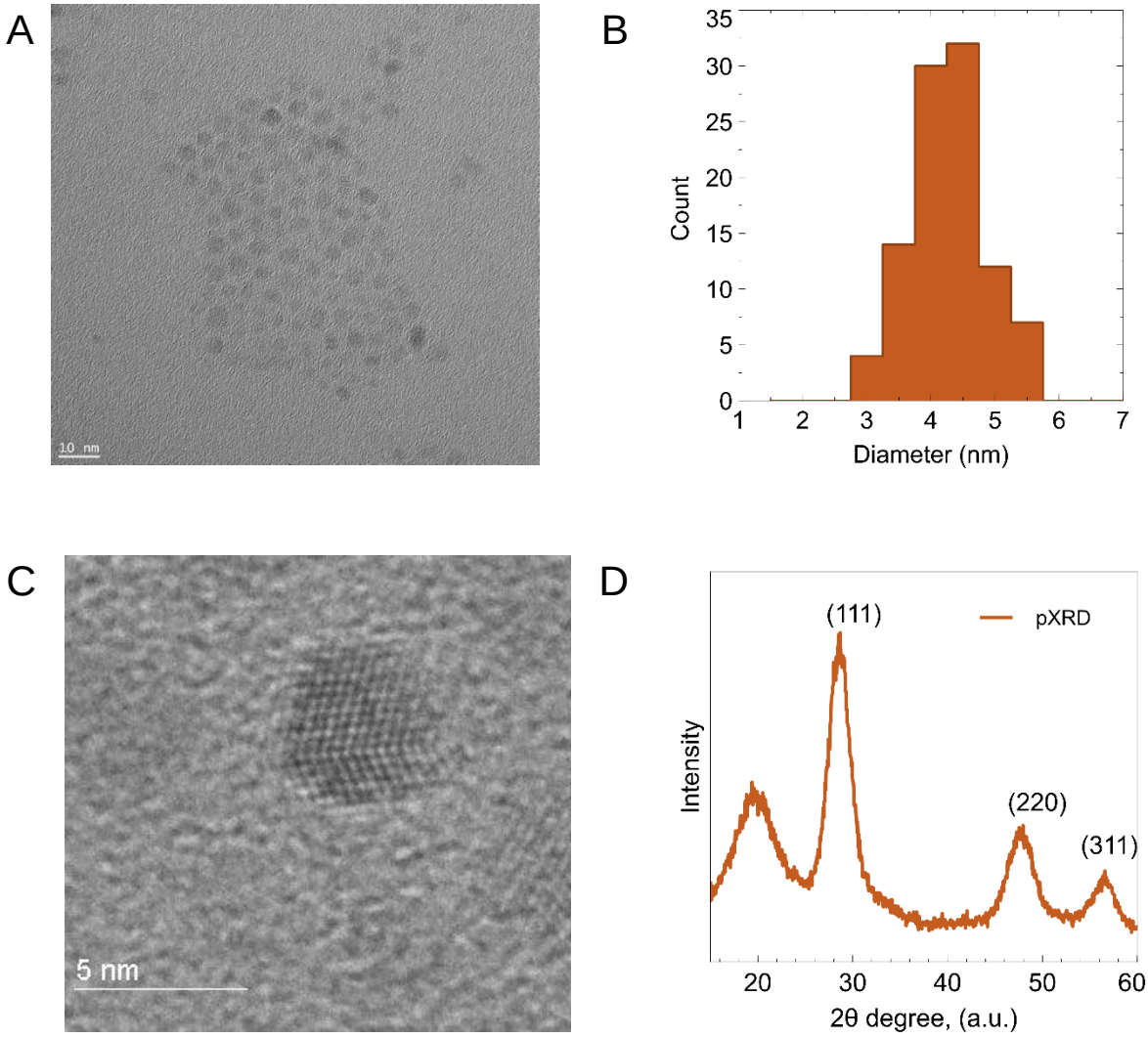

Figure S3-14: (A) Representative ZnS TEM image and (B) ZnS size distribution (n=100) (C) Representative ZnS TEM image displaying crystallinity of particle and (D) pXRD of ZnS NPs

The addition of PEI&E3P onto these particles was conducted in the same manner as CdSe/ZnS (see main text for procedure).

3.8.6 Hydrodynamic radius and zeta potential measurements

DLS and Zeta potential measurements were conducted with Wyatt Möbiuζ with Atlas attachment at 25 °C with a background concentration of electrolyte (0.01 mM KCl) at 0.3 mg/mL

CdSe/ZnS-PEI&E3P. The hydrodynamic size of each sample was calculated using the correlation function in the Wyatt proprietary software, DYNAMICS. Errors represent the standard deviation of three measurements. PDI of each of the samples was 0.57, except for the sample at pH 8 after 1 day (PDI=0.47).

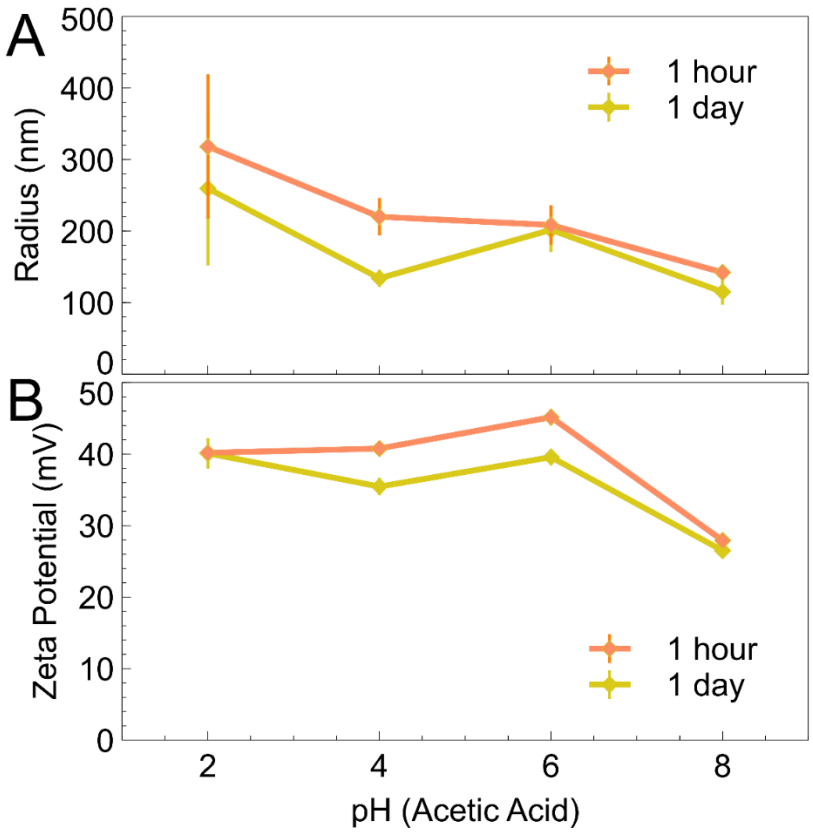

Figure S3-15: (A) Zeta Potential of CdSe/ZnS-PEI&E3P suspended in 0.1 mM KCl with pH adjusted with acetic acid. (B) Hydrodynamic radius of CdSe/ZnS-PEI&E3P suspended in 0.1 mM KCl with pH adjusted with acetic acid. Error bars represent the standard deviation of three measurements

3.8.7 Fluorescence of QDs after exposure to pH 2-8

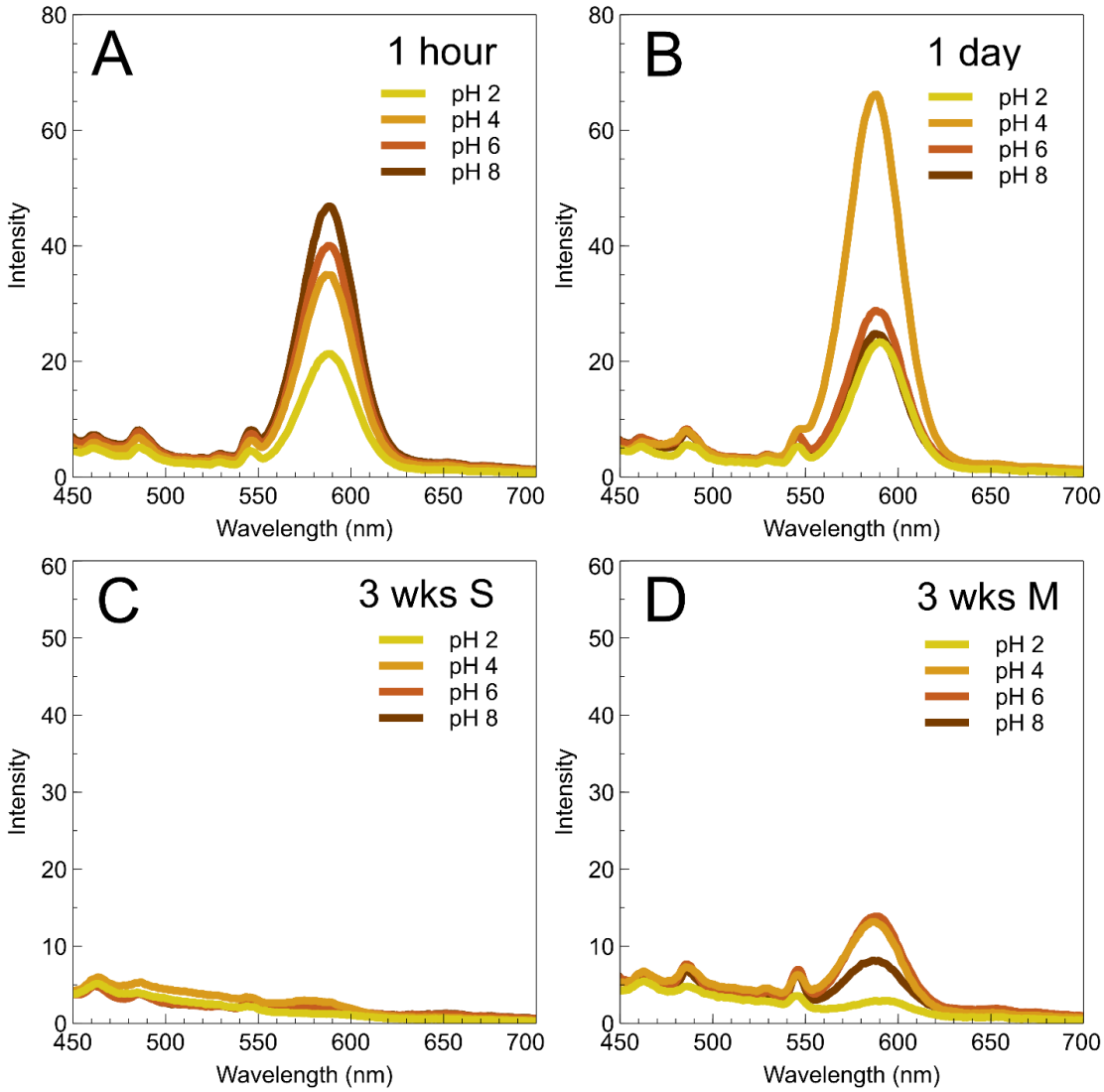

Figure S3-16: Fluorescence spectra of QDs aged at pH 2-8 after 1 hour (A), 1 day (B), 3 weeks (C,D) using acetic acid and under aerobic conditions. After 3 weeks, settling of the QDs occurred, and therefore spectra were taken of the supernatant solution (C) and the solution after mixing (D).

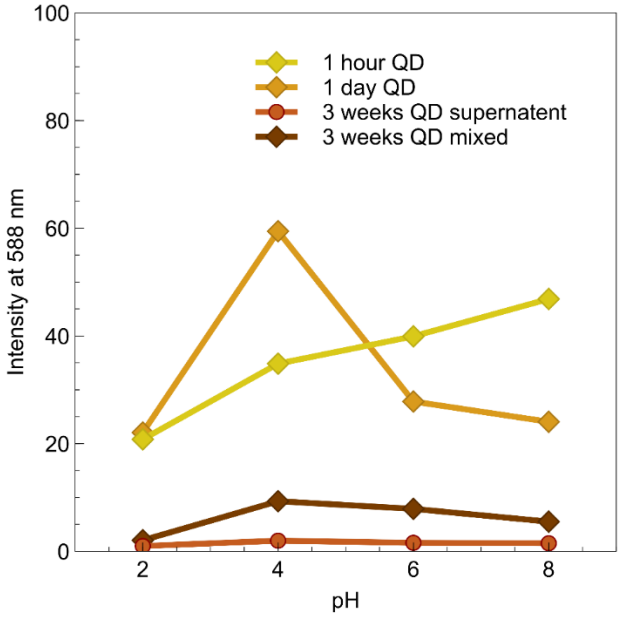

Figure S3-17: Intensity of fluorescence spectra at 588 nm after QDs aged at pH 2-8 after 1 hour, 1 day, and 3 weeks using acetic acid and under aerobic conditions. After 3 weeks, settling of the QDs occurred, and therefore spectra were taken of the supernatant solution and the solution after mixing.

3.8.8 CellTiter-Glo HepG2 cell viability curves and IC_{50} data

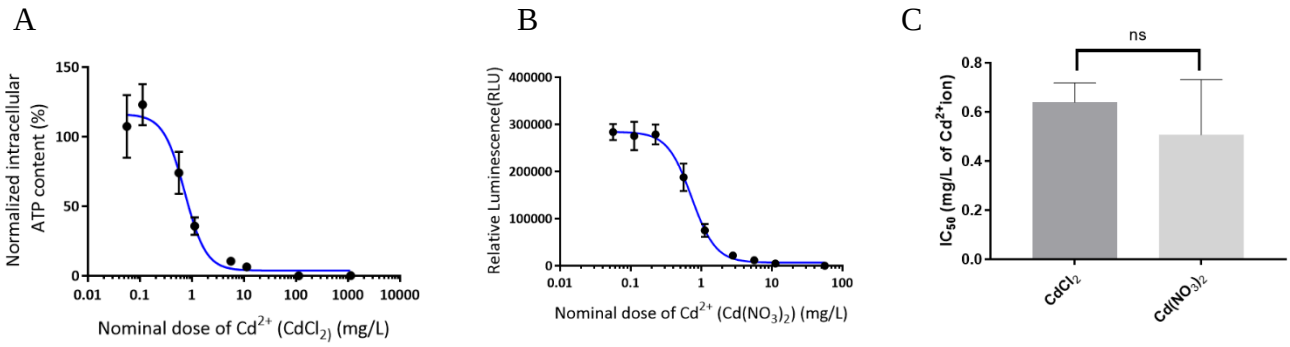

Figure S3-18: Cytotoxicity of cadmium ion in HepG2 cell model. A) Representative cell viability measured using $CdCl_2$ B) Representative cell viability measured using $Cd(NO_3)_2$. C) Comparison of IC_{50} values calculated using $CdCl_2$ and $Cd(NO_3)_2$.

Graph represents the mean and standard deviation from three biological experiments. Unpaired t-test confirm no significant difference (p = 0.38) between the IC_{50} measured using these two different cadmium compounds.

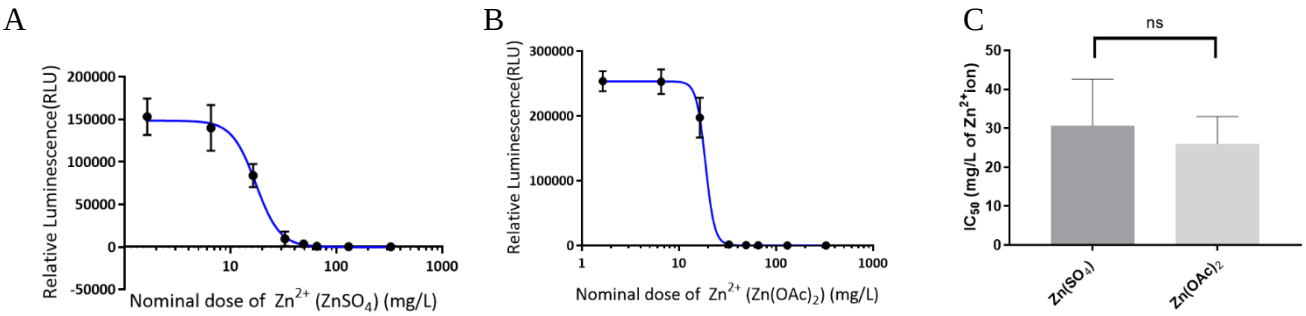

Figure S3-19: Cytotoxicity of zinc ion in HepG2 cell model. A) Representative cell viability measured using Zn(SO4) B) Representative cell viability measured using Zn(OAc)2. C) Comparison of IC50 values calculated using Zn(SO4) and Zn(OAc)2.

Graph represents the mean and standard deviation from three biological experiments. Unpaired t-test confirm no significant difference (p = 0.59) between the IC_{50} measured using these two different zinc compounds.

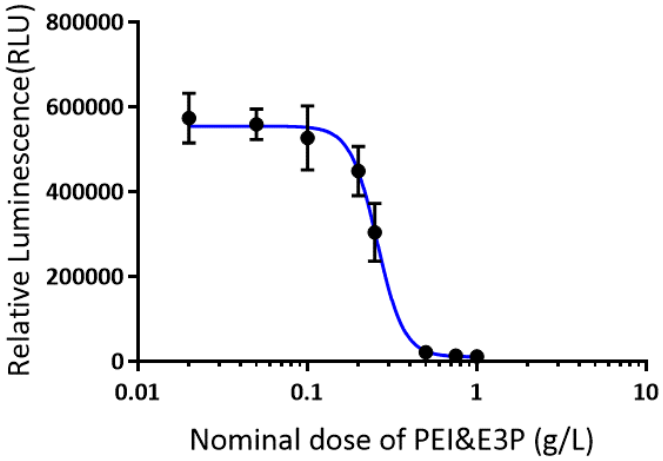

Figure S3-20: Representative cell viability results for determining the cytotoxicity of PEI&E30 in the HepG2 cell model.

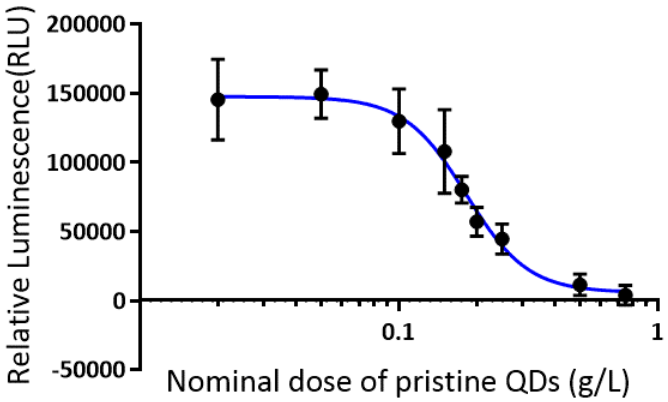

Figure S3-21: Representative cell viability results for determining the cytotoxicity of pristine QDs in the HepG2 cell model.

HepG2 cell were seeded onto cover slips in a 6-well microplate. Specifically, the coverslips were autoclaved and kept sterile before being put into wells. 600,000 cells were seeded in each well and left to attach to the coverslips in 2 mL media. After 24 hours, the media was carefully replaced with fresh media containing QDs and HepG2 cells incubated for 24 hours. QDs were then removed and cells were washed carefully with PBS. Cells were fixed using 4% PFA and stained with 300 nM DAPI for 5 minutes followed by rinsing with PBS and mounting with ProLong™ Gold Antifade Mountant on a slide for confocal imaging. Images were taken using a TCS Leica SP8 Multiphoton and analyzed with ImageJ.

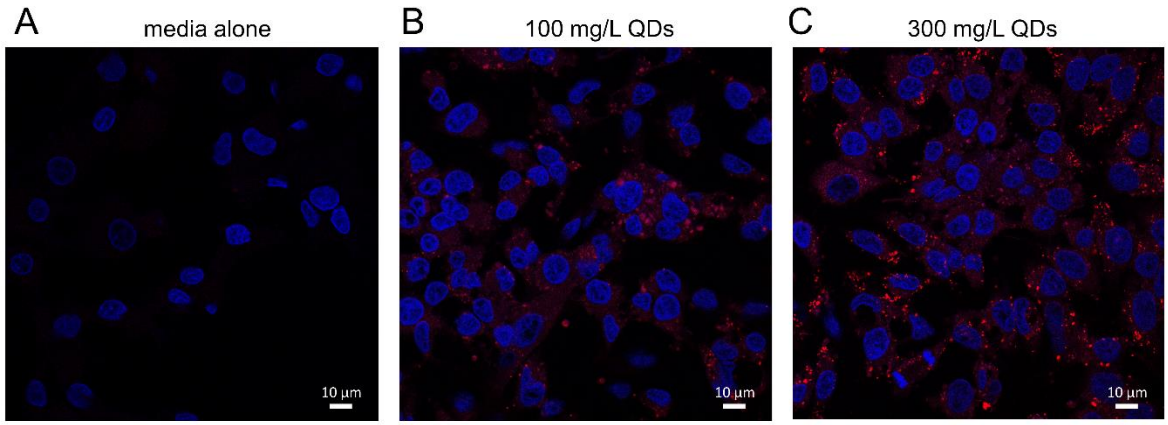

Figure S3-22: HepG2 cells were incubated for 24 hours with (A) cell media alone or with concentrations of QDs (B) below and (C) above the IC_{50}. Cells were washed, fixed, stained with DAPI and analyzed by confocal laser scanning microscopy using a TCS Leica SP8 Multiphoton. Images were analyzed with ImageJ 1.47c. Blue = DAPI; Red = QDs.

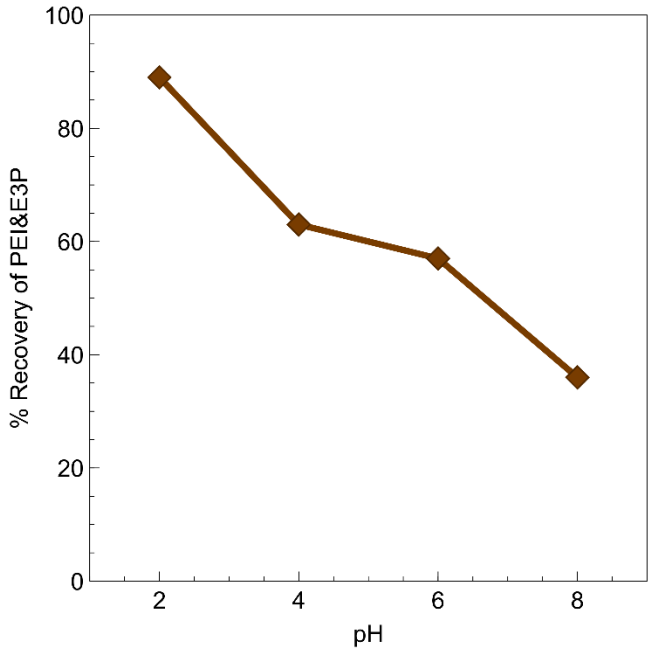

Figure S3-23: Percent recovery of PEI&E3P in 3 kDa filter after ageing for 1 day at pH 2-8.

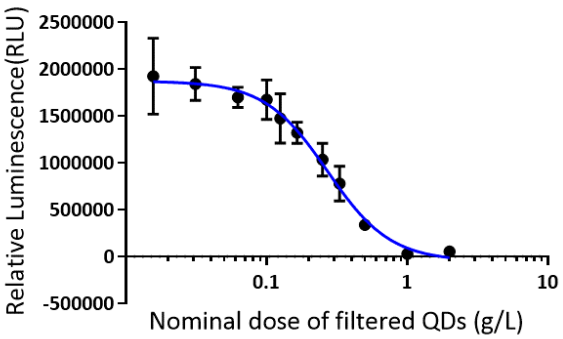

Figure S3-24: Representative cell viability results for determining the cytotoxicity of aged, filtered QDs in the HepG2 cell model.

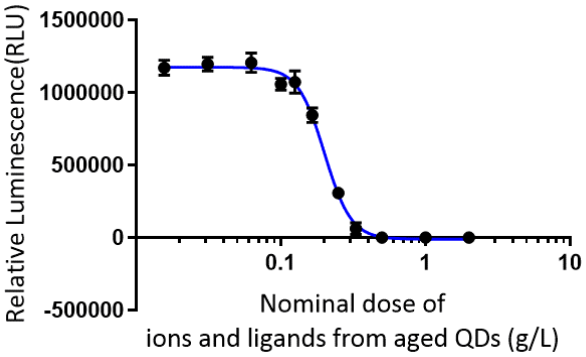

Figure S3-25: Representative cell viability results for determining the cytotoxicity of ions and ligands leached from QDs in the HepG2 cell model.

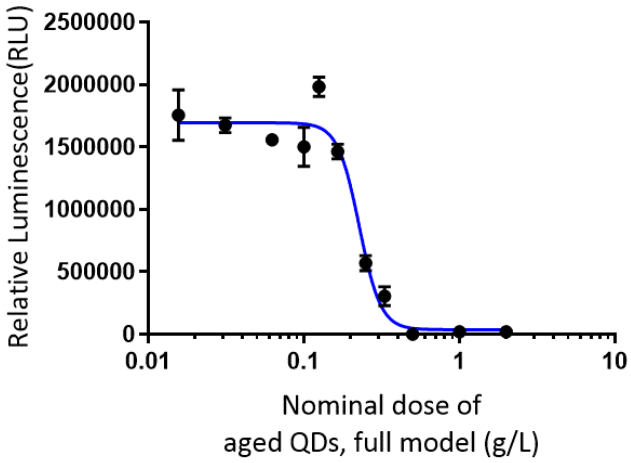

Figure S3-26: Representative cell viability results for determining the cytotoxicity of the full aged model of QDs in the HepG2 cell model.

Table S3-3: IC_{50} values from each trial and the calculated average and standard deviation.

	$CdCl_2$ (mg/L)	**$Cd(NO_3)_2$ (mg/L)**	**$Zn(SO_4)$ (mg/L)**	**$Zn(OAc)_2$ (mg/L)**	**PEI-E3P (g/L)**	**Pristine QDs**	**Filtered QDs**	**Ions and Ligands**	**Full model**
Trial 1	0.73	0.28	36	26	0.23	0.13	0.25	0.14	0.23
Trial 2	0.6	0.51	39	19	0.26	0.17	0.27	0.2	0.16
Trial 3	0.59	0.73	17	33	0.17	0.16	0.36	0.16	0.18
Average	0.64	0.51	30.67	26.00	0.22	0.15	0.29	0.17	0.19
St Dev	0.08	0.23	11.93	7.00	0.05	0.02	0.06	0.03	0.04

3.8.9 References for Supporting Information:

(1) Johnson, R. L.; Schmidt-Rohr, K. Quantitative Solid-State 13C NMR with Signal Enhancement by Multiple Cross Polarization. *J. Magn. Reson.* **2014**, *239*, 44–49. https://doi.org/10.1016/j.jmr.2013.11.009.

(2) Schmidt-Rohr, K.; Spiess, H. W. *Multidimensional Solid-State NMR and Polymers.*; Elsevier Science: Jordan Hill, 2012.

(3) Holycross, D. R.; Chai, M. Comprehensive NMR Studies of the Structures and Properties of PEI Polymers. *Macromolecules* **2013**, *46* (17), 6891–6897. https://doi.org/10.1021/ma4011796.

(4) Zhou, J.; Zhu, M.; Meng, R.; Qin, H.; Peng, X. Ideal CdSe/CdS Core/Shell Nanocrystals Enabled by Entropic Ligands and Their Core Size-, Shell Thickness-, and Ligand-Dependent Photoluminescence Properties. *J. Am. Chem. Soc.* **2017**, *139* (46), 16556–16567. https://doi.org/10.1021/jacs.7b07434.
(5) Xie, R.; Kolb, U.; Li, J.; Basché, T.; Mews, A. Synthesis and Characterization of Highly Luminescent CdSe−Core CdS/Zn 0.5 Cd 0.5 S/ZnS Multishell Nanocrystals. *J. Am. Chem. Soc.* **2005**, *127* (20), 7480–7488. https://doi.org/10.1021/ja042939g.
(6) Chen, X.; Hutchison, J. L.; Dobson, P. J.; Wakefield, G. Highly Luminescent Monodisperse CdSe Nanoparticles Synthesized in Aqueous Solution. *J. Mater. Sci.* **2009**, *44* (1), 285–292.
(7) Metz, K. M.; Mangham, A. N.; Bierman, M. J.; Jin, S.; Hamers, R. J.; Pedersen, J. A. Engineered Nanomaterial Transformation under Oxidative Environmental Conditions: Development of an in Vitro Biomimetic Assay. *Environ. Sci. Technol.* **2009**, *43* (5), 1598–1604. https://doi.org/10.1021/es802217y.
(8) Wiecinski, P. N.; Metz, K. M.; King Heiden, T. C.; Louis, K. M.; Mangham, A. N.; Hamers, R. J.; Heideman, W.; Peterson, R. E.; Pedersen, J. A. Toxicity of Oxidatively Degraded Quantum Dots to Developing Zebrafish (Danio Rerio). *Environ. Sci. Technol.* **2013**, *47* (16), 9132–9139. https://doi.org/10.1021/es304987r.
(9) Li, Y.; Zhang, W.; Li, K.; Yao, Y.; Niu, J.; Chen, Y. Oxidative Dissolution of Polymer-Coated CdSe/ZnS Quantum Dots under UV Irradiation: Mechanisms and Kinetics. *Environ. Pollut.* **2012**, *164*, 259–266. https://doi.org/10.1016/j.envpol.2012.01.047.
(10) Rath, T.; Novák, J.; Amenitsch, H.; Pein, A.; Maier, E.; Haas, W.; Hofer, F.; Trimmel, G. Real Time X-Ray Scattering Study of the Formation of ZnS Nanoparticles Using Synchrotron Radiation. *Mater. Chem. Phys.* **2014**, *144* (3), 310–317. https://doi.org/10.1016/j.matchemphys.2013.12.045.

4 Linking transformation of cadmium-containing quantum dots in simulated human digestive system to toxicity.

K. Xu, A. Bechu, N. Basu, S. Ghoshal*, A. Moores*, S. George* "Hazard profiling of components constituting a commercially-relevant functional quantum dot revealed synergistic interactions between heavy metals and polymer" Chem. Res. Tox. 2021 (submitted Nov. 10 2021, ID: tx-2021-00382n)

Bechu & K. Xu. N. Basu, S. Ghoshal*, A. Moores*, S. George* "Linking transformation and toxicity of Cd-containing quantum dots in the simulated human digestive system" manuscript in preparation.

4.1 Connecting text

With the synthesis of this commercially relevant QD, we explored the impact of oxygen and pH in dark aqueous conditions. There are many other species in the environment that could interact with QDs, such as light and humic acids. As we mentioned in the introduction, there has been significant work with these environmental factors, but less work in biologically relevant environments. We identified a particularly interesting environment, the human digestive system, as the next environment for these QDs. We partnered with toxicologists to find out whether the commercial QDs were more toxic than their components to intestinal epithelial cells. Then, we decided to probe the transformations of QDs in a simulated human digestive system.

4.2 Abstract:

Nanomaterials are increasingly complex and increasingly ingested by the general population, which exposes the nanomaterials to a new environment and set of human cells. These complexities cannot be explored for each circumstance – there are simply too many nanoparticles and factors relating to digestion. We therefore used a well-characterized multi-

component nanomaterial (quantum dots) to explore complexities inherent to nanomaterial structure. We compared synergistic toxicity effects of coating and inorganic shells of pristine samples. With this baseline, we then tracked the transformation the nanoparticles in a simulated human digestion system to identify key transformations. We observed dissolution and increased dispersion of quantum dots and association of quantum dots with biomolecules in solution. We propose that these transformations are necessary to interpret the changing toxicity of nanoparticles throughout human digestion. This work enabled further investigation on toxicity by our collaborators.

4.2.1 Introduction:

Cytotoxicity of quantum dots (QDs) was first reported in the early 2000s.[1] Almost 20 years later, mechanistic questions still remain because of the complex nature and shifting applications of QDs. Initially designed as biosensors[2] and for probing fundamental behaviors of excitons,[3] quantum dots are now commercially used as color converters in electronic display screens.[4] This expansion of applications is partly due to the tunability of the core, shell, and coating of quantum dots. This tunability has enhanced the light emission and stability of QDs and allowed for their dispersion into various media.

The varied uses of QDs makes it important to assess their safety to human health. The cytotoxicity and subcellular effects of a diverse set of QDs has therefore become more heterogenous as well. Early on, a decrease in cytotoxicity was linked to the addition of ZnS shells.[5] Studies have also shown that the coating of QDs with positive charges increases cytotoxicity.[6] Such studies are difficult to compare to one another to determine which component of a quantum dot (shell, coating etc.) has the largest impact. This is due to the different conditions of the studies, such as organism, dose, and specific QD structure. Analyzing many QD toxicity studies to determine trends has been partly addressed by thorough meta-analyses of toxicity data of QDs.[7,8] These studies combed through 307-517 studies of QD toxicity and extracted key attributes such as QD structure, dose, organism and exposure time. They then calculated LD_{50} 7uy6uuuuui8and ran a random forest or Bayesian network analysis to determine which attributes had the largest impacts on the outcome. Depending on the analysis method used though, slightly different prioritizations have been assigned (e.g. the shell is more important than

the ligand in one analysis, but not the other). In addition, these meta-analyses do not tend to focus on QDs currently used on commercial applications. Quantum dots in commercial applications were primarily designed for long term stability and integration into plastics, rather than benign behavior in biologically-relevant situations.

We established a commercially relevant quantum dot model in our previous work[9] that was based on a patent for QDs in devices.[10] This particle, CdSe/ZnS-P&E had a CdSe core because this material can be tuned to emit at specific green and red wavelengths desirable for display applications.[10] The CdS/ZnS shells allowed for enhanced stability of the core, compared to a ZnS shell.[11] Lastly, the polymer P&E was synthesized from polyethylene imine and 1,2-epoxy-3-phenoxypropane.[10] This polymer allowed for integration of the CdSe/ZnS QD into plastic films needed for display applications.[10]

This complex nanoparticle, CdSe/ZnS-P&E, can have toxicity and subcellular impacts arising from either different components, or a combination of these components. We define component as one part of the CdSe/ZnS-P&E (Figure 4-1). The simplest components are CdSe and ZnS QDs (no polymer) as well as the polymer alone (P&E). Combining two of these simplest components yielded CdSe-P&E, ZnS-P&E and CdSe/ZnS. We ran a series of toxicity and subcellular effect tests to establish the toxicity of different components. To quantitively compare these combinations, we applied a combination index (CI). CI compares the modeled additive toxicity of components to the actual toxicity of a mixture to determine whether components had interactions that led to higher or lower toxicity. This method is commonly used for additive effects of mixtures of drugs, but we hypothesized that its application to nanomaterials can also help to decipher the relative importance of different components. This work will be presented in the first section of this chapter.

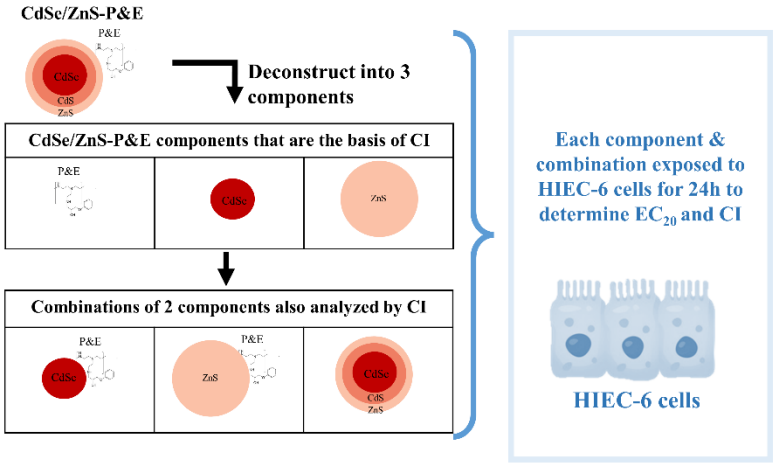

Figure 4-1: Schematic of commercially-relevant CdSe/ZnS-P&E as well as its basic components (P&E, CdSe, and ZnS) and combinations of 2 basic components (CdSe-P&E, ZnS-P&E, and CdSe/ZnS).

The objective of this first section was to quantitatively examine the impact of different components of quantum dots onto intestinal epithelial cells. This first objective prompted the question as to whether, in a real-world scenario, pristine quantum dots could encounter cells in the human intestine. The short answer is no. Only QDs transformed by the GI tract environment (or other nanoparticles) would encounter cells in the human intestine in a real-world scenario. The GI tract can be simulated using three different environments: salivary, gastric, and intestinal phases.[12]

The incorporation of certain nanoparticles into foods and food packaging is currently allowed by regulatory bodies in most countries.[13] For example, TiO_2 and SiO_2 for whitening and anti-clumping agents, FeO used for nutrition, and Ag used as an antimicrobial.[14] In North America, the lack of regulation pushing for nanoparticle designation in food ingredients has complicated exact ingestion estimates. Concurrently, risk assessment methods for nanoparticles in the intestinal system remaining under development.[15] A recent review of studies probing the toxicity of nanomaterials in the digestive tract found that only 12% of studies considered the dissolution kinetics of nanoparticles.[16] Most of these studies are therefore disconnected from the transformation of nanomaterials from simulated human digestion.

In general, nanoparticle toxicity can be altered after transformation in certain environments due to a change in speciation, dissolution, or hetero-aggregation (i.e. the formation of an eco-corona).[17] Such transformations have been noted for nanomaterials exposed to simulated human digestive system. For example, the formation of an enzyme corona has been observed for magnetite nanoparticles.[18] The dissolution of ZnO and SiO_2 (and subsequent reprecipitation of SiO_2) has also been observed.[19] Abdelkhaliq et al. recently reported on the transformation and toxicity of Ag NPs, finding that a significant amount of Ag dissolved and that transformed NPs (100% cell viability at 2,500 μg/L) were less toxic than the equivalent amount of pristine Ag NPs (80% cell viability at 2,500 μg/L).[20] Abdelkhaliq et al.'s work laid important grounds for this study, but we propose examining transformation at each digestion step separately.

Subsequently, the objective of the second part of this chapter is to identify transformations of CdSe/ZnS_P&E in the simulated digestive system at each step that could be correlated to toxicity changes in subsequent studies. We focused on changes in nanoparticle dissolution and dispersion in the gastric phase that are maintained in the intestinal phase. Later studies by our collaborators [data not shown here] will associate changes in toxicity of CdSe/ZnS_P&E as they travel through the simulated human digestive system. We hope that this work can serve as an example of pairing transformation and toxicity to strengthen studies probing the safety of nanoparticles in the digestive system.

4.3 Results and Discussion:

4.3.1 Pristine Toxicity Study

Our first goal was to investigate the toxicity of specific components of quantum dots. Each component was synthesized independently (Figure 4-2). The complete quantum dot system has a CdSe core protected by a ZnS shell and is coated with a polyethylene imine-based polymer (P&E) from a previous study. For this study, we considered three of its components; CdSe quantum dots, ZnS quantum dots, as well as the P&E alone. These components were combined into CdSe-P&E or ZnS-P&E as well.

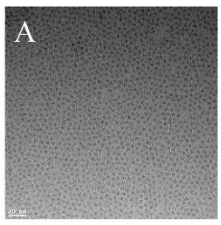

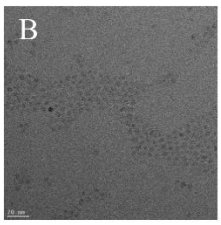

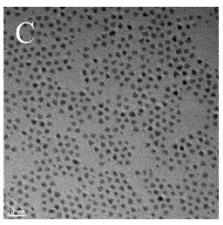

D

QD	Zeta Potential (mV)	Diameter (DLS, nm)
CdSe _P&E	15 ± 6	85 ± 6
ZnS_P&E	7 ± 4	66 ± 6
CdSe/ZnS_ P&E	14 ± 6	141 ± 33

E

Weight Percent (% wt)	CdSe	CdSe_P&E	ZnS	ZnS_P&E	CdSe/ZnS	CdSe/ZnS _P&E	P&E
%wt Cd	13	2	0	0	30	2	0
%wt Zn	0	0	31	1	15	1	0
%wt P&E	0	83	0	95	0	93	100

Figure 4-2: TEM images of (A) CdSe QDs, (B) ZnS QDs, (C) CdSe/ZnS QDs. The zeta potential and hydrodynamic size of the polymer-capped QDs (D) is presented. E) Cd and Zn contents were measured with ICP-OES and P&E contents were calculated from the synthesis. The remaining percent weight of the compounds is composed Se and/or S and different organic ligand resulting from the synthesis

Next, Human Intestinal Epithelial Cell-6 (HIEC-6) cells were exposed to each of these components. The dose-response (mortality) relationship of these components was then measured (see SI 4.7.1 for results gathered by Ke Xu). The EC_{20} (20% of the effective concentration that caused mortality over the fixed exposure time of 24h) was then determined from these dose response curves (

Table S4-1). For our purposes EC_{20} serves as a benchmark to compare each of the components (see SI 4.7.2). This comparison is done quantitatively using a combination index, CI[21] (eq. 1) which compares the expected contribution of toxicity of a component (using its EC_{20} and concentration in the mixture) to the entire mixture (using the mixtures EC_{20}).

$$CI = \frac{C_{1M}}{E_{C_1}/E_M} + \frac{C_{2M}}{E_{C_2}/E_M} + \frac{C_{nM}}{E_{C_n}/E_M} \quad (1)$$

Where C_n is the concentration of the component in the mixture. The denominator is E_{Cn}/E_M which represents the ratio between the benchmark toxicity of the component to the total

toxicity benchmark of the mixture. In the case of additive toxicity (i.e. no synergism or antagonism) this number should be the same as C_n, which is the concentration of the component in the mixture. In summary, the expected contribution of toxicity of a component is in the numerator, while the actual contribution of the component in the mixture is in the denominator. Therefore, if the mixture is more toxic than the sum of its individual components (denominator > numerator) then the CI<1, indicating that the components had a synergistic effect on toxicity. A synergistic effect occurs when the two components dosed together are more toxic than the toxicity of the expected sum of the individual components. This calculation indicated that QD combinations that included the polymer (P&E) has synergistic interactions (Figure 4-3).

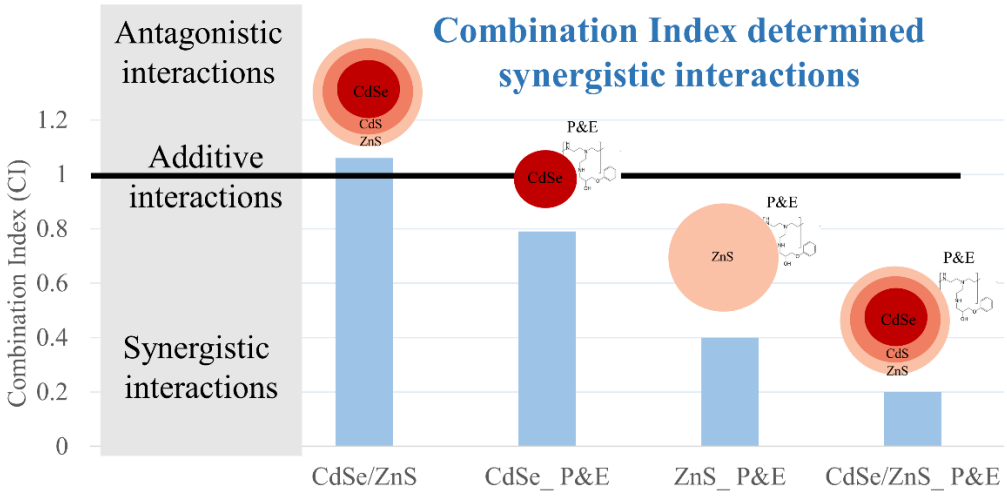

Figure 4-3: Combination Index of QD mixtures, with synergistic interactions (CI<1) and antagonistic interactions (CI>1) indicated on the left side of the graph. CIs are based on toxicity data gathered by Ke Xu (see appendix).

Interestingly, we found that the CdSe/ZnS-P&E combination had highest synergistic effects (CI= 0.2), even though CdSe/ZnS had slightly antagonistic effects (CI=1.1). An antagonistic effect (CI>1) occurs when the toxicity of a mixture is less than that expected from its components. In this study, we observed slight mediation of toxicity by the addition of one component (a ZnS shell, CI= 1.1). However, adding the polymer P&E, decreased the CI to 0.2,

demonstrating synergistic interactions. We decided to investigate whether this decrease in CI (i.e. synergistic toxicity) could be linked to increased cell uptake of CdSe/ZnS.

Therefore, we measured the uptake of the inorganic elements of the CdSe/ZnS_P&E into the cells (Figure 4-4). CdSe/ZnS-P&E demonstrated 6× higher uptake than CdSe/ZnS at the same dose (25 µg/mL after 3h exposure). This same dose of the QD mixture, however, indicates a different dose Cd because of the different percentage of Cd in the two mixtures (30% vs. 2% for non-polymer capped and polymer-capped, respectively, see Figure 4-2). When considering only Cd, we calculated that the uptake of Cd is 77-fold higher when Cd is present in polymer-capped QDs compared to Cd in non-polymer capped QDs. Although the different initial dose of Cd in this Cd-only comparison could play a role in the higher Cd uptake of the polymer-capped QDs, we concluded that the presence of the polymer increases the uptake of CdSe/ZnS QDs.

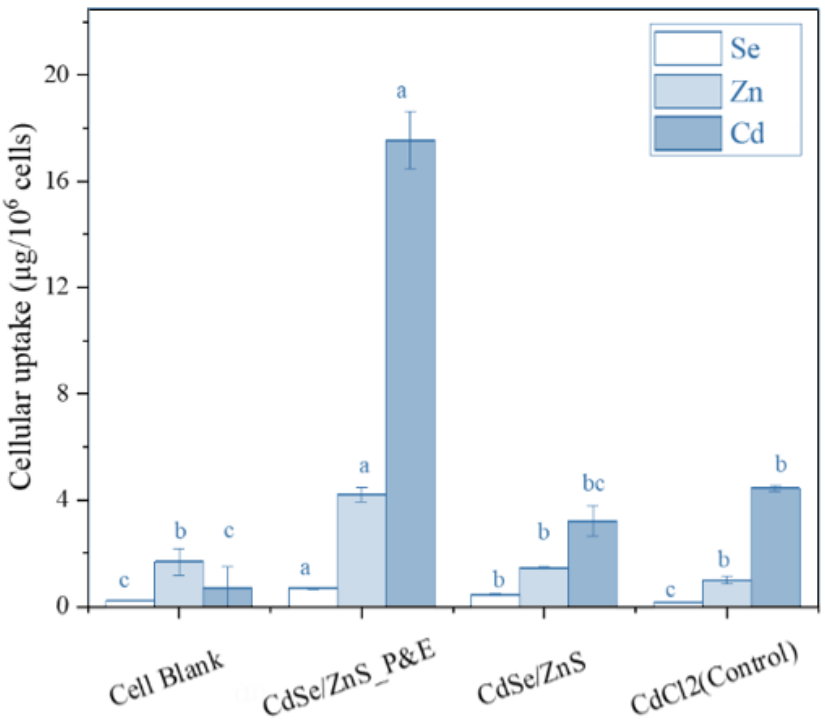

Figure 4-4: Cellular uptake comparison of polymer-capped and non-capped CdSe/ZnS quantum dots compared to a blank and $CdCl_2$ controls after exposure for 3h to 25 µg/mL.

Changing nanoparticle coatings to mediate uptake is a well-known technique for both nanoparticles[22] and well as different drugs.[23] Polyethylene imine, which is the base structure in the P&E polymer, is also a well-known gene transfer agent, albeit with a higher than desirable cell toxicity.[24] However, it is often difficult to compare the exact increase in uptake due to the vast differences in nanoparticle and coating syntheses.[7] For this study, we quantitatively determined that the P&E coating is the main driver for increased QD toxicity.

With the quantitative CI, we also conclude that CdSe/ZnS_P&E has more synergy than just CdSe/P&E. We hypothesize that a reason for this could be that CdSe/ZnS_P&E dissolve in the low pH environments of the cells (but not before), delivering more Cd than CdSe_P&E, which is less stable and could leave Cd outside of the cell. This insight can inform nanoparticle design as well as provide a quantitative structure to comparing the toxicity of complex nanoparticle mixtures.

4.3.2 Simulated digestion system overview and sampling method:

The simulated digestion of CdSe/ZnS_P&E was then employed to explore the transformation of these particles and the impact of that transformation on the toxicity. For the remainder of this chapter, CdSe/ZnS_P&E will be referred to as simply QDs, since we only tested this complex particle (rather than components). The digestion method employed was the standardized Infogest procedure,[12] with a starting concentration of 1250 ppm quantum dots in non-serum media (Figure 4-5). This starting concentration was chosen such that the final concentrations after work-up would match the previously discussed pristine toxicity tests [data not shown here].

A

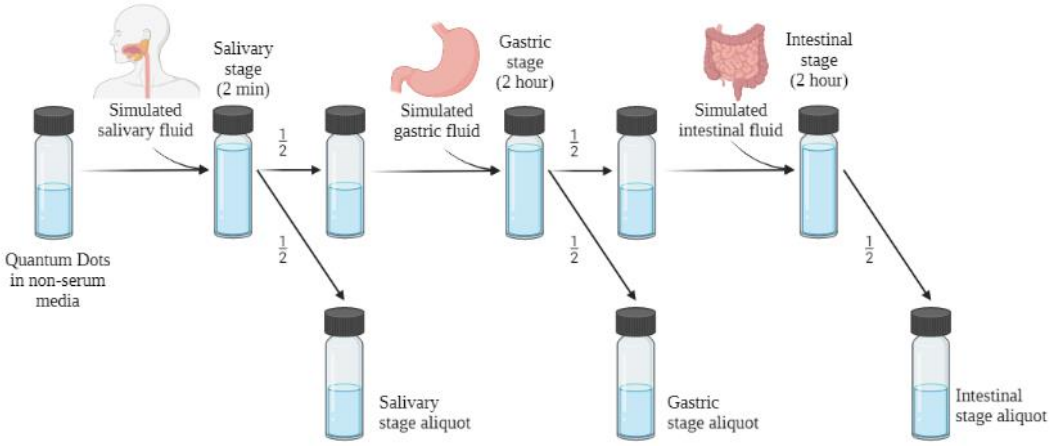

B

Dig. Stage:	Salivary	Gastric	Intestinal
Biomolecule	Salivary amylase	Pepsin	Pancreatin, Bile
Biomolecule concentration	0.005 mg/mL	6.0 mg/mL	30, 15 mg/mL
Ionic Strength (mM)	38	98	142
CdSe/ZnS_P&E	1.250 mg/mL	0.625 mg/mL	0.313 mg/mL

Figure 4-5:(A) Simulated digestion steps, with aliquot (1/2 total sample) removed at every stage. (B) Brief description of added components each stage, which was adapted from Infogest and the activity of enzymes of this specific study. Ionic strength calculated from the added salt solutions. Concentrations of CdSe/ZnS_P&E were set such that toxicity tests could be compared to pristine CdSe/ZnS_P&E toxicity tests.

4.3.3 Transformation of QD metals in simulated digestive system:

After each stage of the simulated digestion, we investigated changes to the structure of the quantum dot (Figure 4-6). Fluorescence was used because it traditionally indicates changes in the shelling of quantum dots,[11] or non-radiative recombination increases as ligands are exchanged [25] (Figure 4-6A). We analyzed the portion of quantum dots that remained by centrifugal filtration with a >3 kDa cutoff (Figure 4-6B). This method separates CdSe/ZnS_P&E that are >1 nm from dissolved ions in solution, and we have previously proven that the presence of the polymer does not impact its effectiveness (> 95% recovery of ions and 100% recovery of

NPs).[9] We discovered that this separation technique is slightly complicated by the presence of enzymes, which will be elaborated on below.

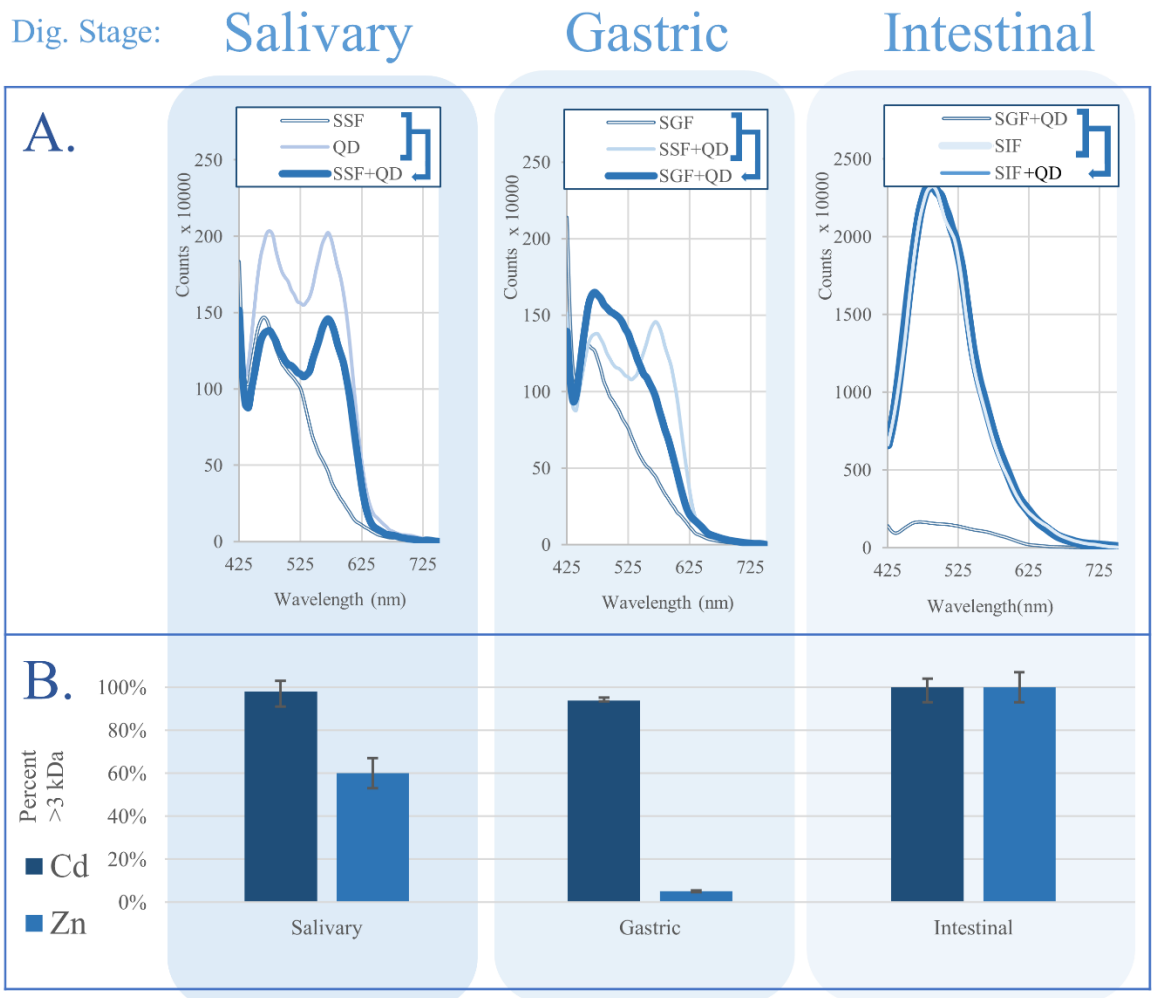

Figure 4-6: (A) Fluorescence of CdSe/ZnS_P&E (labelled QD) at each digestion stage. Note that the peak at 450 nm represents phenol red from non-serum cell media. (B) Percent of the metal constituent of CdSe/ZnS QD in nanoparticle form, measured using centrifugal ultrafiltration. The remainder of the metal constituent of the CdSe/ZnS QD was in 'dissolved' form (<3 kDa).

Fluorescence and dissolution of CdSe/ZnS_P&E demonstrate changes to the surface of individual QDs (Figure 4-6A,B). A 100% loss of CdSe/ZnS_P&E fluorescence occurs at the gastric stage, where the peak at 600nm indicating QD fluorescence disappears. This loss of fluorescence is accompanied by the dissolution of 95% of the Zn-containing shell (Figure 4-6B).

Although this dissolution was initiated at the salivary stage (with 40% dissolution), we hypothesize that the almost complete loss of the Zn-shell at the gastric stage is due to low pH. In our previous work, 80% of the Zn-shell was lost after 24 h exposure to acetic acid at pH 3.[9] In this study, despite these changes to the surface of the quantum dot, the preservation of 95% of Cd in nanoparticle form (i.e. >3 kDa) indicates that the core of the particles is still almost completely intact in the gastric stage. This would also align with past work, which did not demonstrate >10% dissolution of Cd after 24h exposure to acetic acid at pH 3.[9] Therefore, we hypothesize that Cd-containing nanoparticles remain intact after the gastric phase.

The complete recovery of >3 kDa Cd and Zn at the intestinal could indicate re-precipitation of these metals or the absorption of these metals onto biomolecules in solution. Simulated digestions with only Cd and Zn ions only (no QDs present) indicated that 100% and 75% of ions, respectively, were >3 kDa after the intestinal phase (see Figure S4-10). Therefore, the intestinal would cause either CdSe/ZnS_P&E or dissolved ions to be in the >3 kDa fraction. The intestinal phase has a higher concentration of biomolecules than the gastric (Figure 4-5B). One of these biomolecules, bile, has been shown to absorb Cd ions,[26] so we hypothesize that association between bile and QDs with Cd-containing surfaces could occur. Due to a neutral intestinal pH, we also hypothesize that Cd in QDs will persist in nanoparticle form.

We also examined Cd with single particle inductively coupled mass spectrometry (spICP-MS). The size detection limit for spICP-MS was 2.66×10^{-17} gram of Cd per nanoparticle, which we calculated to equate to an aggregate of ~210 CdSe/ZnS QDs (see SI for calculation). Due to the unknown behavior of the polymer P&E in these solutions, we only estimate sizes of the inorganic CdSe/ZnS portion of QDs. spICP-MS generated data regarding the size of Cd-containing nanoparticles in solution (Figure 4-7B) as well as the percentage of quantum dots that were aggregated into aggregates of >210 CdSe/ZnS QDs (Figure 4-7A). These techniques are also presented at each digestion stage for clarity.

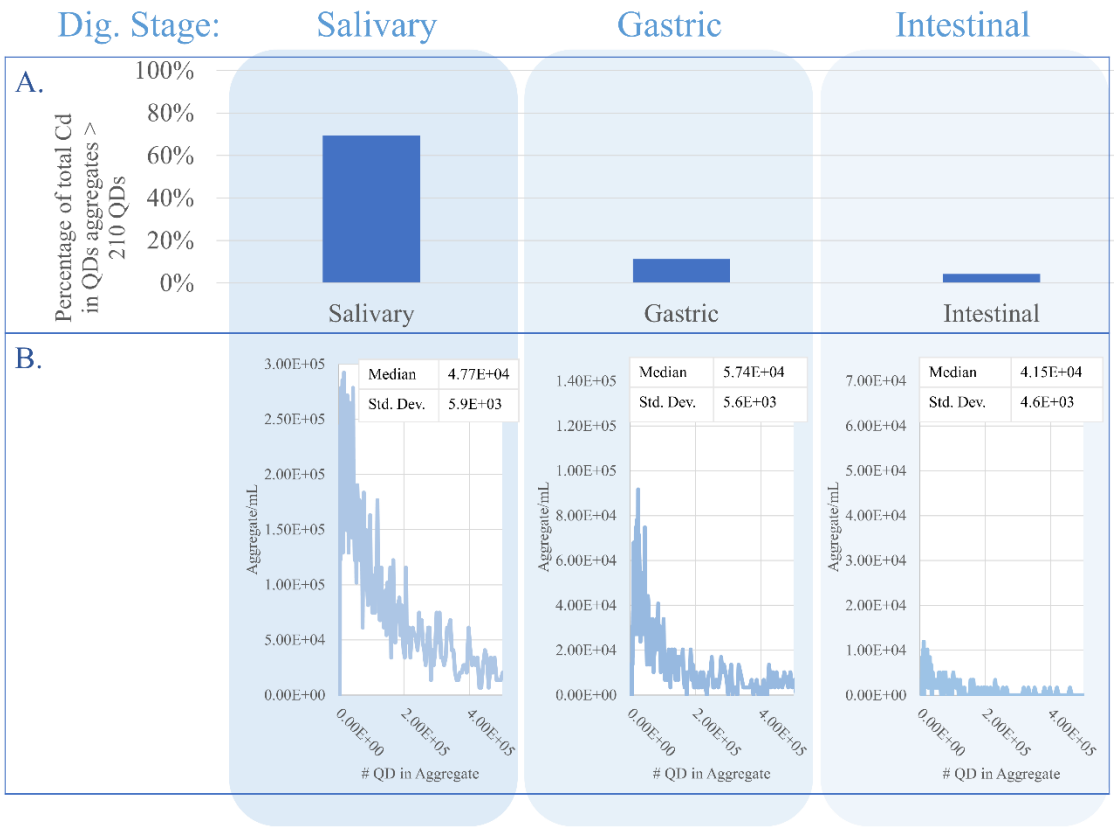

Figure 4-7: (A) Percentage of Cd aggregates over 210 CdSe/ZnS QDs compared to total amount of Cd measured in the sample. (B) Lognormal fitting of size range of inorganic portion quantum dots (calculated) based on spICP-MS data of cadmium at each digestion stage. Median particle size and standard deviation are reported in number of CdSe/ZnS QD aggregates. Note that the Y-axis are set such that the maximum is ½ of the previous stage, which would represent the maximum expected amount of particles in the aliquot.

The examination of Cd-containing nanoparticle revealed two key points. First, 70% of Cd-containing nanoparticles are initially aggregated in the salivary stages into clusters that are larger than 210 QDs (Figure 4-7A, Figure S4-11). This changes during the gastric stage. At the end of the gastric stage, only 15% of Cd is measured to be in aggregates of larger than 210 CdSe/ZnS QDs. This small amount of Cd in aggregates of larger than 210 QDs gets slightly smaller after the intestinal phase (to 10%). Second, the size of the large aggregates of CdSe/ZnS

QDs observed (Figure 4-7B) remains consistently higher than the limit of detection (4.7E+04-5.7E+04 compared to 2.1E+02).

The changes in aggregation extent at the different stages reflect another aspect of the transformations of CdSe/ZnS QDs in the simulated digestive system. When CdSe/ZnS QDs are aggregated (i.e. salivary stage), they also demonstrate a stable fluorescence and some ZnS shell stability. However, during the gastric stage, CdSe/ZnS QDs become more dispersed while loosing the remaining ZnS shell and fluorescence. Although the intestinal phase brings with it a higher pH and a higher ionic strength, CdSe/ZnS QDs do not form aggregate into aggregates of larger than 210 CdSe/ZnS QDs. We hypothesized that this could be due to the association of QDs with biomolecules in solution. To understand the interplay between QD and biomolecules, we tracked red traces of QD fluorescence with the presence of biomolecules using confocal microscopy (Figure 4-8).

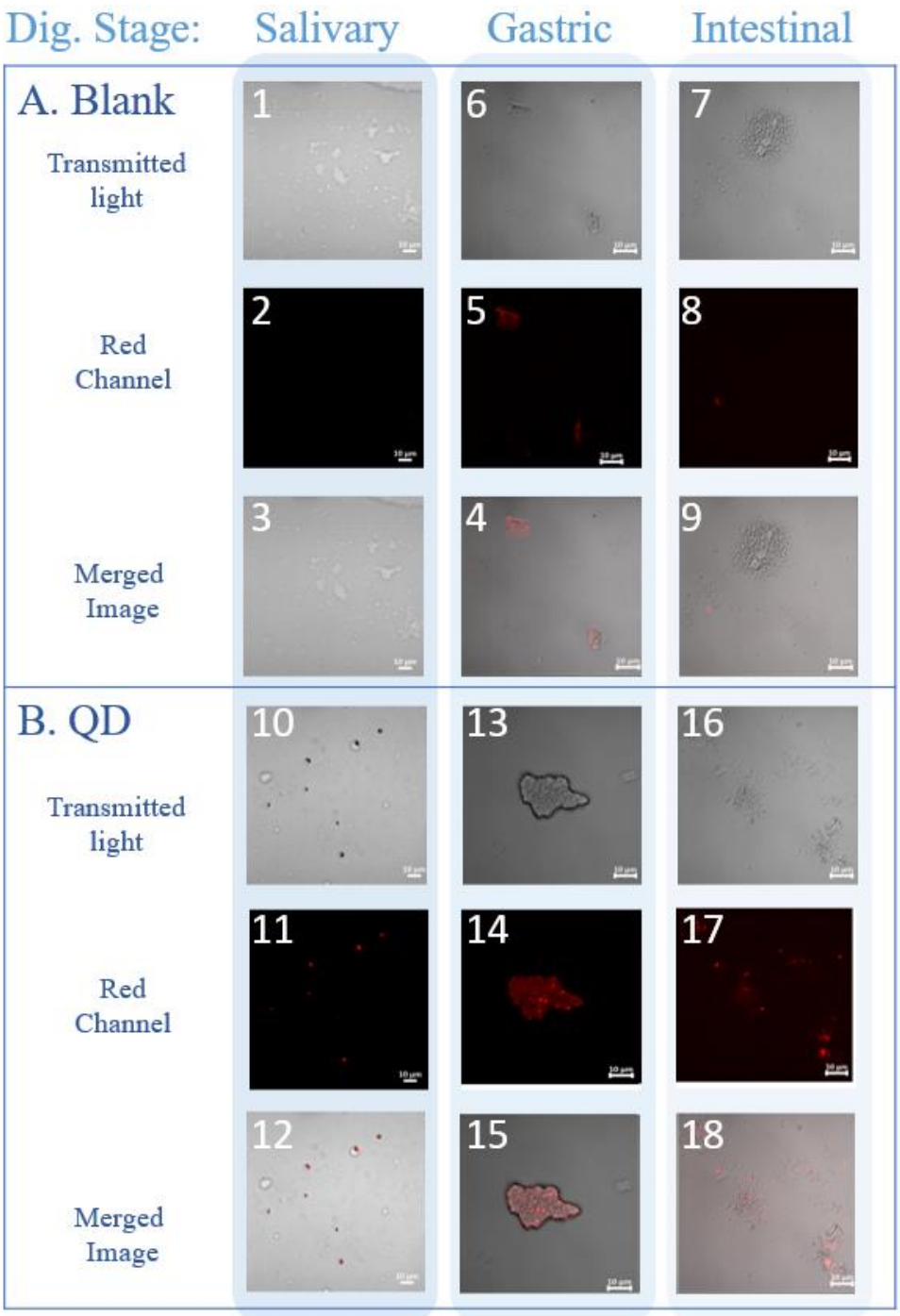

Figure 4-8: Confocal microscopy images of (A) three digestion stages without QDs present and (B) three digestion stages with QDs present, with QD presence indicated by red fluorescence (red channel).

These confocal images demonstrate the co-localization of QDs (red fluorescence signal) with biomolecules in solution (dark grey shapes). The salivary stage indicates brighter quantum dots because of the preserved fluorescence at this stage (see Figure 4-6A for aggregate fluorescence). At the salivary stage, there is also a lack of dispersion in the fluorescence, which aligns with the spICP-MS results. The particles observed in the salivary stage (~1 μm) correlate to CdSe/ZnS QD aggregates of >2E+06 QDs, which would be above the size range of spICP-MS data in this work (calculation is done assuming random close packing of CdSe/ZnS QDs into a spherical aggregate).

The gastric phase shows QDs co-localized with the gastric biomolecules. The presence of biomolecules and cell culture media does not significantly impact the particle size of ENPs measured by spICP-MS due to the dilution needed before sample introduction.[27] The intestinal stage shows a higher dispersion of both biomolecules and QDs, even though the signals for QDs are more muted. We hypothesize that the association of QDs to biomolecules could be stronger than the homo-aggregation of QDs that can be observed by spICP-MS, especially in the intestinal phase.

4.4 Conclusions:

Although nanoparticle structures and transformations in the digestive system are inherently complex, the use of a well-characterized model nanoparticle can help to distinguish the key changing contributions to toxicity. The multi-component, commercially-relevant model of CdSe/ZnS, complete with its separately synthesized components, was exposed to intestinal epithelial cells. The resulting set of EC20s was compared using a combination index to determine that the polymer imparts a higher synergistic effect than the inorganic shell. The polymer-capped zinc-shelled CdSe had more synergistic toxicity (and a lower EC20) than the non-shelled polymer-capped CdSe.

This initial study led to questions regarding the integrity of the coating after transformations in the digestive system. We chose a simulated human digestive model and fine-tuned an aliquot work-up so that polymer-capped CdSe/ZnS could be exposed to intestinal cells

after transformation. We determined that the gastric stage was a key stage for the transformation of quantum dots – leading to surface defects (i.e. loss of fluorescence), loss of the ZnS shell, and decreased proportion of Cd-containing aggregates larger than 210 CdSe/ZnS QDs. These transformations seem to be preserved in the intestinal stage. These transformations will then be correlated to our collaborator's observations of increased intestinal cell toxicity of transformed QDs compared to pristine QDs, which are to be reported elsewhere.

4.5 Methods:

4.5.1 Cellular Uptake:

Cells were exposed to 25 μg/mL of each component for 6 h. The supernatant media was removed (cells adhered to the 24 well plate). Cells were then washed 3x with fresh serum-free culture media. Cells were then trypsinized and centrifuged (Eppendorf 5430R Refrigerated centrifuge, 255×g, 5 min). The pellets were then digested with 400 μL 70 % (v/v) HNO_3 in open 15ml DigiTUBEs at 90 °C using a heating block for 1 h, followed by 400 μL H_2O_2 digestion in the same condition. The digestion product was diluted with Milli-Q water to 1.3% (v/v) HNO_3 acid for ICP-MS analysis. Total amounts of Cd, Se and Zn in the cells were determined in Perkin Elmer NexION 300X ICP-MS at 82, 66, 114 for Se, Zn, Cd respectively.

4.5.2 Simulated Human Digestion:

The simulated salivary, gastric, and intestinal digestions were carried out according to Recio et al,[12] and are described briefly below. QDs were initially dispersed in non serum containing media at 1250 ppm. Then, 1 mL of this solution was mixed with the same volume of simulated salivary fluid (SSF) in the salivary digestion stage (2 mL final volume). The mixture was placed on an orbital shaker (Forma Scientific 420) and incubated at 120 rpm at 37°C for 2 min. Samples were taken as SSF digested QDs, and the mixture was further mixed in 1:1 ratio with simulated gastric fluid (SGF) and incubated on the shaker for 2 h. After incubation, the pH of the solution was adjusted to pH=7 with 1M NaOH before samples were taken. Then, simulated intestinal fluid (SIF) was mixed at the ratio of 1:1 with the solution in previous step. The mixture was kept in the incubated orbital shaker for another 2 h at 120 rpm, 37°C. To stop enzyme digestion,

samples take at each stage were subjected to heat-shock treatment (placed in boiling water for 5 min) to inactivate enzymes.

Potassium chloride (>98%), monopotassium phosphate (99%), sodium bicarbonate (≥99.7%), sodium chloride (≥ 99%), magnesium chloride (99%), calcium chloride (≥99%), sodium hydroxide (99.99%), and hydrochloric acid (37% v/v) were purchased from Sigma and used as received. These chemicals were used to make stock solutions, which were then combined into electrolyte-only simulated digestive fluids (see Table 3 in Recio et al.[12])

Enzymes (and their activities) used in the digestions were salivary amylase (400 U/mg solid), pepsin (400 U/mg solid), pancreatin (4 U/mg solid) and bile salts (0.78 mmol of bile salts/g bile). These enzymes were used as received. Except for salivary amylase, enzymes were stored at -20°C as dry powders until the day they were suspended for use in a simulated digestion. Salivary amylase was suspended in solution at the concentration needed for digestion then stored at -20°C.

The amounts of electrolyte-only solutions, enzyme solutions, acid, and base used in the digestions are outlined in the table below (modeled after Table 2 in Recio et al. [12]). Each digestion step was preformed with prewarmed solutions (10 minutes) at 37°C, and each digestion step itself was preformed at 37°C after mixing solutions at room temperature. Digestions were carried out in 20mL glass vials.

4.5.3 Centrifugal filtration of QDs aliquots after digestion

Samples were separated using Amicon Ultra 3 kDa centrifugal units. These tubes were spun for 45 minutes at 4500 rpm. The <3 kDa fraction is referred to as the filtrate (or dissolved), while the >3 kDa fraction is the retentate.

After separation, the sample was acid digested with DigiTubes. The filtrate was added to a 50 mL tube, followed by 1 mL of H_2O_2 (Sigma, 50% reagent grade), and the resulting solution was digested at 95°C for 30 minutes. Then 1 mL of HNO_3 (99.999%, Trace Metal Grade) was

added and the solution was digested at 95°C for 1 hour. After the two digestions the samples were diluted to 15 mL with water and transferred to tubes for ICP-OES analysis.

When the retentate sample was examined, H_2O_2 was first added to the filter and allowed to sit for 10 minutes. Then, it was transferred to the digestion tube for digestion at 95°C for 30 minutes. 1 mL of HNO_3 was also added to the filter for 10 min before being transferred to the digestion tube for digestion at 95°C for 30 minutes.

ICP-OES was performed on a Perkin Elmer Optima 8300 using wavelengths 206.20 nm and 228.80 nm for Zn and Cd, respectively. Zn and Cd standards of 1-1000 ppb were made from TraceCERT standard solutions.

4.5.4 Fluorescence:

The emitted fluorescence intensity of the digested QDs sampled at each stage of the simulated digested was measured with a Spectramax i3x plate reader (Molecular Devices, San Jose, USA) at excitation 400 nm and presented as emission spectrum. At each stage of digestion, the spectrum of both the digestive fluid and the QD containing digestive fluid were measured and compared. Serum free media and the undigested QD suspended in serum free media were also used as negative and positive control, respectively. For SGF-QD, pH was adjusted to 7 before measurement.

4.5.5 Confocal Microscopy

The aliquots from each digestion phase were de-activated (5 min boiling) then drop-cast onto a microscope slide. The dried samples were then analyzed with the LSM 710 confocal laser scanning microscopy (Carl Zeiss, Oberkochen, Germany).

4.5.6 spICP-MS:

spICP-MS was conducted on a PerkinElmer NexION 300X ICP-MS running Syngistix software (V1.1). Dwell time for experiments was set at 100 μs with a sampling time of 100s.

Flowrate and transport efficiency were measured daily. Transport efficiency (8.9 ± 0.9%) was assessed using 30nm Au NPs ultra-uniform with PEG-carboxyl in 2 mM sodium citrate, nanoComposix (53 mg Au/L) diluted to 26 ng Au/L in deionized water. Dissolved calibrations (0.05 – 10 ppb Cd) were prepared with 1% nitric acid (PlasmaPure Plus 67 – 70%, SCP Science, Canada) and Cd standard solution (TraceCert, 10000 mg/L).

4.6 References:

(1) Hoshino, A.; Fujioka, K.; Oku, T.; Suga, M.; Sasaki, Y. F.; Ohta, T.; Yasuhara, M.; Suzuki, K.; Yamamoto, K. Physicochemical Properties and Cellular Toxicity of Nanocrystal Quantum Dots Depend on Their Surface Modification. *Nano Lett.* **2004**, *4* (11), 2163–2169. https://doi.org/10.1021/nl048715d.

(2) Ma, F.; Li, C.; Zhang, C. Development of Quantum Dot-Based Biosensors: Principles and Applications. *J. Mater. Chem. B* **2018**, *6* (39), 6173–6190. https://doi.org/10.1039/C8TB01869C.

(3) Inoshita, T.; Sakaki, H. Electron Relaxation in a Quantum Dot: Significance of Multiphonon Processes. *Phys. Rev. B* **1992**, *46* (11), 7260–7263. https://doi.org/10.1103/PhysRevB.46.7260.

(4) Moon, H.; Lee, C.; Lee, W.; Kim, J.; Chae, H. Stability of Quantum Dots, Quantum Dot Films, and Quantum Dot Light-Emitting Diodes for Display Applications. *Adv. Mater.* **2019**, *31* (34), 1804294. https://doi.org/10.1002/adma.201804294.

(5) Pelley, J. L.; Daar, A. S.; Saner, M. A. State of Academic Knowledge on Toxicity and Biological Fate of Quantum Dots. *Toxicol Sci* **2009**, *112* (2), 276–296. https://doi.org/10.1093/toxsci/kfp188.

(6) Tang, Y.; Han, S.; Liu, H.; Chen, X.; Huang, L.; Li, X.; Zhang, J. The Role of Surface Chemistry in Determining in Vivo Biodistribution and Toxicity of CdSe/ZnS Core–Shell Quantum Dots. *Biomaterials* **2013**, *34* (34), 8741–8755. https://doi.org/10.1016/j.biomaterials.2013.07.087.

(7) Oh, E.; Liu, R.; Nel, A.; Gemill, K. B.; Bilal, M.; Cohen, Y.; Medintz, I. L. Meta-Analysis of Cellular Toxicity for Cadmium-Containing Quantum Dots. *Nature Nanotechnology* **2016**, *11* (5), 479–486. https://doi.org/10.1038/nnano.2015.338.

(8) Bilal, M.; Oh, E.; Liu, R.; Breger, J. C.; Medintz, I. L.; Cohen, Y. Bayesian Network Resource for Meta-Analysis: Cellular Toxicity of Quantum Dots. *Small* **2019**, *15* (34), 1900510. https://doi.org/10.1002/smll.201900510.

(9) Bechu, A.; Liao, J.; Huang, C.; Ahn, C.; McKeague, M.; Ghoshal, S.; Moores, A. Cadmium-Containing Quantum Dots Used in Electronic Displays: Implications for Toxicity and Environmental Transformations. *ACS Appl. Nano Mater.* **2021**, *4* (8), 8417–8428. https://doi.org/10.1021/acsanm.1c01659.

(10) Dubrow, R. S.; Freeman, W. P.; Lee, E.; Furuta, P. Quantum Dot Films, Lighting Devices, and Lighting Methods. US9199842B2, December 1, 2015.

(11) Talapin, D. V.; Mekis, I.; Götzinger, S.; Kornowski, A.; Benson, O.; Weller, H. CdSe/CdS/ZnS and CdSe/ZnSe/ZnS Core−Shell−Shell Nanocrystals. *J. Phys. Chem. B* **2004**, *108* (49), 18826–18831. https://doi.org/10.1021/jp046481g.

(12) Brodkorb, A.; Egger, L.; Alminger, M.; Alvito, P.; Assunção, R.; Ballance, S.; Bohn, T.; Bourlieu-Lacanal, C.; Boutrou, R.; Carrière, F.; Clemente, A.; Corredig, M.; Dupont, D.; Dufour, C.; Edwards, C.; Golding, M.; Karakaya, S.; Kirkhus, B.; Le Feunteun, S.; Lesmes, U.; Macierzanka, A.; Mackie, A. R.; Martins, C.; Marze, S.; McClements, D. J.; Ménard, O.; Minekus, M.; Portmann, R.; Santos, C. N.; Souchon, I.; Singh, R. P.; Vegarud, G. E.; Wickham, M. S. J.; Weitschies, W.; Recio, I. INFOGEST Static in Vitro Simulation of Gastrointestinal Food Digestion. *Nature Protocols* **2019**, *14* (4), 991–1014. https://doi.org/10.1038/s41596-018-0119-1.

(13) Baranowska-Wójcik, E.; Szwajgier, D.; Oleszczuk, P.; Winiarska-Mieczan, A. Effects of Titanium Dioxide Nanoparticles Exposure on Human Health—a Review. *Biol Trace Elem Res* **2020**, *193* (1), 118–129. https://doi.org/10.1007/s12011-019-01706-6.

(14) McClements, D. J.; Xiao, H. Is Nano Safe in Foods? Establishing the Factors Impacting the Gastrointestinal Fate and Toxicity of Organic and Inorganic Food-Grade Nanoparticles. *npj Sci Food* **2017**, *1* (1), 6. https://doi.org/10.1038/s41538-017-0005-1.

(15) More, S.; Bampidis, V.; Benford, D.; Bragard, C.; Halldorsson, T.; Hernández-Jerez, A.; Hougaard Bennekou, S.; Koutsoumanis, K.; Lambré, C.; Machera, K.; Naegeli, H.; Nielsen, S.; Schlatter, J.; Schrenk, D.; Silano (deceased), V.; Turck, D.; Younes, M.; Castenmiller, J.; Chaudhry, Q.; Cubadda, F.; Franz, R.; Gott, D.; Mast, J.; Mortensen, A.; Oomen, A. G.; Weigel, S.; Barthelemy, E.; Rincon, A.; Tarazona, J.; Schoonjans, R. Guidance on Risk Assessment of Nanomaterials to Be Applied in the Food and Feed Chain: Human and Animal Health. *EFSA J* **2021**, *19* (8), e06768. https://doi.org/10.2903/j.efsa.2021.6768.

(16) Sohal, I. S.; O'Fallon, K. S.; Gaines, P.; Demokritou, P.; Bello, D. Ingested Engineered Nanomaterials: State of Science in Nanotoxicity Testing and Future Research Needs. *Particle and Fibre Toxicology* **2018**, *15* (1), 29. https://doi.org/10.1186/s12989-018-0265-1.

(17) Spurgeon, D. J.; Lahive, E.; Schultz, C. L. Nanomaterial Transformations in the Environment: Effects of Changing Exposure Forms on Bioaccumulation and Toxicity. *Small* **2020**, *16* (36), 2000618. https://doi.org/10.1002/smll.202000618.

(18) Di Silvio, D.; Rigby, N.; Bajka, B.; Mackie, A.; Baldelli Bombelli, F. Effect of Protein Corona Magnetite Nanoparticles Derived from Bread in Vitro Digestion on Caco-2 Cells Morphology and Uptake. *The International Journal of Biochemistry & Cell Biology* **2016**, *75*, 212–222. https://doi.org/10.1016/j.biocel.2015.10.019.

(19) Sohal, I. S.; Cho, Y. K.; O'Fallon, K. S.; Gaines, P.; Demokritou, P.; Bello, D. Dissolution Behavior and Biodurability of Ingested Engineered Nanomaterials in the Gastrointestinal Environment. *ACS Nano* **2018**, *12* (8), 8115–8128. https://doi.org/10.1021/acsnano.8b02978.

(20) Abdelkhaliq, A.; van der Zande, M.; Undas, A. K.; Peters, R. J. B.; Bouwmeester, H. Impact of in Vitro Digestion on Gastrointestinal Fate and Uptake of Silver Nanoparticles with Different Surface Modifications. *Nanotoxicology* **2020**, *14* (1), 111–126. https://doi.org/10.1080/17435390.2019.1675794.

(21) Chou, T.-C. Theoretical Basis, Experimental Design, and Computerized Simulation of Synergism and Antagonism in Drug Combination Studies. *Pharmacol Rev* **2006**, *58* (3), 621–681. https://doi.org/10.1124/pr.58.3.10.
(22) Freese, C.; Gibson, M. I.; Klok, H.-A.; Unger, R. E.; Kirkpatrick, C. J. Size- and Coating-Dependent Uptake of Polymer-Coated Gold Nanoparticles in Primary Human Dermal Microvascular Endothelial Cells. *Biomacromolecules* **2012**, *13* (5), 1533–1543. https://doi.org/10.1021/bm300248u.
(23) Chen, W.; Zhou, S.; Ge, L.; Wu, W.; Jiang, X. Translatable High Drug Loading Drug Delivery Systems Based on Biocompatible Polymer Nanocarriers. *Biomacromolecules* **2018**, *19* (6), 1732–1745. https://doi.org/10.1021/acs.biomac.8b00218.
(24) Cortez, M. A.; Godbey, W. T.; Fang, Y.; Payne, M. E.; Cafferty, B. J.; Kosakowska, K. A.; Grayson, S. M. The Synthesis of Cyclic Poly(Ethylene Imine) and Exact Linear Analogues: An Evaluation of Gene Delivery Comparing Polymer Architectures. *J. Am. Chem. Soc.* **2015**, *137* (20), 6541–6549. https://doi.org/10.1021/jacs.5b00980.
(25) Koole, R.; Schapotschnikow, P.; de Mello Donegá, C.; Vlugt, T. J. H.; Meijerink, A. Time-Dependent Photoluminescence Spectroscopy as a Tool to Measure the Ligand Exchange Kinetics on a Quantum Dot Surface. *ACS Nano* **2008**, *2* (8), 1703–1714. https://doi.org/10.1021/nn8003247.
(26) Elinder, C. G.; Kjellstöm, T.; Lind, B.; Molander, M. L.; Silander, T. Cadmium Concentrations in Human Liver, Blood, and Bile: Comparison with a Metabolic Model. *Environ Res* **1978**, *17* (2), 236–241. https://doi.org/10.1016/0013-9351(78)90025-7.
(27) Peters, R.; Herrera-Rivera, Z.; Undas, A.; van der Lee, M.; Marvin, H.; Bouwmeester, H.; Weigel, S. Single Particle ICP-MS Combined with a Data Evaluation Tool as a Routine Technique for the Analysis of Nanoparticles in Complex Matrices. *Journal of Analytical Atomic Spectrometry* **2015**, *30* (6), 1274–1285. https://doi.org/10.1039/C4JA00357H.
(28) Gao, X.; Spielman-Sun, E.; Rodrigues, S. M.; Casman, E. A.; Lowry, G. V. Time and Nanoparticle Concentration Affect the Extractability of Cu from CuO NP-Amended Soil. *Environ. Sci. Technol.* **2017**, *51* (4), 2226–2234. https://doi.org/10.1021/acs.est.6b04705.

4.7 Supporting information:

4.7.1 Cell Toxicity Data: (Collected by Ke Xu)

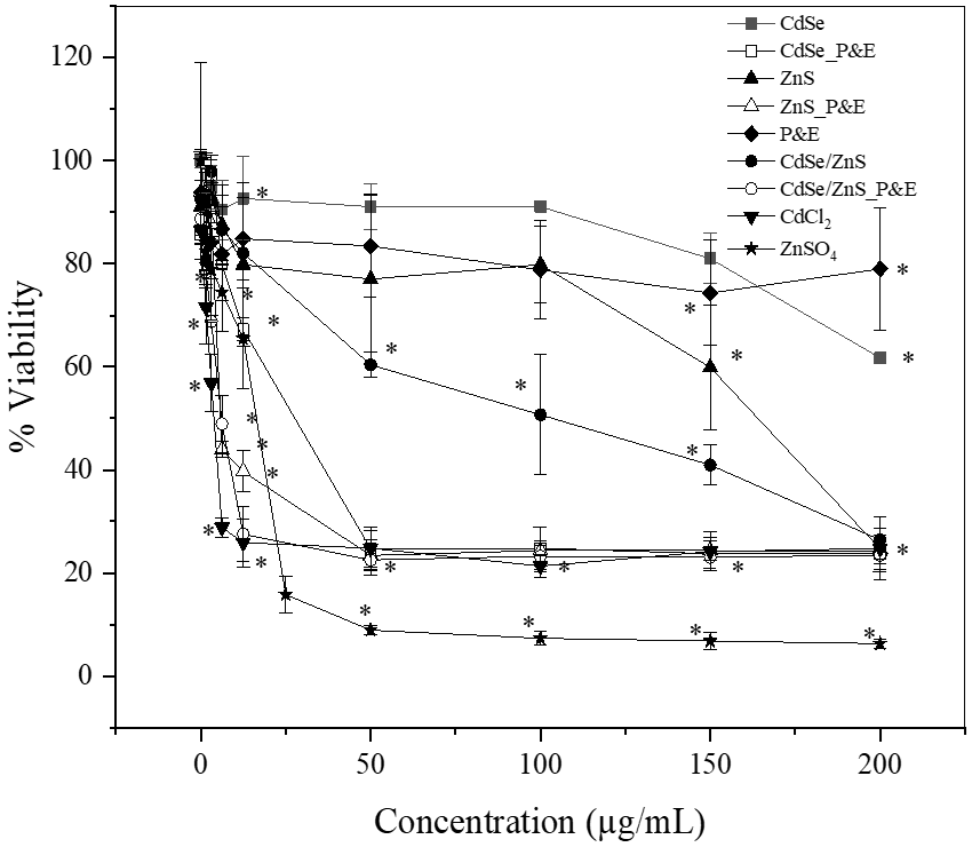

Figure S4-9: Cell toxicity data (as % viability of HIEC-6 cells) compared to the dose of the QDs and QD mixtures (n=3, *p<0.05)

The % viability of HIEC-6 cells was measured with the resaszurin assay (Abcam, USA) after an exposure time of 24h. The % viability of HIEC-6 cells is derived from the measured viability of cells exposed to QDs compared to the viability of a cell culture without particle exposure.

4.7.2 Combination Index Calculation:

Curve fitting was performed using 4 parameter logistics equation between the concentration of the sample (x) and the % viability (y) (Equation 3), the 4 parameters (A1, A2, x0 and p) were then used to derive EC_{20} (Equation 4). Fitting and parameter calculation were performed by Origin Pro 2018 software (version 95E [2018]; Originlab)

$$y = A2 + \frac{A1-A2}{1+\left(\frac{x}{x0}\right)^{p}} \quad (3)$$

$$EC_{20} = 10^{log(x0)+\frac{log(0.25)}{p}} \quad (4)$$

Specific values of the combination index and EC_{20} are presented below (
Table S4-1).

Component or combination	EC_{20} (µg/mL)	Combination Index
CdSe	150	N/A
ZnS	28.98	N/A
P&E	11.98	N/A
CdSe/ZnS	55.37	1.06
CdSe_ P&E	10.86	0.79
ZnS_ P&E	4.89	0.4
CdSe/ZnS_ P&E	2.47	0.2

Table S4-1: EC_{20} and CI of QD components and combinations

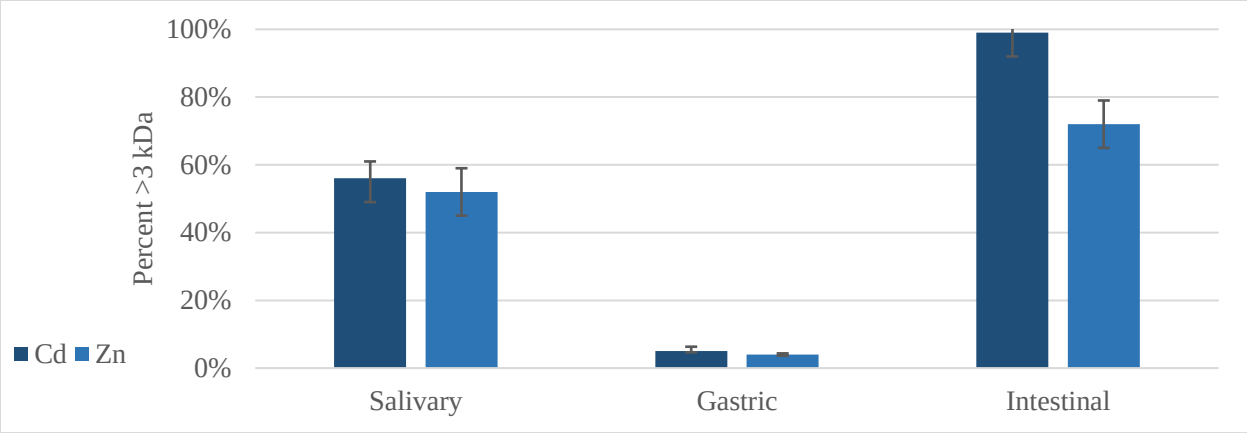

Figure S4-10: Percent >3 kDa for ions (no QDs present) and polymer throughout digestion.

4.7.3 Calibration of spICP-MS:

The calibration of the single particle mode requires two key calibrations and method validation. The first key calibration step is transport efficiency. We used 30 nm Au NPs from NIST because preliminary tests of QDs in water indicated that their size range was ~25nm. We verified that transportation efficiency of gold nanoparticles would not change significantly depending on the digestion stage (all were within the average 8.9 ± 0.9%).

The next calibration necessary for measuring Cd in single particle mode is the dissolved ion calibration, which was achieved with an $R^2 = 0.9999$. However, Cd ions were not stable in de-ionized water, so spiking and recovering dissolved Cd in the presence of Cd-containing QDs was adjusted. Inspired by the work of Gao et al,[28] we added 100 ppb EDTA to solutions of 10 ppb Cd ions in deionized water and stirred at 100 rpm for 2 h. Although this only kept ~10% of Cd ions in solution, subsequent dilutions into DI water were stable and we used these Cd ion solutions to spike solutions of QDs in different diluted digestion solutions (Table S4-2)

Table S4-2: Recoveries of ions, nanoparticle size, and nanoparticle concentration after the addition of 0.5 ppb of Cd ions.

Sample Matrix	Recovery of spiked dissolved ion as dissolved ion in reading	Recovery of same particle size of QDs after ion spike	Recovery of same particle concentration of QDs after ion spike
Media	N/A	96%	96%
Salivary	111%	98%	99%
Gastric	112%	83%	98%

These results demonstrate that nanoparticle size and concentration were very stable in the presence of spiked Cd ions. The expected ionic content of the solution was 10% higher than expected, so this consistent increase was accounted for in subsequent calculations for the main text.

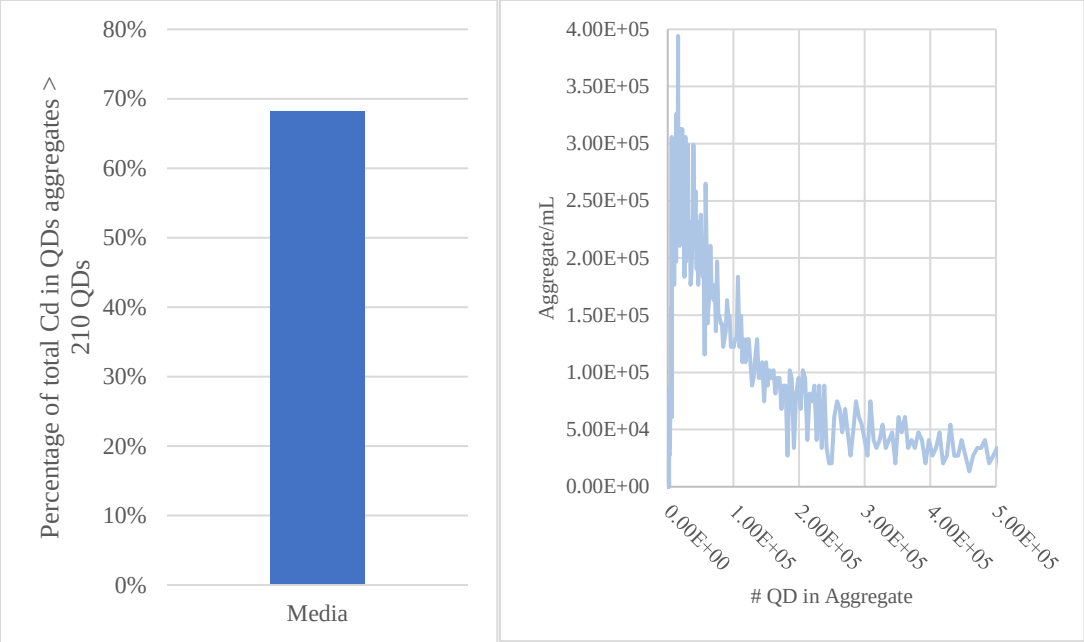

Figure S4-11: (A) Amount of QD aggregates in media > 210 QDs and (B) distribution of aggregates in the diluted media.

4.7.4 Calculating number of QDs in aggregate compared to Cd particle size

$$N_{QD} = \frac{\frac{4}{3}\pi(d_{Cd}/2)^3\rho_{Cd}}{f_{Cd}}/m_{QD}$$

Where the N_{QD} is the number of QDs in the aggregate, d_{Cd} is the diameter of the Cd particle (generated by spICP-MS), $\boldsymbol{\rho_{Cd}}$ is the density of Cd, $\boldsymbol{f_{Cd}}$ is the weight fraction of Cd in the QD, and $\boldsymbol{m_{QD}}$ is the mass of one QD. Please note that these calculations only account for the inorganic portion of QDs, and do not include the polymer coating. This calculation allowed for the correlation of the Cd particle LOD to the LOD of QD aggregates (Figure).

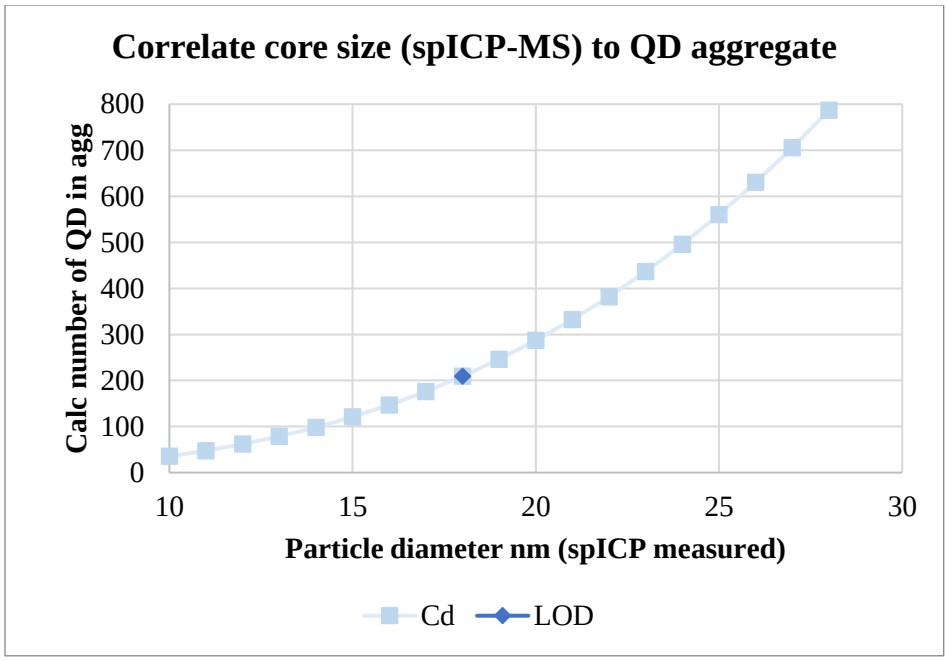

Figure S4-12: Relationship between Cd in Cd particle (spICP-MS result) and number of QD in aggregate (calculated).

5 Are substitutes to Cd-based quantum dots in displays more sustainable, effective, and cost competitive? An alternatives assessment approach

A. Bechu, S. Ghoshal, A. Moores,* N. Basu* "Are substitutes to Cd-based quantum dots in displays more sustainable, effective, and cost competitive? An alternatives assessment approach" ACS Sustainable Chem. Eng. 2022, 10,7, 2294-2307.
https://doi.org/10.1021/acssuschemeng.1c04909

Also available on ChemRxiv: https://doi.org/10.26434/chemrxiv-2021-sjv53

5.1 Connecting text

The previous chapter explored the possible transformations in the simulated human digestive system, with the goal of probing transformations to inform the design of safer NPs. However, as noted in the introduction, the commonly employed green chemistry metrics do not link hazard to design. Therefore, we decided to explore the use of an alternatives assessment to probe the safety of the next generation of emissive materials. We designed the alternatives assessment such that it would be accessible to researchers developing materials.

5.2 Abstract

Light emissive organics and inorganic nanoparticles are substance classes competing for applications in displays in the form of organic LEDs (OLEDs) and quantum LEDs (QLEDs), respectively. Upcoming substance classes (perovskites) and Q-OLED displays also contain novel nanomaterials and organics for these applications. However, the sustainability of these emissive substances is difficult to assess quickly and broadly because of their complexity, their inherently different structures, and their rapid evolution in the literature. We propose the use of an alternatives assessment to compare the hazard, cost, and performance of these possible substitute substances, with a focus on replacing cadmium-containing quantum dots. This assessment type is used in industry and government to inform chemical substitution. It uses available information,

while pointing out important data gaps, for decision making. The cost assessment highlights competitiveness of OLEDs because of their low amounts needed per display, but performance assessments do not identify a preferred alternative. The hazard results indicate there is no clear alternative either, with each novel nanomaterial or organic substance having different negative aspects. These results identify the need for a low-hazard high-performing alternative substance, and the assessment provides a framework for researchers to evaluate their own novel substances.

5.3 Introduction

Globally, the fate of 83% of electronic waste (E-waste) is unknown, likely dumped or dismantled in potentially hazardous circumstances.[1] This undocumented E-waste (44 million metric tons generated in 2019 alone) has embedded chemicals and substances that are commonly released into the environment.[1] One type of electronic good with increasingly diverse chemicals are screens and monitors, which currently make up 12.5 wt% of global E-waste. Contrary to global E-waste trends, the total weight of disposed screens and monitors is decreasing slightly (by 1% over 4 years). This shift is attributed to the replacement of traditional heavy cathode ray tube (CRT) monitors with lighter flat panel displays in waste streams.[1] These two screens rely on different technologies and heavy metals, with CRT relying heavily on lead while flat screens have a cocktail of heavy metals.[2] This technology shift has represented an overall decrease in certain end-of-life impacts,[2] although unknown risks remain.

The next generation of flat screen televisions currently has many different emissive substance classes vying for dominance.[3] These classes use novel substances that convert charge or light into specific colors. The main substance of concern is cadmium-containing quantum dots (Cd-QDs), due to the known toxicity of Cd.[4] This substance of concern has led to numerous studies reviewing the sustainability of the Cd-QDs and competing substances.[5] For example, life cycle assessments (LCAs) have been performed to compare the cumulative energy demand of Cd-QDs and indium-containing QDs (In-QDs).[6] After updating these assessments with new data on the amount of materials in televisions, In-QDs were found to require approximately 13 times more energy (MJ cm^{-2}) than Cd-QDs.[7] LCAs have also been used to point out areas of concern in

the manufacturing of Cd-QDs into quantum light emitting diode displays (QLEDs), such as the aquatic acidification and ecotoxicity of a Cd-QD encapsulating polymer.[8]

Another substance class of interest to displays, perovskites, have attracted significant research attention for their use in photovoltaic panels, and sustainability assessments have mostly focused on that application. Studies have weighed the risks of using lead in perovskites versus lead alternatives using a variety of metrics, with some concluding that lead-based perovskites performance outweighs the possible risk,[9] while others encourage the development of lead-free materials.[10] Lastly, QLEDs are functionally matched by organic LEDs (OLEDs), which rely on specific organic emitters (OEs). In sustainability assessments, however, OLEDs are commonly compared to traditional liquid crystal displays (LCDs). OLEDs require less energy over their lifetime,[11] but assessments focused on the end of life of these materials caution the higher toxicity potential.[12] In summary, these Cd-QD, In-QD, perovskite and OLED assessments have pointed out sustainability concerns unique to each substance class.

The sustainability studies mentioned above employ LCA, which has provided in-depth and useful comparisons between two substance classes. However, there are challenges with LCA in assessing all emissive substances that are still at the research stage.[13] For example, modelling a scale-up scenario is time consuming and involves various assumptions to cover missing impact data. [13] In addition, the toxicity profiles of these research-stage nanomaterials of complex composition are not often known and cannot be easily predicted by models.[13] These challenges, and many others, hinder the use of LCAs for nanomaterials at the research stage.[14,15] A high-level yet simple evaluation is needed that encompasses all substance classes while remaining accessible to researchers developing these substances.

The alternatives assessment framework was developed by the US EPA to help identify safer and effective alternatives to a chemical of concern.[16,17] Alternatives assessment is a powerful method in the context of sustainable chemistry and engineering because it enables research on the design and synthesis of safer alternative molecules and materials, even emerging ones that have not yet left the laboratory.[18] This methodology prioritizes reducing the potential harm of new substances, while also recognizing only the alternatives that are feasible (e.g. in

terms of cost and performance). It works with available data and available substitutes, while pointing out the need for additional data or substitutes.

This framework was built to help enable decision making, yet it is also a great too to and to identify areas where further research would be useful. Alternatives assessment is established in chemicals regulations in both the United States[19,20] and Europe[21,22] so that manufacturers and government officials can survey different available substitutes for hazardous chemicals with chemical safety in mind. In short, alternatives assessment is a key piece of industry and government's response to pressing sustainability challenges linked to substances of concern.

This framework is not commonly used in academic literature, but it has great potential as a holistic assessment of emerging substances that is accessible to researchers. In industry, it is used during R&D and early manufacturing to inform chemical substitution, which is the replace a hazardous product with the use of a process or substance that decreases hazard without compromising function.

The established framework is not to be confused with risk assessment or life cycle assessment common in academia, although it is complimentary. While both alternatives assessments and life cycle assessments rely on similar data, they differ in the scope of their analysis, with AA bringing cost and function in to the evaluation. The focus of alternatives assessment is also on the comparison of competing technologies. AA thus help identify promising substance classes, while pointing at the need for further investigation via LCA or other sustainability assessment methods. In short, alternatives assessment is a great way to narrow down the focus of research on most promising candidates in terms of sustainability (as well as function and cost), while offering information about the areas to improve to reach better performances on these points.

It is a flexible assessment that allows for comparison of numerous options and materials classes if desired. For example, Gilbertson and Ng compared organics to minerals to nanomaterials in a search for alternatives to brominated fire retardants.[23] We have previously published an alternatives assessment on 46 perovskites in solar cells, which has identified the least hazardous alternative as well as the steps needed for that alternative to be more competitive

with the highest-performing lead-based material.[24] We hypothesize that this flexible assessment could also be used by substance researchers to identify promising responsible replacements for Cd-QDs for displays.

The objective of this study is to analyze Cd-QDs and its possible replacement substance classes with an alternatives assessment to foster a broad understanding of the field. We followed the US National Research Council guidelines[17] and made the assessment fit for the purpose of analyzing emissive substances in displays. We produced three evaluations: performance, cost, and hazard. Using substance syntheses and reported performance metrics as inputs, we output a score in each evaluation. Then, we compared the scores of different substance classes with the goal of finding a viable substitution. We also qualitatively examined possible regulatory barriers for the different substances. We aimed to structure this alternatives assessment so that materials researchers can add in their own chemicals (in a reasonable timeframe) and compare them to other emerging substance classes. In short, an alternatives assessment for emissive substances can help point researchers to an informed substitution of Cd-QDs.

5.4 Methods

This assessment follows the steps of the US National Academy's Framework to Guide Selection of Chemical Alternatives.[17] Steps 1-4 are outlined in the following section "Identify substance class of concern & scoping problem formulation". Step 5-7 and 9 encompass the Cost, Performance and Hazard assessments sections of the methods. Step 8 involved integrating life cycle analysis, which we did not pursue due to the early research stage (and therefore high uncertainty) of some analyzed substances. Step 10 and 11 involves bringing together all evaluations to compare and identify an acceptable alternative. These steps are addressed in the "Multiparameter Evaluation" section. All steps and methods sections are represented schematically below (Figure 5-1), and details will be reported in the following sections.

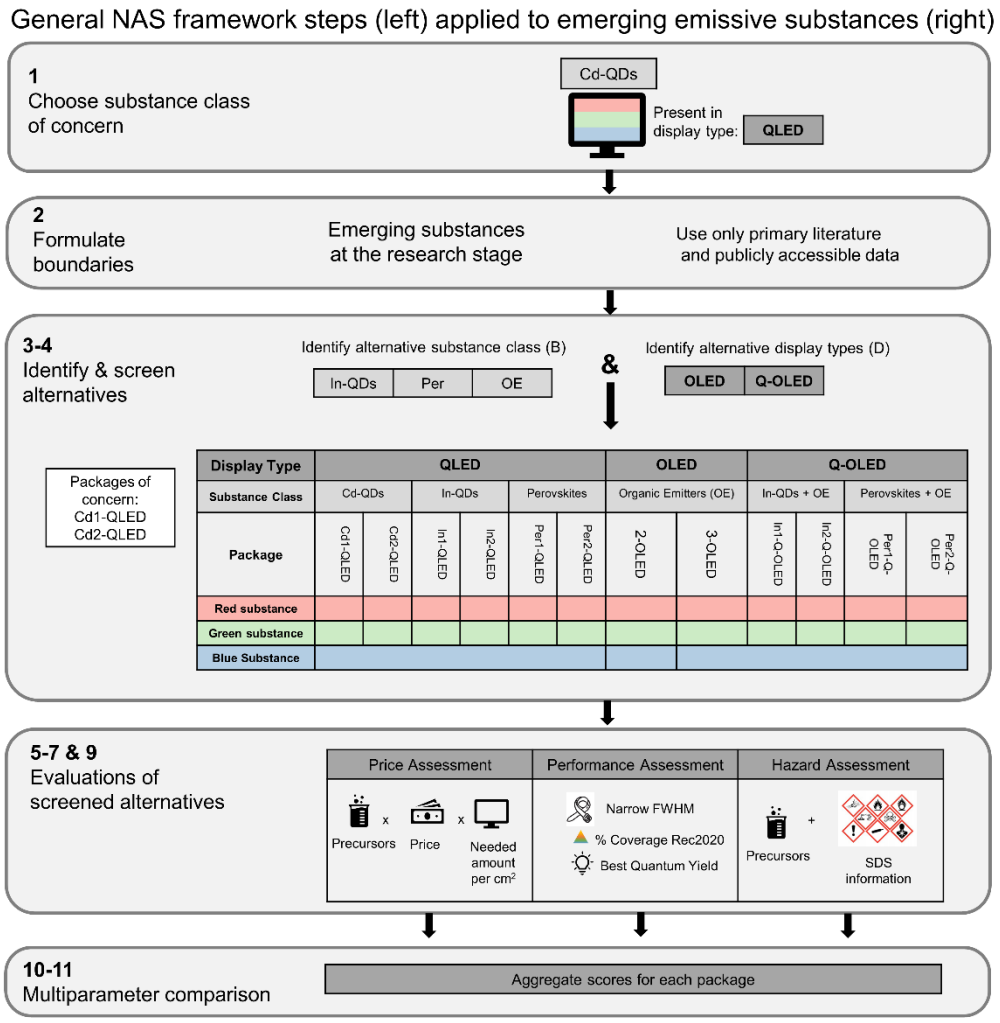

Figure 5-1: Outline of substance class of concern and alternatives packages examined in this alternatives assessment. Step 1 identifies the substance class of concern, Cd-QDs, which are integrated into displays. Step 2 points out two different boundaries employed in this assessment. Four key terms are bolded in the large table of steps 3-4: substances, substance class, packages, and display types. These terms are all significant to categorizing alternatives. Steps 5-7 & 9 illustrate the three different evaluations conducted for each package: price, performance, and hazard. Steps 10-11 indicate that these three evaluations will be aggregated into one score for each package.

5.4.1 Identify substance class of concern & scoping problem formulation

The first four steps of this framework involve (1) choosing a substance of concern, (2) formulating the boundaries of the assessment (3), identifying alternatives, and (4) screening the alternatives. We decided to abide by the following three decision rules as boundaries to the assessment. First, the foundational data for this assessment is based on public knowledge. Second, the alternatives presented are emerging substance classes, which are highlighted to spur development. Third, the scaling up of the production of these alternatives is not considered.

The four steps mentioned above were informed by a search of both the scientific literature and press releases from display and QD companies. Literature was searched before April 2021 and considered for use in this assessment if it met the following criteria: (1) use of developed substance in a device; and (2) explicitly outlined steps and procedures in chemical and device fabrication. Since only a few substances could be chosen, we chose the best performing in terms of external quantum efficiency or quantum yield for each substance class (See SI for all papers screened). Patents were excluded from the search. We also consulted with scientists developing these substances as well as those assessing the degradation and subsequent toxicity of these substances through the McGill Sustainability Systems Initiative (MSSI).

As noted in the introduction, we aim to identify responsible replacements of Cd-QDs in displays using alternatives assessment. We defined Cd-QDs as a substance class that is made up of many substances (different Cd-containing QDs from different syntheses). We chose two different syntheses of cadmium-containing quantum dots, therefore having Cd1-QDs[25] and Cd2-QD[26] substances. We chose two syntheses to demonstrate possible differences inherent to one substance class (in the case of QDs there are different shell compositions and precursors). We chose these two syntheses specifically because they both produce high performing Cd-QDs.

To connect these substances to their end use in displays and rely on uniform nomenclature, we organized the assessment according to four key designations (highlighted as A-D in this paragraph, also displayed in Figure 5-1). (A) Substances are individual single or multiple mineral phases or organic compounds that achieve a desired function (emitting red,

green, or blue light in this case). Substances belong to a (B) substance class. A substance class is composed of substances that are generally similar in structure. For example, Cd-QDs are a substance class. Returning to (A) substances, we chose to group red, green, and blue emitting substances together because they make up the three colored pixels in displays (Table S5-1). Each such group was designated as a (C) package. These packages will essentially be the units analyzed in this alternatives assessment. Lastly, there are (D) display types. We decided to integrate display types because these are known by consumers and marketed by the industry. The Cd-QDs substance class is used in a display type (QLEDs). QLEDs have blue substances that emit light from charge, and red and green substances that emit light by down-converting blue light.

According to the above definitions, Cd-QD substance class cannot make up a package on its own because it must have a blue emissive material. To complete the package, we added InGaN substance as a blue emitting material.[27,28] InGaN also provides the blue backlight necessary for QDs, which down-convert the light.[29] InGaN is therefore an integral part of the display type, QLED. In summary, the substance class of concern was grouped into two packages: Cd1-QLED and Cd2-QLED. These packages are labelled such a way that the display type (QLED) and the substance class (Cd-QDs) can be identified. The 1 and 2 refer to different synthetic methods for slightly different chemical compositions of the substances (Cd1-QDs and Cd2-QDs).

5.4.2 Identify and screen alternatives

In a similar manner as the substance class of concern, alternative substance classes were grouped in packages of red, green, and blue emissive materials. Alternatives to Cd-QDs were chosen to represent three different emerging substance classes: In-based QDs, perovskites, and organic emitters (OEs). Chosen alternative substances were high performers in their respective substance classes (see SI excel sheet for complete list of alternatives screened). Performance was based on high quantum yield (QY) and external quantum efficiency (EQE), both of which indicate that the material is adept at transforming light or charge into a given wavelength.

In-based QDs are currently replacing Cd-based QDs in some displays because of their lack of Cd, due to the latter's toxicity concerns. The synthesis of In-based QDs is less mature

than that of Cd-based QDs, and was challenged by initially with a lower quantum yield and broader emission.[29] Two In-based QD substances were explored, and since they need an InGaN backlight (and therefore QLED display type), they are identified as In1-QLED[30] and In2-QLED.[31]

Perovskites are presented in literature as having a similar emissive tunability as QDs, but with simpler syntheses. These materials are promising because of their defect tolerance and high rates of emission, but the development of a blue material lags behind green and red ones.[32] Two green/red perovskite alternative substances were chosen, one which contains lead,[33] while the other is lead-free.[34] Although the lead-based perovskite alternative has high performance, we anticipate the presence of lead could create a similar situation as Cd, as both elements are heavy metals with known adverse health effects covered by the same EU regulations.[35] There are various lead-free perovskites, which our group recently assessed for use in solar panels. [24] The most promising lead-free alternative in terms of display performance was a cesium antimony halide.[34] These perovskites also retain the InGaN backlight, and are identified as Per1-QLED[33] and lead-free Per2-QLED.[34]

OEs are currently being developed as alternative substances and have the advantage of generating all colors from charge, rather than needing a blue color excitation which must be down converted. This means that OEs have their own display type: OLEDs. OEs are a rapidly evolving field, but recent developments can be approximately categorized according to their method of exciton recombination: phosphorescence (Ph) and thermally activated delayed fluorescence (TaDF).[36] These categories are thoroughly explored in several reviews[37–39], but we chose to focus on the best-performing materials identified by Bräse et al.[36] For OEs, a green, red, and blue chemical substance of each generation were chosen for packages 2-OLED[40–42] (Ph) and 3-OLED[43–45] (TaDF). It is unclear which alternative substance is used by industry, but we decided to investigate these because of their impressive performance in academic papers.

Lastly, we looked ahead to upcoming market-ready developments (which we could emulate here) to showcase the versatility of the alternatives assessment approach. The development of Q-OLEDs aimed to address separate issues with QLED and OLED display types by combining different substance classes.[46] This substance class promises “lower cost, higher brightness, improved power efficiency and more accurate color reproduction”.[46] In this next

generation substance class, blue OEs substances are matched with emerging green and red substances.[46] For our assessment, we consider these emerging substances from the In-QDs or perovskites substance classes. This creates the following alternative packages: In1-Q-OLED,[30,45] In2-Q-OLED,[31,45] Per1-Q-OLED,[33,45] and Per2-Q-OLED.[34,45]

In short, there are 12 packages evaluated in this assessment (see Table S5-1 for summary). There are 2 packages of known concern, Cd1-QLED and Cd2-QLED. There are 4 packages of alternative QLED displays based on In-QDs (In1-QLED and In2-QLED) and perovskites (Per1-QLED and Per2-QLED) substance classes. There are 2 packages based on the alternative OLED display types which use OEs (2-OLED and 3-OLED). Then there are 4 packages of Q-OLED display types, which use a combination of OEs for blues and either In-QDs or perovskites for green and red (In1-Q-OLED, In2-Q-OLED and Per1-Q-OLED, Per2-Q-OLED). In total, these 12 packages span different display types and substance classes.

5.4.3 Price Assessment

We followed the method set up by Chen *et al.*[31] to estimate the costs of each alternative package. The amounts of each alternative substance was calculated based on the needs to cover 1 cm^2 of screen area, and then added to the cost of the other substances in the package. This calculation involved finding the cost of each chemical used in the synthesis, estimating the yield of the synthesis, and determining how much of each chemical is used in 1 cm^2 of screen area. Without adequate stability metrics (see discussion in performance assessment section), we did not factor the lifetime of the substance in the screens into the cost. This cost assessment involved certain assumptions described below.

After the precursors of each substance were identified, their cost was found by searching for the chemical on Sigma Aldrich 2021 catalogue and choosing the price ($ CAD) of the largest container size (up to 1 kg for solids or 4L for liquids). The purity examined matched that described in the syntheses. The costs of manufacturing different alternatives were not considered due to the large differences between small-scale syntheses and industrial operations.

After the price of each precursor was established, the final price of the alternative material was estimated based on certain yields. The yields of OLED materials are stated in the

literature,[40–45] however the yield of QDs and perovskites are not stated in the cited papers.[25,30,33,34,47,48] To account for this, we averaged the yield in all steps of the OLEDs synthesis and applied this yield to the limiting reagent in the QDs and perovskites syntheses (see SI spreadsheet for each calculation). For InGaN, the reagents were chosen based on fundamental knowledge of the syntheses[28,49] and the same OLED-based yield was applied (no one limiting reagent).

With the cost of 1 kg of each alternative material calculated, costs were combined with estimated costs of other materials into a given package (of red, green, and blue materials). We assumed QDs concentrations from concentrations of Cd and In from commercial televisions.[7] We assumed that perovskites would be present in displays at the same concentrations as Cd-QDs. For OLEDs, we assumed that the amount of In present aligned with estimates by Zink et al.[50] We also assumed that In-free OLED alternatives would be present in the same molar concentration as In-containing OLEDs. For InGaN, we chose the amount necessary in a display based of a detailed life cycle assessment. [28]

5.4.4 Performance Assessment

Successful materials for color generation in television must meet a variety of performance requirements. Two favorable characteristics are widely reported; [26,48,51] photoluminescence quantum yield (QY) and narrow emission spectra as quantified by full width at half maximum (FWHM). We chose these as two out of three performance metrics. FWHM can also be translated into color purity (see SI and online tool for calculation). We decided to use FWHM rather than color purity to simplify this assessment.

In addition, it is key to determine if the material produces the exact wavelength necessary for displays. ITU-R Recommendation 2020 (Rec. 2020) color standard is the benchmark of colors possible in a display based on a combination of the ideal red, green and blue pixels.[52] To calculate whether a material meets this standard, the peak wavelength of emitted light was converted to X,Y space in the CIE color graph (Commision Internationale de L'Eclairage). These (X,Y) values were then plotted on a graph and the overlap with Rec. 2020 color standard was calculated (see online tool[53] and SI for details). Although there are numerous examples of

>90% coverage of Rec. 2020 with certain combinations of QDs,[54] and perovskites,[52] 100% coverage has not yet been achieved (to the best of the our knowledge).

These three metrics (quantum yield, FWHM, and percent coverage Rec 2020) were collected for each material from their respective sources. InGaN performance information was gathered from the Ullman Encyclopedia of Industrial Chemistry (QY and peak wavelength)[27] as well as the review by T. Wang (FWHM).[55] These values did not contain associated errors, so error values are not included in this assessment.

For each package, the red, green, and blue values for each metric were averaged. For example, an alternatives' FWHM values for red (30 nm), green (50 nm) and blue (60 nm) were combined such that the FWHM value for the alternative package would be 46.7 nm. Then, each averaged metric for each package was compared, with the best value ranked as 1 and the worst 0.1. For quantum yield and percent coverage Rec 2020, the highest percentages were considered best, while for FWHM, the lowest value was considered best. Then, each metric score was added together to obtain the final performance score. For example, if a package had the most Rec 2020 coverage (rank =1), the highest quantum yield (rank = 1) and the lowest FWHM (rank = 1), then its combined performance score would be 3.

5.4.5 Hazard Assessment

Hazard assessments are difficult to construct due to lack of data for most chemicals in commerce. Following a study by Llanos et al.,[24] precursor substances were selected as the inputs to the hazard assessment. This aligns with certain chemical regulations, which determine the inherent hazard of a product from its chemical inputs at the manufacturing stage, rather than possible end of life issues.[56] We also assume that the correct use of PPE cannot be guaranteed, which aligns with recent methodology of the US EPA.[57]

Hazard data was obtained using the Toxics Use Reduction Institute's Pollution Prevention Options Analysis System Tool.[58] This tool process data from Safety Data Sheets and the GHS into subcategory and category scores for different hazards for each chemical (See SI excel sheet for full list of subcategories and categories). The most hazardous score for each subcategory was 10, the least hazardous was 2, and if data was missing, we entered in 0 (see SI

excel sheet for full assessment). The worst variable in each subcategory score of the P2OAsys analysis was used as the final subcategory score (irrespective of exposure route). The score of each category was the average of the subcategory scores. The most common assessors of hazard present in the Safety Data Sheets studied were combined into three metrics; Human Health, Environment, and Physical Properties (see SI Table S5-2 for category combinations for each). In short, human health encompasses all exposure routes causing acute and chronic effects on humans. The environment metric covers the acute and chronic effects on aquatic organisms, as well as persistence and bioaccumulation potentials. Physical properties covers flammability, reactivity, corrosivity, and volatility.

The use of GHS metrics as the basis for this assessment makes error analysis difficult. Errors involved in the various toxicity metrics (some based on expert judgement), or physical properties hazards (specific tests) are not communicated on safety data sheets. [59]

5.4.6 Multiparameter Evaluation:

The cost, performance and hazard assessments were combined to highlight the overall feasibility of the packages. This was done by first ranking the scores of the packages per evaluation on a scale of 1 (best) to 0.1 (worst). The best scores were awarded to the most cost attractive, the highest performing and the safest. A theoretical package, that scored best in all evaluations, would score a 3 (1+1+1) in the multiparameter evaluation.

5.5 Results and Discussion

5.5.1 Cost assessment

Figure 2 presents the cost in Canadian dollars of each substance and each package per cm^2 of display area. These costs vary dramatically, from \$1.30 to \$0.001 CAD/cm^2 (Cd2-QLED and 3-OLED, respectively). The cost of each individual material was not correlated to the number of steps in the synthesis or the number of chemicals involved in the synthesis (Table S5-1). We acknowledge that since the cost estimates were based on precursor prices in the Sigma Aldrich catalog, these costs do not reflect the savings that manufacturers can achieve by buying

chemicals in bulk or at slightly lower purity. Such purity adjustments to the syntheses could be achieved in a later stage of development. For the purposes of this research-stage substance assessment, we will focus on the trends and reasons for the relatively different costs of packages (Figure 5-2).

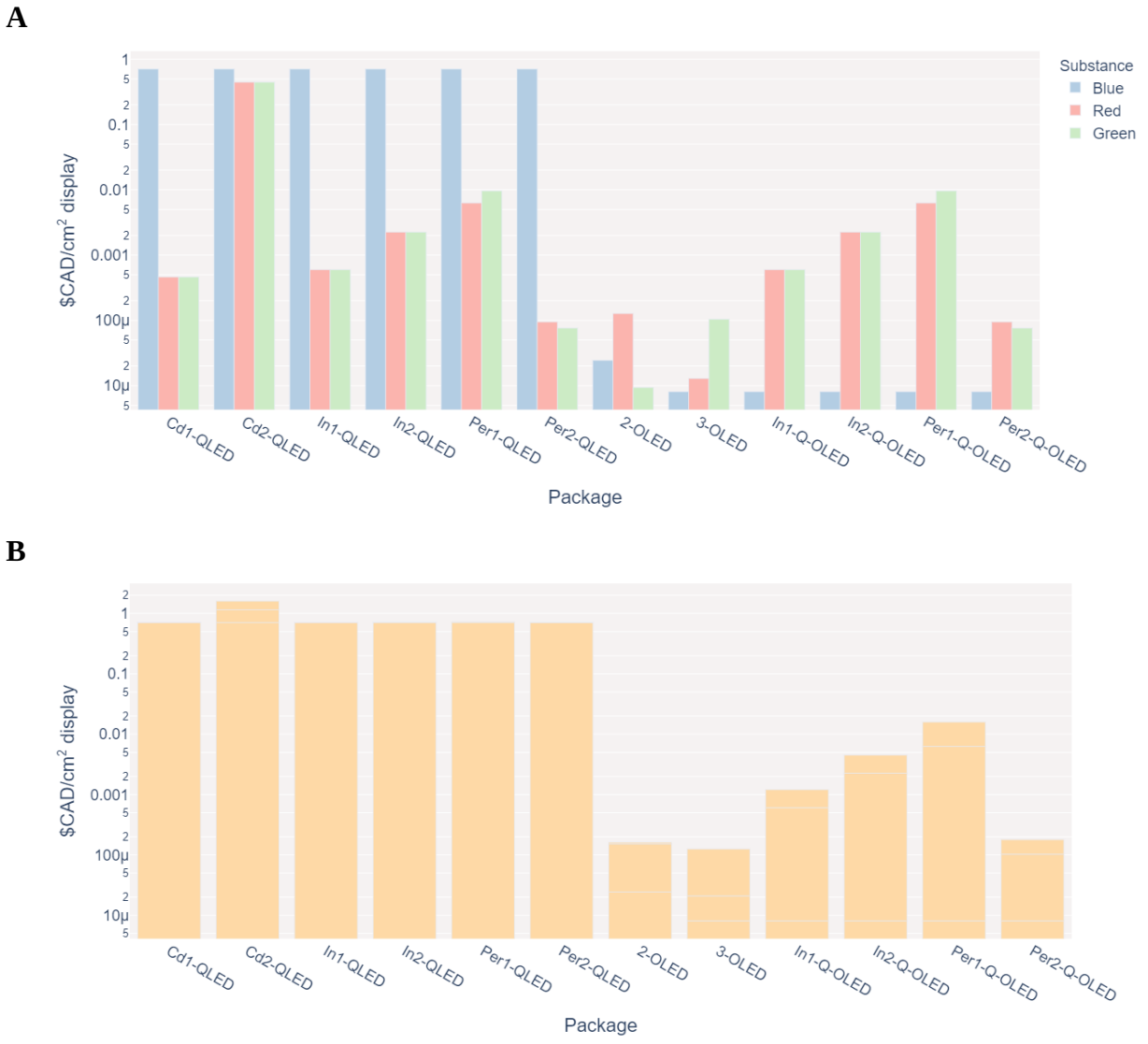

Figure 5-2: (A) Price assessment results, grouped by package of red, green, and blue pixels with a logarithmic y-axis. (B) Total prices of the packages, again on a logarithmic y-axis (see spreadsheet for table of values).

Most of the cost incurred by Cd2-QLED (and other QLEDs) arises from the blue emissive material, InGaN. This material is costly to produce because its precursors are costly deposition-grade metal organics (e.g. trimethylindium). In addition, the amount of InGaN per television is ~20x more than the next highest amount of chemical (Red-Cd2-QLED) and ~70,000x more than the least amount of chemical needed (Blue-3-OLED). Therefore, improvements in both the type or precursors and the amount of Blue-QLED would decrease the cost of the material. It is unclear whether efforts to introduce micro-LEDs (μ-LEDs) with smaller area backlights of InGaN will reduce the total amount and cost of InGaN used in the product.

OLED materials (including the Blue-Q-OLED) have the advantage of needing ~100x less mass of material compared to perovskites (Per) and InP QDs. These lower material requirements absorb the high cost per gram of OLEDs precursors. Such estimates of material requirements have been amended in the past due to examination of actual products.[7]

Figure 2 also demonstrates differences between specific procedures making the similar materials. For example, Cd1-QDs costs >0.01 $CAD/cm^2 of display, while Cd2-QDs costs 0.60 CAD/cm^2 of display. These differences do not lie in the amounts of materials in the television, but rather in the amount and price of the precursors compared to the yields of the syntheses. 80% of the cost of Cd2-QDs is driven using trioctlyamine, a solvent which is ~10x more expensive than the solvent used in Cd1-QDs (octadecene). In addition, Cd2-QDs uses ~3x as much solvent as Cd1-QDs. Another example of a cost difference in the same material is between Per1-Green and Per2-Green. Specifically, Per2-Green uses much less solvent than Per1-Green (13 mL octadecene and 990 mL octane per gram of substance, respectively), which is reflected in the price (18 and 1,514 $CAD/g substance, respectively). These specific precursors could be substituted or reduced to significantly change the rankings in price. Such a substitution can be informed by functional substitution methods,[60] but the ultimate feasibility of these price-centric substitutions will have to be tested by substance researchers themselves.

We acknowledge that a key factor in the cost assessment is missing: the cost of encapsulation. In other words, the cost of other layers in a display is not included, even though certain layers may change depending on the package employed. For example, blue OLED materials need to be more encapsulated than blue QLED,[61] which increases costs.

In addition, the cost of manufacturing the materials at scale is not considered because these substances were analyzed at the lab scale. Purchasing bulk chemicals could also introduce significant cost savings, as the "bulk" metric here is maximum 1 kg of precursor from Sigma Aldrich. Scaling up could also change the purity of chemicals needed, as high-quality materials can be synthesized from low quality precursors.[62] The cost of manufacturing could increase if there are many steps involved in a substance synthesis. For example, QDs need purification between core synthesis and shelling steps.[25,26] The cost of manufacturing may also increase due to the inherent instability of certain substances. For example, perovskites are air and water sensitive,[63] which could call for more specialized equipment at the manufacturing stage. The manufacturing of these substances may also be spread across various stakeholders with different amounts of experience. For example, we anticipate InGaN, as a mature backlight technology, may not be produced by the same company producing QD color filters.

Another consideration of manufacturing are labor costs. Heben et al detailed the scale-up costs of a cost-competitive perovskite solar cell, and found that labor accounted for 5% of the total cost of production.[64] We therefore did not include labor costs in the price assessment.

Lastly, a low cost does not necessarily equate to an available material on the market. For example, the EU designated certain raw materials that were economically important, but had a high supply risk in their list of Critical Raw Materials. A few elements present in this list are also key to substances mentioned here: Gallium, Indium, Phosphorous, Iridium.[65] The substance classes that have a high supply risk are therefore In-QDs and certain OEs. In addition, In and Ga are the backbone to the blue substance in QLEDs, InGaN.

5.5.2 Performance assessment

The best performers had low FWHM, high quantum yield, and high Rec. 2020 overlap (e.g. Cd2-QLED, Figure 5-3). The three highest ranking packages were Cd2-QLED, In2-QLED and Per1-QLED. These three packages had favorable (i.e. low) FWHM and high Rec 2020 overlap.

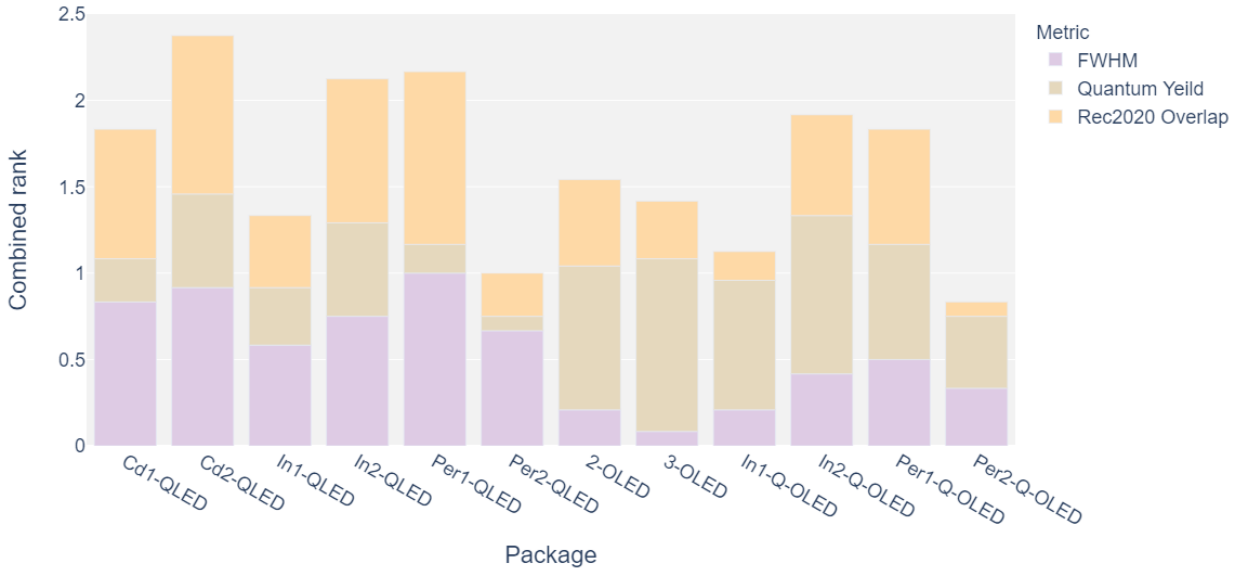

Figure 5-3: Performance Assessment results, grouped by FWHM (purple), Quantum Yield (brown) and Rec 2020 overlap (yellow). The highest rank possible for each performance indicator is 1 and the lowest is 0.1.

These linear rankings have the possibility of obscuring non-linear trends in each of these performance metrics. However, we observed that the trends of ranking vs. performance metric were relatively linear (R^2 = 0.93-0.98, see Figure S5-3). In other words, these rankings do not hide a large disparity between packages, substance classes or display types.

However, the high performance of one package was not linked to high performance of the other package of the same substance class. For example, In2-QLED performed well overall (score of 2.2), but In1-QLED did not perform as well (score of 1.4). Different syntheses led to very different performance scores.

For QDs or perovskites, we propose that the simplest improvement to overall performance could be made by improving the Rec. 2020 overlap. The needed wavelengths to meet this standard[66] could be reached by these substance classes by changing particle size (QDs)[67] or elemental ratios (perovskites).[33] For OEs, the tuning of emission is reliant on tuning ligands.[68]

The performance assessment also highlights that there are differences between OLEDs and QLEDs. Blue-OLEDs have higher quantum yields and worse (i.e., higher) FWHM values than the Blue-QLEDs (which are InGaN based). In addition, the Blue-3-OLED (which is also the blue color in Q-OLEDs) has an emission at 480 nm, which lowers the Rec.2020 overlap (Figure S5-2). These FWHM and emission peak (both attributed to the blue colors) decreased the overall scores of the Q-OLEDs. This need for improvement in the blue emitters is highlighted by others as well. [32,69]

The lowest performing packages were Per2-QLED and Per2-Q-OLED. These lead-free perovskites had low quantum yields and low overlaps with Rec. 2020. These design considerations are necessary to produce viable lead-free perovskite alternatives. Although only one lead-free perovskite alternative was explored here, other lead-free perovskite alternatives have been compared elsewhere for solar applications.[24] These perovskite variations may be applicable to displays as well.

This performance assessment did not encompass all possible measures of performance. Low performance in metrics not measured here could lead to serious issues as substance classes are evaluated for implementation at scale. One such performance metric not analyzed here is stability. For each substance class, we found that researchers experienced issues with the stability of the substances. [63,70,71] However, the discussions regarding stability of different substance classes is often qualitative. We don't have a quantitative way to compare these statements for the specific substances assessed here– broadly applicable quantitative tests are needed for stability evaluation.

In addition, encapsulation's impacts on stability need to be well established for each substance class. Encapsulation can also have impacts on the performance metrics reviewed here. The quantum yield for substances in this assessment were measured in solution, not in the powder form or embedded in plastic. This change in environment typically does not affect QDs performance, but has been known to impact perovskites.[63] Perovskites suffer from quenching in powder and color segregation in mixtures (in other words, ion exchange which could muddle colors). Encapsulation also affects InP QDs. In-QDs that do not have excellent electron confinement (which originates from imperfect shell structure or incompatible ligands) can also

have unwanted emission and loss of color purity (i.e. FWHM suffers). [72] InP QDs mechanisms of degradation are not as studied in the literature as those affecting Cd-QDs. Their structural similarities between In-QDs and Cd-QDs have meant that often Cd-relevant designs for QLEDs are used. A deeper understanding of InP-specific instability can help overcome this barrier.[72] The scaling up of technologies could also change their performance, but often these substance adjustments are often considered trade secrets and concealed by broad language in patents (e.g. for Cd-based QDs[73]).

In summary, these performance metrics are not perfect, but they do highlight certain essential properties of successful emissive materials. No one substance class had overall better performance than the rest, indicating that an individual synthesis can be the key to high scores.

5.5.3 Hazard assessment

The hazard scores for each package were averaged (Fig. 4A) which broadly demonstrates that there is no fully innocuous package. In addition, no package stands out as less hazardous than the others. To investigate differences that could be averaged out, we chose to expand the data into a heat map (see Table S5-3 for specific scores). A heat map that separates hazards by type (health, environment, and physical properties) as well as by substance (red, green, and blue) demonstrates the nuances in the data (Figure 5-4).

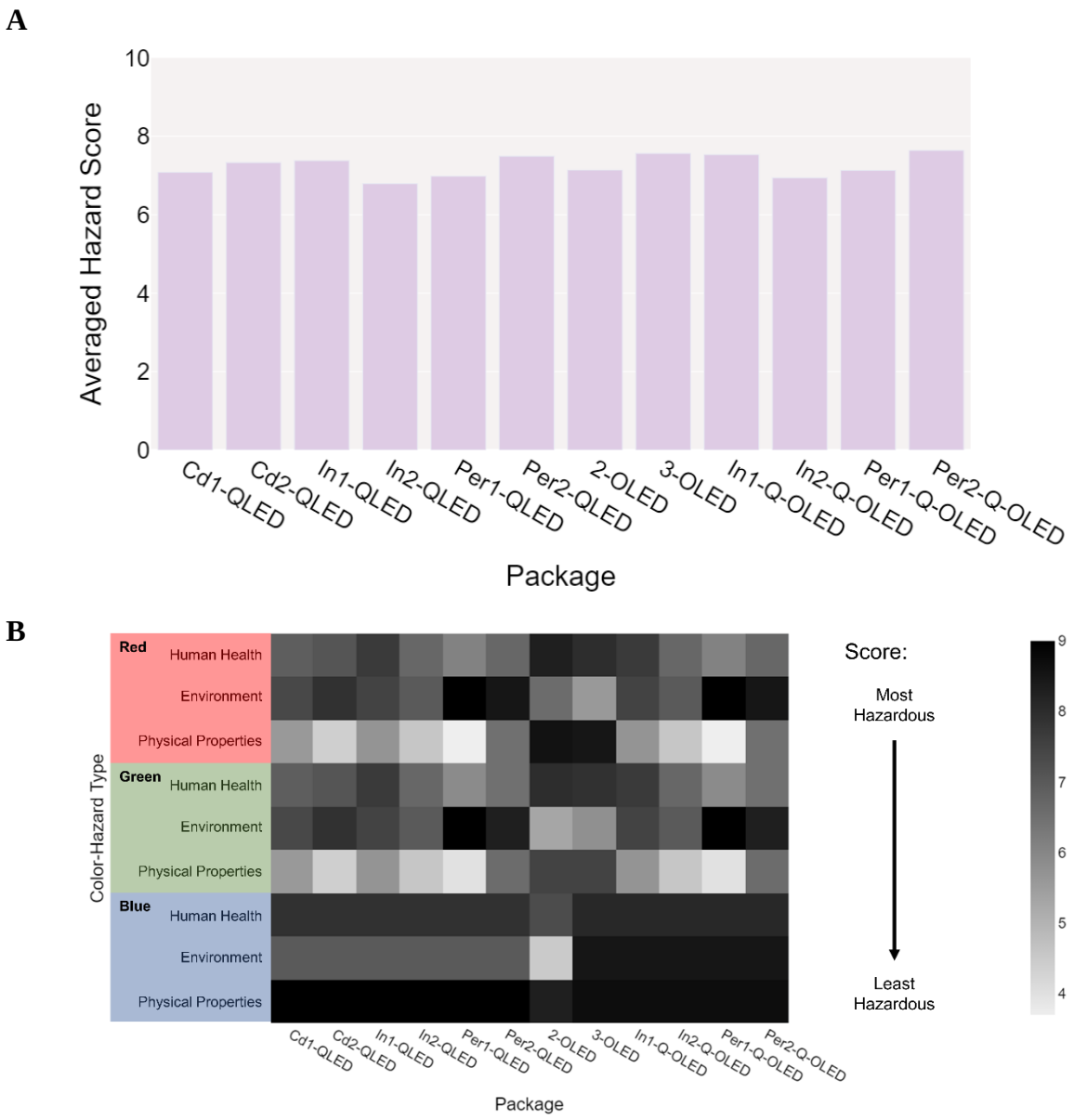

Figure 5-4: (A) averaged hazard assessment results and (B) hazard heat map, where dark indicates the most hazard, while light indicates the least hazard per substance (y-axis, red/green/blue) in a package (x-axis)

Touted as more sustainable than Cd-QDs in industry,[74] In-QDs do not score as less hazardous in this assessment. Although In-QDs do score better than Cd-QDs in their environmental safety by 1 point, In-QDs score an average of 0.3 and 0.1 worse in health and

physical properties, respectively, than Cd-QDs. These results contradict the Cd-QDs and In-QDs toxicity to human cells, which has been compared in a side-by-side manner by Pompa et al.[75] These QDs demonstrated similar instability and ion release.[75] However, because In ions were less toxic, so too were the In-QDs compared to Cd-QDs.[75] These side-by-side toxicity assessments are crucial, but the chemicals involved in the synthesis of QDs must also be less harmful, which is not the case.

Lead-based perovskites (Per1 packages) have low relatively health and physical properties hazards (average is 4.9 compared to the average of other packages which is 7.0). In contrast, they have a higher environmental hazard (average is 9 compared to the average of other packages which is 7.5), which roughly translates to LC_{50} for a 96h exposure to fish that is ≤ 1 mg/L. Surprisingly, the lead-free perovskite package (Per2 packages) was assessed here to be just as hazardous to the environment as the lead-containing Per1 packages. This is interesting because the drop-in replacement for lead bromide, antimony (III) bromide, is less hazardous. Therefore, one could expect Per2 to be less hazardous. However, there is increased hazard associated with the use of cesium bromide in Per2, compared to cesium carbonate in Per1. Also, various solvents in Per2 are harmful to the environment, such as oleylamine and octane, similar to the solvents found in Per1. In conclusion, Per2 packages employ more hazardous solvents and other precursors, increasing its average hazard. This conclusion illustrates that "lead-free" perovskites need to be studied with as much scrutiny as lead-based materials. In addition, these hazard conclusions about Per1 and Per2 focus on the inputs of the substances, the possible end-of-life impacts are not considered.

OLEDs were assessed here to be just as hazardous as the QLED alternatives. Although the OEs are associated with organic precursors, some of their inorganic precursors were the most hazardous precursors used in their synthesis. For example, palladium acetate and copper cyanide precursors in OEs (from both packages 2-OLED and 3-OLED) scored the highest hazard possible, 10. More broadly, 53% of the precursors for OLEDs that scored 10 (most hazardous) in at least one category had metals present, while metals only made up 30% of the precursors. The 3rd generation OLEDs (package 3-OLED), which are free of iridium, scored better or similarly as

2nd generation OLEDs (package 2-OLED) in health and environmental hazard, but worse (by 1.7) in terms of physical properties.

The combined hazards in Figure 4 demonstrate the hazard data that was gathered from safety data sheets (SDS) for this alternatives assessment. Missing data was not represented in Figure 5-4, but a lack of data has led to regrettable substitutions in the past. Data missing from this assessment is plotted in Figure 5-5.

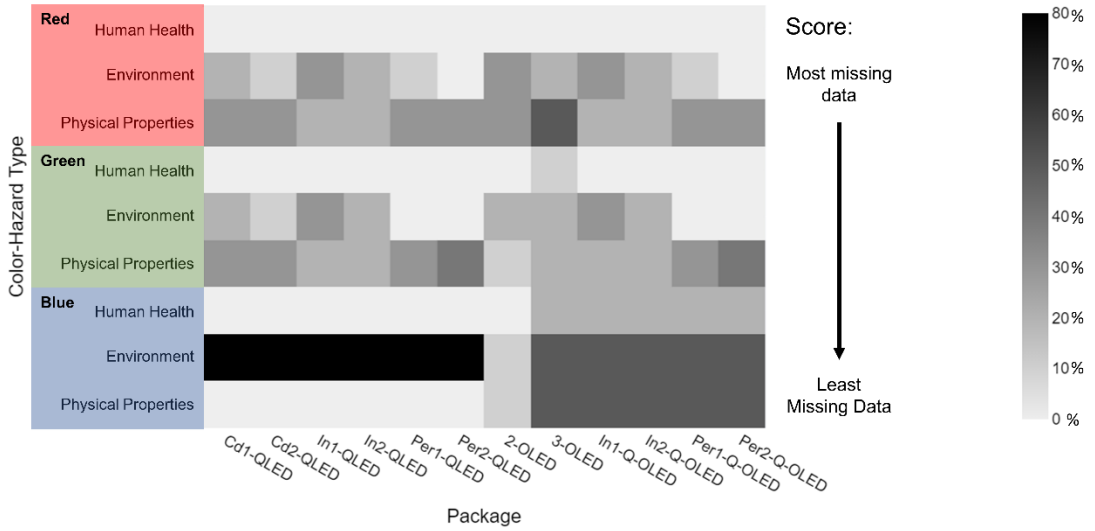

Figure 5-5: Initial missing hazard data results presented as a heatmap, where darker points indicate more missing data. At the maximum of the scale, 80% indicates that 80% of the precursors of a certain substance (color in the x axis) in a package (y-axis) had no data found in the SDS corresponding to the specific hazard (e.g. Environment in the x-axis). 0% indicates that all precursors of a substance had information regarding the specific hazard.

The least amount of missing data in Figure 5-5 is in the health hazard categories (see Table S5-4 for values). On average, only 1% of the precursors in all substances had data missing in both acute and chronic human health tests. This compares to 23-28% of the missing data for the environment and physical properties hazards. This points to the general lack of environmental hazard and stability data for many commercial chemicals.[76]

The largest amount of missing data is from the InGaN material, which forms the blue material of QLED displays. We hypothesize that lack of environment data is due to the high instability of the precursors (e.g. triethylgallium). These precursors decompose violently after contact with air and water and have been the cause of numerous workplace incidents.[77,78] Investigation into their possible byproducts after the reaction is complete (metal oxides) also yielded missing environmental data.[79] However, data gaps such as these should be addressed before choosing such an alternative over another with a more complete dataset.

Also, it is important to note the data that is missing from the health, environment, and physical properties categories. The P2OASys tool has three categories that were not integrated into Figure 5-4 and Figure 5-5; Atmospheric Hazard, Process Factors and Life Cycle Factors. These three categories had 75-76% missing data, which we deemed not robust enough for inclusion in the results. Of course, other key sustainability impact metrics, such as greenhouse gas emissions could also be explored further for promising alternatives using other sustainability assessment methods, such as LCA. However, if an alternative is identified, these categories must be explored more thoroughly to avoid regrettable substitutions.

Lastly, we acknowledge a lack of missing data about the end of life of these substances. Nanomaterials (e.g. Cd-QDs, In-QDs, perovskites) are known to undergo transformations which could impact their toxicity to humans, animals, or plants.[80] In addition, the encapsulation of these emissive substances for use in displays could have large impacts on their eventual behavior in the environment, and pose occupational risks to workers who tend to dismantle electronic items.[81] For ease of use of this assessment by other scientists, we decided to omit these end-of-life considerations. We hypothesize that decreasing the inherent hazard of the precursors of emissive substances could translate into less concern at their end of life.

5.5.4 Aggregation of Evaluations

With the three separate evaluations complete, the results were combined to determine if one alternative presented an optimal combination of high performance, competitive cost, and low hazard (Figure 6). To do this, the packages were assigned a rank per evaluation (e.g., the best performing material received a 1, least hazardous received a 1 and the lowest cost received a 1).

Then the three ranks were combined equally (Figure 5-6A). If a package scored a '3', this would indicate that it had the 'best'/ideal combination of performance, cost, and hazard. However, this was not the case for any package, and the best total score was 2.3 (In2-Q-OLED, Figure 5-6B), closely followed by 2.2 (In2-QLED) and 2.0 (2-OLED). The lowest total ranks were 1.0 (Per2-Q-OLED and Per2-QLED) and 1.1 (In1-QLED).

To demonstrate the versatility of the alternatives assessment, different weights were given to each evaluation (Figure 5-6C), and the scores changed (Figure 5-6D). With the weights being 1 for cost, 0.5 for performance, and 2 for environment, the highest possible score was 3.5. This did not change the top and bottom ranked packages mentioned above, but it did slightly increase the rank of Per1-QLED and decrease the rank of Per2-Q-OLED. Such a method could also be applied to the hazard assessment, where different types of hazards (e.g. carcinogenicity) could be weighted more than others (e.g. ecotoxicity).

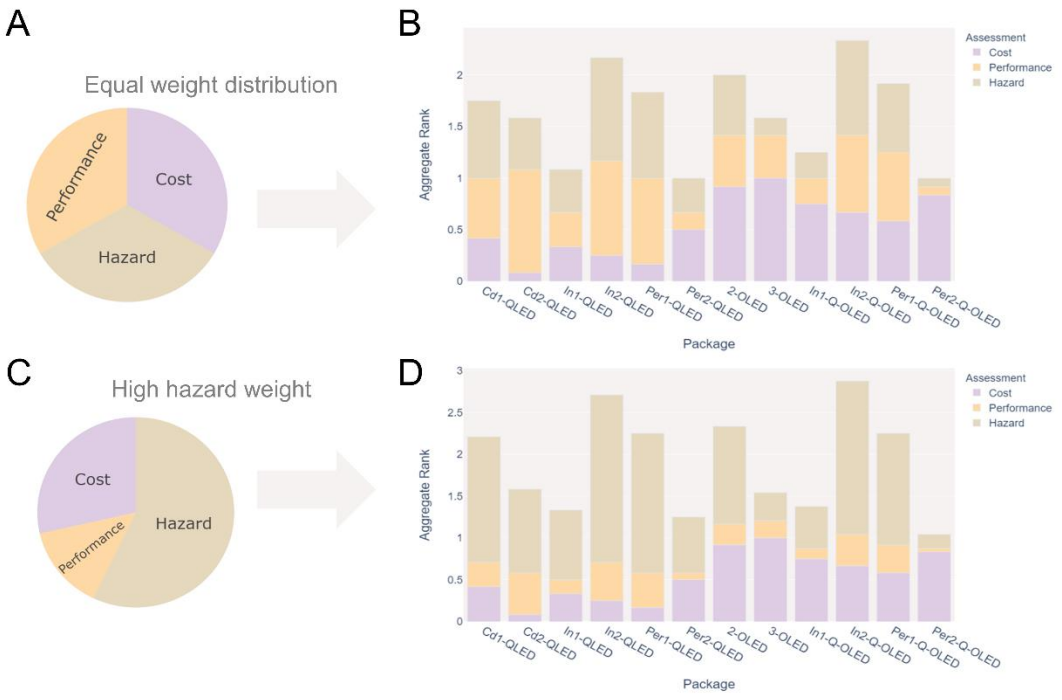

Figure 5-6: (A,B) Combined assessments with weight of 1 for each assessment (best in a category has a score of 1) (C,D) Combined assessments with (starting from the bottom) a weight of 1 for cost, 0.5 for performance, and 2 for hazard (best in the category has a score of 1, 0.5 and 2 respectively).

These aggregate rankings both smooth out large differences in the packages (e.g. cost where variation is 5000 fold, Figure 5-2) while increasing the differences between packages (e.g., hazard, where all average scores are within 6% of the average). However, keeping these factors in mind, it is still possible to draw a couple of conclusions.

First, there is no substance class that is better than the others based on the findings of our assessment. The average score of all packages was 1.63, and each substance class had one package that scored above this, and another that scored below. In other words, there is no substance class with both packages having a better aggregate score than the other substance classes. This, however, can be seen as an opportunity to develop safer, cheaper, higher-performing synthesis in any substance class. The more mature substance class, Cd-QDs in QLEDs, gave very similar aggregate scores, while newer substance classes like perovskites in QLEDs gave different scores.

Second, there is variation within substance classes, except for Cd-QDs. Cd-QDs containing packages scored within 0.5 of each other. The packages representing other substance classes (In-QDs, perovskites, and OEs) scored father apart from each other. This indicates the importance of individual syntheses. Since only 12 packages were chosen for analysis, there is the possibility that a superior synthesis was overlooked. For this reason, the assessment is structured such that it can be reproduced and updated with the latest innovation in these varied substance classes.

The example given in Figure 5-6C,D illustrates how changing priorities can change the overall score of different packages. This set of weights could be the priorities of a company that wants to make a cheap, safe display that does not compete at the top of the line in terms of performance. This set of priorities would probably lead to more development of In1-QDs, which scored relatively well in both QLED and Q-OLEDs.

5.5.5 Regulatory Assessment

This regulatory assessment covers the United States and Canada and is meant to simply identify specific substances that could encounter regulatory barriers from current policies. In

Europe, Cd-QDs were initially exempt from regulations limiting Cd in electronic, but this expired in 2018.[82] Some companies work around this regulation by introducing low-Cd alternatives, which includes mixing with In-QDs. Lead in perovskites could be regulated by the same Restriction on Hazardous Substances (RoHs) regulation as Cd, albeit at a higher amount (100 ppm Cd vs 1000 ppm Pb).[83] The electronics industry has made a regulatory-induced transition away from Pb in its soldering materials, so the adoption of a new lead-containing substance seems unlikely.[84] Cesium and antimony, which are used in lead-free perovskite studied here, are not restricted for use in electronics in the United States and Europe to the best of the authors knowledge.

In-QDs are currently undergoing consultation as to whether to introduce restrictions under RoHs in Europe.[85] A document submitted by Nanosys, a QD company, indicated that In-QDs currently had no feasible substitutions and should therefore continue to be sold until a substitution is found.[46] Non-radioactive iridium (present in 2-OLED packages) is not currently restricted by the RoHs or US EPA. The other OLED substances will have to demonstrate a certain level of safety to be approved for use in Europe on an industrial scale. Substance researchers can estimate possible hazards for OLEDs by using well established tools for toxicity prediction of organic molecules.[86]

In conclusion, this qualitative discussion on regulatory barriers indicates large barriers for Cd-QDs and Pb-containing perovskites. In-QDs are currently being examined, while the remainder of the substances are not currently restricted. However, these substances will be examined if they do prove to be commercialized substitutes for Cd-QDs. During that process, alternatives assessment could be used to determine whether there are feasible and less hazardous alternatives.

5.6 Conclusions

This alternatives assessment introduced different metrics for the emissive substance scientist to consider when developing their materials. Along with performance, cost and hazard are important considerations for the eventual manufacturers and end-users of these materials. This study highlighted the cost, performance, and hazard of emerging emissive substance classes by combining substances into packages. We found that the synthesis of the substance has a large

impact on its performance and cost, while hazards (when averaged) were largely the same. Combining these results highlighted that no one substance class is better than the others. This was surprising to us given the excitement in the literature regarding the sustainability of perovskites[63] and In-QDs.[74]

However, this alternatives assessment was not meant to conclusively rank all different substance classes or substances in this field, but rather to illustrate a method that could be used to assess new materials. There are many other nanocrystals and organic emitters that were not covered in this work. For example, there are many different lead-free perovskites in development for solar cells[24] that have not been tested for use in display applications. These perovskites could be safer and higher performing than the 1 lead free perovskite we analyzed here.

This method also has data gaps in each assessment that can be filled by other researchers. In the cost assessment, we do not consider the possible impacts of encapsulation of each material, or the amount that could be wasted during manufacturing. In the performance assessment, there is no consideration of a materials stability because of a lack of standardized reporting by the primary sources. In the hazard assessment, we acknowledge that the hazard of a material is not simply the sum of its precursors and solvents. Work correlating the hazard of the precursors of a substance to the actual hazard of that substance at its end of life is necessary. There are also hazards such as contribution to climate change which were not considered.

Despite these gaps, this alternatives assessment did serve its original purpose of identifying possible issues with alternatives for Cd-QDs. We identified that the presence of lead in perovskites will introduce similar hazards as Cd and may cause the enforcement of same metal-based regulations that stopped Cd-QDs. This work thus challenges the assumption sometimes made by researchers that lead-based perovskites are inherently safer or greener alternatives to Cd-QDs. Lead-free perovskites need major improvements in performance and a decrease in use of hazardous precursors (both solvents and reactants). Other substances that need substantial improvement in hazard are blue emitters, which can be difficult to design considering only performance metrics. Currently, however, we conclude that all available drop-in replacements for Cd-QDs may one day be considered regrettable substitutions.

If this alternatives assessment had identified a preferable alternative, more research would be needed. To improve this alternatives assessment, we designate stability metrics as well as life cycle and expanded hazard metrics, as keys to the next steps to determine the suitability for a substance's use in displays. Different assessment methodologies, such as life cycle impact analysis or risk analysis (considering exposure) must also inform decisions regarding the next generation of emissive substances.

In addition, there are many more applications that have the potential to benefit from an alternatives assessment to distinguish the most promising substance classes. Just as alternatives assessment has guided industry and government regulation, we hypothesize that there is a place for alternative assessment to drive sustainable (and functional and cost competitive) innovation in an academic context.

5.7 References

(1) Forti, V.; Balde, C. P.; Kuehr, R.; Bel, G. *The Global E-Waste Monitor 2020: Quantities, Flows and the Circular Economy Potential.*; United Nations University (UNU)/United Nations Institute for Training and Research (UNITAR) – co-hosted SCYCLE Programme, International Telecommunication Union (ITU) & International Solid Waste Association (ISWA),: Bonn/Geneva/Rotterdam, 2020; pp 1–15.

(2) Lim, S.-R.; Schoenung, J. M. Human Health and Ecological Toxicity Potentials Due to Heavy Metal Content in Waste Electronic Devices with Flat Panel Displays. *Journal of Hazardous Materials* **2010**, *177* (1), 251–259. https://doi.org/10.1016/j.jhazmat.2009.12.025.

(3) Zhao, X.; Ng, J. D. A.; Friend, R. H.; Tan, Z.-K. Opportunities and Challenges in Perovskite Light-Emitting Devices. *ACS Photonics* **2018**, *5* (10), 3866–3875. https://doi.org/10.1021/acsphotonics.8b00745.

(4) Fawell, J. *Cadmium in Drinking-Water*; Background document for development of WHO Guidelines for Drinking-water Quality; WHO/SDE/WSH/03.04/80/Rev/1; World Health Organization: Geneva, 2011; pp 1–16.

(5) Chen, H.-W.; Lee, J.-H.; Lin, B.-Y.; Chen, S.; Wu, S.-T. Liquid Crystal Display and Organic Light-Emitting Diode Display: Present Status and Future Perspectives. *Light Sci Appl* **2018**, *7* (3), 17168–17168. https://doi.org/10.1038/lsa.2017.168.

(6) Chopra, S. S.; Theis, T. L. Comparative Cradle-to-Gate Energy Assessment of Indium Phosphide and Cadmium Selenide Quantum Dot Displays. *Environ. Sci.: Nano* **2017**, *4* (1), 244–254. https://doi.org/10.1039/C6EN00326E.

(7) S. Chopra, S.; Bi, Y.; C. Brown, F.; L. Theis, T.; D. Hristovski, K.; Westerhoff, P. Interdisciplinary Collaborations to Address the Uncertainty Problem in Life Cycle Assessment of Nano-Enabled Products: Case of the Quantum Dot-Enabled Display.

Environmental Science: Nano **2019**, *6* (11), 3256–3267. https://doi.org/10.1039/C9EN00603F.
(8) Scalbi, S.; Fantin, V.; Antolini, F. Environmental Assessment of New Technologies: Production of a Quantum Dots-Light Emitting Diode. *Journal of Cleaner Production* **2017**, *142*, 3702–3718. https://doi.org/10.1016/j.jclepro.2016.10.098.
(9) Schileo, G.; Grancini, G. Lead or No Lead? Availability, Toxicity, Sustainability and Environmental Impact of Lead-Free Perovskite Solar Cells. *Journal of Materials Chemistry C* **2021**, *9* (1), 67–76. https://doi.org/10.1039/D0TC04552G.
(10) Ke, W.; Kanatzidis, M. G. Prospects for Low-Toxicity Lead-Free Perovskite Solar Cells. *Nature Communications* **2019**, *10* (1), 965. https://doi.org/10.1038/s41467-019-08918-3.
(11) Amasawa, E.; Ihara, T.; Ohta, T.; Hanaki, K. Life Cycle Assessment of Organic Light Emitting Diode Display as Emerging Materials and Technology. *Journal of Cleaner Production* **2016**, *135*, 1340–1350. https://doi.org/10.1016/j.jclepro.2016.07.025.
(12) Yeom, J.-M.; Jung, H.-J.; Choi, S.-Y.; Lee, D. S.; Lim, S.-R. Environmental Effects of the Technology Transition from Liquid–Crystal Display (LCD) to Organic Light-Emitting Diode (OLED) Display from an E-Waste Management Perspective. *Int J Environ Res* **2018**, *12* (4), 479–488. https://doi.org/10.1007/s41742-018-0106-y.
(13) Curran, M. A. Strengths and Limitations of Life Cycle Assessment. In *Background and Future Prospects in Life Cycle Assessment*; Klöpffer, W., Ed.; Springer Netherlands: Dordrecht, 2014; pp 189–206. https://doi.org/10.1007/978-94-017-8697-3_6.
(14) Gallagher, M. J.; Allen, C.; Buchman, J. T.; Qiu, T. A.; Clement, P. L.; Krause, M. O. P.; Gilbertson, L. M. Research Highlights: Applications of Life-Cycle Assessment as a Tool for Characterizing Environmental Impacts of Engineered Nanomaterials. *Environ. Sci.: Nano* **2017**, *4* (2), 276–281. https://doi.org/10.1039/C7EN90005H.
(15) Gilbertson, L. M.; Wender, B. A.; Zimmerman, J. B.; Eckelman, M. J. Coordinating Modeling and Experimental Research of Engineered Nanomaterials to Improve Life Cycle Assessment Studies. *Environ. Sci.: Nano* **2015**, *2* (6), 669–682. https://doi.org/10.1039/C5EN00097A.
(16) Jacobs, M. M.; Malloy, T. F.; Tickner, J. A.; Edwards, S. Alternatives Assessment Frameworks: Research Needs for the Informed Substitution of Hazardous Chemicals. *Environ Health Perspect* **2016**, *124* (3), 265–280. https://doi.org/10.1289/ehp.1409581.
(17) Council, N. R.; Studies, D. on E. and L.; Toxicology, B. on E. S. and; Technology, B. on C. S. and; Decisions, C. on the D. and E. of S. C. S. A. F. to I. G. and I. *A Framework to Guide Selection of Chemical Alternatives*; National Academies Press, 2014.
(18) Chen, J.; Zhang, S.; Allen, D. T.; Subramaniam, B.; Licence, P. Expectations for Manuscripts Contributing to the Field on Management of Synthetic Chemicals in ACS Sustainable Chemistry & Engineering. *ACS Sustainable Chem. Eng.* **2021**, *9* (9), 3376–3378. https://doi.org/10.1021/acssuschemeng.1c01134.
(19) Oregon Health Authority : Toxic Free Kids Act: Rules and Implementation https://www.oregon.gov/oha/ph/healthyenvironments/healthyneighborhoods/toxicsubstances/pages/toxic-free-rules.aspx (accessed 2021 -09 -27).
(20) Eliason, P.; Morose, G. Safer Alternatives Assessment: The Massachusetts Process as a Model for State Governments. *Journal of Cleaner Production* **2011**, *19* (5), 517–526. https://doi.org/10.1016/j.jclepro.2010.05.011.

(21) *Regulation (EC) No 1272/2008 of the European Parliament and of the Council of 16 December 2008 on Classification, Labelling and Packaging of Substances and Mixtures, Amending and Repealing Directives 67/548/EEC and 1999/45/EC, and Amending Regulation (EC) No 1907/2006 (Text with EEA Relevance)*; 2008; Vol. 353.
(22) *Current Landscape of Alterntivaes Assessment Practice: A Meta-Review*; Risk Management; 26; Organization for Economic Co-operation and Development: Paris, 2013; pp 1–41.
(23) Gilbertson, L. M.; Ng, C. A. Evaluating the Use of Alternatives Assessment To Compare Bulk Organic Chemical and Nanomaterial Alternatives to Brominated Flame Retardants. *ACS Sustainable Chem. Eng.* **2016**, *4* (11), 6019–6030. https://doi.org/10.1021/acssuschemeng.6b01318.
(24) Llanos, M.; Yekani, R.; Demopoulos, G. P.; Basu, N. Alternatives Assessment of Perovskite Solar Cell Materials and Their Methods of Fabrication. *Renewable and Sustainable Energy Reviews* **2020**, *133*, 110207. https://doi.org/10.1016/j.rser.2020.110207.
(25) Zhang, H.; Sui, N.; Chi, X.; Wang, Y.; Liu, Q.; Zhang, H.; Ji, W. Ultrastable Quantum-Dot Light-Emitting Diodes by Suppression of Leakage Current and Exciton Quenching Processes. *ACS Appl. Mater. Interfaces* **2016**, *8* (45), 31385–31391. https://doi.org/10.1021/acsami.6b09246.
(26) Zhu, R.; Luo, Z.; Chen, H.; Dong, Y.; Wu, S.-T. Realizing Rec. 2020 Color Gamut with Quantum Dot Displays. *Opt. Express, OE* **2015**, *23* (18), 23680–23693. https://doi.org/10.1364/OE.23.023680.
(27) Theis, D. Display Technology. In *Ullmann's Encyclopedia of Industrial Chemistry*; Wiley-VCH Verlag GmbH & Co. KGaA, Ed.; Wiley-VCH Verlag GmbH & Co. KGaA: Weinheim, Germany, 2008; p a08_603.pub2. https://doi.org/10.1002/14356007.a08_603.pub2.
(28) Carter, C. M.; Cho, J.; Glanzer, A.; Kamcev, N.; O'Carroll, D. M. Cost, Energy and Emissions Assessment of Organic Polymer Light-Emitting Device Architectures. *Journal of Cleaner Production* **2016**, *137*, 1418–1431. https://doi.org/10.1016/j.jclepro.2016.07.186.
(29) Luo, Z.; Xu, D.; Wu, S. Emerging Quantum-Dots-Enhanced LCDs. *Journal of Display Technology* **2014**, *10* (7), 526–539. https://doi.org/10.1109/JDT.2014.2325218.
(30) Brown, R. P.; Gallagher, M. J.; Fairbrother, D. H.; Rosenzweig, Z. Synthesis and Degradation of Cadmium-Free InP and InPZn/ZnS Quantum Dots in Solution. *Langmuir* **2018**, *34* (46), 13924–13934. https://doi.org/10.1021/acs.langmuir.8b02402.
(31) Chen, Y.; Li, S.; Huang, L.; Pan, D. Low-Cost and Gram-Scale Synthesis of Water-Soluble Cu–In–S/ZnS Core/Shell Quantum Dots in an Electric Pressure Cooker. *Nanoscale* **2014**, *6* (3), 1295–1298. https://doi.org/10.1039/C3NR05014A.
(32) Li, C.-H. A.; Zhou, Z.; Vashishtha, P.; Halpert, J. E. The Future Is Blue (LEDs): Why Chemistry Is the Key to Perovskite Displays. *Chem. Mater.* **2019**, *31* (16), 6003–6032. https://doi.org/10.1021/acs.chemmater.9b01650.
(33) Protesescu, L.; Yakunin, S.; Bodnarchuk, M. I.; Krieg, F.; Caputo, R.; Hendon, C. H.; Yang, R. X.; Walsh, A.; Kovalenko, M. V. Nanocrystals of Cesium Lead Halide Perovskites (CsPbX3, X = Cl, Br, and I): Novel Optoelectronic Materials Showing Bright

Emission with Wide Color Gamut. *Nano Lett.* **2015**, *15* (6), 3692–3696. https://doi.org/10.1021/nl5048779.
(34) Zhang, J.; Yang, Y.; Deng, H.; Farooq, U.; Yang, X.; Khan, J.; Tang, J.; Song, H. High Quantum Yield Blue Emission from Lead-Free Inorganic Antimony Halide Perovskite Colloidal Quantum Dots. *ACS Nano* **2017**, *11* (9), 9294–9302. https://doi.org/10.1021/acsnano.7b04683.
(35) *Commission Delegated Directive (EU) 2015/863 of 31 March 2015 Amending Annex II to Directive 2011/65/EU of the European Parliament and of the Council as Regards the List of Restricted Substances (Text with EEA Relevance)*; 2015; Vol. OJ L.
(36) Hong, G.; Gan, X.; Leonhardt, C.; Zhang, Z.; Seibert, J.; Busch, J. M.; Bräse, S. A Brief History of OLEDs—Emitter Development and Industry Milestones. *Adv. Mater.* **2021**, *33* (9), 2005630. https://doi.org/10.1002/adma.202005630.
(37) Li, T.-Y.; Wu, J.; Wu, Z.-G.; Zheng, Y.-X.; Zuo, J.-L.; Pan, Y. Rational Design of Phosphorescent Iridium(III) Complexes for Emission Color Tunability and Their Applications in OLEDs. *Coordination Chemistry Reviews* **2018**, *374*, 55–92. https://doi.org/10.1016/j.ccr.2018.06.014.
(38) Teng, J.-M.; Wang, Y.-F.; Chen, C.-F. Recent Progress of Narrowband TADF Emitters and Their Applications in OLEDs. *Journal of Materials Chemistry C* **2020**, *8* (33), 11340–11353. https://doi.org/10.1039/D0TC02682D.
(39) Kim, K.-H.; Kim, J.-J. Origin and Control of Orientation of Phosphorescent and TADF Dyes for High-Efficiency OLEDs. *Advanced Materials* **2018**, *30* (42), 1705600. https://doi.org/10.1002/adma.201705600.
(40) Liao, J.-L.; Rajakannu, P.; Gnanasekaran, P.; Tsai, S.-R.; Lin, C.-H.; Liu, S.-H.; Chang, C.-H.; Lee, G.-H.; Chou, P.-T.; Chen, Z.-N.; Chi, Y. Luminescent Diiridium Complexes with Bridging Pyrazolates: Characterization and Fabrication of OLEDs Using Vacuum Thermal Deposition. *Advanced Optical Materials* **2018**, *6* (11), 1800083. https://doi.org/10.1002/adom.201800083.
(41) Yang, X.; Guo, H.; Liu, B.; Zhao, J.; Zhou, G.; Wu, Z.; Wong, W.-Y. Diarylboron-Based Asymmetric Red-Emitting Ir(III) Complex for Solution-Processed Phosphorescent Organic Light-Emitting Diode with External Quantum Efficiency above 28%. *Adv. Sci.* **2018**, *5* (5), 1701067. https://doi.org/10.1002/advs.201701067.
(42) Shin, H.; Ha, Y. H.; Kim, H.; Kim, R.; Kwon, S.; Kim, Y.; Kim, J. Controlling Horizontal Dipole Orientation and Emission Spectrum of Ir Complexes by Chemical Design of Ancillary Ligands for Efficient Deep-Blue Organic Light-Emitting Diodes. *Adv. Mater.* **2019**, *31* (21), 1808102. https://doi.org/10.1002/adma.201808102.
(43) Wu, T.-L.; Huang, M.-J.; Lin, C.-C.; Huang, P.-Y.; Chou, T.-Y.; Chen-Cheng, R.-W.; Lin, H.-W.; Liu, R.-S.; Cheng, C.-H. Diboron Compound-Based Organic Light-Emitting Diodes with High Efficiency and Reduced Efficiency Roll-Off. *Nature Photon* **2018**, *12* (4), 235–240. https://doi.org/10.1038/s41566-018-0112-9.
(44) Zhang, Y.; Ran, Q.; Wang, Q.; Liu, Y.; Hänisch, C.; Reineke, S.; Fan, J.; Liao, L. High-Efficiency Red Organic Light-Emitting Diodes with External Quantum Efficiency Close to 30% Based on a Novel Thermally Activated Delayed Fluorescence Emitter. *Adv. Mater.* **2019**, *31* (42), 1902368. https://doi.org/10.1002/adma.201902368.
(45) Lin, T.-A.; Chatterjee, T.; Tsai, W.-L.; Lee, W.-K.; Wu, M.-J.; Jiao, M.; Pan, K.-C.; Yi, C.-L.; Chung, C.-L.; Wong, K.-T.; Wu, C.-C. Sky-Blue Organic Light Emitting Diode

with 37% External Quantum Efficiency Using Thermally Activated Delayed Fluorescence from Spiroacridine-Triazine Hybrid. *Adv. Mater.* **2016**, *28* (32), 6976–6983. https://doi.org/10.1002/adma.201601675.
(46) Nanosys. Review of Impact of Potential New RoHS Substance Restrictions for Indium-Phosphide. Nanosys November 2019.
(47) Li, Y.; Hou, X.; Dai, X.; Yao, Z.; Lv, L.; Jin, Y.; Peng, X. Stoichiometry-Controlled InP-Based Quantum Dots: Synthesis, Photoluminescence, and Electroluminescence. *J. Am. Chem. Soc.* **2019**, *141* (16), 6448–6452. https://doi.org/10.1021/jacs.8b12908.
(48) Jang, E.; Jun, S.; Jang, H.; Lim, J.; Kim, B.; Kim, Y. White-Light-Emitting Diodes with Quantum Dot Color Converters for Display Backlights. *Advanced Materials* **2010**, *22* (28), 3076–3080. https://doi.org/10.1002/adma.201000525.
(49) Shenai-Khatkhate, D. V.; Goyette, R. J.; DiCarlo Jr., R. L.; Dripps, G. Environment, Health and Safety Issues for Sources Used in MOVPE Growth of Compound Semiconductors. *Journal of Crystal Growth* **2004**, *272* (1), 816–821. https://doi.org/10.1016/j.jcrysgro.2004.09.007.
(50) Volz, D.; Wallesch, M.; Fléchon, C.; Danz, M.; Verma, A.; M. Navarro, J.; M. Zink, D.; Bräse, S.; Baumann, T. From Iridium and Platinum to Copper and Carbon: New Avenues for More Sustainability in Organic Light-Emitting Diodes. *Green Chemistry* **2015**, *17* (4), 1988–2011. https://doi.org/10.1039/C4GC02195A.
(51) Sun, Y.; Jiang, Y.; Sun, X. W.; Zhang, S.; Chen, S. Beyond OLED: Efficient Quantum Dot Light-Emitting Diodes for Display and Lighting Application. *The Chemical Record* **2019**, *19* (8), 1729–1752. https://doi.org/10.1002/tcr.201800191.
(52) Yang, C.; Zhuang, B.; Lin, J.; Wang, S.; Liu, M.; Jiang, N.; Chen, D. Ultrastable Glass-Protected All-Inorganic Perovskite Quantum Dots with Finely Tunable Green Emissions for Approaching Rec. 2020 Backlit Display. *Chemical Engineering Journal* **2020**, *398*, 125616. https://doi.org/10.1016/j.cej.2020.125616.
(53) Bechu, A.; Griffin, H. Emissive Substance Spectral Overlap with Rec. 2020, 2021.
(54) Chen, H.-W.; Zhu, R.-D.; He, J.; Duan, W.; Hu, W.; Lu, Y.-Q.; Li, M.-C.; Lee, S.-L.; Dong, Y.-J.; Wu, S.-T. Going beyond the Limit of an LCD's Color Gamut. *Light: Science & Applications* **2017**, *6* (9), e17043–e17043. https://doi.org/10.1038/lsa.2017.43.
(55) Wang, T. Topical Review: Development of Overgrown Semi-Polar GaN for High Efficiency Green/Yellow Emission. *Semicond. Sci. Technol.* **2016**, *31*, 093003. https://doi.org/10.1088/0268-1242/31/9/093003.
(56) *Regulation (EC) No 1907/2006 of the European Parliament and of the Council of 18 December 2006 Concerning the Registration, Evaluation, Authorisation and Restriction of Chemicals (REACH), Establishing a European Chemicals Agency, Amending Directive 1999/45/EC and Repealing Council Regulation (EEC) No 793/93 and Commission Regulation (EC) No 1488/94 as Well as Council Directive 76/769/EEC and Commission Directives 91/155/EEC, 93/67/EEC, 93/105/EC and 2000/21/EC*; 2006; Vol. 396.
(57) US EPA. EPA Announces Path Forward for TSCA Chemical Risk Evaluations https://www.epa.gov/newsreleases/epa-announces-path-forward-tsca-chemical-risk-evaluations (accessed 2021 -09 -24).
(58) P2OASys - Tool - About https://p2oasys.turi.org/GetStarted/About/about.html (accessed 2021 -01 -11).

(59) GHS (Rev.8) (2019) | UNECE https://unece.org/ghs-rev8-2019 (accessed 2021 -09 -28).
(60) Tickner, J. A.; Schifano, J. N.; Blake, A.; Rudisill, C.; Mulvihill, M. J. Advancing Safer Alternatives Through Functional Substitution. *Environ. Sci. Technol.* **2015**, *49* (2), 742–749. https://doi.org/10.1021/es503328m.
(61) Chen, Z.; Yan, S.; Danesh, C. MicroLED Technologies and Applications: Characteristics, Fabrication, Progress, and Challenges. *J. Phys. D: Appl. Phys.* **2021**, *54* (12), 123001. https://doi.org/10.1088/1361-6463/abcfe4.
(62) Jean, J.; Xiao, J.; Nick, R.; Moody, N.; Nasilowski, M.; Bawendi, M.; Bulović, V. Synthesis Cost Dictates the Commercial Viability of Lead Sulfide and Perovskite Quantum Dot Photovoltaics. *Energy Environ. Sci.* **2018**, *11* (9), 2295–2305. https://doi.org/10.1039/C8EE01348A.
(63) Wang, X.; Bao, Z.; Chang, Y.-C.; Liu, R.-S. Perovskite Quantum Dots for Application in High Color Gamut Backlighting Display of Light-Emitting Diodes. *ACS Energy Lett.* **2020**, *5* (11), 3374–3396. https://doi.org/10.1021/acsenergylett.0c01860.
(64) Song, Z.; L. McElvany, C.; B. Phillips, A.; Celik, I.; W. Krantz, P.; C. Watthage, S.; K. Liyanage, G.; Apul, D.; J. Heben, M. A Technoeconomic Analysis of Perovskite Solar Module Manufacturing with Low-Cost Materials and Techniques. *Energy & Environmental Science* **2017**, *10* (6), 1297–1305. https://doi.org/10.1039/C7EE00757D.
(65) *Critical Raw Materials Resilience: Charting a Path towards Greater Security and Sustainability*-; Communication COM(2020) 474 final; European Commission: Brussels, 2020.
(66) Recommendation ITU-R BT.2020-2: Parameter Values for Ultra-High Definition Television Systems for Production and International Programme Exchange. International Telecommunication Union 2015.
(67) Yu, W. W.; Qu, L.; Guo, W.; Peng, X. Experimental Determination of the Extinction Coefficient of CdTe, CdSe, and CdS Nanocrystals. *Chemistry of Materials* **2003**, *15* (14), 2854–2860.
(68) Chen, L.; You, H.; Yang, C.; Zhang, X.; Qin, J.; Ma, D. Tuning the Saturated Red Emission: Synthesis, Electrochemistry and Photophysics of 2-Arylquinoline Based Iridium(III) Complexes and Their Application in OLEDs. *J. Mater. Chem.* **2006**, *16* (32), 3332–3339. https://doi.org/10.1039/B605783G.
(69) Lee, J.-H.; Chen, C.-H.; Lee, P.-H.; Lin, H.-Y.; Leung, M.; Chiu, T.-L.; Lin, C.-F. Blue Organic Light-Emitting Diodes: Current Status, Challenges, and Future Outlook. *J. Mater. Chem. C* **2019**, *7* (20), 5874–5888. https://doi.org/10.1039/C9TC00204A.
(70) Liu, Z.; Lin, C.-H.; Hyun, B.-R.; Sher, C.-W.; Lv, Z.; Luo, B.; Jiang, F.; Wu, T.; Ho, C.-H.; Kuo, H.-C.; He, J.-H. Micro-Light-Emitting Diodes with Quantum Dots in Display Technology. *Light Sci Appl* **2020**, *9* (1), 83. https://doi.org/10.1038/s41377-020-0268-1.
(71) Moon, H.; Lee, C.; Lee, W.; Kim, J.; Chae, H. Stability of Quantum Dots, Quantum Dot Films, and Quantum Dot Light-Emitting Diodes for Display Applications. *Adv. Mater.* **2019**, *31* (34), 1804294. https://doi.org/10.1002/adma.201804294.
(72) Wu, Z.; Liu, P.; Zhang, W.; Wang, K.; Sun, X. W. Development of InP Quantum Dot-Based Light-Emitting Diodes. *ACS Energy Lett.* **2020**, *5* (4), 1095–1106. https://doi.org/10.1021/acsenergylett.9b02824.
(73) Dubrow, R. S.; Freeman, W. P.; Lee, E.; Furuta, P. Quantum Dot Films, Lighting Devices, and Lighting Methods. US9199842B2, December 1, 2015.

(74) Ko, Y.-H.; Prabhakaran, P.; Choi, S.; Kim, G.-J.; Lee, C.; Lee, K.-S. Environmentally Friendly Quantum-Dot Color Filters for Ultra-High-Definition Liquid Crystal Displays. *Sci Rep* **2020**, *10* (1), 15817. https://doi.org/10.1038/s41598-020-72468-8.
(75) Brunetti, V.; Chibli, H.; Fiammengo, R.; Galeone, A.; Ada Malvindi, M.; Vecchio, G.; Cingolani, R.; L. Nadeau, J.; Paolo Pompa, P. InP/ZnS as a Safer Alternative to CdSe/ZnS Core/Shell Quantum Dots : In Vitro and in Vivo Toxicity Assessment. *Nanoscale* **2013**, *5* (1), 307–317. https://doi.org/10.1039/C2NR33024E.
(76) Ingre-Khans, E.; Ågerstrand, M.; Beronius, A.; Rudén, C. Transparency of Chemical Risk Assessment Data under REACH. *Environ. Sci.: Processes Impacts* **2016**, *18* (12), 1508–1518. https://doi.org/10.1039/C6EM00389C.
(77) Wojcik, S. M. OSHA issues $28,000 in fines for Upper Macungie lab explosion https://www.mcall.com/news/local/parkland/mc-upper-macungie-cyoptics-osha-report-20170725-story.html (accessed 2021 -06 -10).
(78) Dow Chemical Worker Dies After Plant Fire https://cen.acs.org/articles/91/i42/Dow-Chemical-Worker-Dies-Plant.html (accessed 2021 -06 -10).
(79) PubChem. Indium oxide https://pubchem.ncbi.nlm.nih.gov/compound/150905 (accessed 2021 -06 -10).
(80) Zhang, J.; Guo, W.; Li, Q.; Wang, Z.; Liu, S. The Effects and the Potential Mechanism of Environmental Transformation of Metal Nanoparticles on Their Toxicity in Organisms. *Environmental Science: Nano* **2018**, *5* (11), 2482–2499. https://doi.org/10.1039/C8EN00688A.
(81) J. Gallagher, M.; T. Buchman, J.; A. Qiu, T.; Zhi, B.; Y. Lyons, T.; M. Landy, K.; Rosenzweig, Z.; L. Haynes, C.; Howard Fairbrother, D. Release, Detection and Toxicity of Fragments Generated during Artificial Accelerated Weathering of CdSe/ZnS and CdSe Quantum Dot Polymer Composites. *Environmental Science: Nano* **2018**, *5* (7), 1694–1710. https://doi.org/10.1039/C8EN00249E.
(82) *Directive 2011/65/EU of the European Parliament and of the Council of 8 June 2011 on the Restriction of the Use of Certain Hazardous Substances in Electrical and Electronic Equipment Text with EEA Relevance*; 2011; Vol. OJ L.
(83) Wäger, P. A.; Schluep, M.; Müller, E.; Gloor, R. RoHS Regulated Substances in Mixed Plastics from Waste Electrical and Electronic Equipment. *Environ. Sci. Technol.* **2012**, *46* (2), 628–635. https://doi.org/10.1021/es202518n.
(84) Huang, C.-M.; Raj, A.; Osterman, M.; Pecht, M. Assembly Options and Challenges for Electronic Products With Lead-Free Exemption. *IEEE Access* **2020**, *8*, 134194–134208. https://doi.org/10.1109/ACCESS.2020.3010771.
(85) *ROHS Annex II Dossier for Indium Phosphide. Restriction Proposal for Substances in Electrical and Electronic Equipment under RoHS*; Oko-Institut e.V., 2019; pp 1–47.
(86) Bhatia, S.; Schultz, T.; Roberts, D.; Shen, J.; Kromidas, L.; Marie Api, A. Comparison of Cramer Classification between Toxtree, the OECD QSAR Toolbox and Expert Judgment. *Regulatory Toxicology and Pharmacology* **2015**, *71* (1), 52–62. https://doi.org/10.1016/j.yrtph.2014.11.005.

5.8 Supporting Information:

5.8.1 Specific substances used in packages

Table S5-1: Substances used to build the packages in this assessment

Package	Red-	Green-	Blue-
Cd1-QLED	CdSe/ZnS[1]	CdSe/ZnS[1]	InGaN[2,3]
Cd2-QLED	CdSe/CdS/ZnS/CdSZnS[4]	CdSe/CdS/ZnS/CdSZnS[4]	InGaN[2,3]
In1-QLED	InPZnS/ZnS[5]	InPZnS/ZnS[5]	InGaN[2,3]
In2-QLED	InP/ZnSe/ZnS[6]	InP/ZnSe/ZnS[6]	InGaN[2,3]
P1-QLED	CsPbI3[7]	CsPbBr3[7]	InGaN[2,3]
P2-QLED	Cs3Sb2Br9[8]	Cs3Sb2I9[8]	InGaN[2,3]
2-OLED	PyThir[9]	2a[10]	Ir-2[11]
3-OLED	TPAPZCN[12]	CzDBA[13]	spiroAcTRZ[14]
In1-Q-OLED	InPZnS/ZnS[5]	InPZnS/ZnS[5]	spiroAcTRZ[14]
In2-Q-OLED	InP/ZnSe/ZnS[6]	InP/ZnSe/ZnS[6]	spiroAcTRZ[14]
P1-Q-OLED	CsPbI3[7]	CsPbBr3[7]	spiroAcTRZ[14]
P2-Q-OLED	Cs3Sb2Br9[8]	Cs3Sb2I9[8]	spiroAcTRZ[14]

5.8.2 Cost: Detailed Methods

1. See “Cost (CADg)” in spreadsheet. The substance prices are calculated in Rows 1-269, while you can input your own substance in cells 270.
2. Identify the needed chemical names, their purity (column C,D)
3. Find a vendor online (column E), find the CAS numbers (column F), and link the website (column G)
    a. In this assessment, the largest package size (up to 100g for solids or 4L for liquids) was used
4. Input the price of that package size (column H) and convert it to CAD (column I). Place the size of the chemical ordered in Column J

5. Calculate the price per unit (column K) by dividing column I/ the integer in column J
6. Determine the amount used in the synthesis with its unit (column M)
7. Convert this amount to the specified unit, and add to column N
    a. E.g., if the synthesis requires 1kg of NaOH but your 'unit' is grams, simply convert to 1000 and add to column N
8. Multiply the CAD price per unit (column K) by the amount of the unit needed (column N) to get the price for the amount used (column O)
9. Identify the limiting reagent in your synthesis
10. Choose the yield of your synthesis
    a. In this assessment, where no yield was mentioned, the average of all the mentioned yields was used (see cell R3 for calculation)
    b. The following method was used for QDs yield at each step (using R- and G-Cd2-QLED as an example, see cells V21-V37)

i.	Core materials were identified (Cd, Se)
ii.	Limiting reagent of in the core was identified (Cd)
iii.	Amount of Cd in the final product was calculated based on assumed yield (cell T26)
iv.	The amount of Cd used in the next step was estimated. This was estimated from the paper's information that (A) a solution with an absorbance of 0.1 was used and (B) core size is 2 nm and (C) 1 mL of solution was used.
v.	Using these inputs and the exciton coefficient provided by Yu et al,[15] the molarity of CdSe QD used for shelling was calculated. (V21-V25)
vi.	Then, the mols of CdSe in one QD core was calculated (V26-V33)
vii.	These two inputs (molarity of QD core solution and mols of CdSe per QD core) we combined to determine the mols of Cd used in the synthesis.
viii.	Then, a ZnS shell was added. We assumed 68% yield of Cd in that step (T33)

ix. The same procedure as steps iv-vii was used to determine the mol of Cd needed for the last shelling (Z21-Z36)

x. The final yield of mol Cd from the cores was estimated based on a 68% yield (T42)

xi. This mol Cd was converted to grams of inorganic QD using the mol ratios given in the paper (AG21-AG36), with result in T43

11. Integrate the yield at each step to determine the price of materials in the next step
    a. The following equation was used to determine the price of the precursors used in the following step (p_2, see N26-O27 or K136-O137) involving the price of the precursors at the previous step (p_1), the amount produced at that step (y_1) and the subsequent step amount needed (y_2)

$$p_2 = (p_1 * y_1)/y_2$$

    b. The final cost per gram of material was calculated as a final step, where the intended amount (y_2) was 1g.
12. With the cost per gram of material calculated, this value was input into Row 8 of the sheet "Cost (CADcm2)
13. The ug/cm^2 of display of certain key elements (Cd, In, Ir) in the television was added to Row 6
    a. In the case of 3-OLED, there was no key element. However, since 2-OLED is a similar material, we assumed that the average number of moles present/ cm^2 of display in 2-OLED (K85) was the same as 3-OLED. Therefore, we multiplied that average number of moles present/ cm^2 of display (K85) by the molar masses of each of the 3-OLED compounds (N81-P81) to get the amount (g) of 3-OLED compounds/ cm^2 of display.
14. The ug of compound/cm^2 of display was then calculated based on the percent of the key element in the material (see Row 10 and below).
    a. The percent of the key element in the material was calculated based on the stoichiometry of the element in the material (perovskites, OLEDs) or based on the expected/calculated stoichiometry (QDs).

15. The CAD/g of material was then combined with the ug of compound/cm^2 of display to determine the CAD/ cm^2 of display for each material (Row 9).
16. The cost of InGaN was previously calculated in "Cost (CADg)" spreadsheet
17. Each material was combined in a package (T6-Y18)

5.8.3 Hazard: Detailed Methods

To reproduce the calculated hazards, access to the P2OASys - Tool (turi.org) is necessary. The Hazards of each of the chemicals involved in the synthesis will be calculated using this tool using the following steps:

1. Calculating hazard for every chemical. Repeat this step for each chemical involved in the synthesis. Import into the spreadsheet
    a. Load a "New Assessment" on the P2OAsys Tool, adding the CAS number and name of the chemical.
    b. Then add hazard data for this chemical into the tool using one of the "Enter Data" buttons.
    c. To the best of your ability (with chosen SDS), fill in as many hazard metrics as possible.
    d. Save these changes and click on the "Back" button
    e. Click "Export Data to csv" from the main page, and the copy the column where your chemical appears (i.e. column D) into the sheet "Hazard_Raw_Data"
    f. Click "Score Summary" to access the calculated hazard scores for your chemical. Click "Export all scores"
    g. In this csv file, you will need to add a row under row 1. In that row, add the CAS number of the chemical. This is key because chemicals are identified by their CAS number in the excel sheet
    h. Then, copy the necessary columns into the sheet "Hazard_Scored_Raw_Data"
    i. Check that your chemicals appeared in the "Hazard_Subcategory_Scores" sheet, as this sheet is the source for the "Hazard_Results_Category_Scores" sheet

j. Note, that this series of steps can be done for batches of chemicals, as the export function in P2OASys tool can export multiple chemicals. Please keep in mind though that leaving the P2OASys tool unattended may cause it to refresh (and loose hazard data) so export often!

2. Calculate the hazards of one substance from its precursors.
    a. Add the precursors to the material (column E) as well as their CAS #s (Column F)
    b. Add the substance that the precursor is used for (Ex used in cell C158 as an example) as well as the use of that precursor (Solvent, Reactant, Catalyst etc) if desired.
    c. Then, drag and drop the columns G-BT to autofill the contents (from sheet Hazard_Subcategory_Scores)
    d. Then add the package into the BX16 cell, as well as the red, green and blue colors assigned to it.
    e. These substances can also be input into cell BX35, but this is not necessary for the assessment to work
    f. The aggregate hazard scores should be filled in automatically (CD16) as well as the fraction of scores missing (CD37).
    g. Integrating the new package into the rank is a bit trickier. Please extend the formula in cell CR16 (hazard scores) or CR37 (missing scores) up to cells CR4 orCR25, respectively.
        i. This will reset the ranking to be out of 13 rather than out of 12, which was the state of the paper when it was published.
3. Advanced: If ever the precursors pass Row 200.
    a. There are ‘named’ sets of data (e.g. Health, Environment, Physical Properties) that extend to Row 200. If you surpass that row in data inputs, you may need to extend these data sets.
    b. Use the Formulas Tab -> Name Manager -> select the needed row and extend the reference as needed (e.g. to 300)
        i. The four names that will need to be extended are: Alt_ID, Health, Environment, Physical Properties

ii. If you simply extend Alt_ID, this will cause errors in all cells CE4-CQ15. Then, extend the other three to see the columns successively update with results.

5.8.4 Performance: Detailed Methods

1. Locate the quantum yield and the FWHM of the substance in the paper
2. With these three performance metrics in hand, add them to the excel sheet named "Performance"
    a. Add the name of the substance (C19), the QY (E19), the FWHM (F19)
3. Name a new package (C35) and indicate the red, green, and blue substances for that package (D36-F36)
4. The FWHM and QY tables will auto fill (B39, B74)
5. For the emission peaks (B57), please fill in manually the wavelength of highest emission intensity
6. Use the online tool to calculate the Rec. 2020 overlap for the emission peaks of the package
    a. https://www.mooresresearch.org/alternativeassessmentqdot
7. Input this value into cell P16
8. Next, adjust the rankings of all metrics (column L,N,Q,R) using the instructions in box I25
9. The graph of all ranked performance metrics should adjust with these changes in ranking (J31)

5.8.5 Supporting Figures

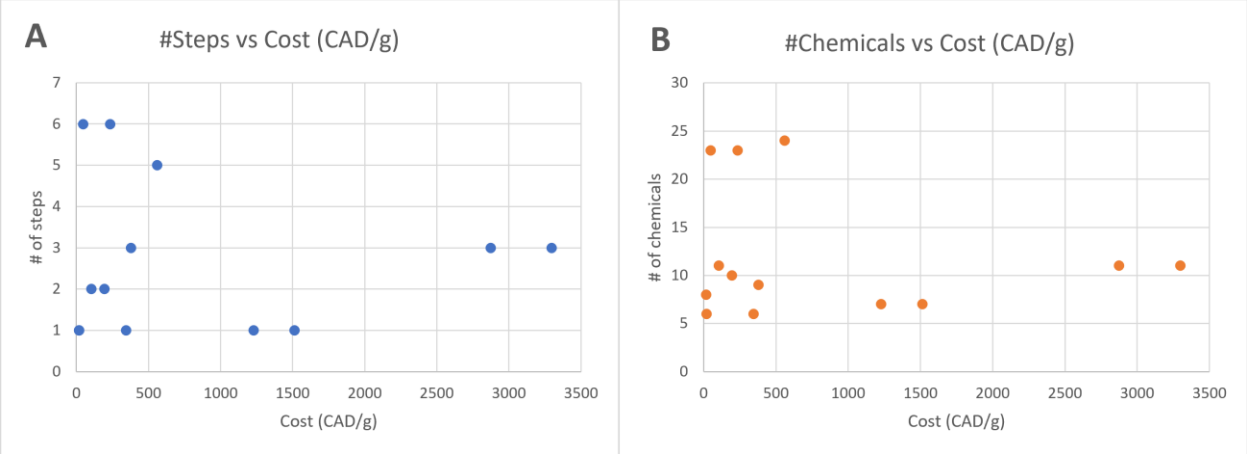

Figure S5-1: Lack of correlations observed for the (A) number of steps versus cost and (B) number of chemicals versus cost (CAD/g).

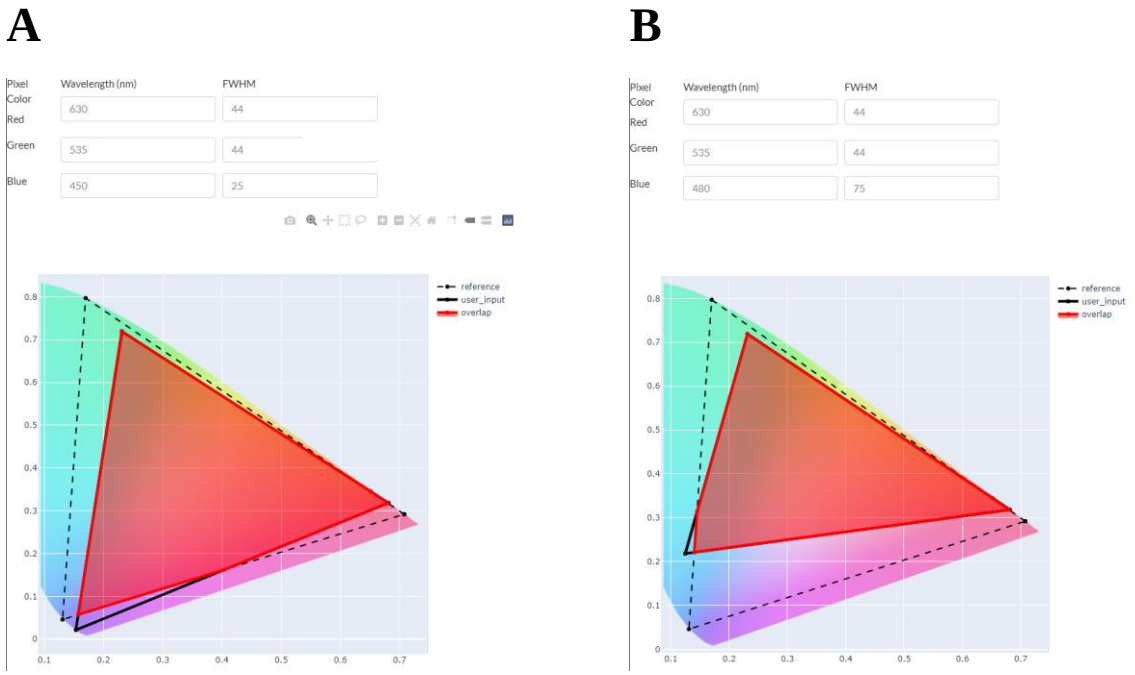

Figure S5-2: Rec. 2020 overlap on (A) In2-QLED and (B) In2-Q-OLED. The resulting Rec.2020 overlaps are outlined in red, with the Rec. 2020 standard in dashed black lines. The only difference between (A) and (B) is the inputs for the blue wavelength.

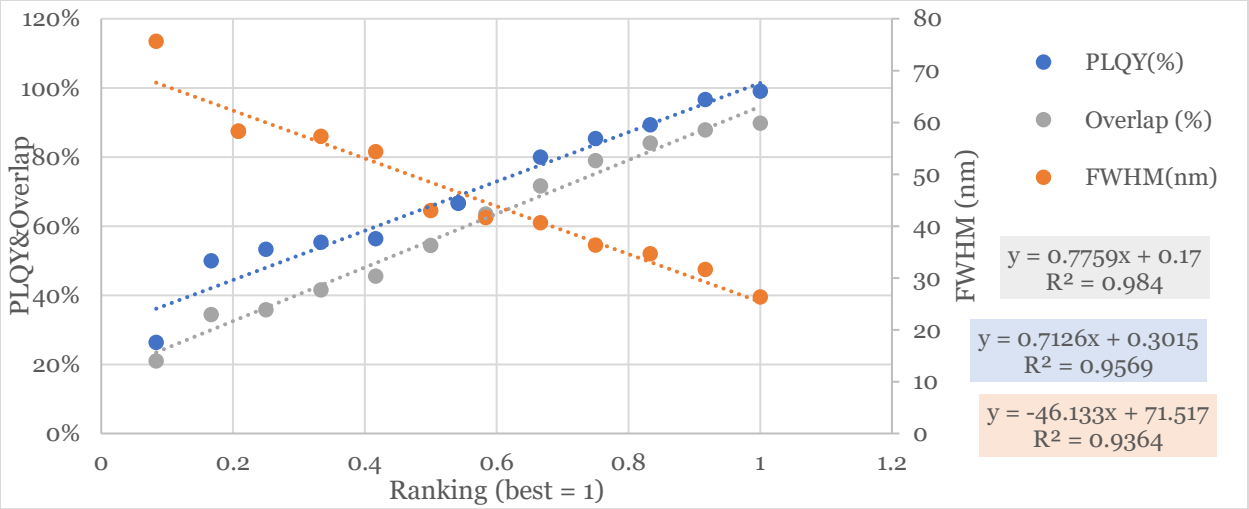

Figure S5-3: Individual performance metrics of packages (y-axis) compared to the package rank (x-axis).

This linear relationship demonstrates that there are no large disparities in performance metrics that are obscured by a linear ranking, where the one difference between two packages (e.g. between 3rd and 4th place) is the same as another (e.g. 4th and 5th place). Note that PLQY & % Overlap increase with increasing rank, while FWHM decreases. FWHM decreases because a smaller FWHM means a higher color purity.

To correlate FWHM to color purity, we used the following equation by Zhang et al.[16]

$$Color\ Purity\ (\%) = \frac{\sqrt{(x - x_i)^2 + (y - y_i)^2}}{\sqrt{(x_d - xi)^2 + (y_d - y_i)^2}}\ x\ 100$$

Where (x,y) are the CIE coordinates of the substance (generated from wavelength of emission and FWHM), (xi,yi) refers to the white illumination on the CIE diagram (0.33, 0.33), and (xd,yd) refers to the CIE coordinate for the "dominated wavelength" or the same wavelength as the sample but with an ideal FWHM (5 nm for this study).

The correlation between color purity ranking and FWHM ranking is demonstrated below (Figure S4). The standard deviation of the differences between the rankings is 0.06, which is much less than the difference between the ranks of 0.12. This small difference in ranking stems from the

green substance, which has a much wider range of color purity than red or blue (54-91% vs 75-99%). This is a result of the larger area of the CIE diagram that is dedicated to green colors.

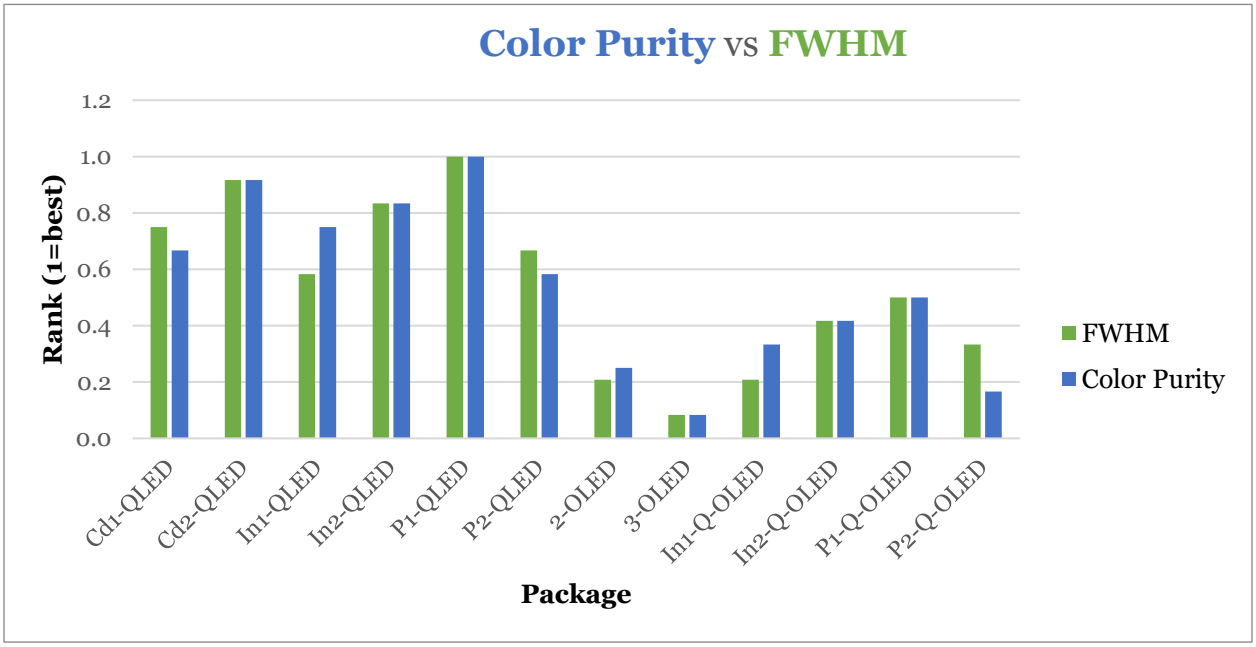

Figure S5-4: Comparison between rank (y-axis) for color purity (blue) and FWHM (green) for packages. See spreadsheet "Performance (Fig3)" sheet for calculations.

Table S5-2: TURI P2OASys category scores used to define the health, environment and physical properties hazards illustrated in Figure 4B and 5 of the main text. Please see spreadsheet : "Hazard_Results (Fig4+5)" sheet for subcategory information.

Aggregate categories	Health	Environment	Physical Properties
TURI P20ASys categories	(1) Acute Human Effects (2) Chronic Human Effects	(1) Ecological Hazards (2) Environmental Fate and Transport	(1) Physical Properties

Table S5-3: Package scores for Hazard Assessment (demonstrated as a heat map in Fig. 4B)

	Health	Environment	Physical_Prop	Health	Environment	Physical_Prop	Health	Environment	Physical_Prop	Health	Environment	Physical_Prop	Average
	R-	R-	R-	G-	G-	G-	B-	B-	B-				
Cd1-QLED	6.91	7.39	5.63	6.91	7.39	5.63	7.90	7.00	9.00	7.24	7.26	6.75	7.08
Cd2-QLED	7.45	7.78	5.80	7.45	7.78	5.80	7.90	7.00	9.00	7.60	7.52	6.87	7.33
In1-QLED	7.95	7.19	6.11	7.95	7.19	6.11	7.90	7.00	9.00	7.94	7.13	7.07	7.38
In2-QLED	7.00	6.10	5.50	7.00	6.10	5.50	7.90	7.00	9.00	7.30	6.40	6.67	6.79
P1-QLED	6.92	8.90	3.50	6.70	8.90	4.00	7.90	7.00	9.00	7.17	8.27	5.50	6.98
P2-QLED	6.67	8.50	6.50	6.64	8.71	6.50	7.90	7.00	9.00	7.07	8.07	7.33	7.49
2-OLED	8.32	7.07	8.43	7.84	4.97	7.37	7.45	4.59	8.19	7.87	5.55	7.99	7.14
3-OLED	7.90	5.56	8.40	7.82	5.78	7.33	8.10	8.50	8.67	7.94	6.61	8.13	7.56
In1-Q-OLED	7.95	7.19	6.11	7.95	7.19	6.11	8.10	8.50	8.67	8.00	7.63	6.96	7.53
In2-Q-OLED	7.00	6.10	5.50	7.00	6.10	5.50	8.10	8.50	8.67	7.37	6.90	6.56	6.94
P1-Q-OLED	6.92	8.90	3.50	6.70	8.90	4.00	8.10	8.50	8.67	7.24	8.77	5.39	7.13
P2-Q-OLED	6.67	8.50	6.50	6.64	8.71	6.50	8.10	8.50	8.67	7.14	8.57	7.22	7.64

Table S5-4: Scores for data missing in Hazard Assessment (demonstrated as a heat map in Fig. 5)

	Health	Environment	Physical_Prop	Health	Environment	Physical_Prop	Health	Environment	Physical_Prop	Health	Environment	Physical_Prop	Average
	R-	R-	R-	G-	G-	G-	B-	B-	B-				
Cd1-QLED	0.00	0.18	0.27	0.00	0.18	0.27	0.00	0.80	0.00	0.15	0.15	0.27	0.19
Cd2-QLED	0.00	0.10	0.50	0.00	0.10	0.50	0.00	0.80	0.00	0.20	0.20	0.27	0.22
In1-QLED	0.00	0.27	0.18	0.00	0.27	0.18	0.00	0.80	0.00	0.15	0.15	0.27	0.19
In2-QLED	0.00	0.29	0.29	0.00	0.29	0.29	0.00	0.80	0.00	0.19	0.19	0.27	0.22
P1-QLED	0.00	0.17	0.33	0.00	0.00	0.40	0.00	0.80	0.00	0.17	0.13	0.27	0.19
P2-QLED	0.00	0.00	0.33	0.00	0.00	0.43	0.00	0.80	0.00	0.11	0.14	0.27	0.17
2-OLED	0.00	0.36	0.36	0.00	0.23	0.14	0.00	0.16	0.16	0.24	0.12	0.11	0.16
3-OLED	0.00	0.20	0.50	0.08	0.25	0.25	0.17	0.50	0.50	0.23	0.19	0.39	0.27
In1-Q-OLED	0.00	0.27	0.18	0.00	0.27	0.18	0.17	0.50	0.50	0.15	0.15	0.39	0.23
In2-Q-OLED	0.00	0.29	0.29	0.00	0.29	0.29	0.17	0.50	0.50	0.19	0.19	0.39	0.26
P1-Q-OLED	0.00	0.17	0.33	0.00	0.00	0.40	0.17	0.50	0.50	0.17	0.13	0.39	0.23
P2-Q-OLED	0.00	0.00	0.33	0.00	0.00	0.43	0.17	0.50	0.50	0.11	0.14	0.39	0.21

5.8.6 Supporting References:

(1) Yang, Z.; Zhang, Y.; Liu, J.; Ai, J.; Lai, S.; Zhao, Z.; Ye, B.; Ruan, Y.; Guo, T.; Yu, X.; Chen, G.; Lin, Y.; Xu, S. Ultrastable Quantum Dot Composite Films under Severe Environments. *ACS Appl. Mater. Interfaces* **2018**, *10* (18), 15880–15887. https://doi.org/10.1021/acsami.8b02790.

(2) Carter, C. M.; Cho, J.; Glanzer, A.; Kamcev, N.; O'Carroll, D. M. Cost, Energy and Emissions Assessment of Organic Polymer Light-Emitting Device Architectures. *Journal of Cleaner Production* **2016**, *137*, 1418–1431. https://doi.org/10.1016/j.jclepro.2016.07.186.

(3) Theis, D. Display Technology. In *Ullmann's Encyclopedia of Industrial Chemistry*; Wiley-VCH Verlag GmbH & Co. KGaA, Ed.; Wiley-VCH Verlag GmbH & Co. KGaA: Weinheim, Germany, 2008; p a08_603.pub2. https://doi.org/10.1002/14356007.a08_603.pub2.

(4) Jang, E.; Jun, S.; Jang, H.; Lim, J.; Kim, B.; Kim, Y. White-Light-Emitting Diodes with Quantum Dot Color Converters for Display Backlights. *Advanced Materials* **2010**, *22* (28), 3076–3080. https://doi.org/10.1002/adma.201000525.

(5) Brown, R. P.; Gallagher, M. J.; Fairbrother, D. H.; Rosenzweig, Z. Synthesis and Degradation of Cadmium-Free InP and InPZn/ZnS Quantum Dots in Solution. *Langmuir* **2018**, *34* (46), 13924–13934. https://doi.org/10.1021/acs.langmuir.8b02402.
(6) Li, Y.; Hou, X.; Dai, X.; Yao, Z.; Lv, L.; Jin, Y.; Peng, X. Stoichiometry-Controlled InP-Based Quantum Dots: Synthesis, Photoluminescence, and Electroluminescence. *J. Am. Chem. Soc.* **2019**, *141* (16), 6448–6452. https://doi.org/10.1021/jacs.8b12908.
(7) Protesescu, L.; Yakunin, S.; Bodnarchuk, M. I.; Krieg, F.; Caputo, R.; Hendon, C. H.; Yang, R. X.; Walsh, A.; Kovalenko, M. V. Nanocrystals of Cesium Lead Halide Perovskites (CsPbX3, X = Cl, Br, and I): Novel Optoelectronic Materials Showing Bright Emission with Wide Color Gamut. *Nano Lett.* **2015**, *15* (6), 3692–3696. https://doi.org/10.1021/nl5048779.
(8) Zhang, J.; Yang, Y.; Deng, H.; Farooq, U.; Yang, X.; Khan, J.; Tang, J.; Song, H. High Quantum Yield Blue Emission from Lead-Free Inorganic Antimony Halide Perovskite Colloidal Quantum Dots. *ACS Nano* **2017**, *11* (9), 9294–9302. https://doi.org/10.1021/acsnano.7b04683.
(9) Yang, X.; Guo, H.; Liu, B.; Zhao, J.; Zhou, G.; Wu, Z.; Wong, W.-Y. Diarylboron-Based Asymmetric Red-Emitting Ir(III) Complex for Solution-Processed Phosphorescent Organic Light-Emitting Diode with External Quantum Efficiency above 28%. *Adv. Sci.* **2018**, *5* (5), 1701067. https://doi.org/10.1002/advs.201701067.
(10) Liao, J.-L.; Rajakannu, P.; Gnanasekaran, P.; Tsai, S.-R.; Lin, C.-H.; Liu, S.-H.; Chang, C.-H.; Lee, G.-H.; Chou, P.-T.; Chen, Z.-N.; Chi, Y. Luminescent Diiridium Complexes with Bridging Pyrazolates: Characterization and Fabrication of OLEDs Using Vacuum Thermal Deposition. *Advanced Optical Materials* **2018**, *6* (11), 1800083. https://doi.org/10.1002/adom.201800083.
(11) Shin, H.; Ha, Y. H.; Kim, H.; Kim, R.; Kwon, S.; Kim, Y.; Kim, J. Controlling Horizontal Dipole Orientation and Emission Spectrum of Ir Complexes by Chemical Design of Ancillary Ligands for Efficient Deep-Blue Organic Light-Emitting Diodes. *Adv. Mater.* **2019**, *31* (21), 1808102. https://doi.org/10.1002/adma.201808102.
(12) Zhang, Y.; Ran, Q.; Wang, Q.; Liu, Y.; Hänisch, C.; Reineke, S.; Fan, J.; Liao, L. High-Efficiency Red Organic Light-Emitting Diodes with External Quantum Efficiency Close to 30% Based on a Novel Thermally Activated Delayed Fluorescence Emitter. *Adv. Mater.* **2019**, *31* (42), 1902368. https://doi.org/10.1002/adma.201902368.
(13) Wu, T.-L.; Huang, M.-J.; Lin, C.-C.; Huang, P.-Y.; Chou, T.-Y.; Chen-Cheng, R.-W.; Lin, H.-W.; Liu, R.-S.; Cheng, C.-H. Diboron Compound-Based Organic Light-Emitting Diodes with High Efficiency and Reduced Efficiency Roll-Off. *Nature Photon* **2018**, *12* (4), 235–240. https://doi.org/10.1038/s41566-018-0112-9.
(14) Lin, T.-A.; Chatterjee, T.; Tsai, W.-L.; Lee, W.-K.; Wu, M.-J.; Jiao, M.; Pan, K.-C.; Yi, C.-L.; Chung, C.-L.; Wong, K.-T.; Wu, C.-C. Sky-Blue Organic Light Emitting Diode with 37% External Quantum Efficiency Using Thermally Activated Delayed Fluorescence from Spiroacridine-Triazine Hybrid. *Adv. Mater.* **2016**, *28* (32), 6976–6983. https://doi.org/10.1002/adma.201601675.
(15) Yu, W. W.; Qu, L.; Guo, W.; Peng, X. Experimental Determination of the Extinction Coefficient of CdTe, CdSe, and CdS Nanocrystals. *Chemistry of Materials* **2003**, *15* (14), 2854–2860.

(16) Zhang, Z.; Sun, L.; Devakumar, B.; Liang, J.; Wang, S.; Sun, Q.; Dhoble, S. J.; Huang, X. Novel Highly Luminescent Double-Perovskite Ca2GdSbO6:Eu3+ Red Phosphors with High Color Purity for White LEDs: Synthesis, Crystal Structure, and Photoluminescence Properties. *Journal of Luminescence* **2020**, *221*, 117105. https://doi.org/10.1016/j.jlumin.2020.117105.

6 Conclusions, Implications and Future Work

6.1 Connecting text

The previous chapter concludes the experimental and assessment work conducted in this thesis. We developed an alternatives assessment to examine the next generation of emissive substances – from perovskites to In-QDs to organic emitters. This assessment did not conclude that one of the alternatives was more safe, cost-effective, and higher performing. We also concluded that there should be a simple way to incorporate the transformation and toxicity data from previous chapters. The following section will survey other conclusions, implications and future work needed.

6.2 Summary

This thesis first explored the synthesis, transformation, and toxicity of commercially-relevant QDs. Second, it assessed whether emerging substances were viable and safe replacements for these Cd-QDs. The thesis' 4 major findings are described below:

1) Commercially relevant QDs were introduced as the basis for transformation and toxicity tests. Using the design reported in a patent for the core, the graded shells, and the large amount of well-characterized polymer, we synthesized QDs that were representative of the ones currently found in displays in **Chapter 3**. The development of this synthesis provided a versatile platform for analyzing each piece of the system, and we subsequently synthesized QD components and combinations in **Chapter 4.**
2) Although commercially relevant QDs may loose their ZnS shells, these QDs are stable in the long term. We studied both the dissolution and aggregation of QDs in solutions of various pHs for 6 months in **Chapter 3**. At circum-neutral pH, we found that Cd had remained in nanoparticle form (> 3 kDa) and had aggregated into ~100 nm tight aggregates. In the dark, the impact of dissolved oxygen was minimal, suggesting at the dominance of a reaction that is different from the oxidations observed under light conditions by other authors.
3) We demonstrated that Cd in QDs remain intact after simulated human digestion, but their degree of dispersion changes significantly in **Chapter 4.** Using spICP-MS for

the first time to examine QDs, we concluded that the cut-off was ~210 QDs and saw the percentage of QDs above that threshold decrease dramatically after the gastric stage. Despite the higher pH conditions in the intestinal stage, the same degree of homo-aggregation was not recovered.

4) Throughout the examination of QD transformations, we partnered with toxicologists to examine the implications of transforming QDs. In **Chapter 3,** we found that QDs exposed to pH 2 for 24 h and separated from dissolved ions were less toxic than either pristine QDs or a model that contained the same polymer and dissolved ion amounts. In **Chapter 4,** we found that the 'complete' QD (CdSe/ZnS-P&E) had synergistic toxicity, rather than simply additive toxicity of its components.
5) Emerging alternatives to Cd-QDs in displays are not yet safer and viable (i.e. cost-competitive and high performing). The alternatives assessment method was adapted to emerging emissive substances in **Chapter 5.** We developed a price, performance, and adapted a hazard assessment for the examination of perovskites, In-QDs, and organic emitters. Based on the 12 packages of red, green, and blue substances examined, we concluded that the emerging alternatives were not less hazardous, higher performing, or more cost effective overall. We identified that regulations could also halt the implication of certain lead-based alternatives, as they had previously restricted Cd-QDs.

6.3 Implications and Future Work

The implications and future work related to the four key findings reflect the four key conclusions of this thesis. It must be noted that these four key conclusions must not be generalized and applied to more complex systems. Our environmental transformation study included different pHs and oxygen conditions, but not the influence of light, humic acids, or changes in concentration of the QDs. The presence of any of these conditions could change aggregation and dissolution trends. Similarly, the examination of QDs in the simulated human digestive system were done on an in vitro system. In vivo, there is a much more complex environment (including the presence of different foods) which may

complicate the behavior of the QDs. Keeping these limitations in mind, the main conclusions of this thesis are:

1) Relevant results start with relevant particles. Environmental and toxicity studies have a moving target to reach as QDs continue to develop into a wide variety of research-stage applications. This work brought currently commercially relevant Cd-QDs, but these Cd-QDs will soon be replaced by Cd-free alternatives in televisions. The fates of these alternatives will need to be examined with the same rigor. We recommend continued collaboration between the researchers developing these substances and the researchers examining the fate and toxicity of the same substances.
2) Long-term stability of QDs in nano-size aggregates could have implications for their transport. These particles could be mobile over long distances in aquatic environments and therefore be more bioavailable than large aggregates of other nanoparticles. Such an implication should be tested with more real-world conditions that include ambient light and other biomolecules in solution. We hope that these systematic studies can be designed for incorporation into models that facilitate the examination of nanoparticles with different safety and sustainability assessments.
3) QDs (and other small stable NPs) should be closely monitored in the human digestive system. The increased dispersion in our study could point to association with biomolecules that facilitate the uptake of QDs in the digestive system. There are a few more layers to the digestive tract that were not examined in our study, such as the microbial community or the mucus layer that protects epithelial cells. These factors should also be included in future tests to determine whether increased dispersion influences toxicity.

Acknowledgement of hazard is needed as emerging emissive substances are developed. These considerations were made accessible to the chemists and materials scientists that are developing new substances through AA. Although risk assessments and LCA may need specialists, relatively simple hazard analyses are attainable through the adaptation of AA. We also identified stability metrics, bulk chemical costs, and unknown life cycle impacts that were missing from our assessment – all of which should be explored in the future.